



**HAL**  
open science

# Stabilization of Water-in-Water emulsions by bishydrophilic microgels

Do Nhu Trang Nguyen

► **To cite this version:**

Do Nhu Trang Nguyen. Stabilization of Water-in-Water emulsions by bishydrophilic microgels. *Polymers*. Le Mans Université, 2024. English. NNT : 2024LEMA1014 . tel-04769476

**HAL Id: tel-04769476**

**<https://theses.hal.science/tel-04769476v1>**

Submitted on 6 Nov 2024

**HAL** is a multi-disciplinary open access archive for the deposit and dissemination of scientific research documents, whether they are published or not. The documents may come from teaching and research institutions in France or abroad, or from public or private research centers.

L'archive ouverte pluridisciplinaire **HAL**, est destinée au dépôt et à la diffusion de documents scientifiques de niveau recherche, publiés ou non, émanant des établissements d'enseignement et de recherche français ou étrangers, des laboratoires publics ou privés.

# THESE DE DOCTORAT

DE  
LE MANS UNIVERSITE  
SOUS LE SCEAU DE  
LA COMUE ANGERS – LE MANS

ECOLE DOCTORALE N° 596  
*Matière, Molécules, Matériaux et Géosciences*  
Spécialité : Chimie et physico-chimie des polymères

Par  
« **Do Nhu Trang NGUYEN** »

« **Stabilization of Water-in-Water emulsions by bishydrophilic microgels** »

Soutenance de thèse à la Salle de conférence IAM, le 01 octobre 2024 à 10h

Unité de recherche : Institut des Molécules et des Matériaux du Mans UMR 6283

Thèse N° : 2024LEMA1014

## Rapporteurs avant soutenance :

Dr. Laurence Navailles                      CNRS, Université de Bordeaux  
Dr. Hans Tromp                                NIZO Food Research

## Composition du Jury :

Président :            Dr. Fabienne Gauffre                      CNRS, Université de Rennes  
Examineurs :        Pr. Valérie Ravaine                      Bordeaux INP  
                             Pr. Fernando Leal-Calderon            Bordeaux INP

Dir. de thèse :        Pr. Lazhar Benyahia                      Le Mans Université  
Co-dir. de thèse : Dr. Taco Nicolai            Le Mans Université



## Remerciements

J'exprime toute ma reconnaissance à mon directeur de thèse, Monsieur Lazhar Benyahia et mon co-directeur de thèse, Monsieur Taco Nicolai pour leurs conseils, leur disponibilité au quotidien et leur grande patience lors de ces trois années de thèse. Je remercie l'équipe à Bordeaux, surtout Léa Waldmann et Madame Valérie Ravaine pour la synthèse des microgels et pour les discussions enrichissantes.

Je souhaiterais également adresser mes remerciements aux membres du jury : Madame Laurence Navailles et Monsieur Hans Tromp d'avoir accepté de rapporter ce travail de thèse, Je remercie aussi Madame Valérie Ravaine, Madame Fabienne Gauffre et Monsieur Fernando Leal-Calderon d'avoir aimablement accepté de participer à mon jury.

Je remercie toute l'équipe PCI du Laboratoire IMMM, au sein de laquelle j'ai passé mes trois ans de thèse, pour leur accueil chaleureux et m'assuré les meilleures conditions de travail. Je remercie Monsieur Frédérick Niepceron de m'avoir formé sur le microscope confocal, LUMiSizer®. Je remercie aussi Monsieur Christophe Chassenieux pour son écoute et ses conseils dispensés au cours des « Biopolymer clubs ».

Je remercie mes collègues : Yuwen, Noémie, Sandra, Maria, Colleen, Hyun Jung, Navya, Gireesh, Ahmad, Paul, Elie ainsi que les autres personnes et étudiants dans mon laboratoire pour leurs propositions précieuses et leur accompagnement tout au long de ce travail de recherche. Je remercie mes chers amis : Oanh, Su, Tran, Thao, Giang, Nghi, Phat et Khoi qui sont toujours de mon côté pour les moments inoubliables qu'on a passé ensemble.

Finalement, je voudrais témoigner ma gratitude et mes remerciements à ma famille : mes parents, mon frère et ma famille française Céline dont les supports et les encouragements m'ont aidé à surmonter les difficultés et à accomplir ce mémoire.





## Abbreviation

|                 |  |
|-----------------|--|
| AA              | acrylic acid   |
| AMP             | amylopectin  |
| AMPS            | aqueous multi-phase systems  |
| ATPS            | aqueous two-phase system   |
| BIS             | bishydrophilic microgels   |
| CLSM            | confocal laser scanning microscopy   |
| DEX             | dextran  |
| D/P             | emulsion of dextran droplets dispersed in poly(ethylene oxide)             |
| DG/P            | emulsion of dextran and gelatin droplets dispersed in poly(ethylene oxide) |
| DLS             | dynamic light scattering   |
| DS              | degree of substitution   |
| F <sub>AA</sub> | fraction of acid acrylic   |
| FITC            | fluorescein isothiocyanate   |
| GEL             | gelatin  |
| G/P             | emulsion of gelatin droplets dispersed in poly(ethylene oxide)             |
| G/D             | emulsion of gelatin droplets dispersed in dextran                          |
| O/W             | Oil-in-Water   |
| PEO             | poly(ethylene oxide)   |
| P/D             | emulsion of poly(ethylene oxide) droplets dispersed in dextran             |
| P/G             | emulsion of poly(ethylene oxide) droplets dispersed in gelatin             |

|                |                                     |
|----------------|-------------------------------------|
| pNIPAM         | poly(N-isopropylacrylamide)         |
| pVPC           | polyvinylpyridinium chloride        |
| PRO            | protein microgels                   |
| PUL            | pullulan                            |
| RhoB           | rhodamin B                          |
| M <sub>w</sub> | molecular weight                    |
| t <sub>c</sub> | characteristic stabilization time   |
| TLL            | tie line length                     |
| VPTT           | Volume Phase Transition Temperature |
| W/W            | Water-in-Water                      |
| WPI            | whey protein isolate                |
| XG             | xyloglucan                          |

# Table of contents

|   |           |
|---|-----------|
| <b>Introduction .....</b>                                   | <b>11</b> |
| <b>Chapter 1. State of the Art .....</b>                    | <b>15</b> |
| <b>1.1. Water-in-Water emulsions .....</b>                  | <b>17</b> |
| 1.1.1. Phase diagram .....                                  | 18        |
| 1.1.2. Properties of Water-in-Water emulsions .....         | 20        |
| 1.1.3. Aqueous multi-phase system.....                      | 21        |
| <b>1.2. Stabilization of Water-in-Water emulsions .....</b> | <b>23</b> |
| 1.2.1. Stabilization by the adsorption of particles .....   | 23        |
| 1.2.2. Stabilization by self-assemble systems .....         | 29        |
| 1.2.3. Stabilization by gelation of a third phase .....     | 32        |
| 1.2.4. Stabilization of aqueous multi-phase system .....    | 33        |
| <b>Chapter 2. Materials and Methods .....</b>               | <b>35</b> |
| <b>2.1. Materials .....</b>                                 | <b>37</b> |
| 2.1.1. Bishydrophilic microgels .....                       | 37        |
| 2.1.2. Protein microgels.....                               | 39        |
| 2.1.3. Emulsion preparation .....                           | 39        |
| <b>2.2. Methods .....</b>                                   | <b>40</b> |
| 2.2.1. Particle size measurement .....                      | 40        |
| 2.2.2. Microstructure observation .....                     | 41        |

|   |           |
|---|-----------|
| 2.2.3. Transmission measurement .....   | 42        |
| <b>Chapter 3. Stabilization of Water-in-Water emulsion by varying the composition of bishydrophilic microgels.....</b>                            | <b>47</b> |
| <b>3.1. Swelling behavior of microgels in suspension.....</b>   | <b>49</b> |
| <b>3.2. Effect of the microgel composition on Water-in-Water emulsion stability .....</b>   | <b>50</b> |
| 3.2.1. Stability of Water-in-Water emulsions at low temperature .....   | 50        |
| 3.2.2. Effect of temperature on Water-in-Water emulsion stability.....  | 62        |
| <b>Conclusion.....</b>  | <b>69</b> |
| <b>Chapter 4. Effect of charge on the stabilization of Water-in-Water emulsions by bishydrophilic microgels.....</b>                              | <b>71</b> |
| <b>4.1. Characterization of the microgels.....</b>  | <b>73</b> |
| <b>4.2. Emulsion microstructure and stability.....</b>  | <b>76</b> |
| 4.2.1 Effect of the pH .....  | 76        |
| 4.2.2. Effect of salt .....   | 80        |
| 4.2.3. Combined effect of pH and salt.....  | 85        |
| 4.2.4. Effect of the fraction of acrylic acids units .....  | 85        |
| <b>Conclusions .....</b>  | <b>88</b> |
| <b>Chapter 5. Interaction between stabilized droplets of different phases in the same continuous phase of an aqueous three-phase system .....</b> | <b>91</b> |
| <b>5.1. Stabilisation of GEL-PEO emulsions by bishydrophilic microgels .....</b>  | <b>93</b> |
| 5.1.1. Effect of microgel composition.....  | 93        |

|   |            |
|---|------------|
| 5.1.2. Effect of the pH .....   | 96         |
| 5.1.3. Effect of charge on the microgels .....  | 100        |
| <b>5.2. Interaction between gelatin and dextran droplets .....</b>  | <b>103</b> |
| 5.2.1. Morphology .....   | 103        |
| 5.2.2. Stability .....  | 110        |
| <b>Conclusion.....</b>  | <b>114</b> |
| <b>Chapter 6. Structure and stabilization of Water-in-Water emulsions in the presence of two types of microgels .....</b> | <b>117</b> |
| <b>6.1. Microgels in water and pure PEO and DEX phases .....</b>  | <b>119</b> |
| <b>6.2. Mixtures of emulsions .....</b>   | <b>120</b> |
| 6.2.1. Gently mixed emulsions .....   | 120        |
| 6.2.2. Vortex mixed emulsions.....  | 125        |
| <b>6.3. Stabilization with microgel co-aggregates.....</b>  | <b>131</b> |
| <b>6.4. Mixtures of an emulsion and a microgel suspension.....</b>  | <b>134</b> |
| <b>Conclusion.....</b>  | <b>138</b> |
| <b>General conclusion .....</b>   | <b>141</b> |
| <b>References .....</b>   | <b>145</b> |



## Introduction

Water-in-Water (W/W) emulsions, also referred to as “aqueous two-phase systems” (ATPS) are generated by mixing two incompatible types of polymers in aqueous solution, which separate into two distinct phases [1]. These systems have attracted interest as a simple route to form aqueous microcompartments [2]. Many molecular species tend to partition preferentially to one phase, which means that they can spontaneously localize and concentrate within the dispersed phase [3]. As such, they are also considered as interesting tools to study rudimentary forms of artificial cells [4].

However, stabilization W/W emulsions is challenging. Compared with Oil-in-Water (O/W) emulsions, the interface separating aqueous phases is thicker and has a much lower interfacial tension [5]. For these reasons, small surfactants are inappropriate to stabilize W/W emulsions, but particles of sufficiently large size will in some cases spontaneously adsorb at the interface leading to an effective stability of W/W emulsions [6-8]. The driving force for the adsorption is the reduction of the total interfacial tension when a particle is located at the interface. This means that the particles need to have some affinity with both phases. In fact, the optimum situation for adsorption is when the particles prefer each phase equally and therefore partition equally between the phases. It has been found, however, that adsorption at the interface is not by itself sufficient to obtain stability and interaction between the particles at the interface appears to play a crucial role. Another interesting feature of W/W emulsions is that the stability generally depends on which phase is the dispersed phase even if the emulsions are situated on the same tie-line and therefore the interfacial tension is the same [9-11].

Examples of amphiphilic block copolymers micelles [12, 13], liposomes [14] and even recently lipidic bilayers [15] have been reported. Different types of particles have been studied



for their ability to stabilize W/W emulsions, such as protein particles [11], fat particles [16], mineral particles [17], rod-like cellulose nanocrystals [18], and synthetic microgels [10].

Among them, bishydrophilic microgels formed by crosslinking dextran (DEX) grafted with poly(N-isopropylacrylamide) (pNIPAM) show interesting effects on the stability of W/W emulsions formed by the mixture of poly(ethylene oxide) (PEO) and DEX [10]. The two components of these microgels present a different affinity for each phase of this system. In addition, the thermosensitivity of pNIPAM causes these microgels to shrink when heated above 32 °C and was found to have an effect on the stability. Notably, at room temperature, emulsions of the DEX rich phase dispersed in the PEO rich phase (D/P) were found to be much more stable than the inverse emulsions (P/D), whereas at 50 °C P/D emulsions were more stable than D/P emulsions even though the emulsions were situated on the same tie-line.

By systematically altering the weight content of DEX, its functionalization degree, and its molecular weight, we aim to finely tune the bishydrophilic balance of these microgels. This tunability is crucial for controlling the affinity of the microgels for different aqueous phases and their adsorption at the W/W interface. In the first instance, our study examines how these modifications influence the stability of W/W emulsions, assessing both types of W/W emulsions to understand the broad impact of microgels composition. Additionally, we explore the effect of temperature on the stability of these emulsions.

The second aim of this investigation was to study the effect of electrostatic interactions on the stabilization of the same model W/W emulsion by these microgels. Beyond the fundamental character aimed at understanding the stabilization mechanisms of W/W emulsions, this study shows that modulating the pH, ionic strength or temperature can be used as triggers to modulate the stability and the behavior of the emulsions for potential applications acrylic acid (AA) groups were incorporated into the otherwise neutral microgels during the synthesis. AA was chosen, because the copolymerization reaction can be easily done with this

monomer, it is well-described in the literature [19-23] and its protonation can be modulated by varying the pH. In this manner, the charge density of the microgels could be modified by varying the pH while the strength of electrostatic interactions could be varied either by changing the charge density or by adding salt. We will show the effect of electrostatic interactions on the size of the microgels and their capacity to stabilize W/W emulsions as a function of the temperature.

Stable W/W emulsions have excellent potential for compartmentalization of ingredients and localized reactions [14, 24, 25]. When more than two types of incompatible polymers are mixed, aqueous multi-phase systems (AMPS) are formed containing droplets of different phases dispersed together in a common continuous phase. Droplets of different phases do not coalesce, but in most cases stick to each other. The contact angle that each phase makes with the two other phases is determined by the ratios of the interfacial tensions between the different phases [26]. Very few studies on the stabilization of W/W emulsions containing more than one type of dispersed droplet have been reported so far, but it has been shown that they can lead to the formation of Janus-type droplets or a space-filling network [27, 28]. In the third part of this thesis, we address this issue by mixing W/W emulsions containing droplets rich in DEX or rich in fish gelatin (GEL) dispersed in a common continuous phase rich in PEO. It will be shown that the droplets immediately associated, whereas droplets of the same phase do not coalesce or only very rarely. The morphology of the Janus droplets was exploited to determine the effect of the adsorbed microgel layer on the effective interfacial tension.

The last part of this these is to study the simultaneous use of two types of particles with distinct properties to benefit from the properties of each particle. This approach has been used to stabilize O/W emulsions, for instance using particles with opposite charge [29, 30] or with different hydrophobicity [31, 32], but not yet for W/W emulsions. The objective of the present investigation was therefore to study the effect of adding two different types of particles on the

microstructure and stability of a W/W emulsion. Here we report on the combined effects of adding bishydrophilic microgels and protein microgels to W/W emulsion containing PEO and DEX. Both types of microgels were evaluated for their individual and synergistic contributions to the emulsion properties. This strategy optimized the stability of W/W emulsions as well as the structuring and organization of the two types of particles at the interface.

The thesis includes 6 chapters:

— Chapter 1 gives a background to the investigation presented in this thesis and a summary of relevant literature.

— Chapter 2 presents the materials and methods used in this work. The synthesis of microgels and the emulsion preparation will be described. Various characterization techniques for assessing the particle size, microstructure as well as emulsion stability will be presented.

— Chapter 3 focuses on a fundamental investigation of the effect of adding bishydrophilic microgels on the stability of W/W emulsions. The results have been published in the *Journal of Colloid and Interface Science* (DOI: 10.1016/j.jcis.2023.09.049).

— Chapter 4 evaluates the effect of electrostatic interactions on the stability of W/W emulsions. The results have been published in *Journal of Colloid and Interface Science* (DOI: 10.1016/j.jcis.2023.05.029).

— Chapter 5 presents an investigation of the interaction between bishydrophilic microgel-stabilized GEL and DEX droplets dispersed in the same continuous phase of PEO. The results have been published in *Soft Matter* (DOI: 10.1039/D3SM01688A).

— Chapter 6 is dedicated to the study of interaction between droplet stabilized by bishydrophilic microgels and protein microgels. The results have been submitted in *Journal of Colloid and Interfacial Science*.

The thesis ends with main conclusions and proposes future research directions.

## **Chapter 1. State of the Art**

In this chapter, the literature on particle stabilization of W/W emulsions is reviewed. Firstly, the definition and fundamentals of W/W emulsions including the principles of phase separation and emulsion properties will be introduced. This section explains the differences between W/W emulsions with classic oil-in-water (O/W) emulsions. The second part of the chapter provides a detailed description of the various types of particles and strategies used to stabilize W/W emulsions. It discusses how particle size, morphologies, and interactions between particles at the interface contribute to the stabilization process.

---

|   |           |
|---|-----------|
| <b>1. Water-in-Water emulsions .....</b>                  | <b>17</b> |
| 1.1. Phase diagram .....                                  | 18        |
| 1.2. Properties of Water-in-Water emulsions .....         | 20        |
| 1.3. Aqueous multi-phase system.....                      | 21        |
| <b>2. Stabilization of Water-in-Water emulsions .....</b> | <b>23</b> |
| 2.1. Stabilization by the adsorption of particles .....   | 23        |
| 2.1.1. Particle size .....                                | 24        |
| 2.1.2. Morphology .....                                   | 24        |
| 2.1.3. Modification of the particle surface .....         | 26        |
| 2.1.4. Electrostatic interaction .....                    | 27        |
| 2.1.5. Thermosensitivity .....                            | 27        |
| 2.1.6. Crosslinking .....                                 | 28        |
| 2.2. Stabilization by self-assemble systems .....         | 29        |
| 2.2.1. Stabilization by block copolymers.....             | 29        |
| 2.2.2. Stabilization by polyelectrolytes.....             | 30        |
| 2.3. Stabilization by gelation of a third phase .....     | 32        |
| 2.4. Stabilization of aqueous multi-phase system .....    | 33        |

### 1.1. Water-in-Water emulsions

Water-in-Water (W/W) emulsions, also referred to as “aqueous two-phase systems” (ATPS), are generated by mixing two incompatible types of polymers in aqueous solution, which form two distinct phases [1]. The ATPS was first discovered by M. W. Beijerinck in 1896 [33]. Its practical applications were later unveiled by P.Å. Albertsson in 1958, who demonstrated its potential for extraction and purification processes [34]. These systems have attracted interest as a simple route to form aqueous microcompartments [2]. The uneven partition of molecular species within the two phases allows them to spontaneously localize and concentrate within the dispersed compartment [3]. As such, they are also considered as interesting tools to study rudimentary forms of artificial cells [4]. Since then, ATPS has been widely used for various purposes including biomedical sciences, chemical analysis, food safety and environmental monitoring [35].

Separation of two solutes in a mixture into two separate parts occurs when the free energy of mixing ( $\Delta G$ ) is positive. This energy is the result of the compensation of the enthalpy ( $\Delta H$ ) and the entropy ( $\Delta S$ ) of the system:

$$\Delta G = \Delta H - T\Delta S$$

In a mixture of two high molecular weight solutes,  $\Delta S$  is much lower and  $\Delta H$  is most often sufficiently large to favor the formation of two-phase systems [36]. The mechanism of phase separation depends on the repulsion or attraction of the polymer [37]. When the two polymers are uncharged or similarly charged, they have the tendency to segregate into two phases with one rich in one polymer and the other rich in the other [1]. In the case that the two have opposite charges, complex formation will result in precipitation into a single phase that is separated from the solvent phase [38]. Phase separation involving charged polymers usually depends on the ionic strength of the system [39].

Phase segregation has been studied with different combinations of components. Grinberg provided a summary of up to one hundred mixtures of proteins (gelatin, albumin, globulin, ...) and polysaccharides (DEX, pullulan, amylopectin, ...) [40]. As reported by Pereira, various pairs of ATPS were listed such as nonionic PEO or DEX-based ATPS, PEO/poly(acrylic acid), sodium dextran sulfate/polystyrene sulfonate, ... [41]. A frequently utilized ATPS consists of mixtures of PEO and DEX [42].

### *1.1.1. Phase diagram*

Phase separation is driven by a decrease in mixing entropy when the polymer solutions reach a certain concentration. At lower concentrations, the polymers are miscible and form a homogeneous phase [43]. This critical concentration depends on the molecular weight of the polymers. Polymers with larger molecular weights tend to form coexisting phases at lower concentrations compared to that with lower molecular weights [44]. Temperature also influences phase separation by changing the solvent quality [45].

**Figure 1.1** illustrates a schematic phase diagram which represents the transition between the single-phase and two-phase regions determined by a coexistence curve called the binodal. Each point plotted on the diagram corresponds to a blend of two polymer solutions, reflecting their initial concentrations in the mixture. In the two-phase region, a W/W emulsion is formed when applying a mechanical force. Afterward, the system has a tendency to separate into two macroscopic phases with the polymer concentrations lying on the binodal. The tie line is a set of aligned emulsion points containing the same final phase composition and therefore having the same interfacial tension. As the tie-line shortens, the two ends approach a single point on the binodal, called the critical point. The interfacial tension depends on the tie line length (TLL), which is directly related to the distance between the tie line and the critical point [1].

The volume fraction of phases can be determined by the ratio between the distance from the point representing the mixture composition to the end points and the total length of the tie

line. The smaller volume phase tends to be dispersed into the larger volume phase, also known as continuous phase. As the binodal often approaches the axes, the concentration after phase separation at the intersection between the tie line and the binodal normally contains a large amount of one polymer and only a small amount of the other polymer. Examples of phase diagrams relevant for this thesis (DEX-PEO, GEL-PEO, DEX-PEO) are shown in **Figure 1.2** [10, 46].

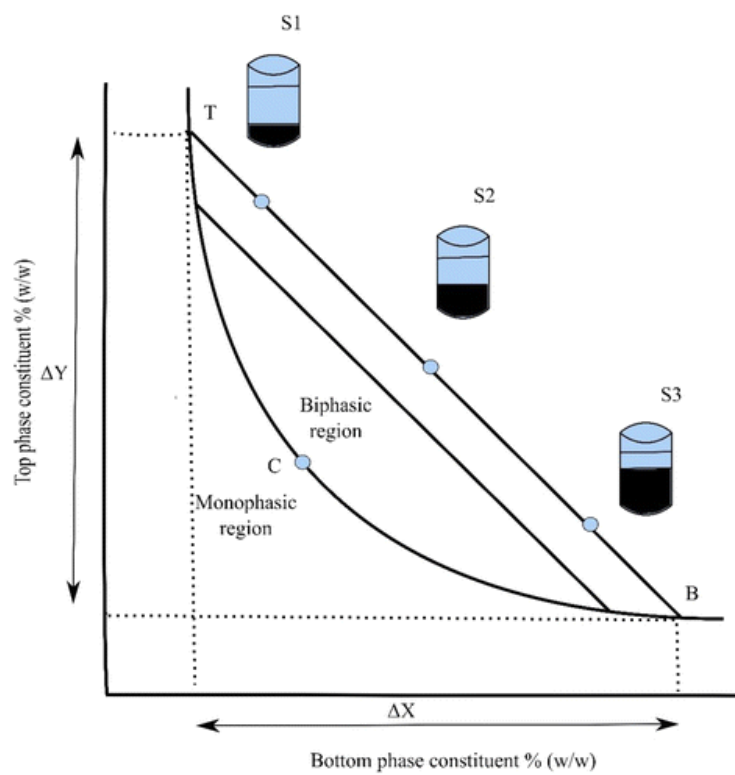


**Figure 1.1.** Schematic phase diagram of an ATPS showing phase separation above the binodal [47]



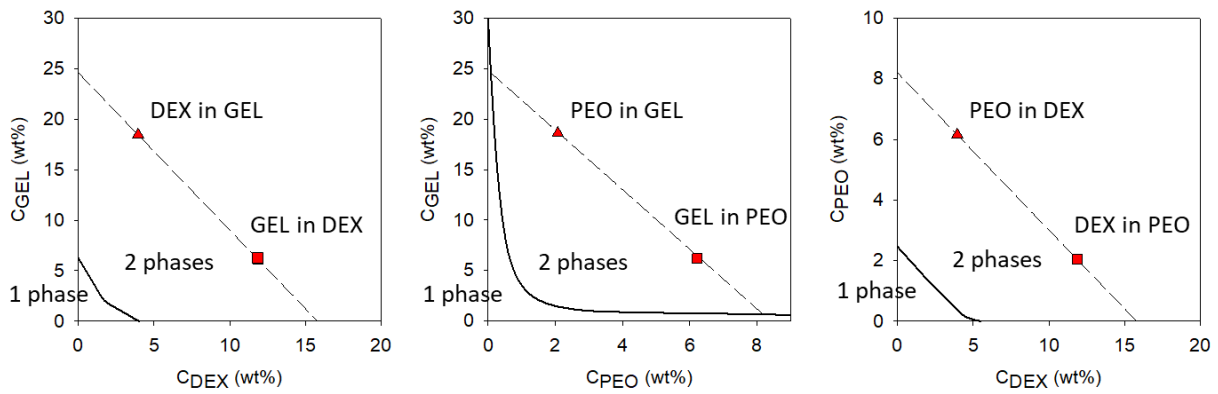


**Figure 1.2.** Phase diagram of the GEL-DEX (left), GEL-PEO (center) and DEX-PEO (right). The solid line represents the binodal. The triangles and squares show the compositions of the emulsions of two volume fractions that situate on the same tie lines indicated by the dashed lines [10, 46]

### 1.1.2. Properties of Water-in-Water emulsions

An important property of the W/W emulsion is its very small interfacial tension that is two to three orders of magnitude lower than that of O/W emulsions [5, 42, 48]. The interfacial tension of W/W emulsion can be measured by different methods, such as spinning drop tensiometers [5], analysis of the shape relaxation of individual droplets after cessation of shear [48] or optical micrographs of capillary rise at a vertical wall [49]. Forciniti et al. [5] have measured the interfacial tension of over sixty PEO-DEX combinations varying molecular weights, concentrations and temperatures. The obtained values range from 1 to 300  $\mu\text{N}\cdot\text{m}^{-1}$ . While the influence of temperature is not so obvious, interfacial tension is more affected by molecular weight and polymer concentration. Balakrishnan et al. investigated mixtures of PEO ( $M_w = 5 \times 10^5$  g/mol) and DEX ( $2 \times 10^5$  g/mol), showing that the interfacial tension decreases with decreasing TLL. The relationship between the interfacial tensions ( $\gamma$ ) and TLL was found to follow a power law :  $\gamma = \text{TLL}^{3.9}$  [48].

Another typical feature of W/W emulsion is the interface thickness. Tromp et al. addressed the concentration profile of polymers across the GEL-DEX interface, estimating its width to be in the range of 8–20 nm [50]. This indicates a significant larger than the thickness

of oil-water interfaces, which is usually around 1–2 nm as noted by Rowlinson [51]. The concentration of proteins is minimum at the middle of the interface, see **Figure 1.3**.

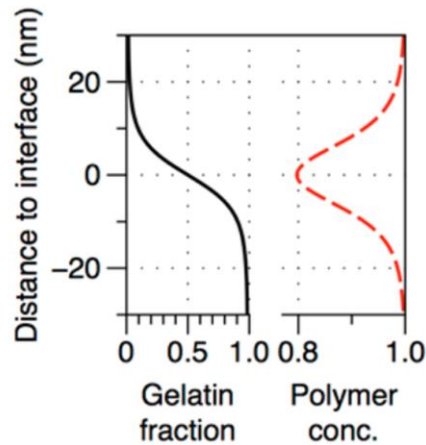


**Figure 1.3.** Gelatin fraction and polymer concentration at the interface [49]

### 1.1.3. Aqueous multi-phase system

When more than two types of incompatible polymers are mixed, aqueous multi-phase systems (AMPS) are formed containing droplets of different phases dispersed together in a common continuous phase. Droplets of different phases do not coalesce, but in most cases stick to each other, forming Janus-like structure [52]. This finding opens the application in the multi-compartmentalization [53]. Water-soluble ingredients can partition preferentially to different compartments in AMPS [3]. The contact between these droplets can induce localized reactions.

If we evaluate the three-phase case containing two immiscible phase droplets A and B in a common continuous phase C, the droplets of two dispersed phases A and B can associate to each other if the interfacial tensions of the three interfaces ( $\gamma_{AB}$ ,  $\gamma_{AC}$ ,  $\gamma_{BC}$ ) is smaller than the sum of the interfacial tensions of the other two interfaces. The contact angle that each phase makes with the two other phases is determined by the ratios of the interfacial tensions between the different phases [54]. Measurements of the contact angles allow calculating the interfacial tensions between the different phases relative to each other:

$$\gamma_{AB}/\gamma_{AC} = \sin(\theta_C)/\sin(\theta_B)$$

$$\gamma_{AB}/\gamma_{BC} = \sin(\theta_C)/\sin(\theta_A)$$

$$\gamma_{BC}/\gamma_{AC} = \sin(\theta_A)/\sin(\theta_B)$$

Nicolai et al. have measured the relative interfacial tension between 15 different pairs of aqueous polymer phases by directly determining the contact angles from images of confocal laser scanning microscopy (CLSM), see **Figure 1.4** [26].

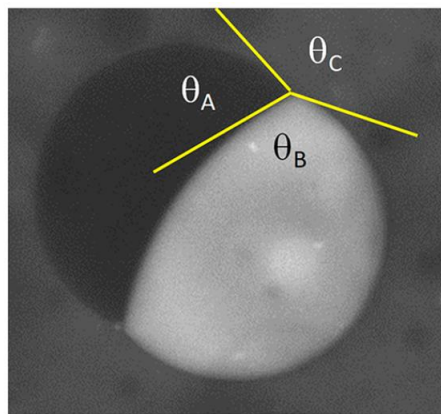


**Figure 1.4.** CLSM image of a three-phase system of a DEX droplet (A) associated with a amylopectin droplet (B) in a continuous PEO phase (C). The angles formed by each phase with the other phases is indicated in the figure [26]

Recently, Meng et al. investigated the morphology of the aqueous three-phase system GEL/DEX/PEO that can be varied by varying the pH [46]. An interesting feature of this emulsion is that the interfacial tension between the GEL and PEO phase decreases sharply at  $\text{pH} < 5$  and  $\text{pH} > 9$  when GEL becomes more strongly positively and negatively charged, respectively. Below and above a critical low and high pH, respectively, all GEL mixed with the PEO, whereas close to the critical values the GEL phase completely wetted the DEX droplets.

## 1.2. Stabilization of Water-in-Water emulsions

### 1.2.1. Stabilization by the adsorption of particles

Small sized surfactants do not adsorb at the interface of W/W emulsions due to the large interfacial thickness and very low interfacial tension. Therefore, they are inappropriate to stabilize W/W emulsions, but particles of sufficiently large size may in some cases spontaneously adsorb at the interface leading to an effective stability of W/W emulsions [6-8].

The driving force for the adsorption is the reduction of the free energy ( $\Delta G$ ) by decreasing the interfacial area when a particle is located at the interface [55]. For a spherical particle, the free energy depends on the particle size ( $R$ ), interfacial tension between two phases ( $\gamma_{AB}$ ) and the contact angle of the particle with the interface ( $\theta$ ):

$$\Delta G = -\pi R^2 \gamma_{AB} (1 - |\cos \theta|)^2$$

The contact angle ( $\theta$ ) depends on the difference between the interfacial tension of the particles with phase A ( $\gamma_{PA}$ ) and phase B ( $\gamma_{PB}$ ) compared to  $\gamma_{AB}$ :

$$\cos(\theta) = \frac{(\gamma_{PA} - \gamma_{PB})}{\gamma_{AB}}$$

The free energy can only be reduced when  $\gamma_{AB} > |\gamma_{PA} - \gamma_{PB}|$ , so that particles can spontaneously adsorb at the interface. The change in free energy will be at its maximum when  $\theta = 90^\circ$ . This suggests that tuning the interfacial tension balance of particles can enhance the stability of the emulsion.

Despite the very low interfacial tension, the  $\Delta G$  is sufficient to overcome the thermal energy ( $kT$ ) provided that the particle size is large enough. Balakrishnan et al. have used latex particles with size around 1  $\mu\text{m}$  can be trapped at the interface of PEO and DEX and did not spontaneously desorb from it without shear forces [48]. However, it was also demonstrated that adsorption of particles cannot guarantee the stability of the corresponding emulsion [48, 56].

The surface coverage is not a sufficient argument to explain emulsion stability, since some particles do not fully cover the droplet surface, but nevertheless stabilize emulsions [11]. It suggests that the interaction between the particles at the interface plays an important role.

Different types of particles have been studied for their ability to stabilize W/W emulsions, such as protein particles [11], fat particles [16], mineral particles [17], rod-like cellulose nanocrystals [18], and thermosensitive microgels [10]. Furthermore, there are other methods to modulate the properties of particles at the W/W interface, such as modifying the surface [9, 57], the morphology [58-60], the electrostatic interaction [61] or crosslinking [62, 63].

#### *1.2.1.1. Particle size*

In order to adsorb at the W/W interface, the particle should have a minimum size. Nguyen et al. found that the native protein with a radius of about 3 nm cannot enter the interface and had no noticeable stabilization [11]. However, forming microgels by heating the protein solution can increase the size and enhance the stability of PEO-DEX emulsion. The microgels were observed to adsorb spontaneously at the interface and inhibited coalescence. The stability against coalescence depended on the concentration and the size of the microgels. The droplet size was smallest when the microgels had a radius of about 100 nm. The recommended optimal particle size for stabilization was suggested to be 100 nm, as larger particles are unfavorable due to decreasing number of particles at the same concentration.

#### *1.2.1.2. Morphology*

Several shapes of particles have been shown to have an effect on the stabilization of W/W emulsions. Gonzalez et al. have tested protein fibrils, microgels, and fractal aggregates produced by heating solutions of protein under various conditions. At pH 7, the D/P emulsion is less stable than the P/D emulsions with all three types of particles. The fibrils were found to be more efficient than microgels at the same concentration, whereas fractals were the least

efficient. Meanwhile, D/P emulsion became more stable at pH 3, especially with fractals. P/D emulsions at pH 3 became less stable with fibrils and more stable with microgels and fractals. The partition of protein particles depends on pH that they prefer DEX at pH 7 and prefer PEO at pH 3, which can partially explain the difference in stability in two cases. The effect of stabilization depends on the morphology of the particles, on which phase is the continuous phase and on the pH [59].

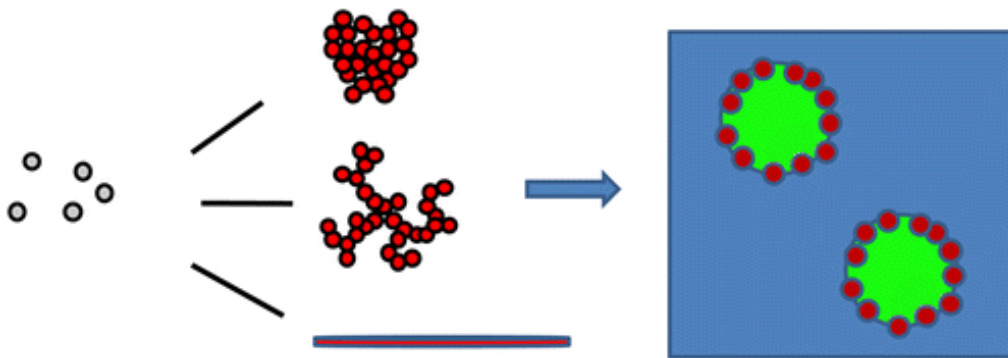


**Figure 1.5.** Protein of different morphologies to stabilize W/W emulsion [59]

Inam et al. have reported the stabilization effect of poly(lactide) platelets to PEO-DEX system. Larger platelets can give smaller droplet sizes and more stable emulsions than smaller platelets [60]. Ganley et al. also shown that Pullulan (PUL) and PEO system can be stabilized by montmorillonite platelets. The platelets can randomly adsorb at the interface and form robust layer around the droplets that strongly prevented the coalescence [58].

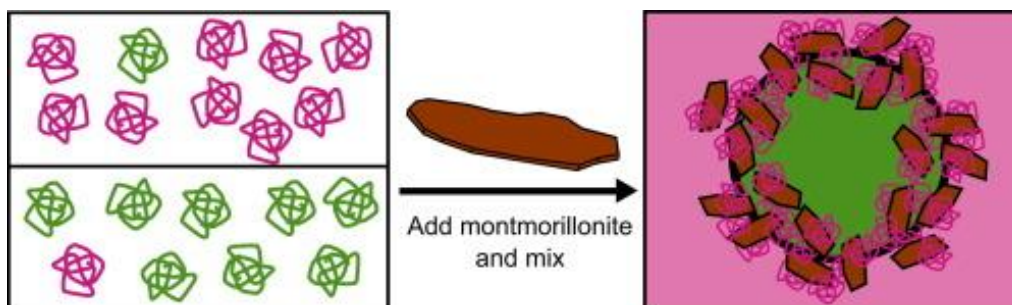


**Figure 1.6.** Stabilization of W/W emulsions using the montmorillonite platelets [58]

### 1.2.1.3. Modification of the particle surface

Modifying the surface properties of the particles is a potential strategy to modulate their adsorption and stabilization capacity. De Freitas et al. found that protein microgels could not stabilize the mixture of amylopectin (AMP) in xyloglucan (XG) at  $\text{pH} > 5.0$  because the microgels had a strong affinity for the AMP phase. However, at  $\text{pH} \leq 5$ , the adsorption of XG onto the surface of the microgel increases the affinity of the microgels for the XG phase and thus their adsorption to the interface and stabilization of the emulsion [9].

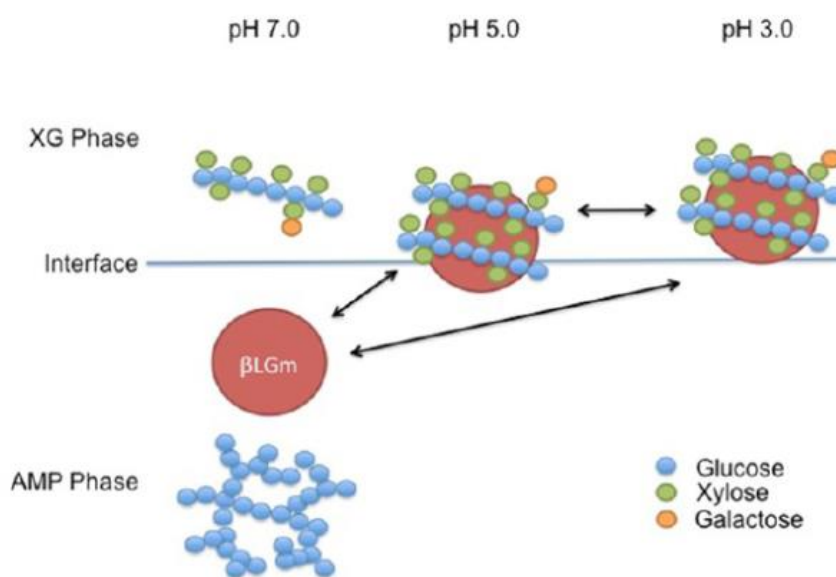


**Figure 1.7.** Schematic representation of interaction of protein microgels ( $\beta\text{LGm}$ ) with XG and its behavior at the interface at different pH [9]

Gonzalez et al. have covered the polystyrene latex particles with protein to stabilize emulsion of PEO and DEX. In the presence of protein, the preference of latex particles changed from PEO to DEX phase. The stability is improved by the high affinity of particles to the continuous phase [57].

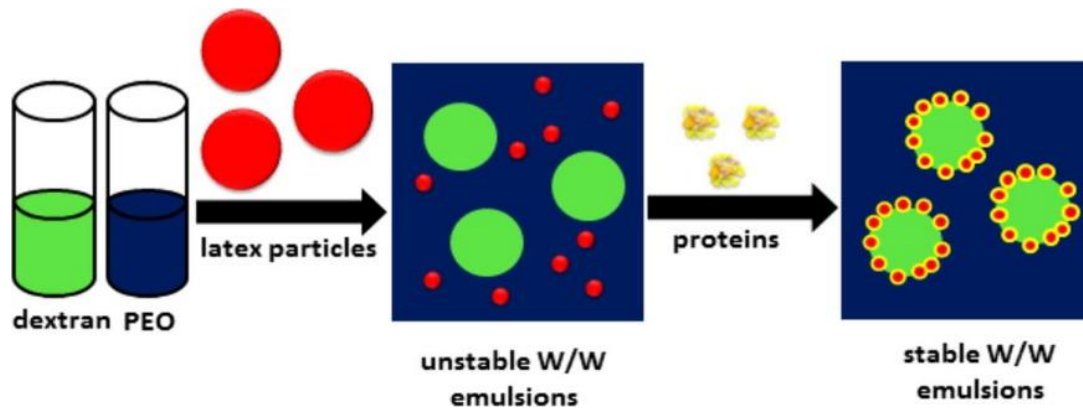


**Figure 1.8.** Stabilization of W/W emulsions by protein-coated latex particles [57]

#### 1.2.1.4. Electrostatic interaction

Nguyen et al. observed the influence of interactions between pH-sensitive microgels at the interface of PEO-DEX mixtures [61]. He noticed that the particles are preferentially situated at the interface and stabilized the emulsions at between 7 and 7,5. However, the destabilization was faster at a lower or higher pH. The interaction between two polymers could be modulated by pH and ionic strength, consequently causing changes in the phase behavior. The addition of 10 mM NaCl led to destabilize the emulsions in one day, whereas they remained stable for more than a week without the addition of salt. Indeed, the addition of salt screens the repulsive interactions of these polyelectrolytes. The interactions between microgels at the interface and between microgels with both phases must play an importance role in stabilization.

#### 1.2.1.5. Thermosensitivity

The effectiveness of particles can be temperature-dependent if they contain heat-sensitive components in their structure. Merland et al. have studied microgels of pNIPAM derivatives, which shrink/swell depending on the temperature [10]. Since pNIPAM has a strong affinity for PEO phase, the adsorption of microgels to the interface of PEO and DEX can be improved by adding a fraction of DEX to microgels, giving it a bishydrophilic character. These microgels can stabilize the D/P emulsion at room temperature and switch to stabilizing the P/D emulsion



when heated above the Volume Phase Transition Temperature (VPTT) of pNIPAM. The temperature effect was not related to a change in the partitioning of the particles between the phases since that did not change when the emulsions were prepared at room temperature and then heated above the VPTT. Thus, the interaction of microgels at the interface during heating has an important role on the stability inversion.

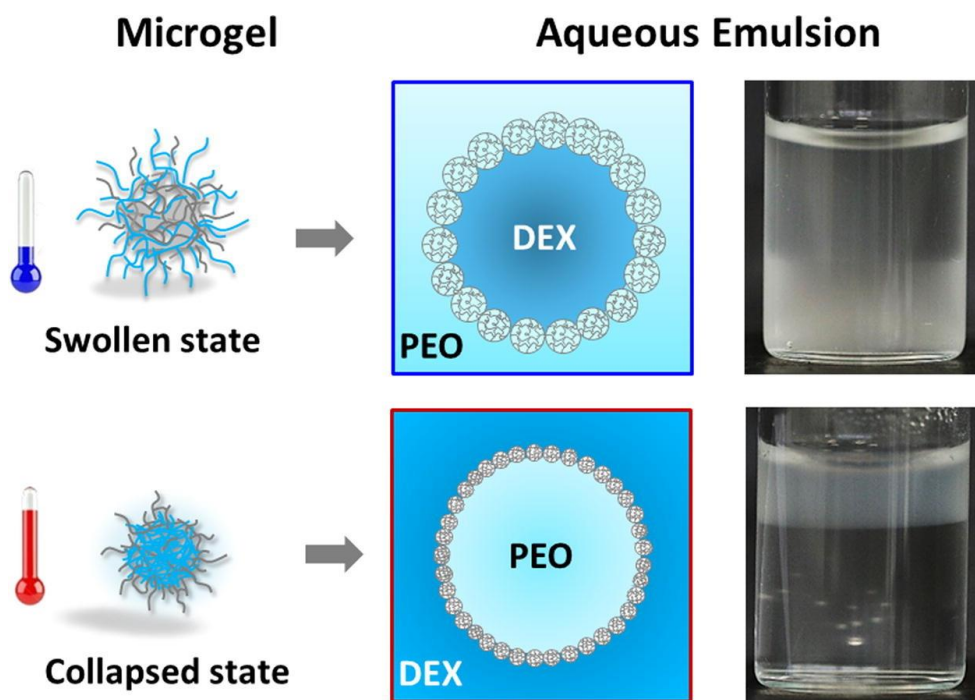


**Figure 1.9.** Thermoresponsiveness of pNIPAM-DEX microgels and its effect on the stability

#### 1.2.1.6. Crosslinking

Another approach to enhance stability is by cross-linking the particles. Zhang et al. used polydopamine nanoparticles as stabilizers for DEX and PEO emulsions [63]. Cross-linking these particles strongly protected emulsion droplets against dilution or surfactant addition. Moutkane et al. have covalently crosslinked the adsorbed protein microgels at the surface of PUL droplets dispersed in AMP by adding the enzyme transglutaminase [62]. The formed microcapsules resisted against dilution for extended times, increasing the pH and heating. To avoid the deformation of the microcapsules, they can be introduced in the DEX phase surrounding PEO droplets dispersed in AMP, see **Figure 1.10**.

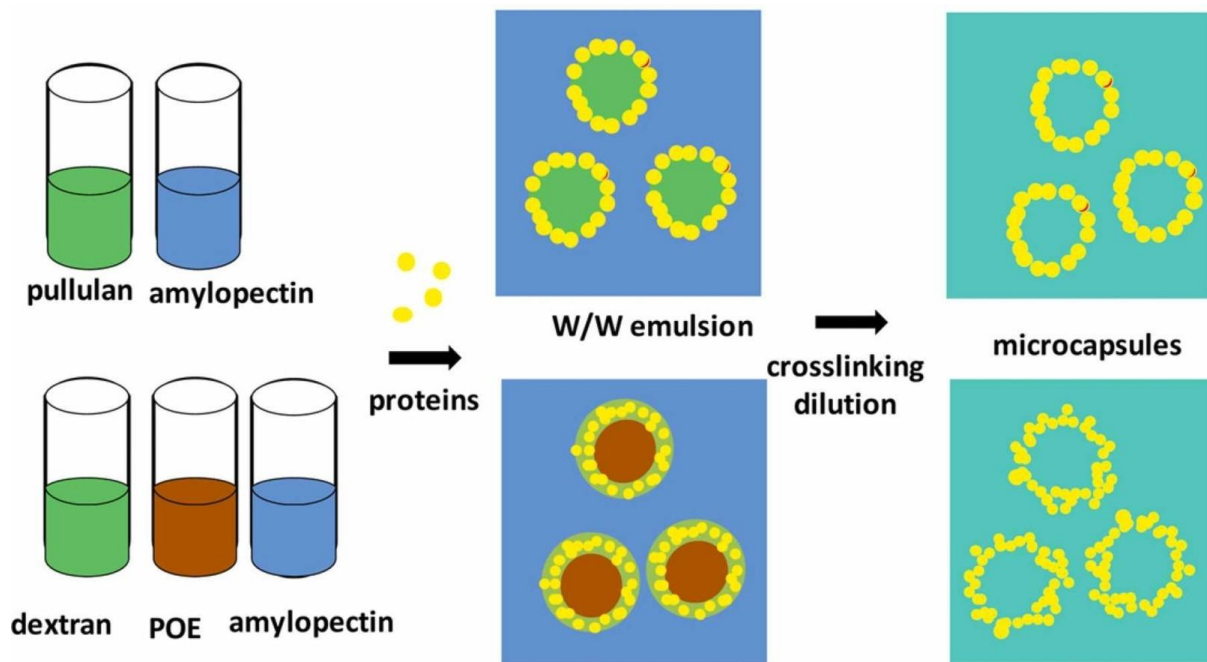


**Figure 1.10.** Formation of microcapsules by crosslinking of microgels to stabilize aqueous droplets in W/W emulsion [62]

### 1.2.2. Stabilization by self-assemble systems

#### 1.2.2.1. Stabilization by block copolymers

Self-assembled block copolymers have also been reported to stabilize W/W emulsions. Ossenbach et al. early described the stabilization of W/W emulsions containing polyvinylpyridinium chloride (pVPC) and PEO with diblock pVPC–PEO copolymers [64]. More recently, Buzza et al. have shown that triblock copolymers with  $P_p$ – $B_b$ – $D_d$  structure can stabilize emulsions of PEO and DEX [13]. Triblock copolymers were formed of two different end blocks, each end preferring one of the two different phases (block P prefers PEO and block D prefers DEX), connected by a central hydrophobic block (block B). A large range of copolymers with different block lengths were tested. Emulsions were better stabilized when blocks B and D were larger. Block P did not show a significant effect of stabilization and the most of triblock structures were less efficient than the B–D diblock. Buzza et al. proposed that the block copolymers form a polymersome-like structure on the surface with each of the two terminal blocks oriented to its preferred phase, see **Figure 1.11**. However, this structure

remains uncertain because it cannot explain why diblocks were more effective than triblocks. As diblock copolymers in solution form a hydrophobic core with a hydrophilic corona, another proposed hypothesis is that the triblock copolymer also formed polymeric micelles that adsorb to the interface and stabilize emulsions just as other types of particles [8].

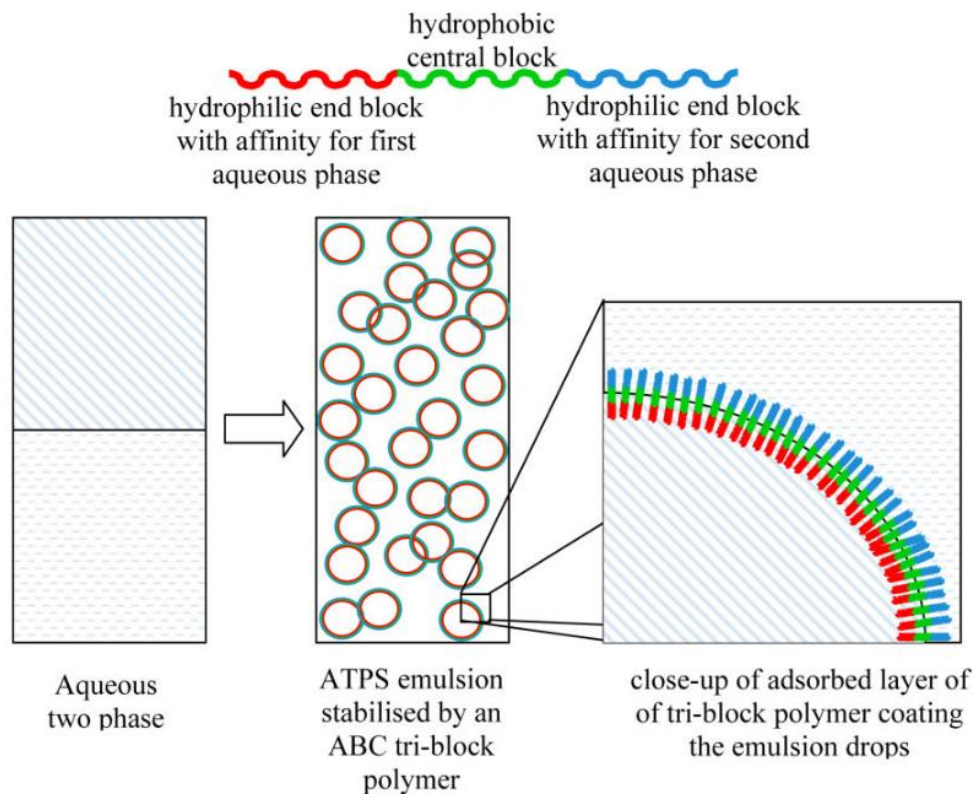


**Figure 1.11.** Illustration of triblock copolymers to stabilize W/W emulsions [13]

#### 1.2.2.2. Stabilization by polyelectrolytes

A potential technique for stabilizing W/W emulsions is forming ionic complexation at the interface. Typically, two oppositely charged polyelectrolytes were added to neutral all-aqueous phase separations [65, 66]. Each polyelectrolyte is dissolved into each phase. When two polyelectrolytes meet each other at the interface of two phases, a complexation can be formed and stabilized the emulsion, see **Figure 1.12**.

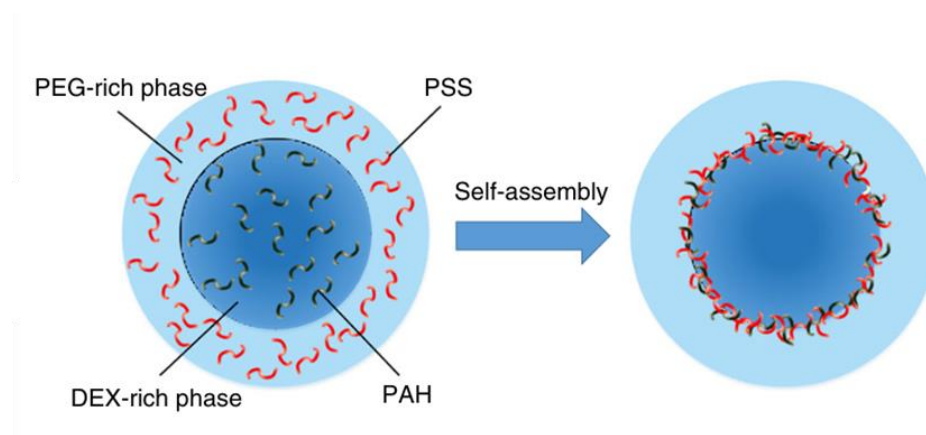


**Figure 1.12.** Schematic of the formation of ionic complexation at water-water interface [65]

Another model is suggested by Tromp et al. to use a polyelectrolyte that has the same chemical properties as one phase and has an opposite charge to the other phase. The studied emulsion consists of one phase rich in DEX and one phase rich in GEL that is positively charged. The fluorescently labeled DEX (FITC-DEX) with a negative charge is added to stabilize the emulsion. The complexation between GEL and FITC-DEX at the interface is expected to cause interfacial gelation and steric or electrostatic repulsion of droplets in W/W emulsions, see **Figure 1.13**. This complexation can be resistant to high salt concentrations which is favorable for applications in the agri-food or pharmaceutical science [67].

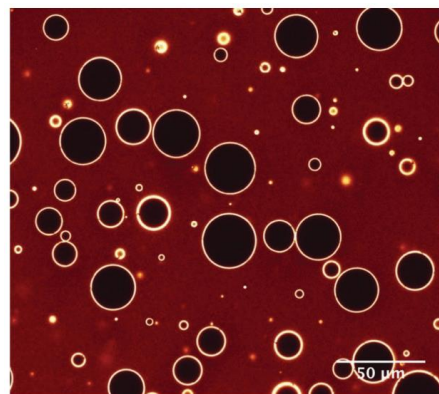


**Figure 1.13.** Confocal image of a DEX/GEL emulsion stabilized by complexation of GEL and FITC-DEX at neutral pH [67]

### 1.2.3. Stabilization by gelation of a third phase

Chen et al. have found that bovine gelatin (GEL B) can phase separate with guar and AMP when being cooling down below 25 °C. An accumulation of gelatin aggregates formed a continuous layer at the surface of the dispersed droplets. A full coverage can enhance the inhibition of coalescence between droplets [68]. Similar phenomena can be found in W/W emulsions formed by other combinations of three incompatible water-soluble macromolecules. Meng et al. have formed a three-phase system by mixing GEL B with DEX and PEO or AMP and XG [46]. The compatibility of GEL B and PEO can be tuned by the pH that changes the contact angles between the three phases. In a narrow range of pH, GEL B can wet completely the DEX droplets and formed a continuous layer around the droplets of the DEX phase. The thickness that can be varied by the concentration of GEL B. After cooling, gelatin microcapsules were formed and preserved stabilization against coalescence and dilution, see

**Figure 1.14.**

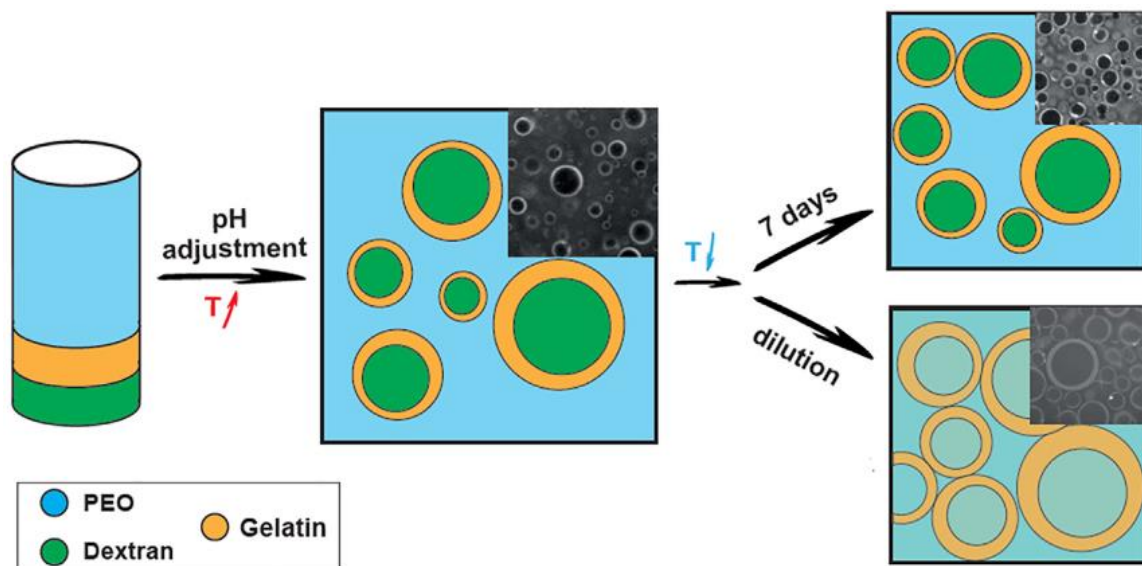


**Figure 1.14.** Schematic of formation of GEL B encapsulation to stabilize DEX-in-PEO emulsion [46]

#### 1.2.4. Stabilization of aqueous multi-phase system

Nicolai et al. have shown that certain AMPS can be stabilized by adding protein microgels as in binary systems [26]. The particles were tested in different pairs of aqueous polymer solutions and were able to adsorb to the interfaces of PEO/DEX, PEO/AMP, PEO/PUL and PEO/XG. For all other mixtures, the microgels preferred to remain within one of the phases. Three-phase systems can be formed by mixing two binary emulsions in a common continuous phase. Droplets of different dispersed phases can associate with each other upon contact. **Figure 1.15** shown the mixture of AMP and PEO droplets in the continuous phase of PUL. The associated droplets of AMP and PEO in PUL form a stable network for several days, even though AMP droplets are unstable without particles at the interface.

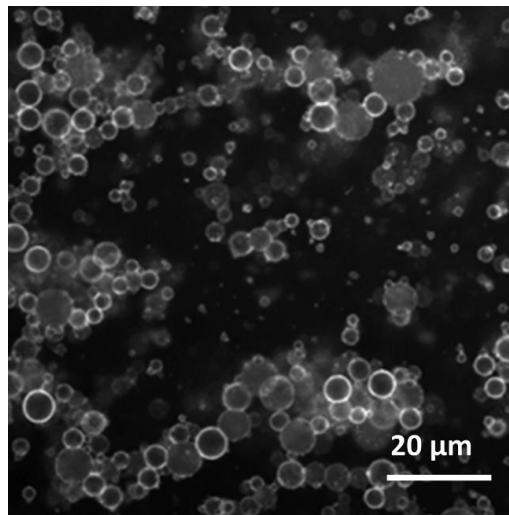


**Figure 1.15.** CLSM images of a network associated AMP and PEO droplets in a continuous PUL phase [26]



## **Chapter 2. Materials and Methods**

In this chapter, I will present the synthesis of different bishydrophilic microgels as well as the preparation of W/W emulsion used in this thesis. Additionally, the various characterization techniques employed to analyze these microgels and emulsions will be discussed.



|   |           |
|---|-----------|
| <b>2.1. Materials .....</b>             | <b>37</b> |
| 2.1.1. Bishydrophilic microgels .....   | 37        |
| 2.1.2. Protein microgels.....           | 39        |
| 2.1.3. Emulsion preparation .....       | 39        |
| <b>2.2. Methods .....</b>               | <b>40</b> |
| 2.2.1. Particle size measurement .....  | 40        |
| 2.2.2. Microstructure observation ..... | 41        |
| 2.2.3. Transmission measurement .....   | 42        |

## 2.1. Materials

### 2.1.1. Bis-hydrophilic microgels

A series of bis-hydrophilic microgels was synthesized by the Institute of Molecular Sciences (ISM) in Bordeaux according to the previously established methodology, consisting in the incorporation of DEX units as cross-linker in the pNIPAM microgel structure [10]. To this end, multifunctional polymerizable DEX were prepared by grafting methacrylate groups on the DEX chains, which were further copolymerized with NIPAM through a precipitation polymerization process.

**Figure 2.1** sketches the structure of the DEX macromers, with the assumption of homogeneous distribution of the methacrylate groups along the chains. Different parameters were modulated to investigate the role of the microgel structure and composition to stabilize W/W emulsions. In addition to adjusting the ratio of DEX to pNIPAM, the molecular weight ( $M_w$ ) of DEX and its degree of substitution by methacrylate (DS) were also considered. Finally, three different DEX chains were used:  $M_w = 6$  kDa and DS = 20;  $M_w = 6$  kDa, and DS = 12;  $M_w = 40$  kDa and DS = 12. The different microgels studied are listed in **Table 2.1**.

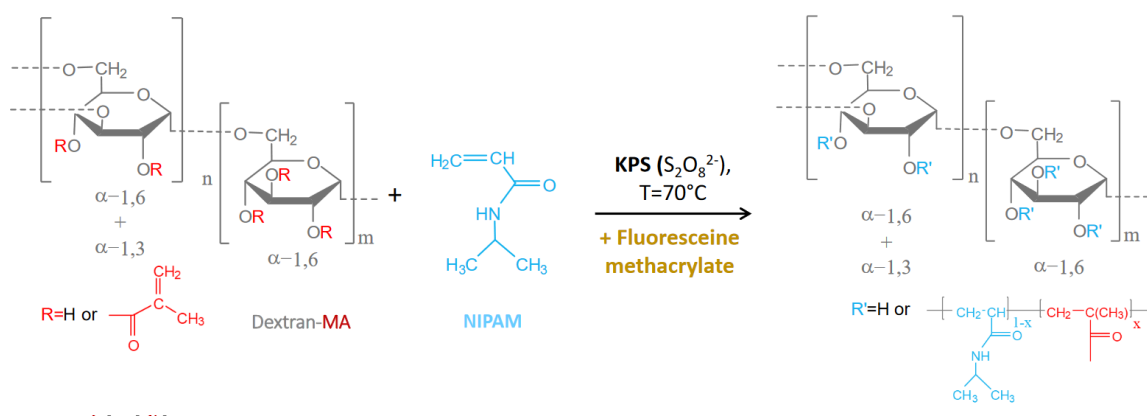


**Figure 2.1.** Scheme of the microgel synthesis and representation of the various DEX macromers

**Table 2.1.** Summary of the microgel composition

| Mw of DEX (kDa) | DS* (mol%) | Weight fraction DEX (wt%) |
|-----------------|------------|---------------------------|
| 6               | 20         | 27                        |
| 6               | 20         | 43                        |
| 6               | 12         | 27                        |
| 6               | 12         | 43                        |
| 6               | 12         | 53                        |
| 6               | 12         | 60                        |
| 40              | 12         | 27                        |
| 40              | 12         | 43                        |

$$*DS \text{ (mol\%)} = \frac{\text{number of MA units}}{\text{number of monomer units in DEX chain}} \times 100$$

Charge was introduced into bishydrophilic microgels by replacing a fraction of NIPAM with acrylic acid (AA) during the synthesis, see **Figure 2.2**. The corresponding neutral microgels that were chosen have a DEX with  $M_w$  of 6 kDa, with  $DS = 12$ . The weight fraction of DEX in the microgel synthesis was 27 wt%. Microgels with 14 mol% NIPAM units replaced by AA units ( $F_{AA} = 14$  mol%) were studied in most detail, but microgels with 5 mol% and 29 mol% AA units were also investigated. For the sake of simplicity, the microgels without AA will be called “neutral” and the ones with AA will be called “charged” microgels whatever the pH, although most AA units are neutral at pH 3.

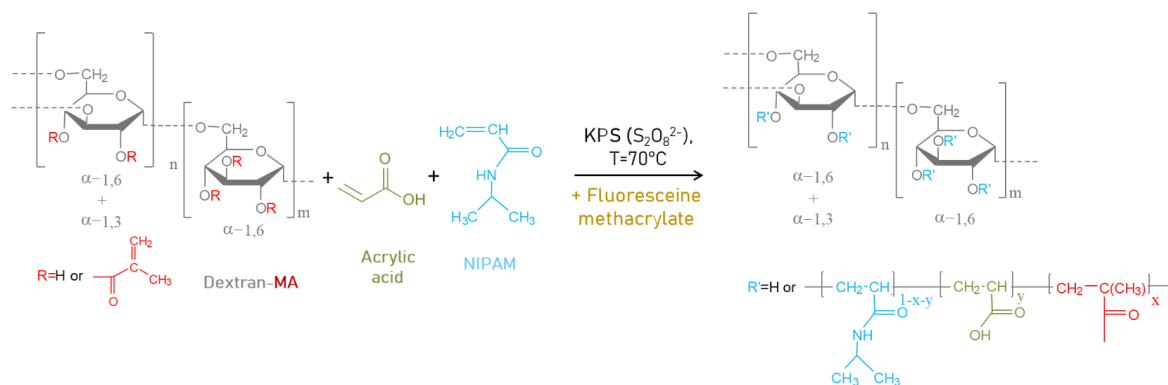


**Figure 2.2.** Scheme of the synthesis of charged microgels

### 2.1.2. Protein microgels

Whey protein isolate (WPI) was purchased from Davisco Foods 167 International, Inc. (Le Sueur, MN, USA). A solution of WPI (4 wt%) was adjusted to pH 5.9 and heated overnight at 80 °C to obtain protein microgels. The protein microgels were characterized as described in detail elsewhere [69]. The protein microgels had a hydrodynamic diameter of 350 nm and a molar mass of  $4 \times 10^7$  g.mol<sup>-1</sup>.

### 2.1.3. Emulsion preparation

#### 2.1.3.1. Biphasic emulsions preparation

DEX (Mw = 4.5-6.5x10<sup>5</sup> g/mol), PEO (Mw = 2x10<sup>5</sup> g/mol) and fish gelatin (GEL) were purchased from Sigma-Aldrich.

Aqueous stock solutions of GEL, DEX and PEO were prepared at 30 wt%, 30 wt% and 15 wt%, respectively, by dissolving the powders in ultrapure water (MilliQ) and stirring for 24 hours. The PEO powder contained a small number of silica particles that was removed by centrifugation of the PEO solutions at 5x10<sup>4</sup> g for 4 h. The phase diagrams of the DEX–PEO, GEL–PEO and GEL–DEX systems used here have already been reported and are reproduced as **Figure 1.2** in the **session 1.1**. Emulsions containing either DEX dispersed in PEO (D/P) or

vice versa (P/D) were formed with a dispersed phase volume fraction of 25%. The emulsions were situated on the same tie-line with one phase containing 8.2 wt% PEO and the other 15.8 wt% DEX with negligible amounts of the other polymer. GEL–DEX (G/D, D/G) and GEL–PEO (P/G, G/P) emulsions with 25% volume fraction the dispersed phase were prepared in the same manner by mixing the required amounts of the stock solutions with water, the GEL rich phases contained 24.6 wt%. No effect of the order of mixing or the strength and duration of vortexing was found. Neutral or charged bishydrophilic microgels were added at a concentration of 0.05 wt%. Protein microgels was fixed at 0.2 wt%.

### *2.1.3.2. Multiphase systems preparation*

The three-phase system with the ratio GEL/DEX/PEO = 12.5/12.5/75 was formed by mixing equal amount of two emulsions G/P (25/75) and D/P (25/75) either gently by bringing them in contact on a microscope slide or vigorously using a vortex mixer.

## **2.2. Methods**

### *2.2.1. Particle size measurement*

The hydrodynamic diameter of the microgels was determined by dynamic light scattering (DLS) using an ALV-5004 correlator in combination with an ALV-CGS3 goniometer (ALV-Langen) [70]. The light source is a He-Ne laser with a wavelength of 632.8 nm. Measurements were made as a function of the scattering wave vector ( $q = (4\pi n/\lambda) \cdot \sin(\theta/2)$ ), where  $n$  is the refractive index of the solution and  $\theta$  is the scattering angle between 20° and 150°. The temperature was controlled by a thermostated bath. The measured intensity autocorrelation functions could be fitted to a single relaxation mode with an average relaxation time ( $\tau$ ) that was used to calculate the translational diffusion coefficient:  $D = 1/(\tau \cdot q^2)$  of the microgels. The average

hydrodynamic diameter ( $d_h$ ) was determined from  $D$  extrapolated to  $q=0$  ( $D_0$ ) using the Stokes-Einstein relation:  $d_h = kT/(3\pi\eta D_0)$ .

Measurements were done at several concentrations of microgels to determine the effect of interactions, which was important for the highly charged microgels in water without added salt. It was found that in this case the microgels needed to be diluted down to 0.005 wt% in order to be able to neglect interactions. All suspensions were filtered through a 0.45  $\mu\text{m}$  pore size filters.

### *2.2.2. Microstructure observation*

A confocal microscope Zeiss LSM 800 (Carl Zeiss Microscopy GmbH, Germany) was used with water immersion objectives (X25 and X63) to image the emulsion morphology.

The bishydrophilic microgels were covalently labeled with the fluorescein isothiocyanate (FITC). A 488 nm wavelength laser was used to excite FITC and the emitted light has a maximum at 517 nm. The protein microgels was labeled with 0.05 ppm of Rhodamin B (RhoB), which was excited at 561 nm and had a maximum emission detected at 573 nm.

For observation, the samples were inserted between slides and coverslips and sealed using a double-sided sticker. The sealed slides were stored vertically in a holder and then observed horizontally at different positions to probe the effects of creaming or sedimentation. The morphology of emulsions was obtained by taking different images along the z-axis from the middle to the surface of the droplets.

A device called RheOptiCAD® was used to control the temperature of the samples during observation with the confocal microscopy (CAD Instruments, Les Essarts-le-Roi, France) [71]. In order to avoid strong temperature gradients, an air objective (X50) was used for observation at high temperatures.

The partition of the microgels between the two phases and at the interface was quantified using fluorescence intensity profiles across droplets, see **Figure 2.3**.

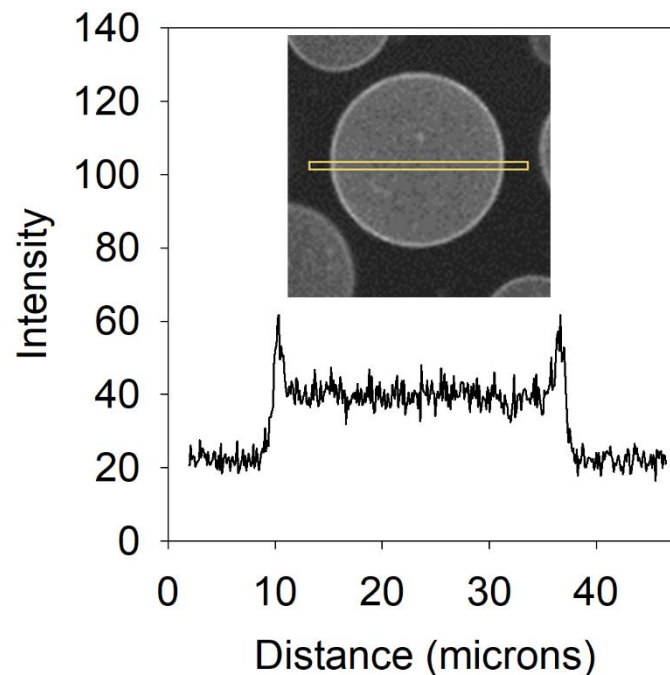


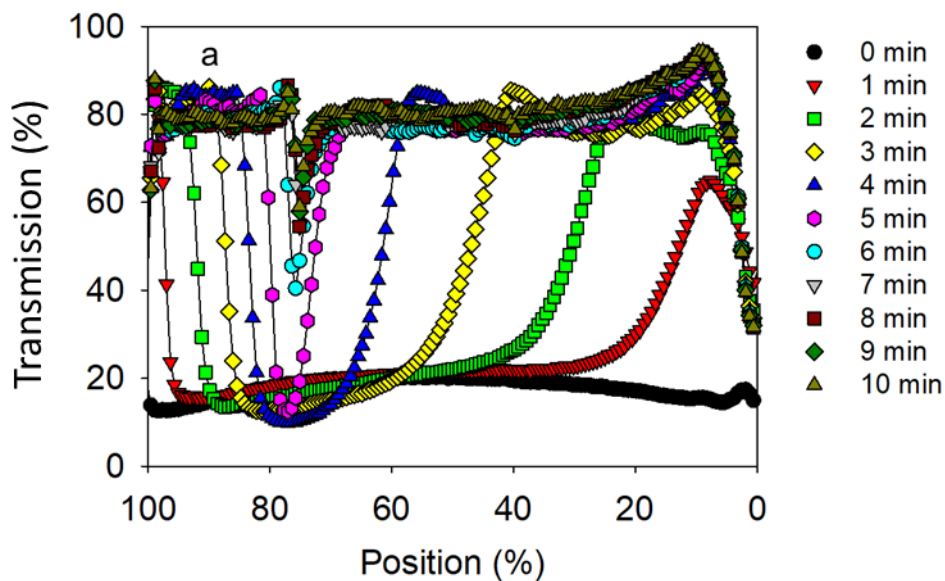
**Figure 2.3.** Example of an intensity profile along a dispersed droplet taken from the image shown in the graph that was used to determine the partition of the microgels between the phases and at the interface.

### 2.2.3. Transmission measurement

The emulsion stability was analyzed by measuring the transmission profile of the samples along the length of the tubes as a function of time. In order to speed up creaming/sedimentation and destabilization, measurements were done under centrifugation (LUMiSizer®, LUM GmbH, Berlin, Germany), the operation of which is explained in detail elsewhere [72, 73]. Its application to study the stability of W/W emulsions was discussed in ref [74]. The tubes are positioned horizontally in the rotor of a centrifuge. A light beam passes through the tubes during centrifugation and the transmitted intensity is measured along the length of the tube. The device allows temperature control between 4 and 60°C. LUMiReader®, a variant of

LUMiSizer®, was also used. It offers the same functions as LUMiSizer® but without centrifugation, thereby observing instability “in real time”, i.e. at 1g.

**Figure 2.4a** and b show examples of transmission profiles during centrifugation at 470g for D/P and P/D emulsions that are not stabilized by microgels. Notice that the centrifugal force is here from the left to the right, which corresponds to from the top (100%) to the bottom (0%) of the sample under gravity. The transmission increased both at the top and the bottom due to the formation of a homogeneous transparent phase of PEO and DEX, respectively. This can be explained by the sedimentation and coalescence of the DEX phase droplets in the D/P emulsion and the creaming of the PEO phase droplets in the P/D emulsion. The sedimentation/creaming front is not sharp because the droplet size is dispersed. The droplets coalesce and form a continuous layer of which the height increases with time until the equilibrium value of 25% of the total height is reached after 10 min. A similar development of the transmission profile was observed for a D/P emulsion in the presence of the microgels, see **Figure 2.4c**, but the time evolution was much slower, and equilibrium had not yet been reached after 10 min, suggesting that the microgels retard droplet coalescence.





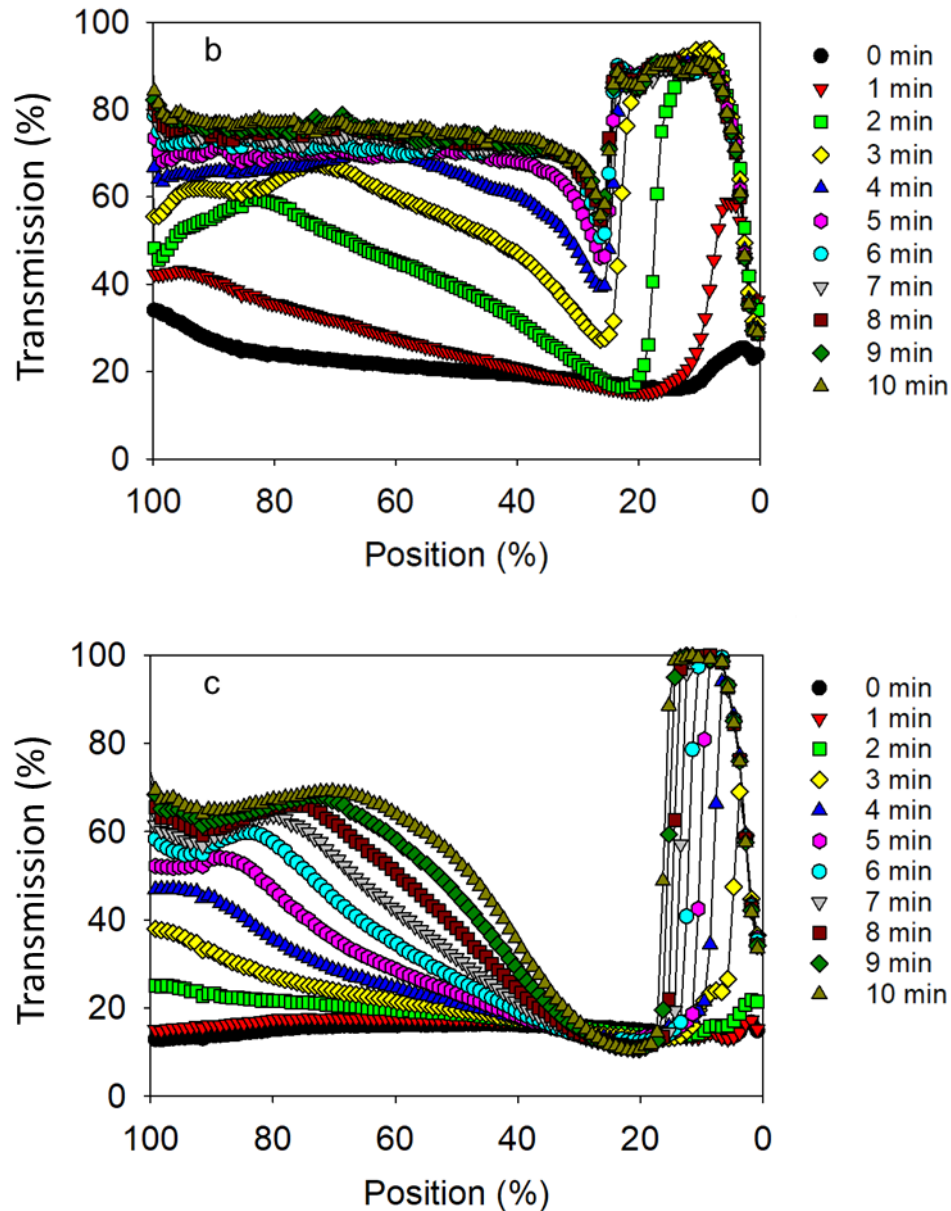


**Figure 2.4.** Evolution of the transmission profile of a P/D (a) and a D/P (b) emulsion without microgels as well as a D/P emulsion with neutral microgels (c).

The rate at which the droplets coalesce into a continuous phase can be quantified by measuring as a function of time the transmission of the section of the sample where the dispersed phase forms a continuous phase at equilibrium (0-25% for D/P and 75-100 % for P/D). An example is shown in **Figure 2.5** for a P/D emulsion without microgels. The transmission gradually increases until it reaches a plateau around 85%, which corresponds to

the value for the homogeneous phase of PEO. A characteristic stabilization time ( $t_c$ ) is defined as the time at which 50% of the transmission change is reached.

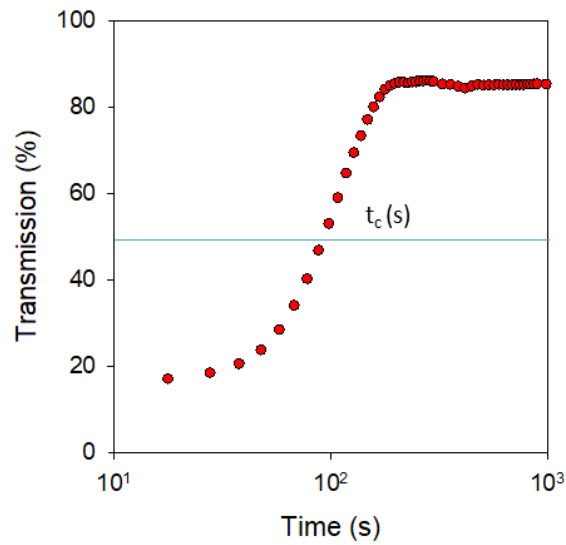


**Figure 2.5.** Evolution of the transmission of the dispersed phase section as a function of time for a P/D emulsion without microgels



## **Chapter 3. Stabilization of Water-in-Water emulsion by varying the composition of bishydrophilic microgels**

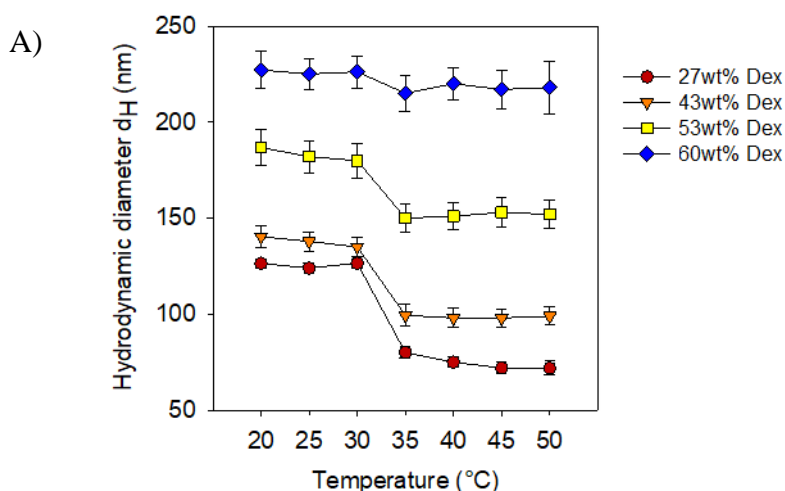
The aim of this study is to evaluate the effect of microgel composition on the stabilization of W/W emulsions. To do this, different microgels were synthesized varying the fraction of DEX from 27 wt% to 60 wt% and used as stabilizers of droplets of the DEX phase dispersed in the PEO phase (D/P) or vice-versa (P/D) at room temperature and at 50 °C. We will first evaluate the deswelling of particle size at high temperature by DLS. Then the structure of the emulsion was determined by CLSM, from which the particle distribution between the two phases was obtained. Finally, the stability of the emulsion was assessed using a LUMiSizer<sup>®</sup>. The obtained results have been published in the *Journal of Colloid and Interface Science*, 2024, 653, 581-593 [75].

|   |           |
|---|-----------|
| <b>1. Swelling behavior of microgels in suspension.....</b>                             | <b>49</b> |
| <b>2. Effect of the microgel composition on Water-in-Water emulsion stability .....</b> | <b>50</b> |
| 2.1. Stability of Water-in-Water emulsions at low temperature .....                     | 50        |
| 2.2. Effect of temperature on emulsion stability .....                                  | 62        |
| <b>Conclusion.....</b>  | <b>69</b> |

### 3.1. Swelling behavior of microgels in suspension

The apparent hydrodynamic diameter of the microgels containing DEX at  $M_w = 6$  kDa and  $DS = 12$  was measured by DLS at various temperatures (**Figure 3.1A**), since this allows exploring the largest range of DEX content. All of them were thermoresponsive and present a volume phase transition temperature (VPTT), except the one with the highest amount of DEX, for which the VPTT is almost invisible. As already pointed out for low DEX contents [10], the VPTT was that of pNIPAM and did not depend on the DEX content, although DEX is hydrophilic. Usually, the copolymerization of NIPAM with hydrophilic monomers leads to an increase of the VPTT [76], except when the the pNIPAM blocks and the hydrophilic ones are spatially separated [19, 77]. This observation implies that DEX and pNIPAM blocks belong to separated domains, or at least that the pNIPAM blocks have a sufficient length to keep the same transition temperature.

The effect of DEX content on the swelling of the particles is also shown in the **Figure 3.1B**. The swelling ratio is defined as the cubic ratio between the diameter in the swollen state and that in the most collapsed state. As expected, the swelling ratio progressively decreases, when the amount of DEX increases.



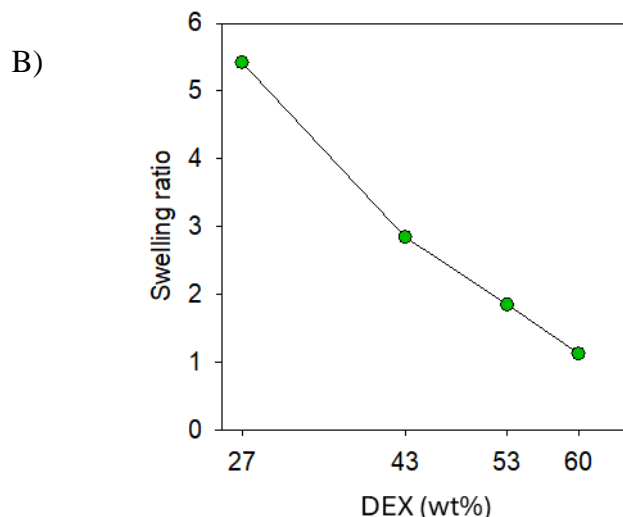


**Figure 3.1.** Behavior of the bishydrophilic microgels (DEX at  $M_w = 6$  kDa and  $DS = 12$ ) in aqueous suspension: A) Hydrodynamic diameter as a function temperature, B) Influence of DEX content on the swelling ratio of the microgels.

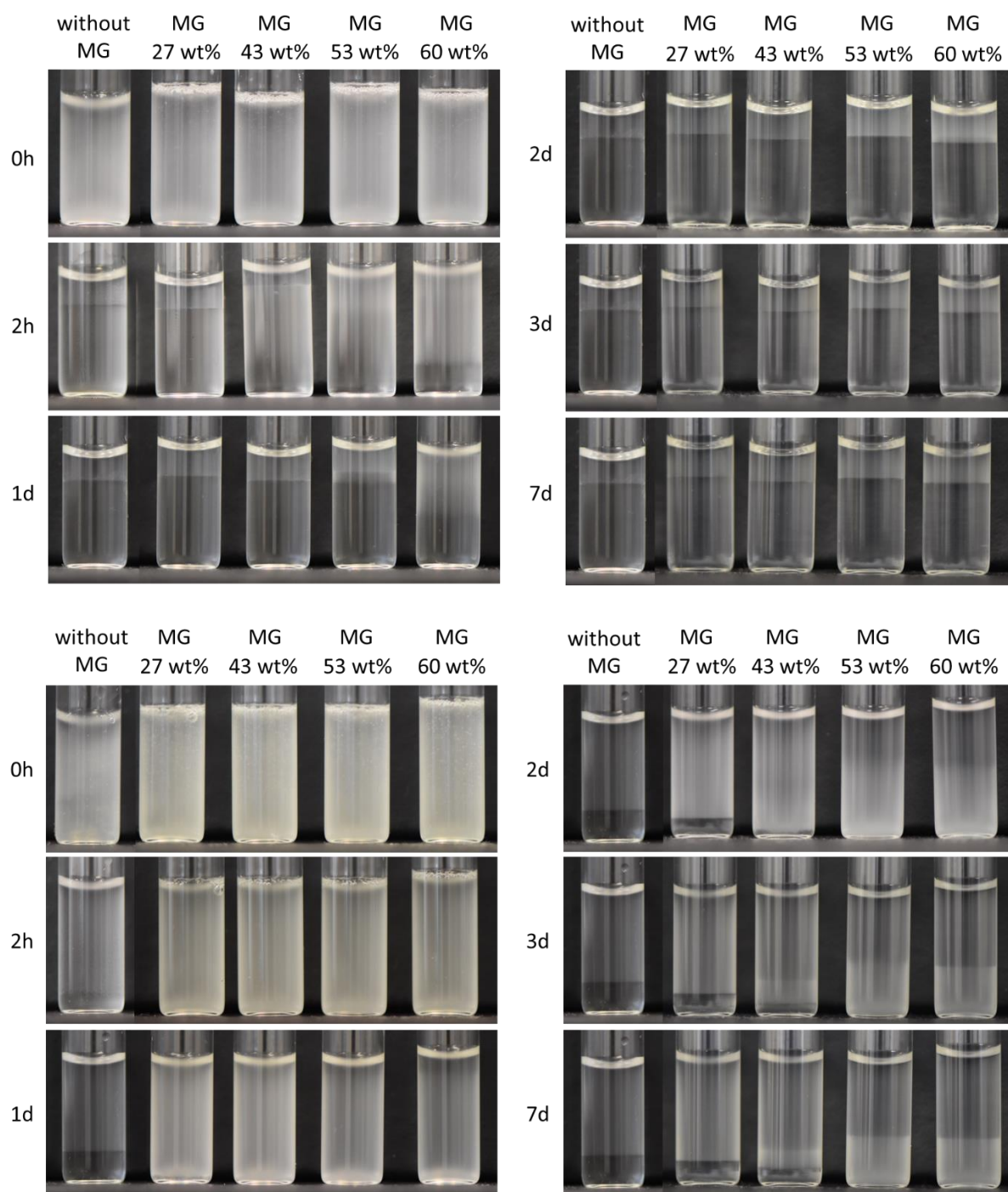
### 3.2. Effect of the microgel composition on Water-in-Water emulsion stability

#### 3.2.1. Stability of Water-in-Water emulsions at low temperature

The stability of W/W emulsions was studied in the presence of microgels, whose concentration was kept constant at 0.05 wt%. Two emulsion compositions were studied: one with an excess of PEO phase (75%), which leads to D/P emulsions, the other with an excess of DEX phase (75%) which leads to P/D emulsions.

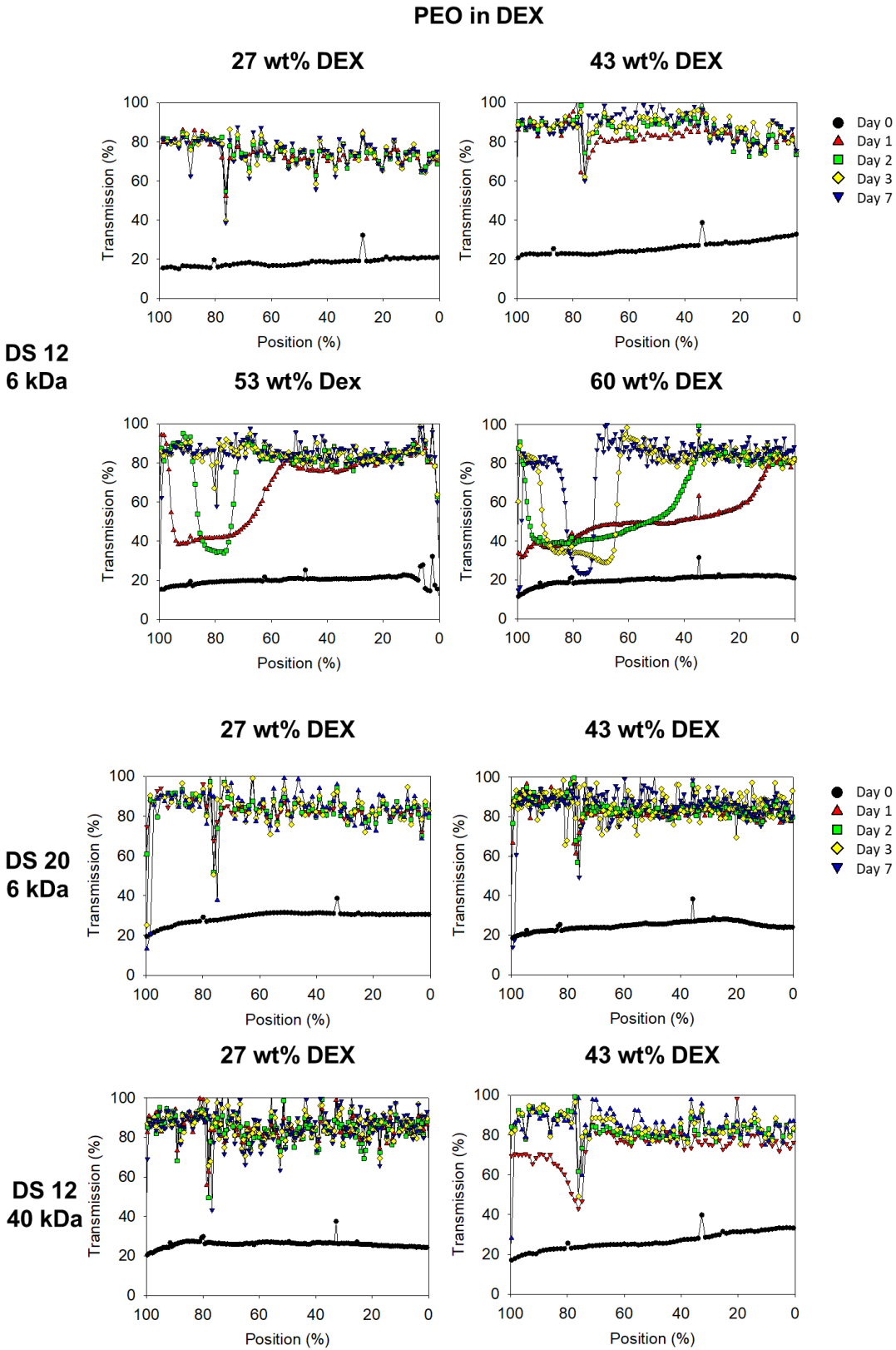
First, the stability of W/W emulsions in the presence of microgels was studied by simple visual inspection (**Figure 3.2**). At short times, just after shaking, the emulsions were equally turbid over the total height of the sample. Upon ageing, sedimentation or creaming occurred. If the drops remained intact, a turbid layer could be seen at the bottom of the vial for D/P emulsions, because DEX-rich droplets sedimented, whereas for P/D, PEO-rich droplets creamed toward the top of the vial. When phase separation occurred due to coalescence, the turbidity was lost. The height profile of the turbidity was also measured using the

LUMiReader® apparatus (**Figure 3.3**). Microgels can stabilize D/P emulsions more than P/D emulsions. No major difference could be observed for different DS or DEX molar mass at the same DEX weight fraction. Interestingly, the microgels at 60 wt% of DEX was the only one to stabilize both the P/D and D/P emulsion.



**Figure 3.2.** Photos of P/D (top) and D/P (bottom) emulsions with and without 0.05 wt% different microgels at different times after preparation as shown in the figure.





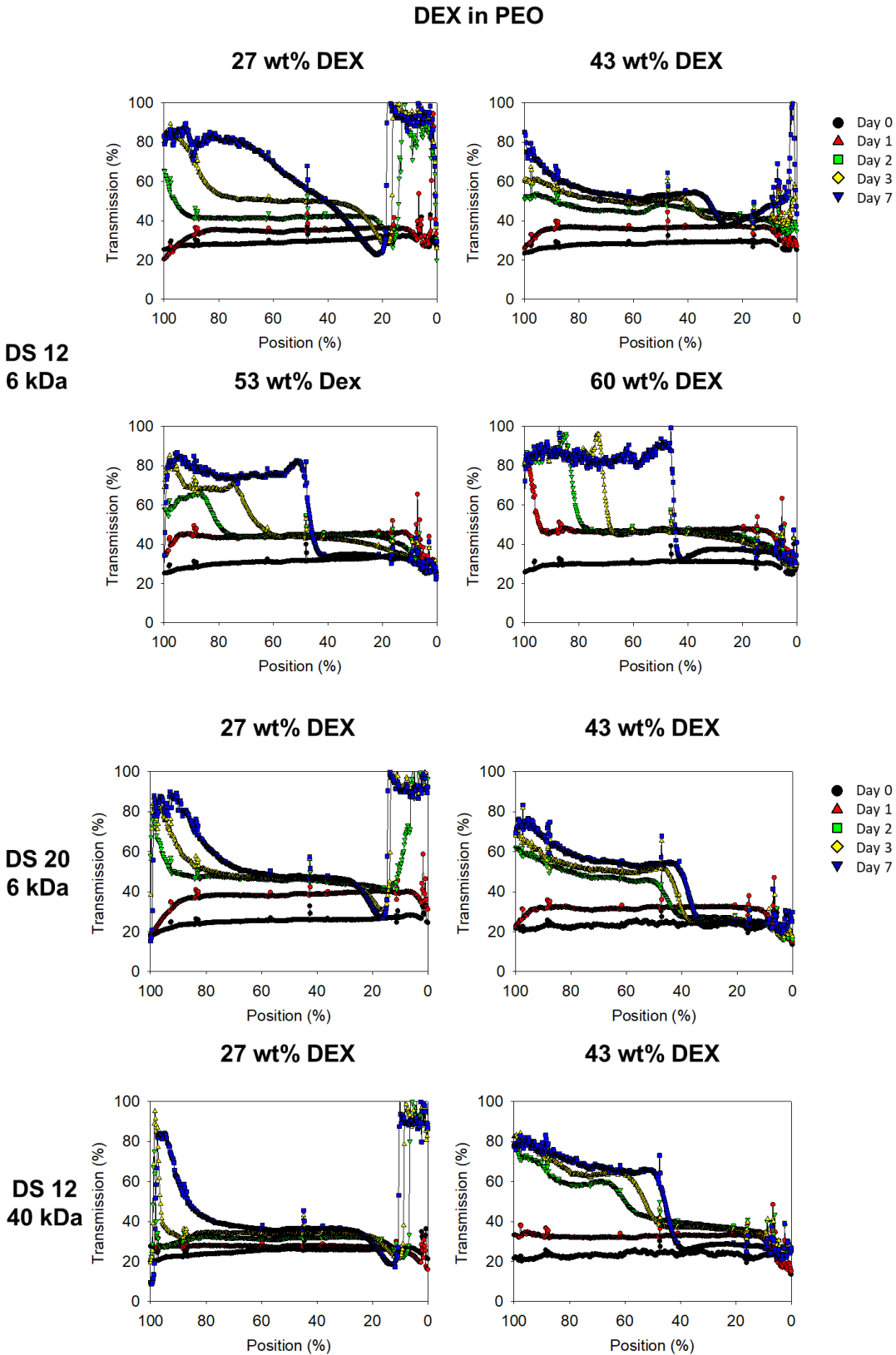
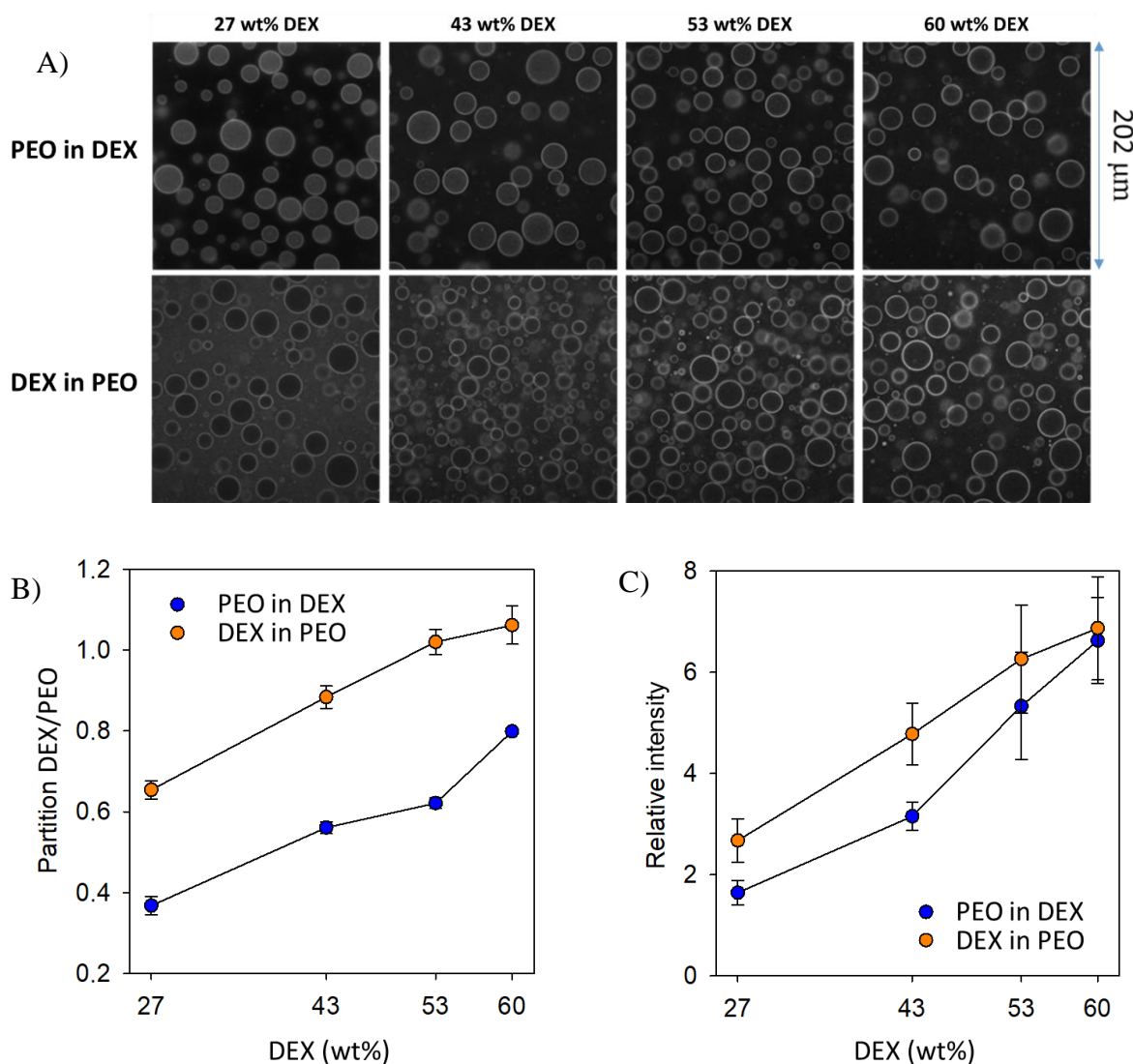


Figure 3.3. Ageing of the emulsions upon gravitational field at 20 °C. Turbidity measurements as a function of height at different times for the various emulsions.

To get a more accurate picture of the stability, the emulsions were observed at the mesoscopic scale by confocal laser scanning microscopy (CLSM) (**Figure 3.4A**). After the preparation, in all the situations, FITC-labelled microgels were visible at the DEX-PEO interface, forming a layer around the droplets. There was no significant effect of the composition on the drop size.

Obviously, the two phases presented different fluorescence intensities, showing an uneven distribution of the microgels in the medium. At low DEX content, an excess of microgels was visible in the PEO phase, which was more fluorescent. The fluorescence intensity of the PEO phase decreases as the DEX content in the microgels increases. For a more quantitative approach, the partitioning between the two phases, given by the fluorescence intensity ratio between these two phases, was plotted in **Figure 3.4B**. It shows that the affinity for the PEO phase decreases as the DEX content increases. The intensity ratio between the DEX and PEO phases evolves from 0.6 to 1.1 when the DEX content raises from 27 wt% to 60 wt% in the case of D/P emulsions. The trend is the same for P/D emulsions, but the ratios are lower.

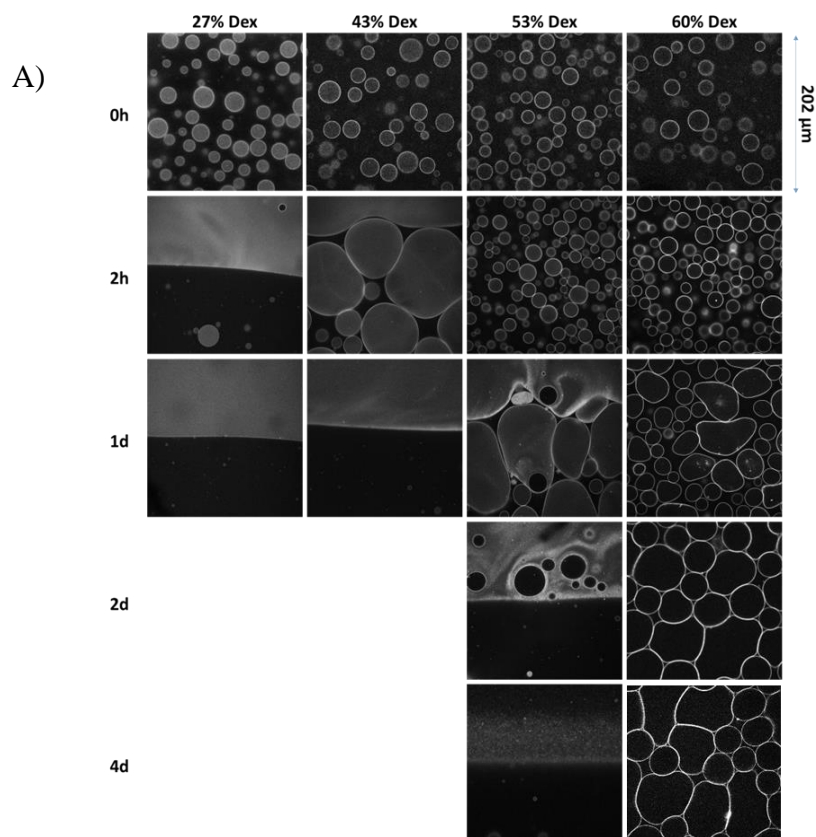
A sharp increase of the intensity at the interface was observed caused by the adsorption of microgels. The relative intensity between the intensity at interface and that of PEO phase is plotted in **Figure 3.4C**. An excess of fluorescence intensity at the interface is observed, which rises with an increasing DEX content. It should be noted that the relative fluorescence intensity at the interface was larger for the D/P emulsions than for P/D emulsions.

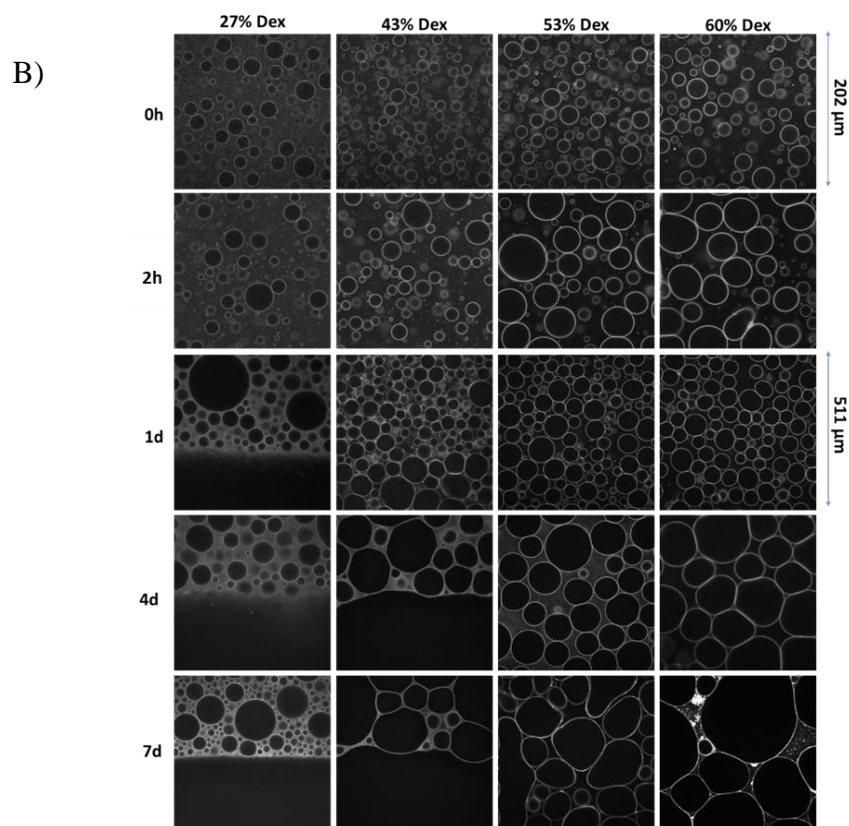


**Figure 3.4.** A) CLSM images of the emulsions immediately after preparation, B) Partitioning between the PEO and the DEX phases when increasing the wt% DEX, C) Relative fluorescence intensity ratios at the interface of P/D and D/P emulsions as function of wt% DEX, extracted from the profile views of the drops. All the emulsions were studied at 20 °C.

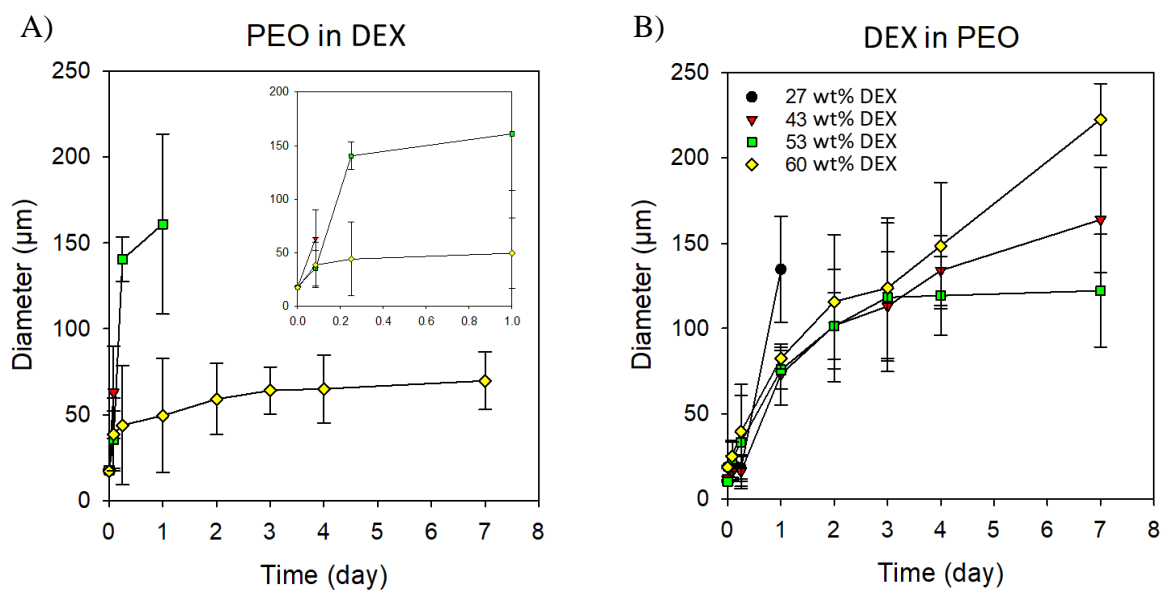
The evolution of the emulsion microstructure during ageing was also monitored by confocal microscopy, by keeping the samples in sealed cells, which were kept vertical and placed horizontally for observations (**Figure 3.5**). For the P/D emulsion with microgels at low DEX contents, a PEO phase is visible at the top after 2 hours. When increasing the DEX content to 53 wt%, coalescence occurred more slowly and the phase separation was observed after one day. Upon further increase to 60 wt%, coalescence was even slower. Droplets grew to reach

65  $\mu\text{m}$  after 1 week but no phase separation was observed. D/P emulsions were more stable than P/D. The DEX phase started to phase separate after 24h for 27 wt% DEX content, and after 4 days for 43 wt%. Droplets were still visible after one week for the two highest contents of DEX, but the drop size was bigger for the 60 wt% content, suggesting an optimal stability for 50 wt%. The kinetic evolution of the drop diameter is given in **Figure 3.6**.



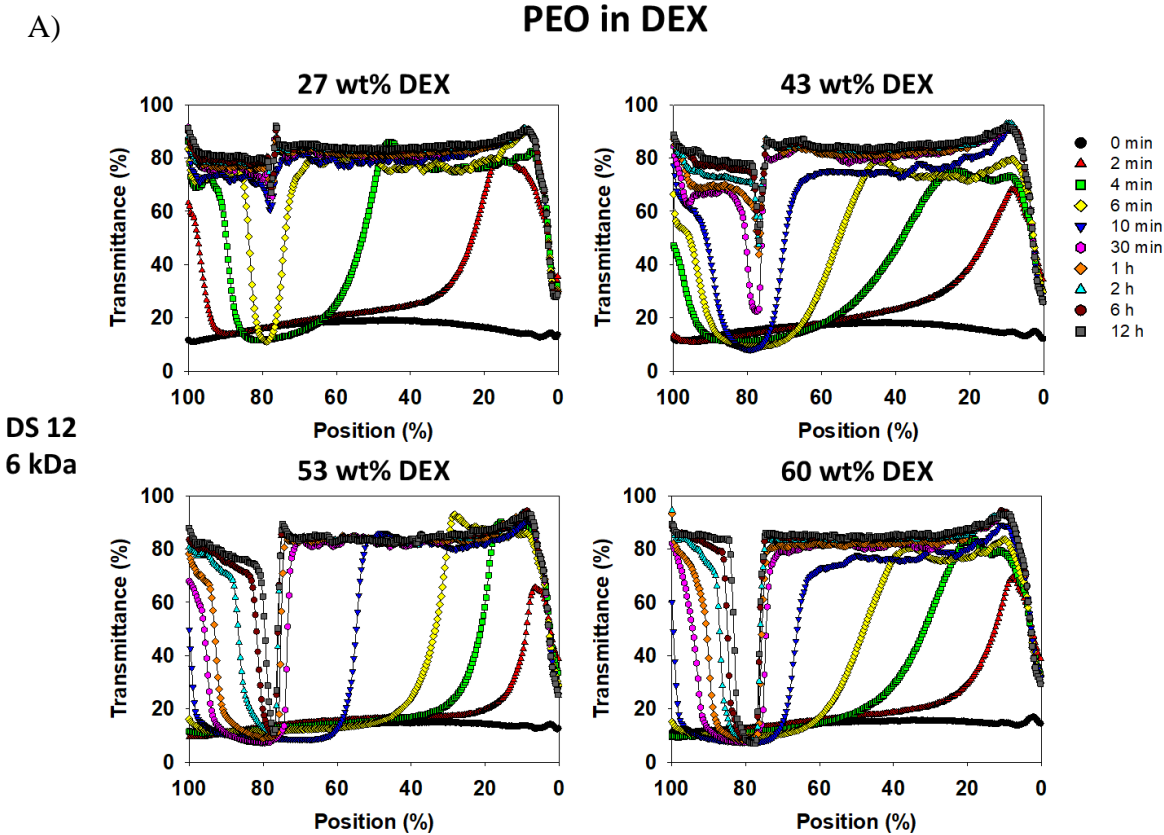


**Figure 3.5.** CLSM images showing the evolution of the microstructure of P/D (A) and D/P (B) emulsions containing 0.05 wt% of microgels with different DEX contents.

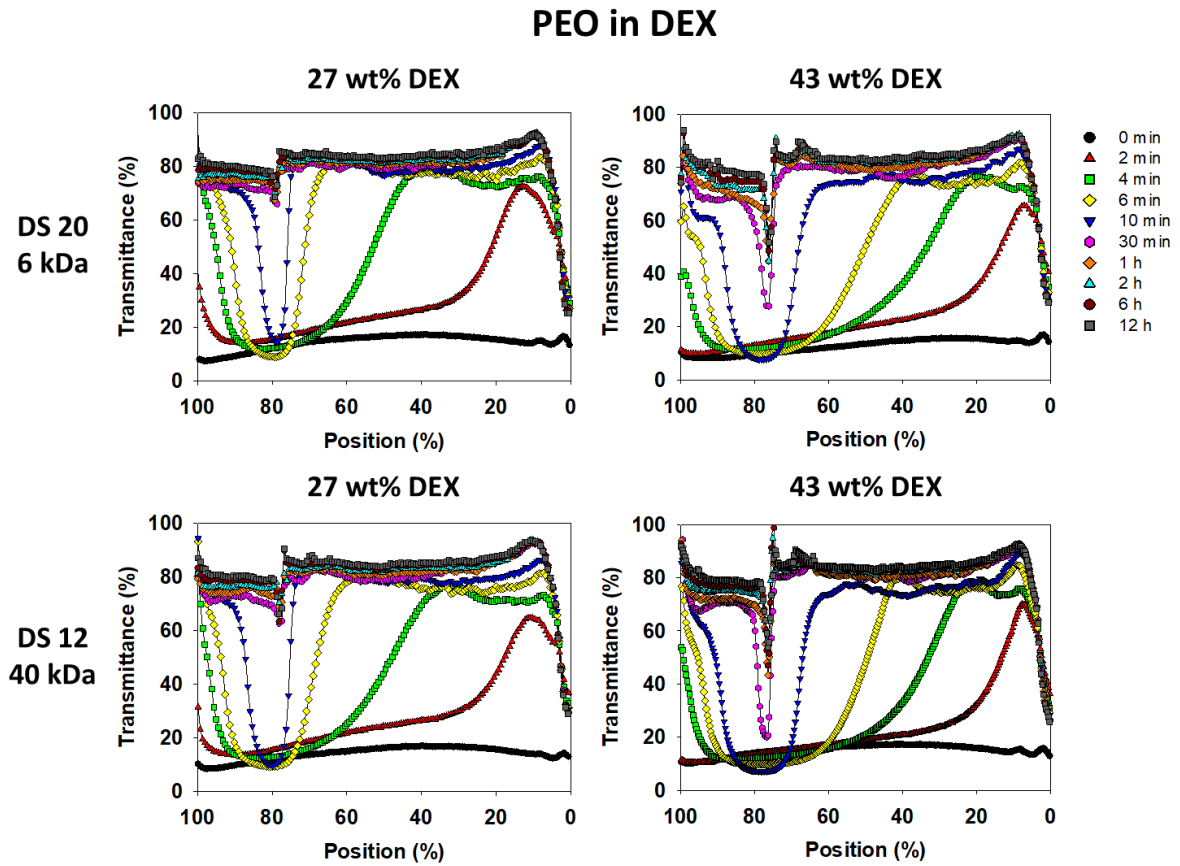


**Figure 3.6.** Mean diameter of the droplets in P/D (A) and D/P (B) emulsions containing 0.05 wt% of microgels with different DEX contents

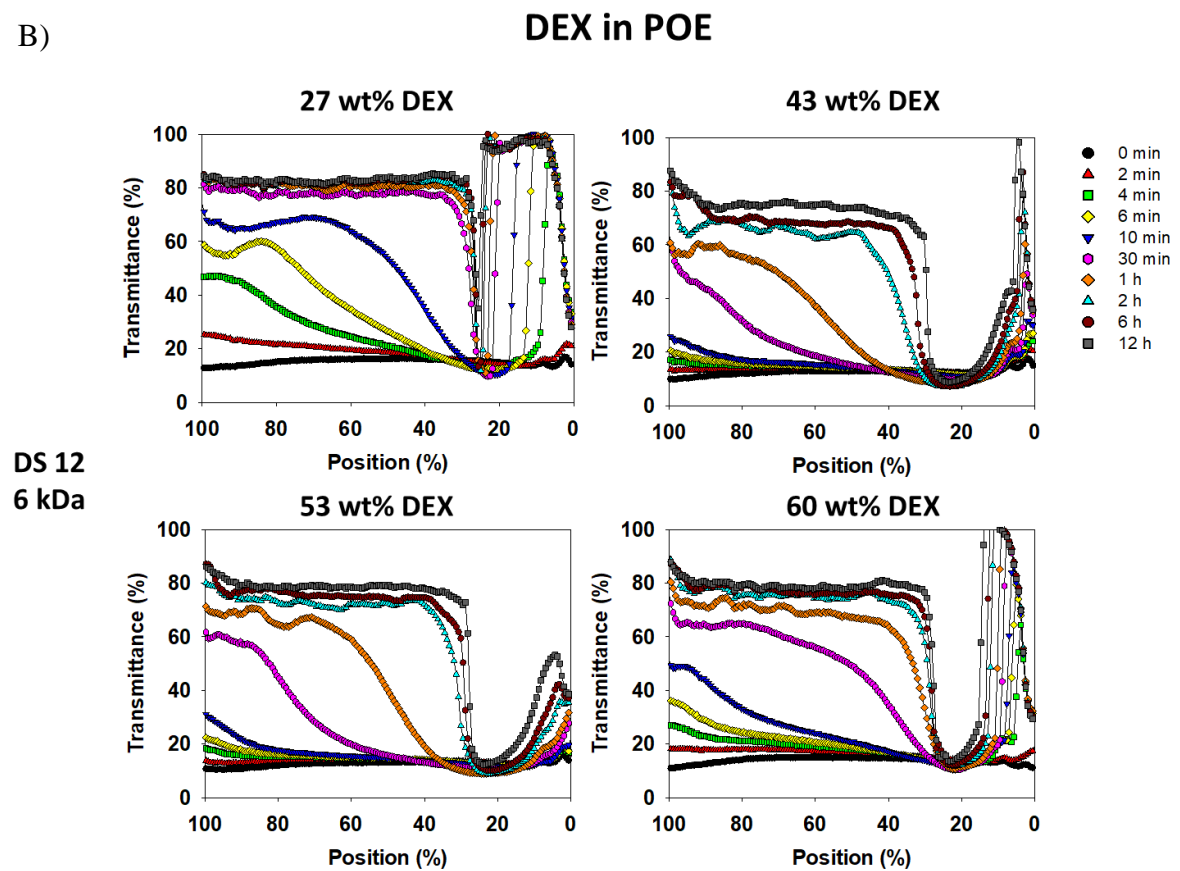
The stability of the different emulsions was also compared during centrifugation (470g), by measuring the turbidity profiles as a function of height in the centrifugation tubes (**Figure 3.7**). Centrifugation accelerates creaming or sedimentation of the droplets and also may accelerate coalescence by compressing the droplets. For both P/D and D/P emulsions, the addition of microgels increased the stability. With 27 wt% DEX microgels, the P/D emulsion phase separated after 10 minutes compared to 1 hour with 43wt%. For the emulsion stabilised with 53 wt% and 60 wt%, phase separation was not observed after 12 hours. A turbid zone corresponding to emulsion droplets could be observed close to the PEO-DEX interface. Similarly to observations under 1G, the D/P emulsions were more stable in the presence of microgels. With 27 wt% DEX microgels, two transparent phases were visible after 2 h. For the emulsions stabilized with the three other microgel candidates, the phase separation was much slower. Maximum stability was observed with the addition of the 53 wt% DEX microgels.







B)





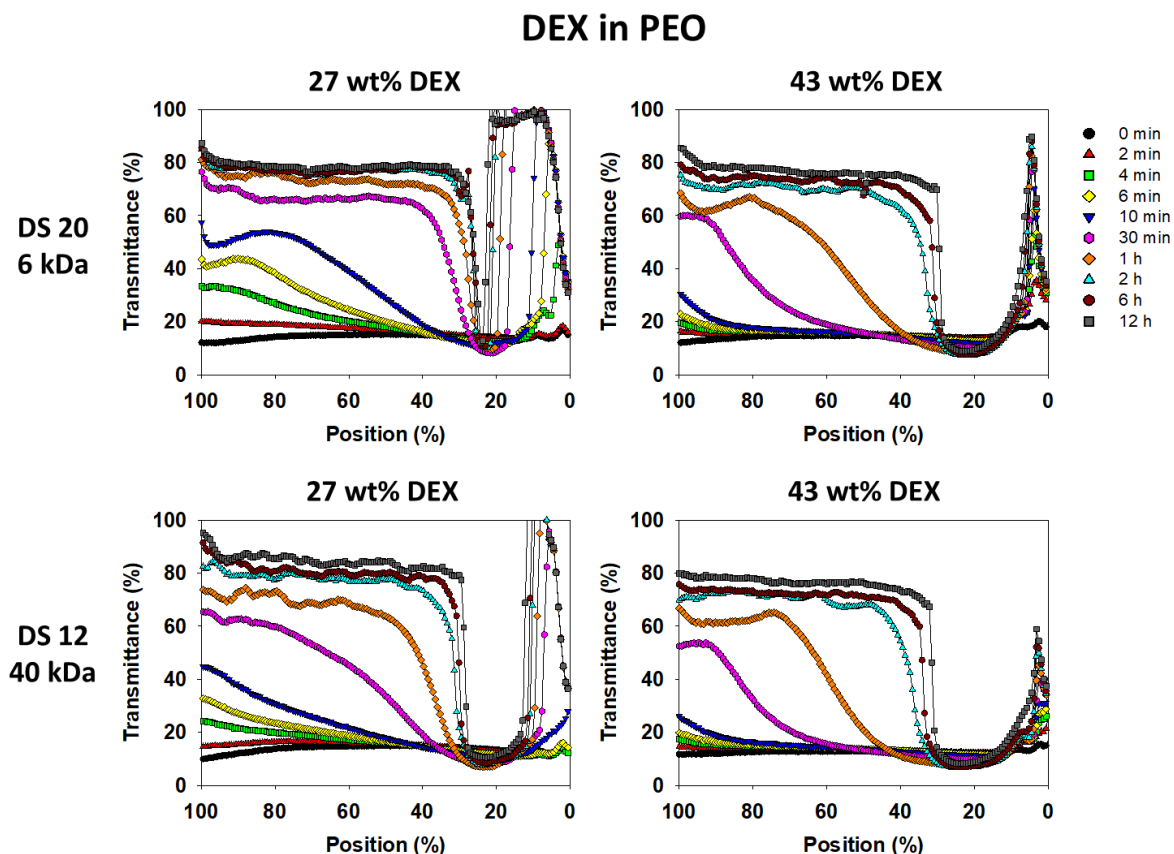


**Figure 3.7.** Ageing upon centrifugation at 470g at 20 °C. Evolution of the turbidity profile for A) P/D emulsion; B) D/P emulsion, with 0.05 wt% microgels with different DEX contents.

These measurements allowed extracting characteristic stabilization times ( $t_c$ ), which correspond to the times taken to reach half of the full transmittance of dispersed phase at the bottom 25% for D/P emulsions and the top 25% for P/D emulsions (**Figure 3.8**), as described in **section 2.2.3**. The  $t_c$  is plotted as a function of microgel composition, for each type of emulsions (**Figure 3.9**). This representation highlights the huge importance of the microgel composition on the mechanical stability of the emulsions. Indeed, the timescale spans over 3 orders of magnitude. At low fraction of DEX (27 wt%), the  $t_c$  were very close for the D/P and P/D emulsions. Increasing the fraction of DEX in the microgels progressively enhanced the stability of the P/D emulsion and further that of D/P, which was maximal close to 50 wt%. Increasing further the fraction of DEX decreased the stability of D/P but continued enhancing that of P/D. Increasing DS and DEX molecular weight also gave a higher  $t_c$  at low content of

DEX, especially in D/P emulsion, but this effect is no longer obvious when increasing the fraction of DEX. The stability mainly depends on the wt% of DEX in the microgel composition.

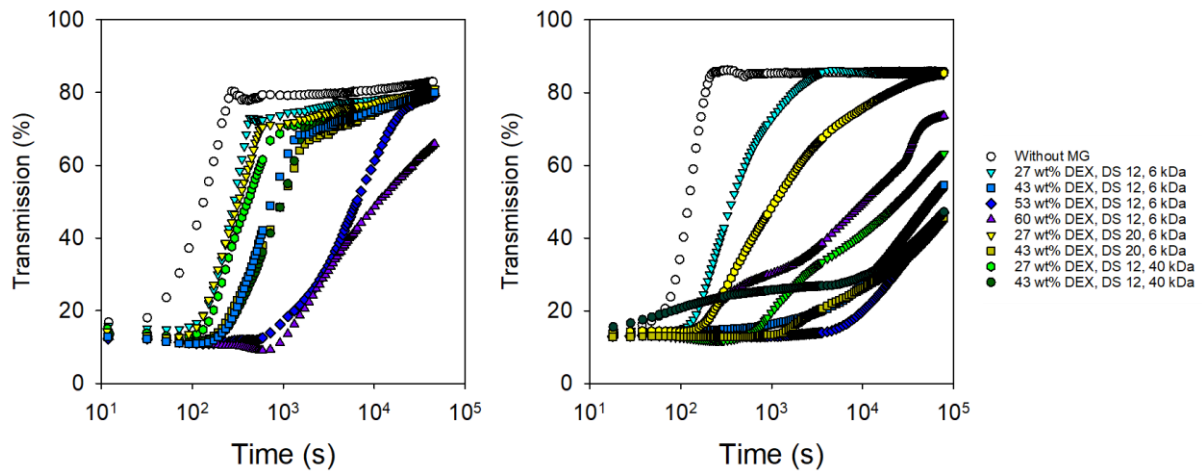


**Figure 3.8.** Evolution of the transmission measured in the section where the dispersed phase forms a continuous phase for P/D (left) and D/P (right) emulsions in the presence of de microgels. Measurements recorded on a LUMiSizer® at 470g.

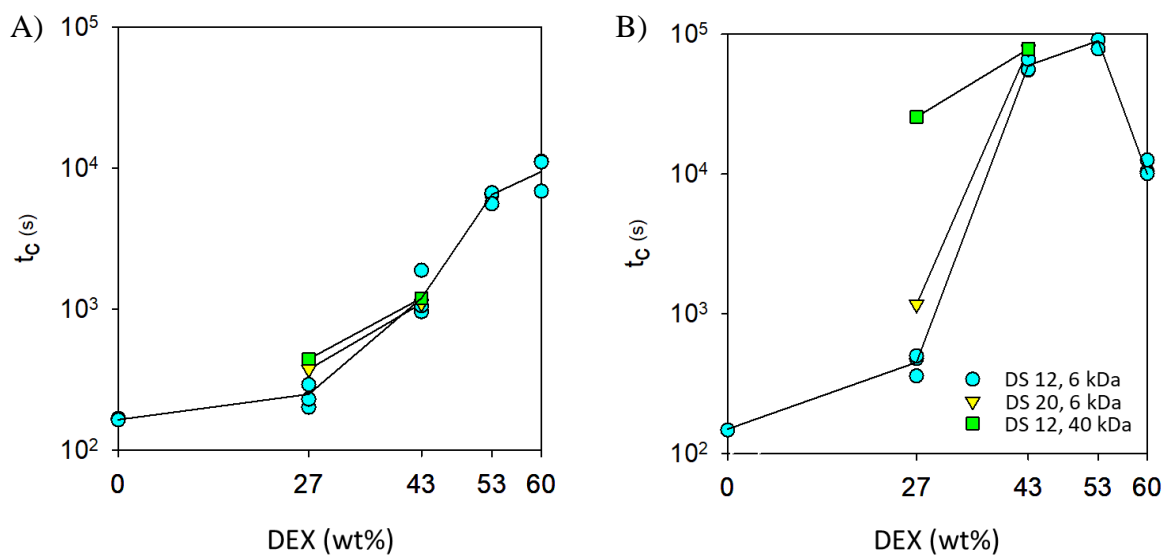
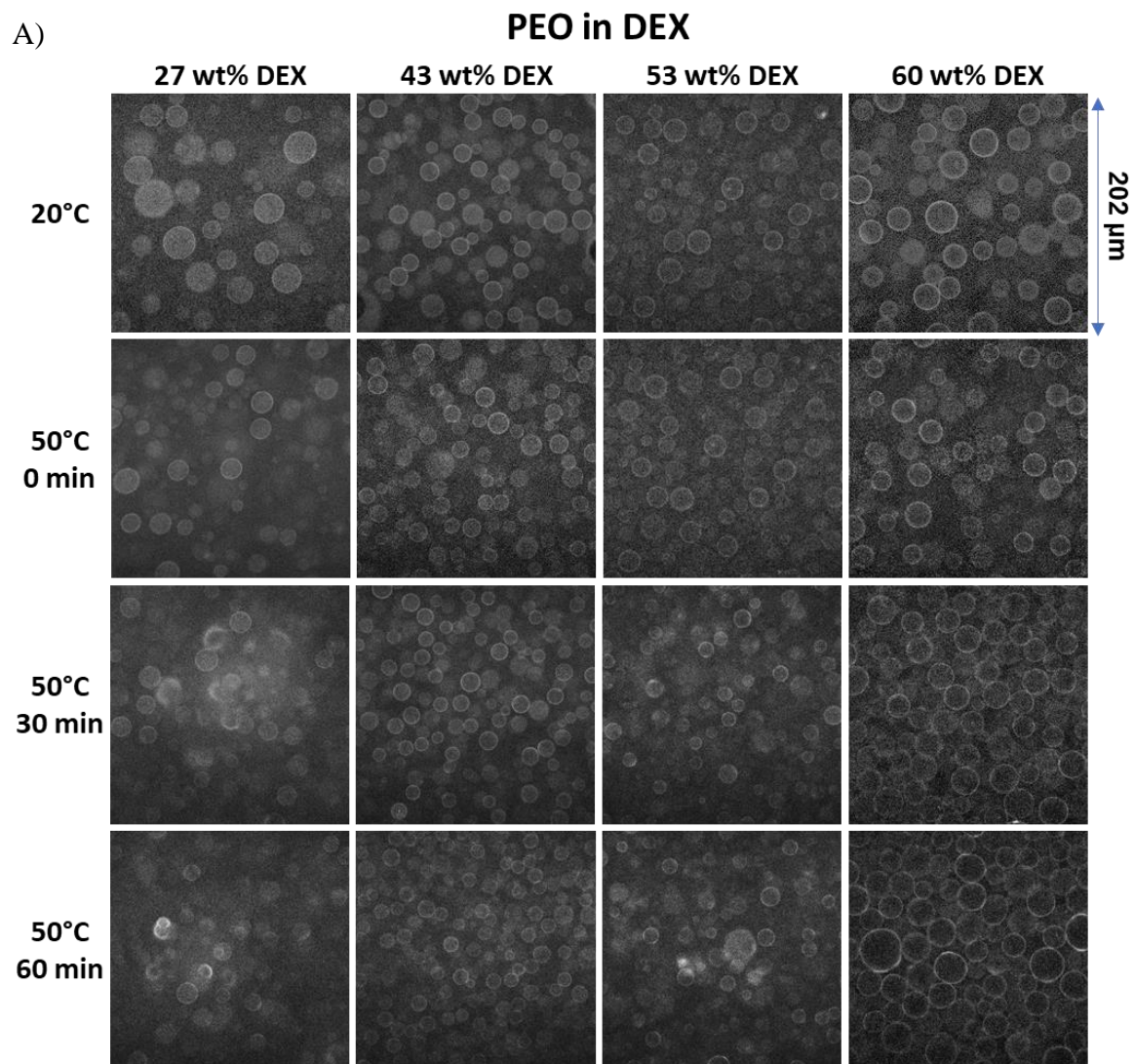


**Figure 3.9.** Characteristic stabilization time of the P/D (A) and D/P (B) emulsions as a function of the DEX fraction in the microgels. 0% DEX corresponds to the emulsion without particles.

### 3.2.2. Effect of temperature on Water-in-Water emulsion stability

As previously described, increasing the temperature induces a sudden drop in the microgel diameter due to the collapse of pNIPAM chains. Previously studied microgels with low DEX contents were found to invert the stability of the W/W emulsion, although the partitioning remained in favour of the PEO phase [10]. It was concluded that the conformational change of the microgels had an influence on their interactions at the interface. The same investigation methodology was applied here to other compositions. Not only ageing at 50 °C was studied, but also the preparation pathway: in one case, the samples were emulsified at room temperature, in the other case, they were heated at 50 °C and then emulsified.

**Figure 3.10** shows the evolution of the microstructure of emulsions prepared at 20 °C and subsequently heated to 50 °C. In this case, the D/P drops coalesced faster than the P/D. This trend was similar for all the microgel compositions. **Figure 3.11** shows the partition between PEO, DEX, and the interface. For both emulsions, heating the emulsion that was initially prepared at 20 °C did not change the partition, whereas the microgels gained more affinity for the DEX phase when they were first heated at 50 °C. Increasing temperature had no effect on the relative intensity of the interface when the emulsion was prepared at 20 °C. However, when the emulsion was prepared at 50 °C the relative intensity at the interface was lower at higher contents of DEX. In this case, a few aggregates of microgels were formed which had a tendency to adsorb at the interface, see **Figure 3.12**.



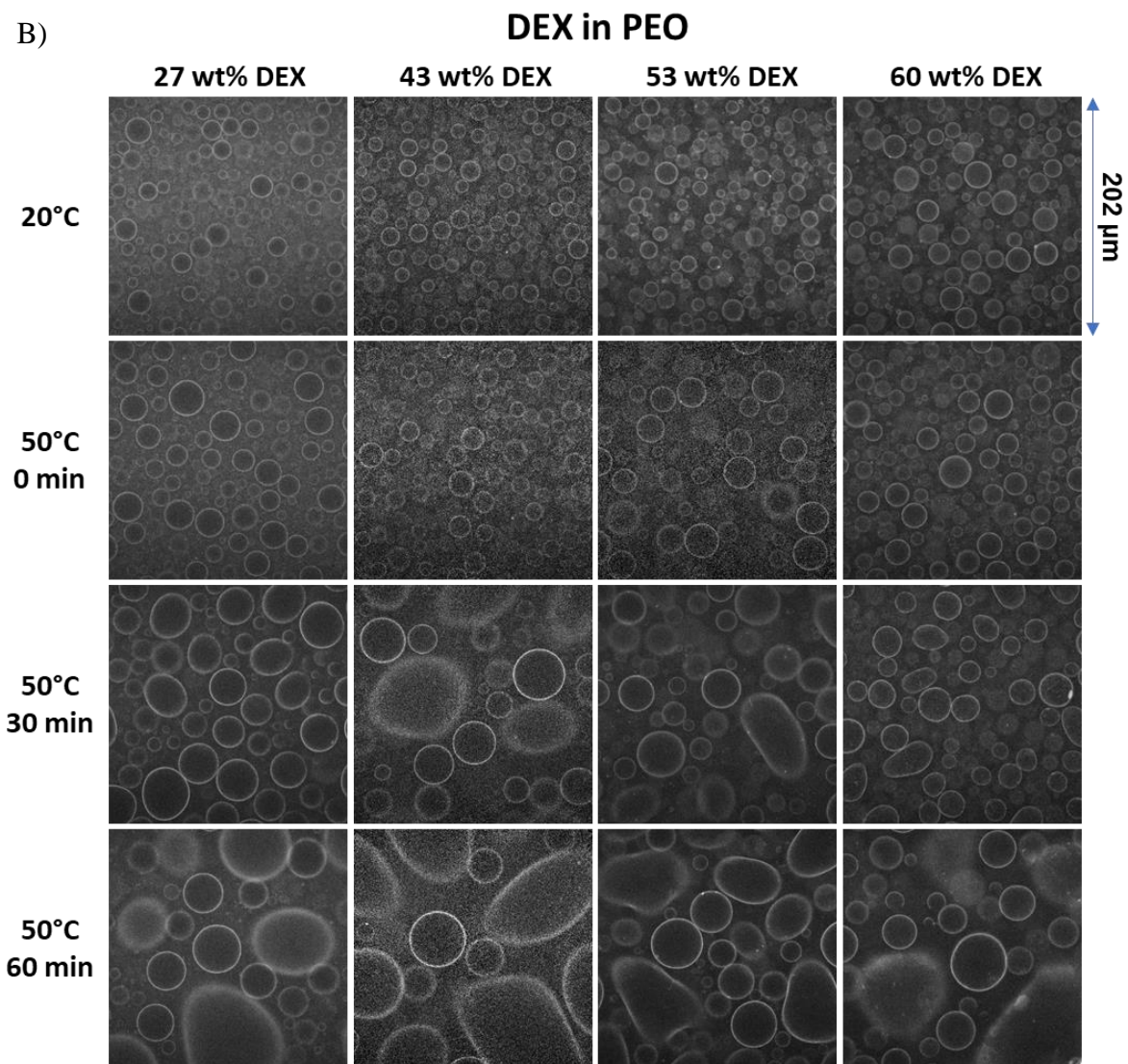


**Figure 3.10.** CLSM images of A) P/D and B) D/P emulsions with 0.05 wt% microgels. The emulsions were prepared at 20 °C and subsequently heated to 50 °C.

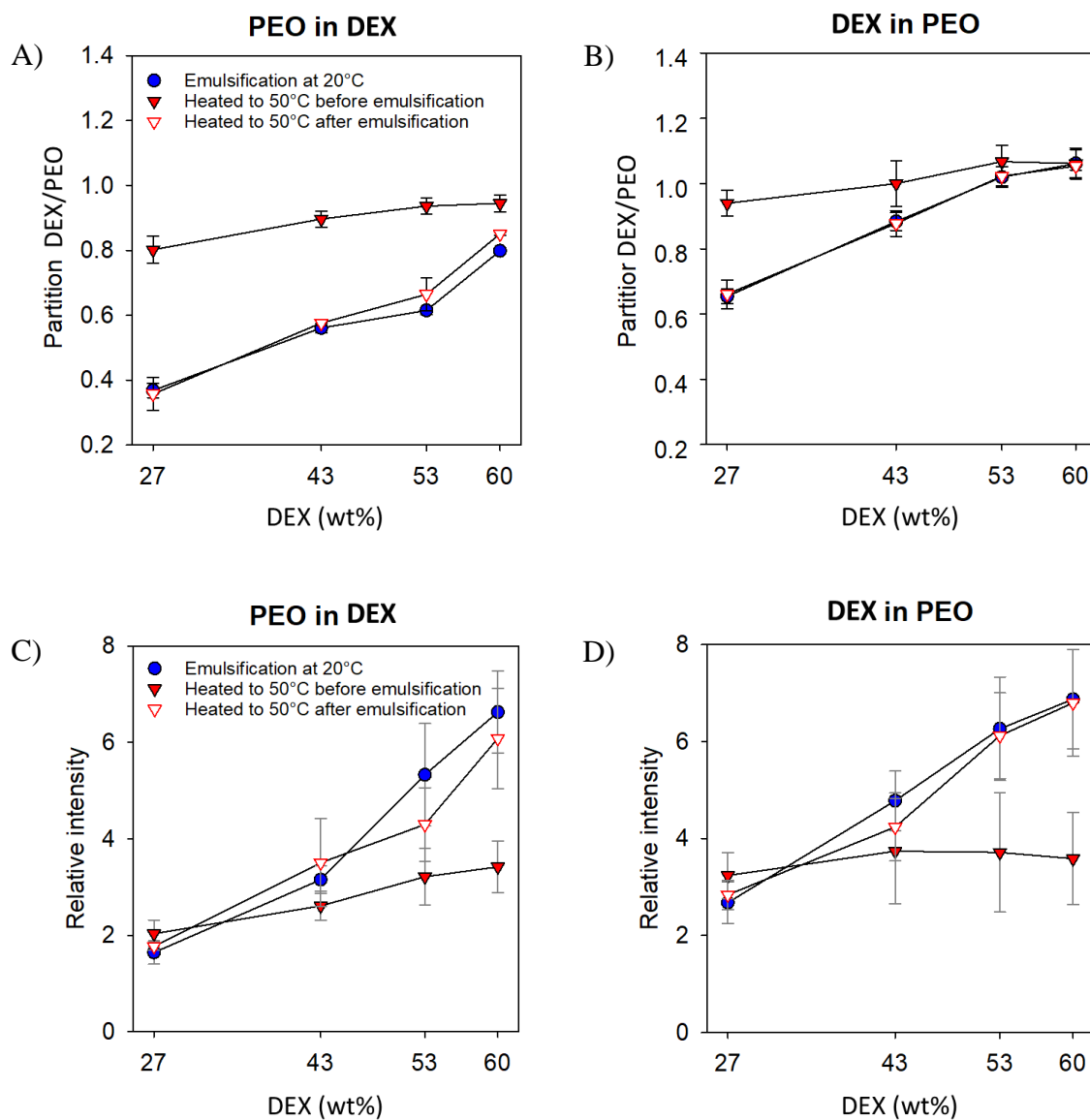


**Figure 3.11.** Effect of temperature on the partition of microgels between the DEX and PEO phases (A, P/D; B, D/P) and on the relative intensity at the interface (C, P/D; D, D/P).



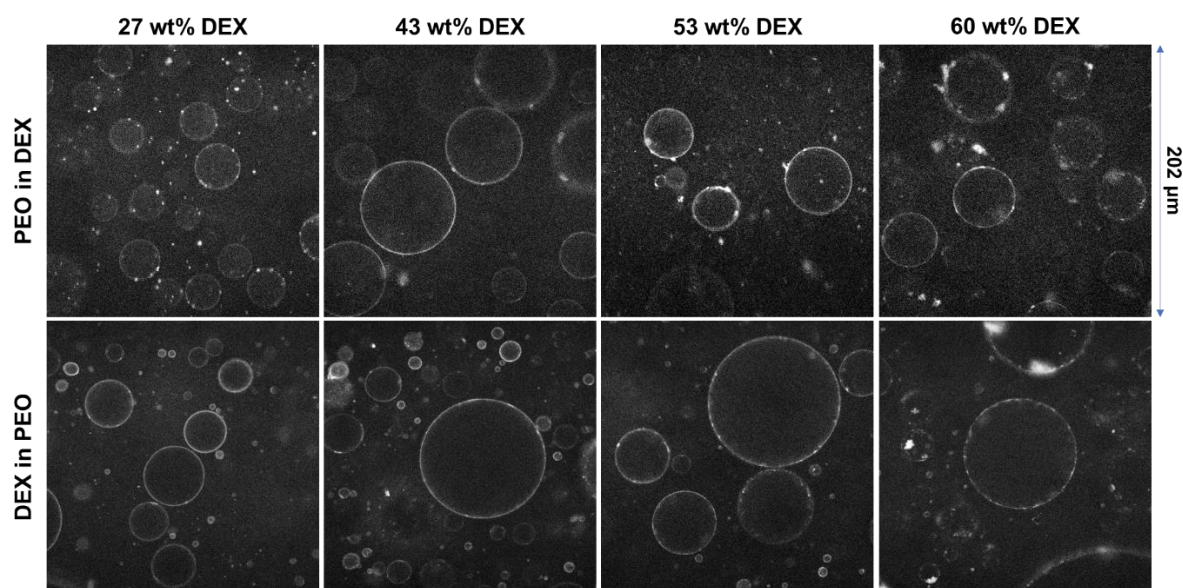


**Figure 3.12.** CLSM images of A) P/D and B) D/P emulsions stabilized by 0.05 wt% microgels at 50 °C that had been prepared at 50 °C.

The stability of the different emulsions was studied during centrifugation at 50 °C (**Figure 3.13** and **Figure 3.14**) and the characteristic stabilization time  $t_c$  was determined, as plotted in **Figure 3.15**. Without microgels, the  $t_c$  decreased, which can be explained by the diminution of the phase viscosity and therefore faster sedimentation or creaming. After the addition of microgels, the D/P emulsion was much less stable than at 20 °C, whatever the preparation pathway. Concerning the P/D emulsion, heating the sample before or after emulsification led to a better stability in presence of 27 wt% DEX and 43 wt% DEX microgels. The emulsion with 50 wt% DEX microgels, was more stable when heated after emulsification and less stable if heated before the sample preparation. Finally, with 60 wt% DEX microgels, both heated emulsions were less stable than at 20 °C. Thus, the previously observed inversion of emulsion stability is confirmed for the DEX contents below 50 wt%. Above 50 wt%, when the stability of P/D is promoted at 20 °C, increasing the temperature decreased the stability.

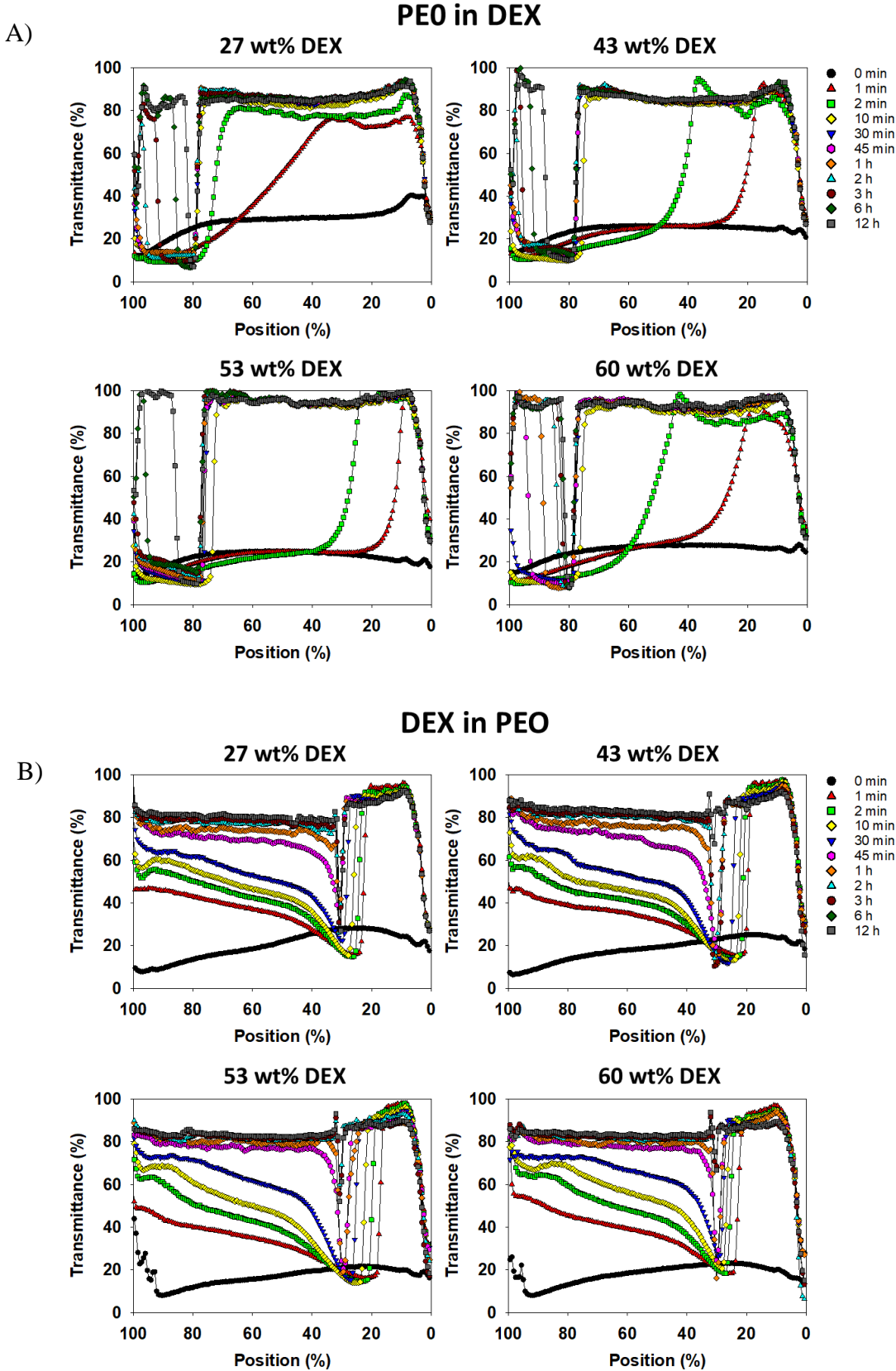


**Figure 3.13.** Ageing of the W/W emulsions upon 470g at 50 °C. Evolution of the transmission profiles measured with LUMiSizer® on A) P/D emulsions; B) D/P emulsions with 0.05wt% microgels.



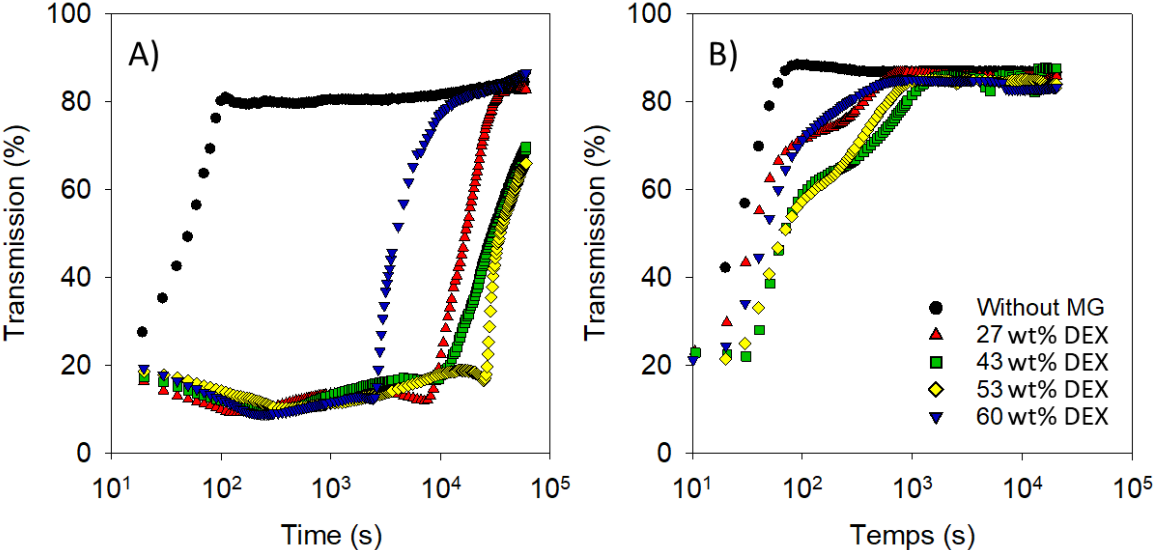


**Figure 3.14.** Evolution of the transmission upon 470g at 50 °C measured in the section where the dispersed phase forms a continuous phase for P/D (A) and D/P (B) emulsions in the presence of de microgels.

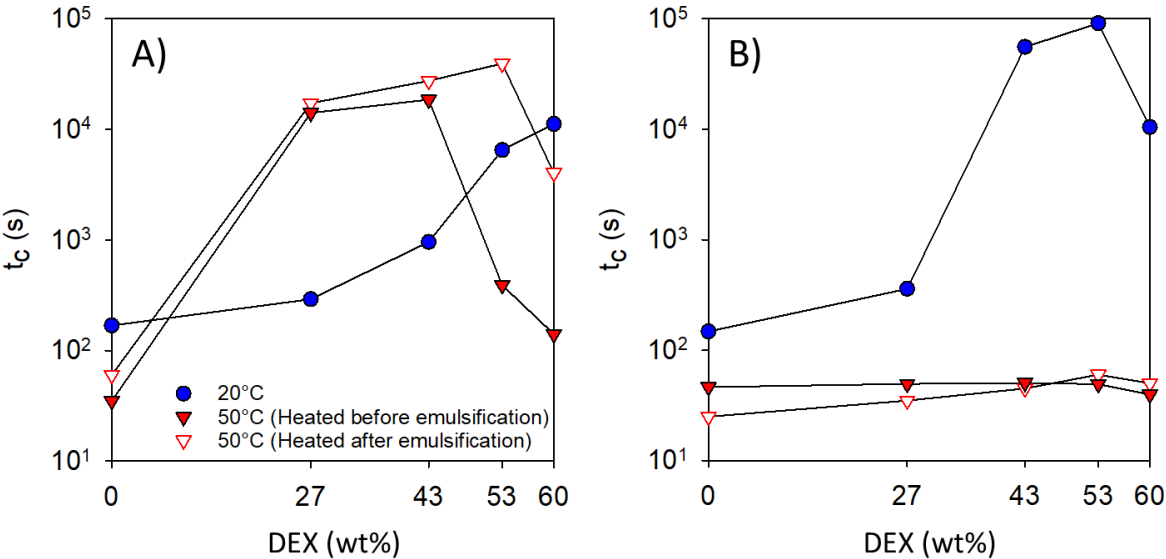


**Figure 3.15.** Characteristic stabilization time of the A) P/D, B) D/P as a function of the DEX fraction in the microgels at 20 °C and 50 °C, for emulsions prepared in different conditions. 0% DEX corresponds to the emulsion without particles.

## **Conclusion**

This study shows how the bishydrophilic balance in particle composition can govern the adsorption energy at the W/W interface, leading to a progressive change in wettability and subsequently affecting the stability of W/W emulsions. Our findings demonstrate the substantial potential of these systems to control W/W emulsion stability through chemical composition, paving the way for novel encapsulation applications. This research provides a critical foundation for chemists aiming to design and develop efficient particle stabilizers with new functionalities, such as catalytic properties. Additionally, the insights gained here are useful for selecting natural biopolymer-based particles, such as denatured proteins, glycoproteins, or polysaccharides, which are naturally bishydrophilic. The strategies outlined are broadly applicable to various W/W emulsion systems where particles exhibit affinity for both phases, thus broadening the scope of practical applications and enhancing the versatility of emulsion-based technologies.



## **Chapter 4. Effect of charge on the stabilization of Water-in-Water emulsions by bishydrophilic microgels**

This chapter discusses the effect of charge on the stabilization of W/W emulsions based on bishydrophilic microgels. To this end, acrylic acid (AA) groups were used to incorporate into neutral microgels during the synthesis. The charge density of the microgels could be modified by varying the pH or adding salt. Microgels with 14 mol% NIPAM units replaced by AA units ( $F_{AA} = 14 \text{ mol\%}$ ) were studied in most detail, but microgels with 5 mol% and 29 mol% AA units were also investigated. The structure of the emulsion and the stability was determined by CLSM and LUMiSizer<sup>®</sup> at room temperature and at 50 °C. The results have been published in *Journal of Colloid and Interface Science*, 2023, 646, 484-492.

|   |           |
|---|-----------|
| <b>1. Characterization of the microgels.....</b>        | <b>73</b> |
| <b>2. Emulsion microstructure and stability.....</b>    | <b>76</b> |
| 2.1 Effect of the pH.....                               | 76        |
| 2.2 Effect of salt.....                                 | 80        |
| 2.3. Combined effect of pH and salt.....                | 85        |
| 2.4. Effect of the fraction of acrylic acids units..... | 85        |
| <b>Conclusions .....</b>                                | <b>88</b> |

#### 4.1. Characterization of the microgels

The hydrodynamic diameter ( $d_h$ ) of the charged microgels with  $F_{AA} = 14$  mol% was determined by dynamic light scattering as a function of the temperature at different pH, with and without 100 mM NaCl, see **Figure 4.1**. At 20 °C,  $d_h = 260$  nm at pH 7 and pH 5 but decreased to 170 nm at pH 4 and 120 nm at pH 3. The decrease can be explained by the deswelling due to a decrease of the charge density of the microgels, given that the pKa of acrylic acid is 4.3.

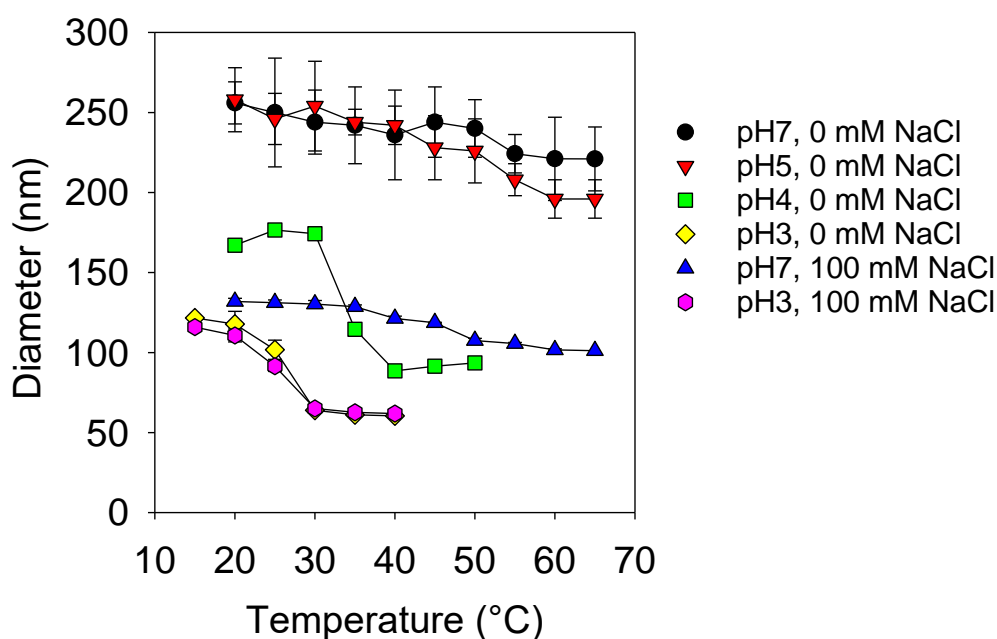


**Figure 4.1.** Temperature dependence of the diameter of charged microgels ( $F_{AA} = 14$  mol%) at different pH with and without added NaCl as indicated in the figure. The error bar is based on the spread of the data as a function of the scattering wave vector.

At pH 7 and 5, the size of the microgels decreased only weakly, down to 230 nm and 200 nm, respectively, when increasing the temperature to 65 °C. However, shrinkage of the microgels was observed at pH 4 starting at 30 °C and at pH 3 starting at 20 °C. At both pH,  $d_h$  decreased by about 2-fold. It appears that the high charge density at pH 5 and pH 7 inhibited shrinkage and countered the hydrophobic attractions between the NIPAM segments at higher

temperatures. The lower charge density at pH 3 compared to at pH 4 may explain why the shrinkage started at a lower temperature at pH 3 than at pH 4.

Addition of NaCl led to shrinkage of the strongly charged microgels at pH 7 and further weak shrinkage during heating starting at 35°C. A more detailed study of the effect of adding salt at 20 °C and 50 °C showed that shrinkage was important already at 5 mM NaCl, see **Figure 4.2**. The effect of NaCl can be explained by screening of electrostatic repulsion. At pH 3, the microgels have very little residual charge, which explains why NaCl had almost no effect on the size of the microgels.

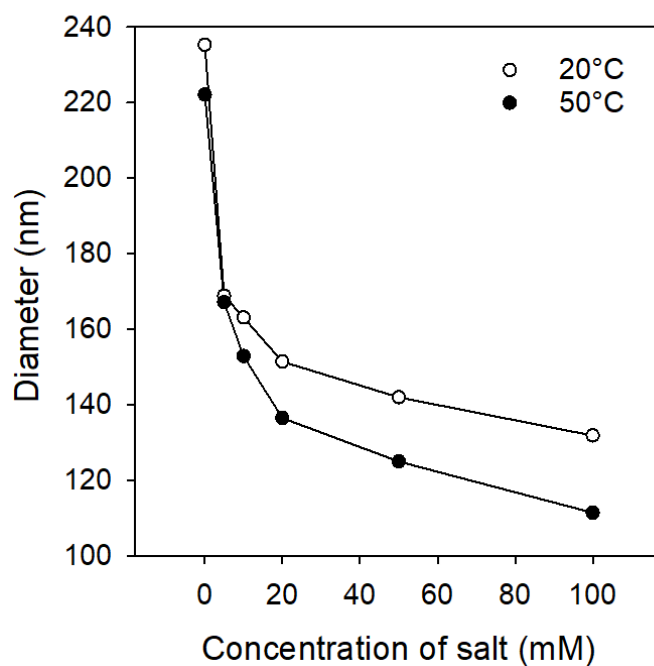
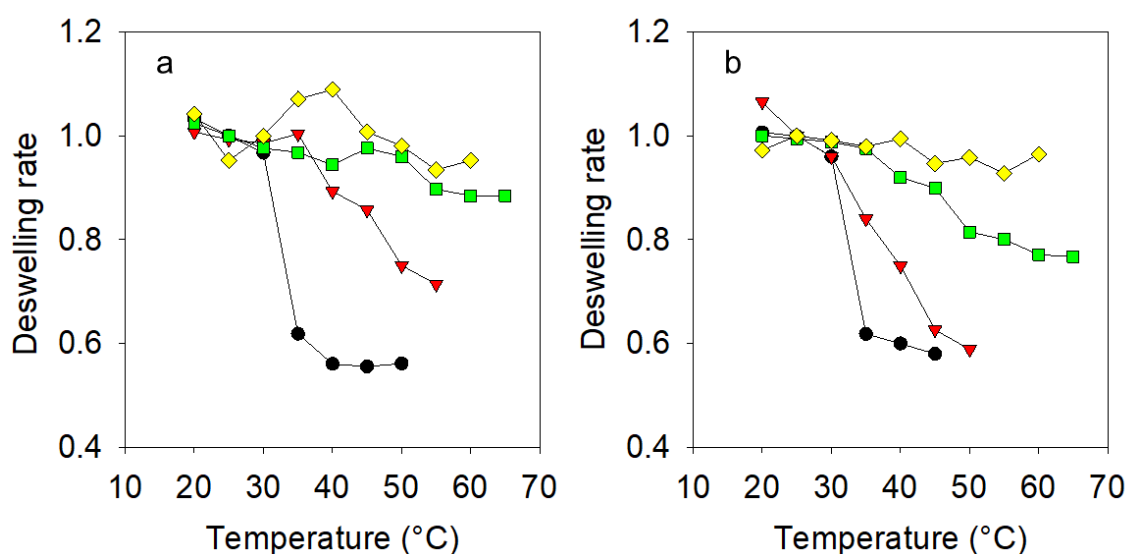


**Figure 4.2.** Dependence of the diameter of charged microgels ( $F_{AA} = 14 \text{ mol}\%$ ) on the NaCl concentration at 20 °C and 50 °C.

Electrostatic repulsion can be reduced either by lowering the charge density through lowering the pH or by screening through salt addition. Both led to shrinkage of highly charged microgels at 20 °C. However, the effect of heating was found to be very different. Lowering the charge density had a much stronger effect on the temperature dependence than screening. The difference is that in the case of screening the AA units are still charged, but the electrostatic

repulsion between the charged is screened, whereas at low pH the AA units are no longer charged. It appears that the presence of charges inhibits temperature induced deswelling even if screened, perhaps because in this case the AA units cannot approach closely. The temperature at which shrinkage began for microgels with low charge density was even lower than for equivalent neutral microgels. This observation shows that neutralized acrylic acid groups promoted shrinkage.

The effect of heating on  $d_h$  was also studied for microgels for which the fraction of AA units was  $F_{AA} = 5 \text{ mol\%}$  or  $29 \text{ mol\%}$ . At  $20 \text{ }^\circ\text{C}$ , the  $d_h$  of these microgels was, respectively,  $280 \text{ nm}$  and  $250 \text{ nm}$  at pH 7 and  $140 \text{ nm}$  and  $90 \text{ nm}$  at pH 3. **Figure 4.3** shows that at pH 7 deswelling is more gradual and occurs at higher temperatures when the microgels contain more charges both in pure water and with  $100 \text{ mM NaCl}$ . The most strongly charged microgels showed no significant deswelling up to  $70^\circ\text{C}$ . At pH 3 where the AA units are neutral, the extent of deswelling did not depend significantly on  $F_{AA}$ , but the temperature where deswelling started decreased with increasing  $F_{AA}$  from about  $35 \text{ }^\circ\text{C}$  at  $F_{AA} = 0 \text{ mol\%}$  to about  $25 \text{ }^\circ\text{C}$  at  $F_{AA} = 29 \text{ mol\%}$ . It should be noted that the microgel suspensions remained colloidally stable whatever the salinity and temperature, thanks to the steric stabilization provide by the DEX chains, as discussed by Merland et al. [10].





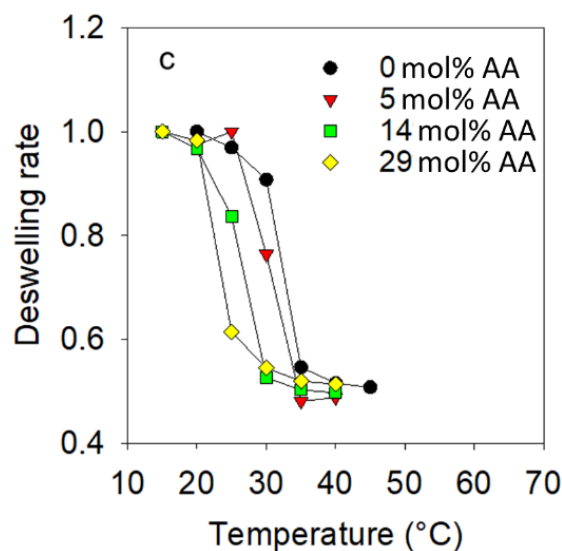


**Figure 4.3.** Deswelling of microgels with different fractions of AA units as a function of the temperature at pH 7 in pure water (a) or in 100 mM NaCl (b) or at pH 3 in pure water (c).

## 4.2. Emulsion microstructure and stability

In first instance, we will focus on the properties of emulsions containing microgels with  $F_{AA} = 14$  mol%. We will present results on the effect of varying the pH without added salt, the effect of the NaCl concentration at pH 7 and the combined effects of reducing the pH to 3 and adding 100 mM NaCl. Measurements were done at 20 °C and 50 °C to see the effect of increased hydrophobic interactions between the NIPAM units. Finally, the effect of varying the fraction of AA units will be discussed.

### 4.2.1 Effect of the pH

The microstructure of D/P and P/D emulsions with charged microgels did not depend significantly on the pH, see Fig. 4. No distinct layer of charged microgels at the interface was observed at any pH. This is in stark contrast with emulsions containing corresponding neutral microgels for which the layer is clearly visible, see **Figure 4.4**. In all systems, the microgels preferred the PEO phase over the DEX phase. The ratio of the microgel concentration in DEX over that in PEO was approximately 0.65 for charged microgels in D/P emulsions and 0.39 in

P/D emulsions independent of the pH, see **Figure 4.5**. The same partition was approximately found for the neutral microgels.

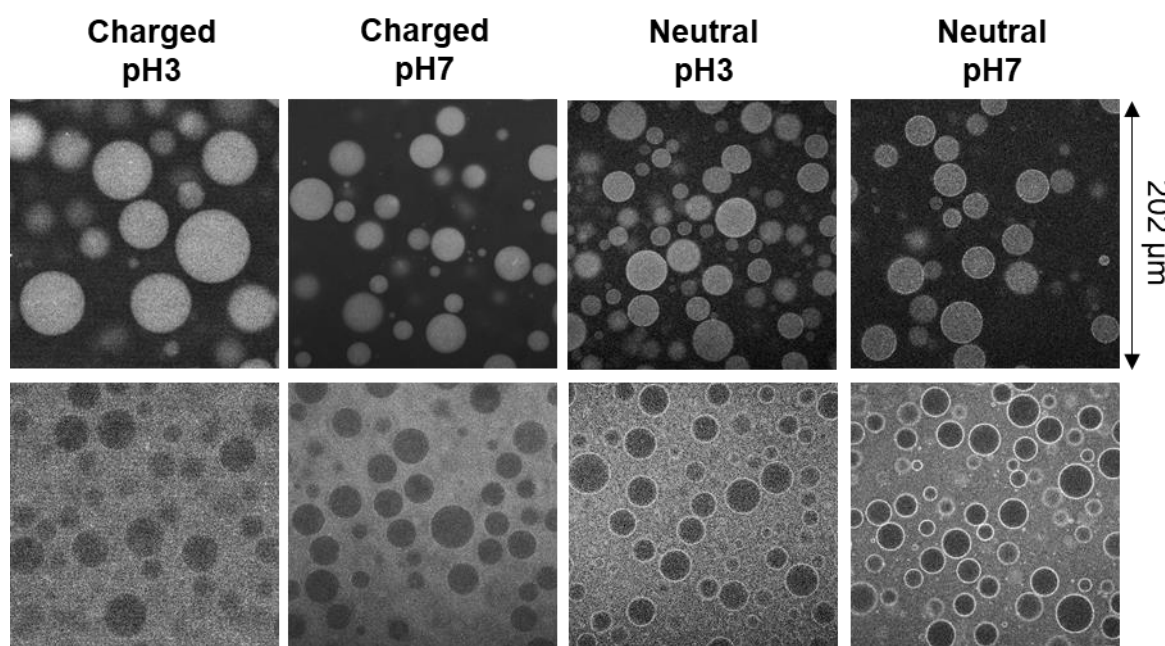


**Figure 4.4.** CLSM images of P/D (top) and D/P (bottom) emulsions at 20 °C with neutral microgels and charged microgels ( $F_{AA} = 14 \text{ mol}\%$ ) at different pH as indicated in the figure.

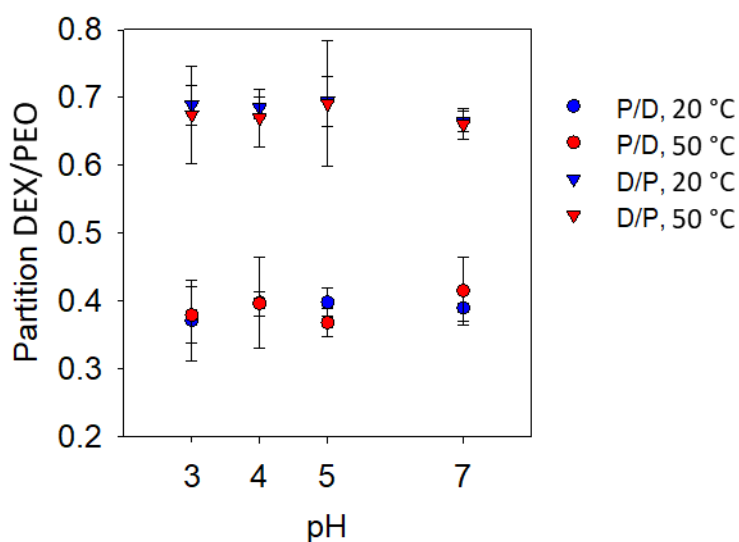


**Figure 4.5.** Partition of charged microgels ( $F_{AA} = 14 \text{ mol}\%$ ) in P/D and D/P emulsions as a function of the pH at 20 °C and 50 °C. Averages over at least 10 droplets and standard deviations are shown.

The stability of the emulsions was quantified by measuring the transmission profiles at different times during centrifugation at 470g and determining a characteristic stabilization time ( $t_c$ ), as was explained in section 2.2.3. The results at 20 °C show that the stability of D/P or P/D emulsions during centrifugation was not clearly improved by the presence of charged microgels with  $t_c \approx 200$  s independent of the pH, whereas  $t_c \approx 150$  s in the absence of microgels, see **Figure 4.6a**. Adding neutral microgels was also not very effective in stabilizing P/D emulsions, but it was more effective in D/P emulsions for which  $t_c \approx 500$  s. There was no significant effect of the pH in the presence of neutral microgels. It's worthy to notice that the trends are similar at 1g and 470g. Centrifugation accelerates destabilization and allows us to distinguish between systems that are stable for more than a week under gravity, which is the case when  $t_c(470G) > 10^3$  s. Under gravity,  $t_c$  is at least two orders of magnitude higher than that under acceleration for neutral particles, see **Figure 4.7**. In addition, D/P emulsions present a higher stability at 1g.

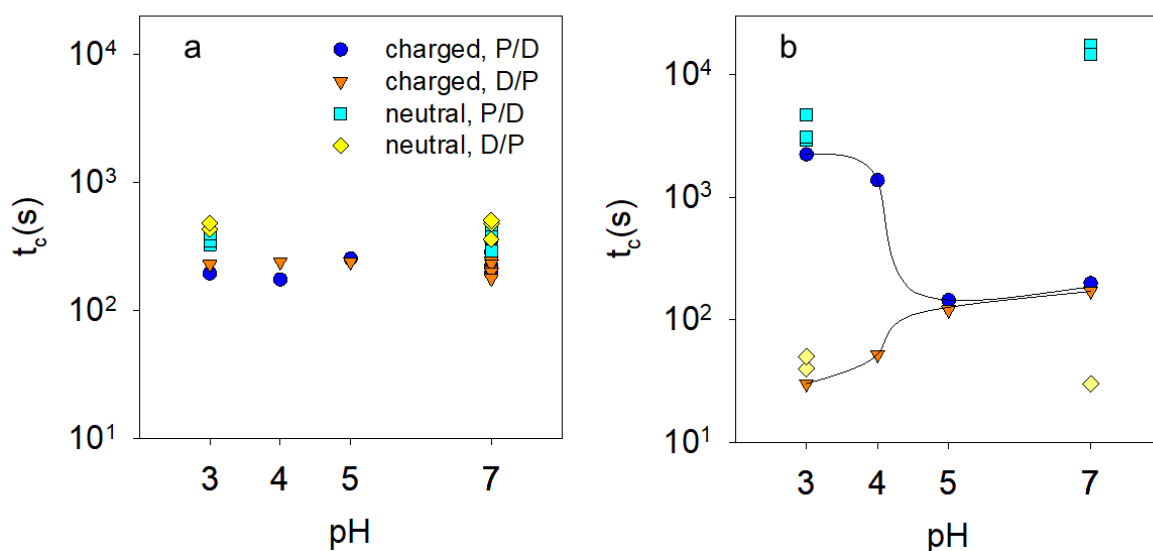


**Figure 4.6.** Characteristic stabilization times of P/D and D/P emulsions at 20 °C (a) or 50 °C (b) with neutral microgels or charged microgels ( $F_{AA} = 14$  mol%) at different pH as indicated in the figure.

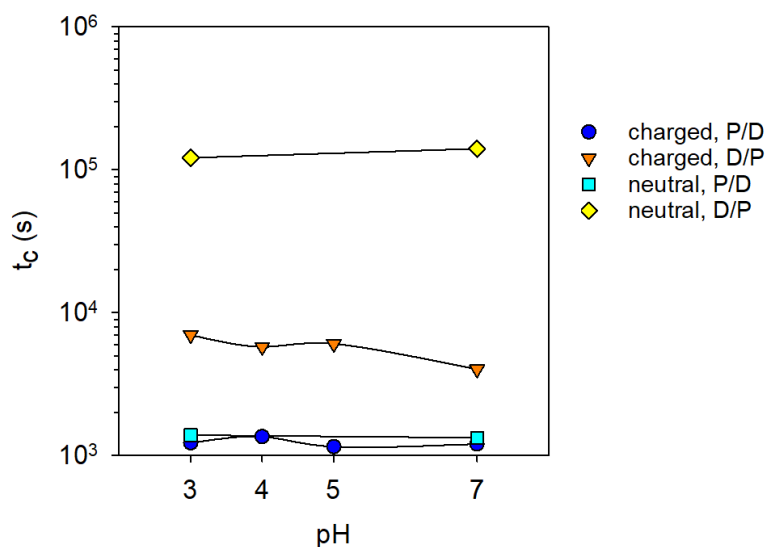


**Figure 4.7.** Characteristic stabilization times of P/D and D/P emulsions under gravity at different pH stabilized by neutral and charged microgels ( $F_{AA} = 14 \text{ mol}\%$ ) at  $20 \text{ }^\circ\text{C}$

The emulsions that were formed at  $20 \text{ }^\circ\text{C}$  did not change their morphology after heating to  $50 \text{ }^\circ\text{C}$ , see **Figure 4.8**. However, some aggregates of microgels were formed at  $50 \text{ }^\circ\text{C}$  in the D/P emulsions at pH 3 and pH 4, which had a tendency to adsorb at the interface, but we don't think that these aggregates had an influence on the stability of the emulsions. The partitioning of the microgels between the phases remained the same after heating to  $50 \text{ }^\circ\text{C}$  within the experimental error, see **Figure 4.5**.

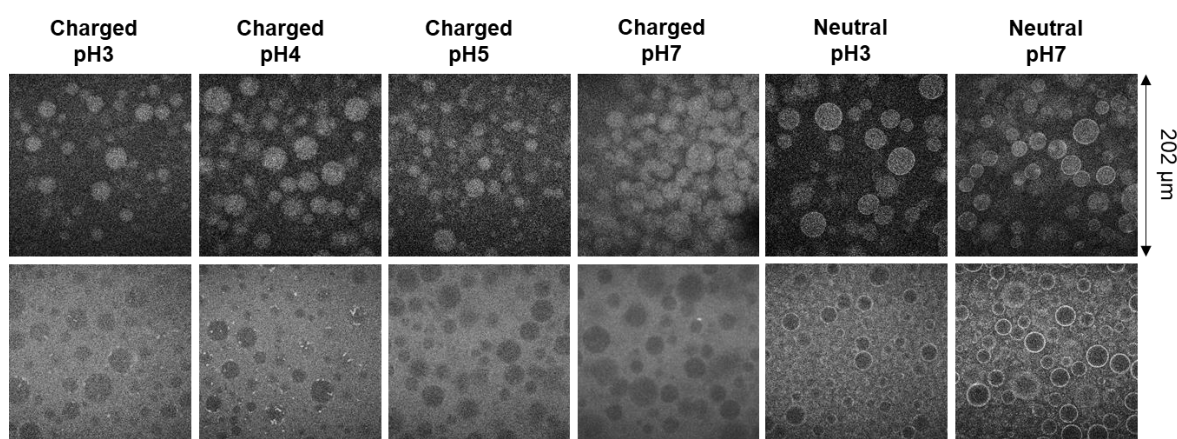


**Figure 4.8.** CLSM images of P/D (top) and D/P (bottom) emulsions at  $50 \text{ }^\circ\text{C}$  with charged microgels ( $F_{AA} = 14 \text{ mol}\%$ ) at different NaCl concentrations at pH 7

At pH 5 and 7, heating to 50 °C did not have a significant effect on the stability of the D/P and P/D emulsions with charged microgels, see **Figure 4.6b**. However, at pH 3 and pH 4, the P/D emulsion was much more stable after heating, whereas the D/P emulsion was less stable. At pH 3, the effect of heating on the stability of the P/D and D/P emulsions with charged microgels was similar to that with the equivalent neutral microgels, but at pH 7 the D/P emulsion was much more stable in the presence of neutral microgels. The strong difference of stability between D/P and P/D emulsions at pH 7 with neutral microgels was not observed with charged microgels, which may be related to the fact that the latter did not shrink much during heating, see **Figure 4.1**.

#### *4.2.2. Effect of salt*

**Figure 4.9** shows CLSM images of emulsions containing fully charged microgels at pH 7 after adding different amounts of NaCl. It is clear that screening the electrostatic interactions by adding NaCl induced adsorption of charged microgels at the interface in both P/D and D/P emulsions, but more strongly in the latter. In addition, the average size of the DEX droplets in D/P emulsion decreased strongly when NaCl was added from 23  $\mu\text{m}$  on average without salt to 10  $\mu\text{m}$  if more than 20 mM NaCl was added, see **Figure 4.10**, whereas for the P/D emulsion, it remained constant at approximately 22  $\mu\text{m}$ . Screening electrostatic interactions through salt addition did not have the same effect as reducing the charge by lowering the pH. The microstructure of emulsions with neutral microgels was not influenced by the addition of salt.

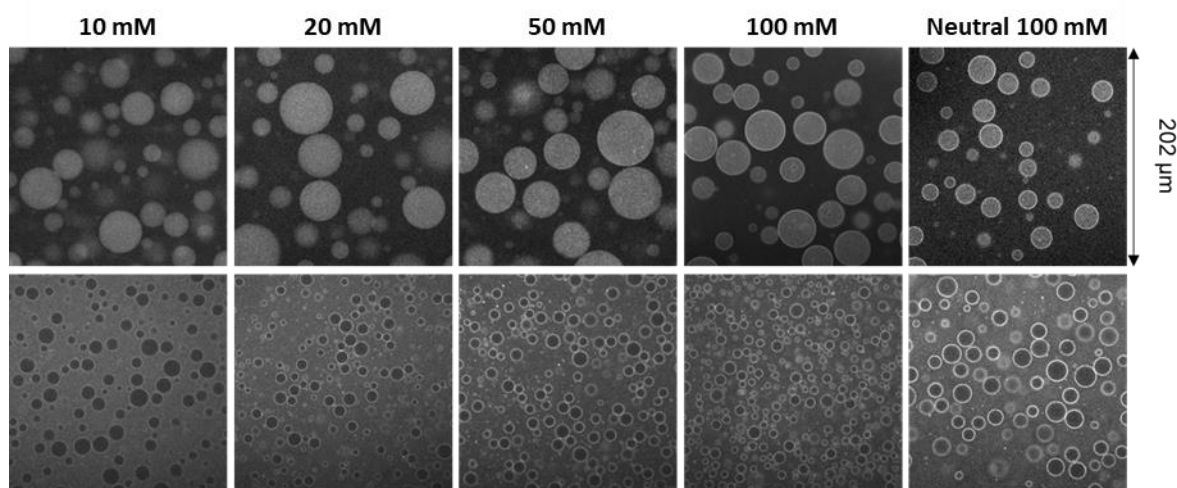


**Figure 4.9.** CLSM images of P/D (top) and D/P (bottom) emulsions at 20 °C with charged microgels ( $F_{AA} = 14 \text{ mol\%}$ ) at different NaCl concentrations at pH 7, as indicated in the figure. Results with neutral microgels at 100 mM NaCl are also shown for comparison.

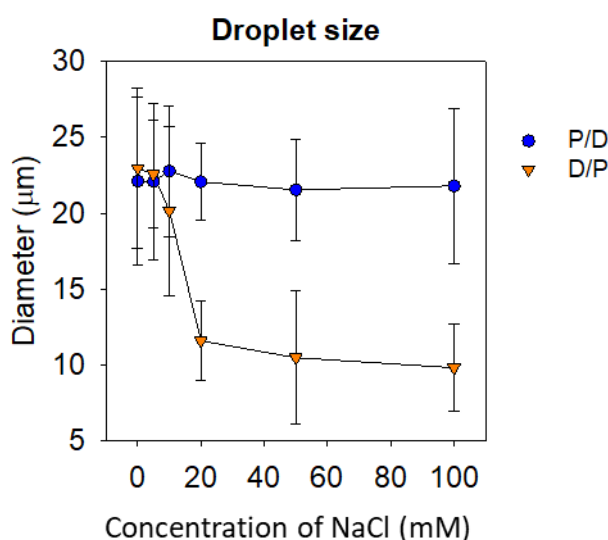


**Figure 4.10.** Average droplet diameter in a P/D and a D/P emulsion with charged microgels ( $F_{AA} = 14 \text{ mol\%}$ ) as a function of the NaCl concentration at pH 7 at 20 °C. Averages from different images containing many droplets and standard deviations are shown.

The concentration ratio of the charged microgels between the DEX and PEO phases increased weakly with increasing NaCl concentration up to 0.89 at 100 mM for the D/P emulsions and remained at 0.39 for the P/D emulsions, see **Figure 4.11**. For the D/P emulsion, the excess fluorescence intensity due to charged microgels at the interface increased progressively with increasing NaCl concentration to about 2.5 times the intensity in PEO phase

at 100 mM NaCl, see **Figure 4.12**. For the P/D emulsion, the excess at the interface was only significant at higher concentrations of NaCl (about 1.5 times that in PEO phase at 100 mM NaCl). It's worth noting that the excess fluorescence at the interface was larger for neutral microgels (about 3.5 times in D/P and 2.2 times in P/D).

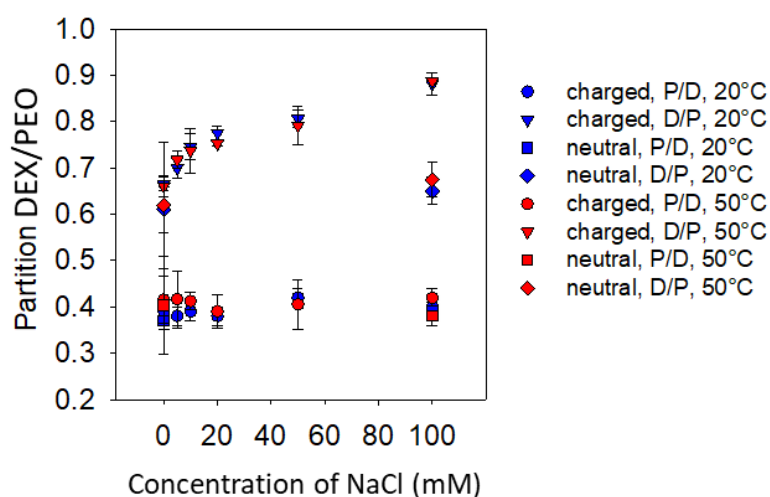


**Figure 4.11.** Partition of charged microgels ( $F_{AA} = 14 \text{ mol}\%$ ) in P/D and D/P emulsion as a function of the NaCl concentrations at pH 7 both at 20 °C and at 50 °C. Averages over at least 10 droplets and standard deviations are shown.

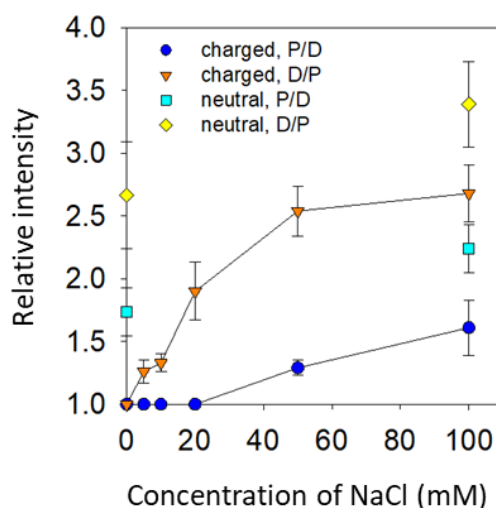


**Figure 4.12.** Excess fluorescence intensity at the interface with respect to that of the PEO phase for neutral and charged microgels ( $F_{AA} = 14 \text{ mol}\%$ ) in P/D and D/P emulsion as a function of the NaCl concentrations at pH 7 at 20 °C. Averages over at least 10 droplets and standard deviations are shown.



The D/P emulsion was found to be much more stable when NaCl was added, whereas the effect was weak for the P/D emulsion. D/P emulsions with charged microgels at 100 mM NaCl were stable for at least one week showing no significant change in the microstructure and no signs of sedimentation under gravity. The characteristic stabilization times are plotted as a function of the NaCl concentration in **Figure 4.13a** showing that the stability improved markedly with increasing NaCl concentration for the D/P emulsion, but the effect was negligible for the P/D emulsion. The effect of adding salt on the stability of emulsions with neutral microgels was small for both P/D and D/P emulsions. At 1g, the trends are the same as at 470g, except that  $t_c$  is much larger especially for charged particles where above 10 mM, no change was observed even after a week, see **Figure 4.14**.

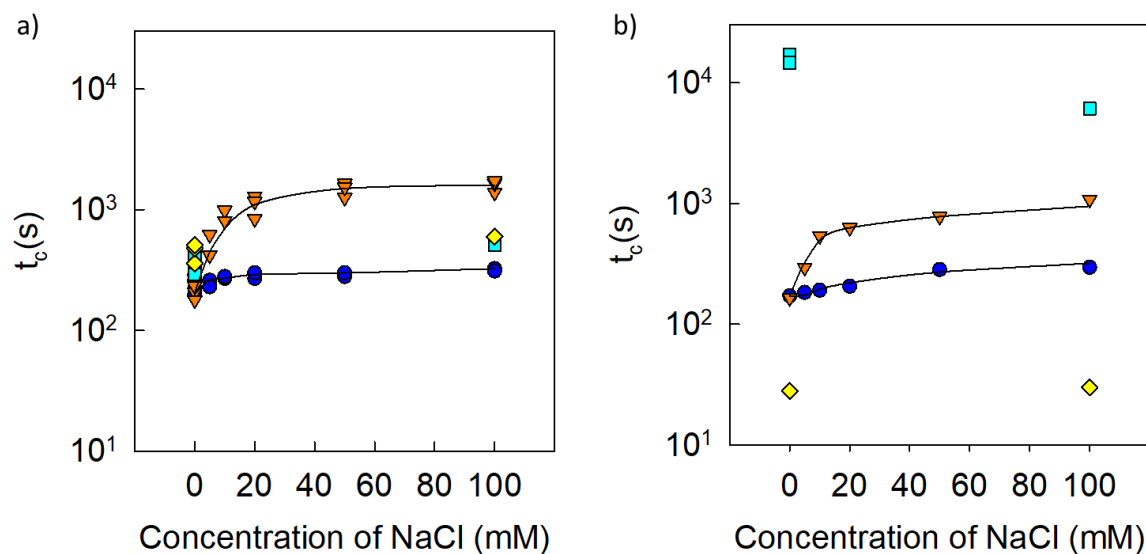


**Figure 4.13.** Characteristic stabilization times of emulsions with neutral and charged microgels ( $F_{AA} = 14 \text{ mol}\%$ ) in different NaCl concentration at 20 °C (a) and 50 °C (b).



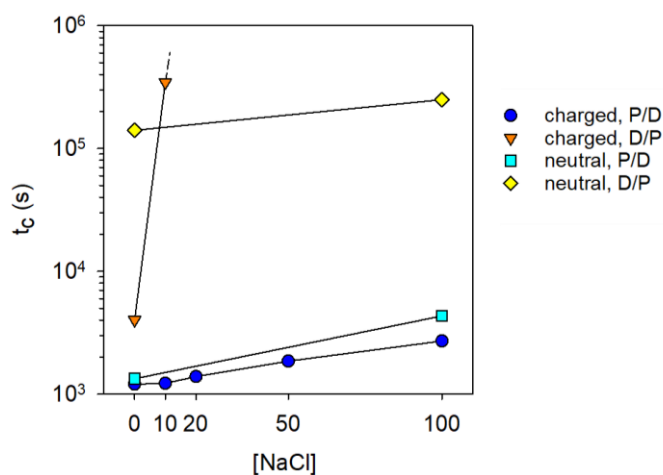


**Figure 4.14.** Characteristic stabilization times of P/D and D/P emulsions at 1g with neutral and charged microgels ( $F_{AA} = 14$  mol%) in different NaCl concentration at 20 °C

Heating solutions prepared at 20 °C to 50 °C did not have a significant effect on the morphology of the emulsions, see **Figure 4.15**, nor on the partitioning, see **Figure 4.11**. The stabilizing effect of adding salt for the D/P emulsion at 20 °C was also observed at 50 °C, albeit to a lesser extent, see **Figure 4.13b**. In fact, the charged microgels behaved similarly at 20 °C and 50 °C, which could be explained by the weak effect of heating on the size of the microgels, see **Figure 4.1**.

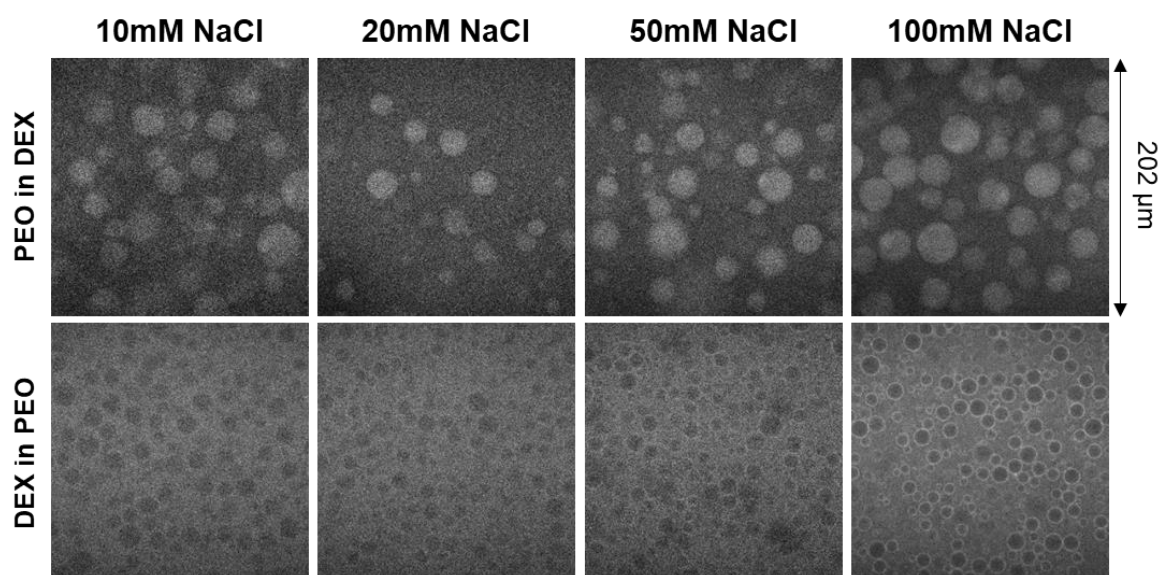


**Figure 4.15.** Microstructure of P/D and D/P emulsions with charged microgels ( $F_{AA} = 14$  mol%) in different NaCl concentrations at pH 7 at 50 °C

#### 4.2.3. Combined effect of pH and salt

To study the combined effects of low charge density and screening, emulsions were prepared at pH 3 and in 100 mM NaCl. **Figure 4.16** shows that adding salt favored adsorption of the microgels at the interface also at pH 3 for both D/P and P/D emulsions even though their charge density at pH 3 was very small. However, adding salt at pH 3 had little effect on the droplet size or the stability either at 20 °C or at 50 °C. Thus, the spectacular effect of the addition of salt on the D/P emulsion observed with the fully charged microgels at pH 7 was not reproduced at pH 3, which means that a high density of charges is necessary to induce the effect. We expect that the effect of salt on the stability of the D/P emulsion will be intermediate at intermediate pH between very strong at pH 7 and very weak at pH 3.

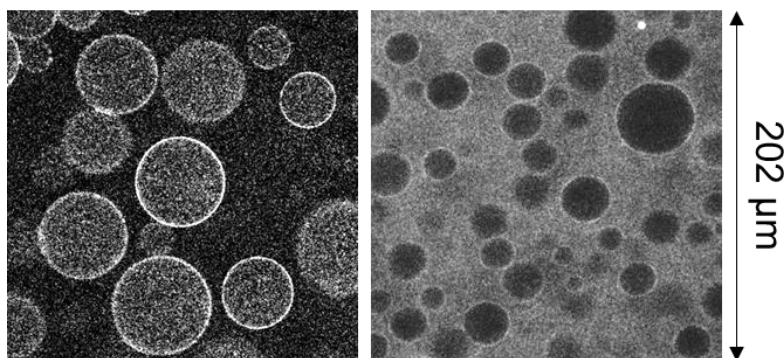


**Figure 4.16.** CLSM images of P/D (left) and D/P (right) emulsions at 20 °C with charged microgels ( $F_{AA} = 14 \text{ mol}\%$ ) in 100 mM NaCl at pH 3.

#### 4.2.4. Effect of the fraction of acrylic acids units

So far we have discussed the properties of emulsions containing microgels with  $F_{AA} = 14 \text{ mol}\%$ . The effect of varying the charge density was investigated by comparing emulsions containing microgels with different fractions of AA units at pH 7. In the absence of salt, even including only 5 mol% AA units inhibited the microgels to accumulate at the interface, see **Figure 4.17**. In the presence of 100 mM NaCl, the microgels accumulated at the interface at all charge densities and the size of the dispersed droplets decreased with increasing charge density.

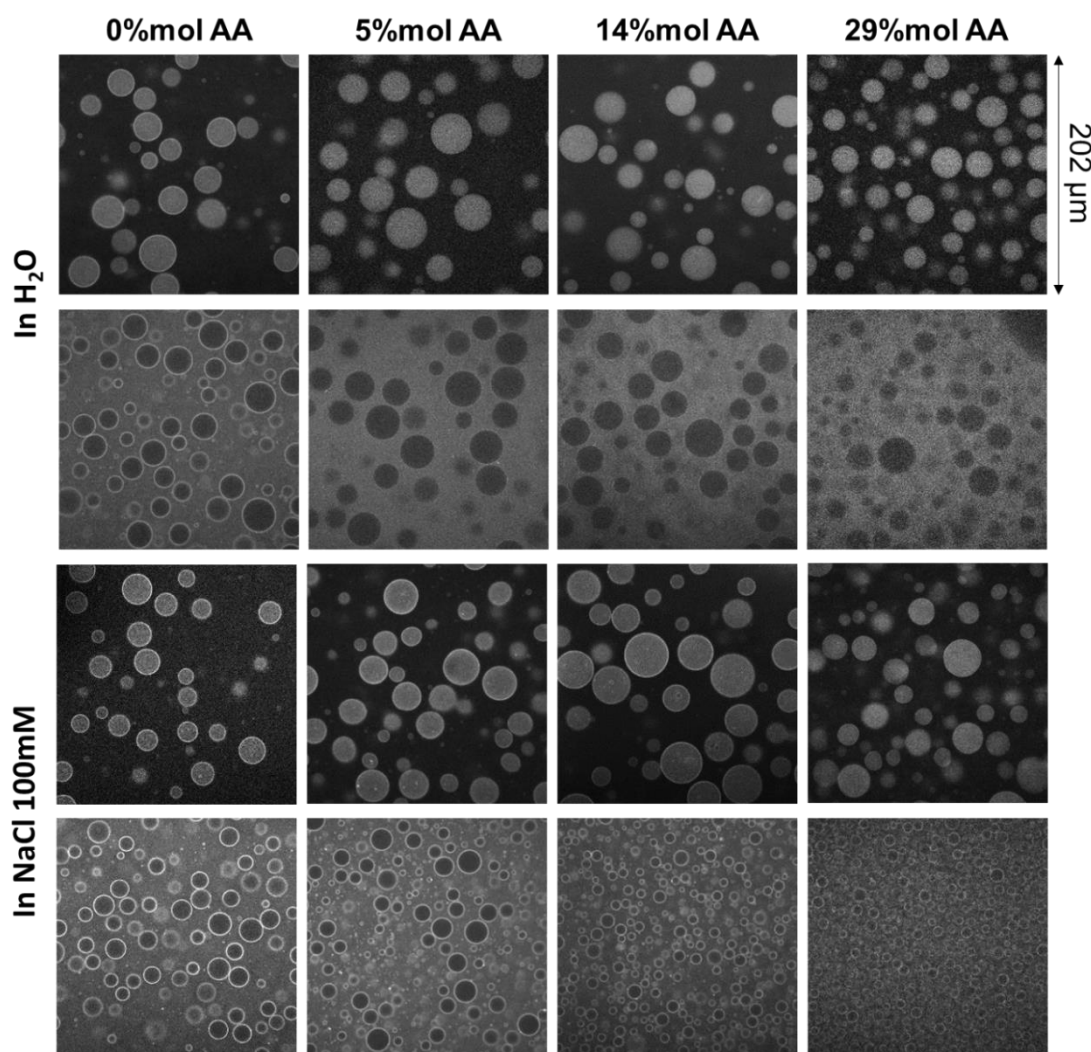


**Figure 4.17.** Microstructure of P/D and D/P emulsions with charged microgels at different fractions of acrylic acid units as indicated in the figure (20 °C, pH 7). The top two rows show the emulsions in pure water and the bottom two rows show the emulsions in 100 mM NaCl.

At 20 °C, the effect of the fraction AA in the microgels on the emulsion stability in the absence of salt was insignificant at pH 7, see **Figure 4.18a**. In section 4.2.1, we showed that the strong increase of the stability of the P/D emulsion with neutral microgels after heating to 50 °C disappeared when 14 mol% AA units were introduced into the microgels. **Figure 4.18a** shows that the effect of heating on the stability is still important at  $F_{AA} = 5$  mol%, albeit less than with neutral microgels. The addition of 100 mM NaCl did not improve the stability of the P/D emulsion at 20 °C, but the stability of D/P increased sharply with increasing fraction of charged units, see **Figure 4.18b**. Heating to 50 °C decreased the stability of the P/D emulsion at low

charge density and the D/P emulsion at high charge density. At pH 3, where the AA units are neutral, the effect of  $F_{AA}$  on the stability was relatively small showing a weak decrease of the stability with increasing fraction of AA units, see **Figure 4.19**.

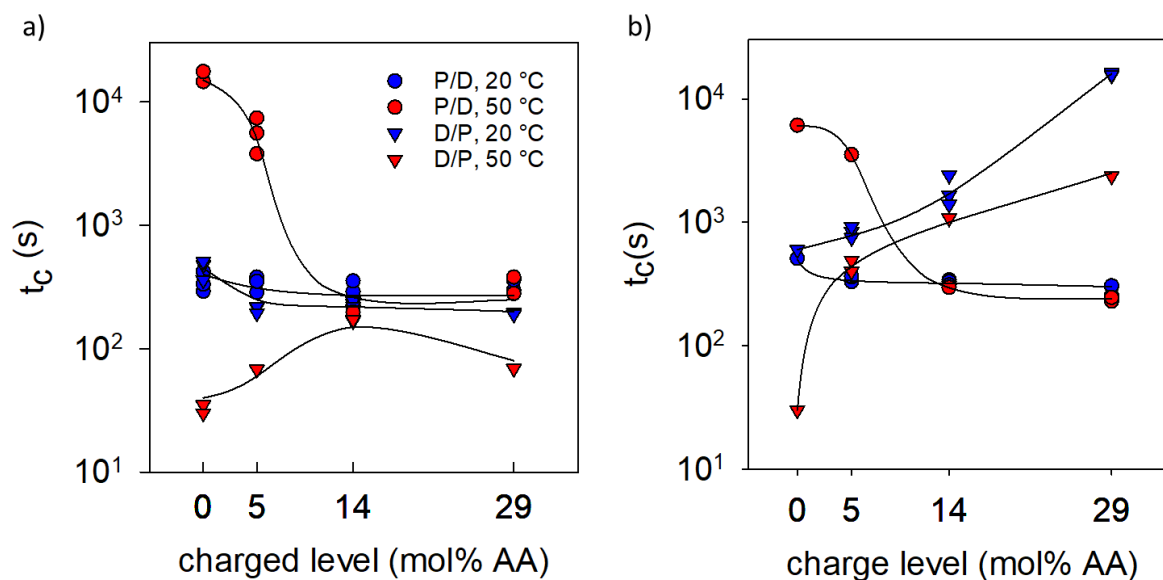


**Figure 4.18.** Dependence on  $F_{AA}$  of the characteristic stabilization time for P/D and D/P emulsions at pH 7 without (a) or with NaCl 100 mM (b) at 20 °C or 50 °C, as indicated in the figure.

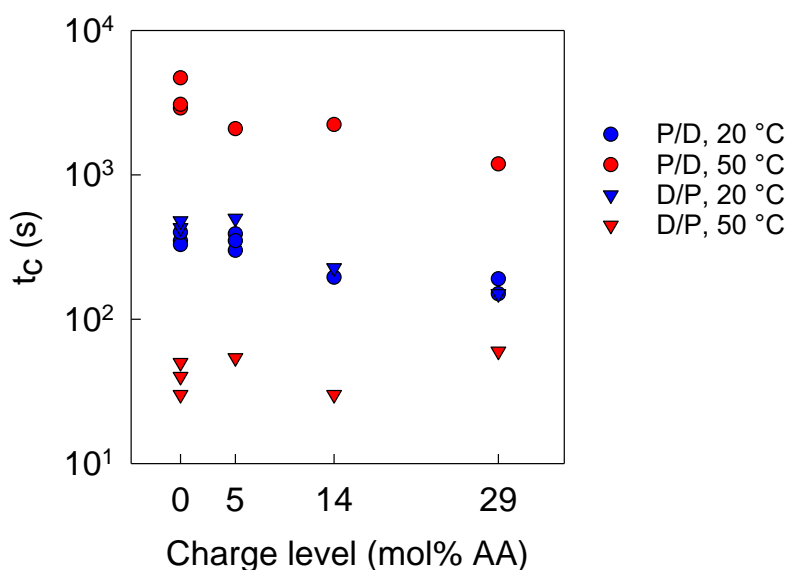


**Figure 4.19.** Characteristic stabilization times of emulsions stabilized by different charged microgels at pH 3 without NaCl at 20 °C and 50 °C

## Conclusions

Charged microgels swell in water due to electrostatic interactions. Decreasing the charge density by decreasing the pH or screening the interaction by the addition of NaCl causes deswelling of the microgels. Merland et al. have already shown that neutral bishydrophilic microgels shrink when the solution is heated above 32 °C [10], because pNIPAM units dehydrate. Here we find that introducing charges into these microgels inhibits deswelling during heating due to strong electrostatic repulsion both in pure water and in the presence of salt. The effect of deswelling during heating is recovered when the charge density is reduced by lowering the pH. At low pH, deswelling starts at lower temperatures when more NIPAM units are replaced by neutral AA units.

Different types of particles have been used in the past to stabilize W/W emulsions [16, 49, 59, 61, 78], but none showed a dependence both on temperature and pH. Elsewhere, Merland et al. [10] showed that by using bis-hydrophilic microgels containing both NIPAM and DEX, the stability of a W/W emulsion depends on the temperature. Here we show that by introducing AA units into the bis-hydrophilic microgels the stability depends on both the temperature and the pH. Charged bis-hydrophilic microgels are less efficient in stabilizing emulsions than the corresponding neutral microgels that were studied in and adsorb less at the interface. Screening the electrostatic repulsion between the microgels at pH 7 by adding salt increases the density of the microgels at the interface and improves the stability, in particular for the D/P emulsion. Adding salt also causes a decrease of the dispersed drop size in D/P emulsions. The stability is not improved at pH 3, where electrostatic repulsion is very small, even though the addition of salt promotes the adsorption of the microgels at the interface also at pH 3.

Elsewhere, it was shown that heating strongly improved the stability P/D emulsions with neutral microgels and decreased the stability of D/P emulsions [10]. No such effect was

observed for strongly charged microgels, but it was recovered when the microgels were neutralized by decreasing the pH. The stabilizing effect of adding salt for D/P emulsions was also observed after heating.

The effects of varying the pH or adding NaCl on the stability of the emulsions cannot be related directly to the partition of the microgels between the phases and the interface as the latter depended little on the pH and the temperature. In an earlier study of the same W/W emulsion with another type of charged microgels, Nguyen et al. [61] showed different and contrary effects of varying the charge density and adding salt on the stability and the partition. The implication is that the chemistry of the microgels is more important than electrostatic interactions.



## **Chapter 5. Interaction between stabilized droplets of different phases in the same continuous phase of an aqueous three-phase system**

Droplets of the dispersed phase can be used to compartmentalize ingredients and induce localized reactions. By mixing more types of incompatible polymers, emulsions containing droplets of different phases can be formed that can potentially capture different ingredients. Here, the interaction between dispersed droplets of different types was studied by gently mixing a W/W emulsion containing droplets rich in DEX dispersed in a continuous phase rich in PEO (D/P) with an emulsion containing droplets rich in GEL dispersed in the same continuous medium (G/P). I will first report here an investigation of the effect of adding bishydrophilic microgels on the stability of G/P system and show that the microgels can also render this type of W/W emulsion very stable. Then I will show that when two microgel-stabilized emulsions are gently mixed, droplets of different dispersed phases are observed with CLSM to coalesce immediately upon contact. Contact angles between the different phases in emulsions with and without microgels are compared and used to determine the effect of the microgels on the interfacial tension between the phases. The obtained results have been published in *Soft Matter*, 2024, 20(15), 3359-3366.



|   |            |
|---|------------|
| <b>1. Stabilisation of GEL-PEO emulsions by bishydrophilic microgels.....</b> | <b>93</b>  |
| 1.1. Effect of microgel composition.....                                      | 93         |
| 1.2. Effect of the pH.....  | 96         |
| 1.3. Effect of charge on the microgels .....                                  | 100        |
| <b>2. Interaction between gelatin and dextran droplets .....</b>              | <b>103</b> |
| 2.1. Morphology .....   | 103        |
| 2.2. Stability .....  | 110        |
| <b>3. Conclusion.....</b>   | <b>114</b> |

## 5.1. Stabilization of GEL-PEO emulsions by bishydrophilic microgels

### 5.1.1. Effect of microgel composition

Binary emulsions of GEL droplets dispersed in a continuous PEO phase (G/P) were prepared with 0.05 wt% neutral bishydrophilic microgels with DEX at  $M_w = 6$  kDa and DS = 12, as described in section 2.1.3. The morphology of the emulsions at pH 7 containing neutral microgels with different DEX wt% observed with CLSM is shown in **Figure 5.1**. The microgels spontaneously adsorbed at the interface between the two phases and formed a layer around the droplets.

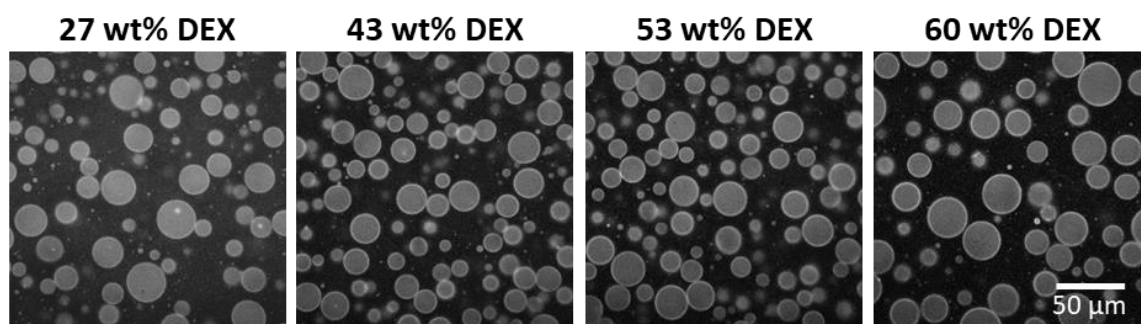


**Figure 5.1.** CLSM images of G/P emulsions at pH7 stabilized by neutral microgels with different DEX contents, as indicated in the figure

The excess of microgels partitioned preferentially to the GEL phase rather than in PEO phase. The contrast between two phases increases when they had a larger DEX content, see **Figure 5.2**. The density of microgels at the interface relative to that in the GEL phase also increased progressively with increasing DEX fraction, see **Figure 5.3**.

**Figure 5.4** shows that the stabilizing effect of the microgels on the P/G emulsion was weak, but it was more efficient for the G/P emulsion. The G/P emulsion containing microgels with 27 wt% DEX began to destabilize after 2 days, whereas emulsions with microgels containing more DEX remained stable for at least one week showing sedimentation of the GEL droplets without formation of a homogeneous GEL layer. As was mentioned in the

Introduction, it is not clear why the effect on the stability can be very different depending on which phase is the dispersed even if the interfacial tension is the same. We speculate that interaction between microgels in different phases plays a role.

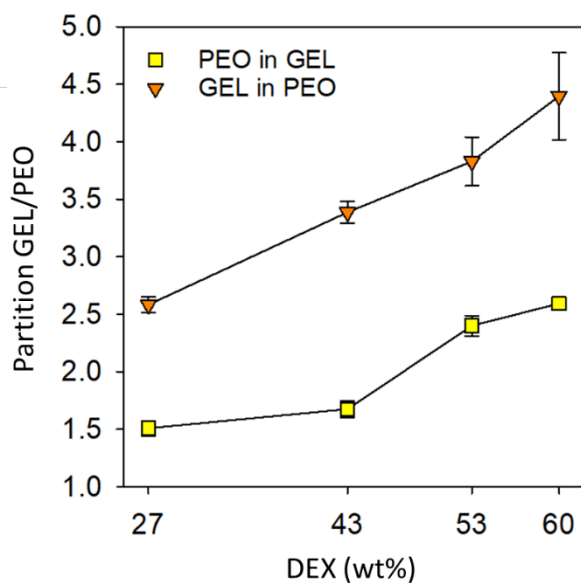


**Figure 5.2.** Partition of microgels in P/G and G/P emulsions as a function of the weight fraction of DEX in the microgels at pH7 at 20°C. Averages over at least 10 droplets and standard deviations are shown.

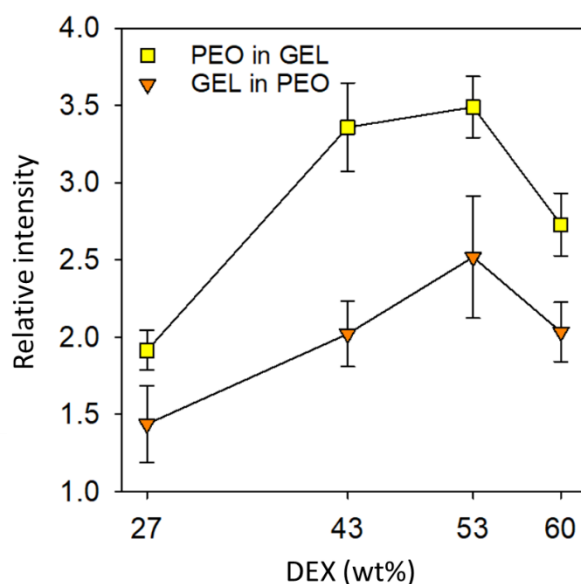


**Figure 5.3.** Excess fluorescence intensity at the interface of droplets compared to that in GEL phase as a function of the weight fraction of DEX in the microgels at pH7 at 20 °C. Averages over at least 10 droplets and standard deviations are shown.

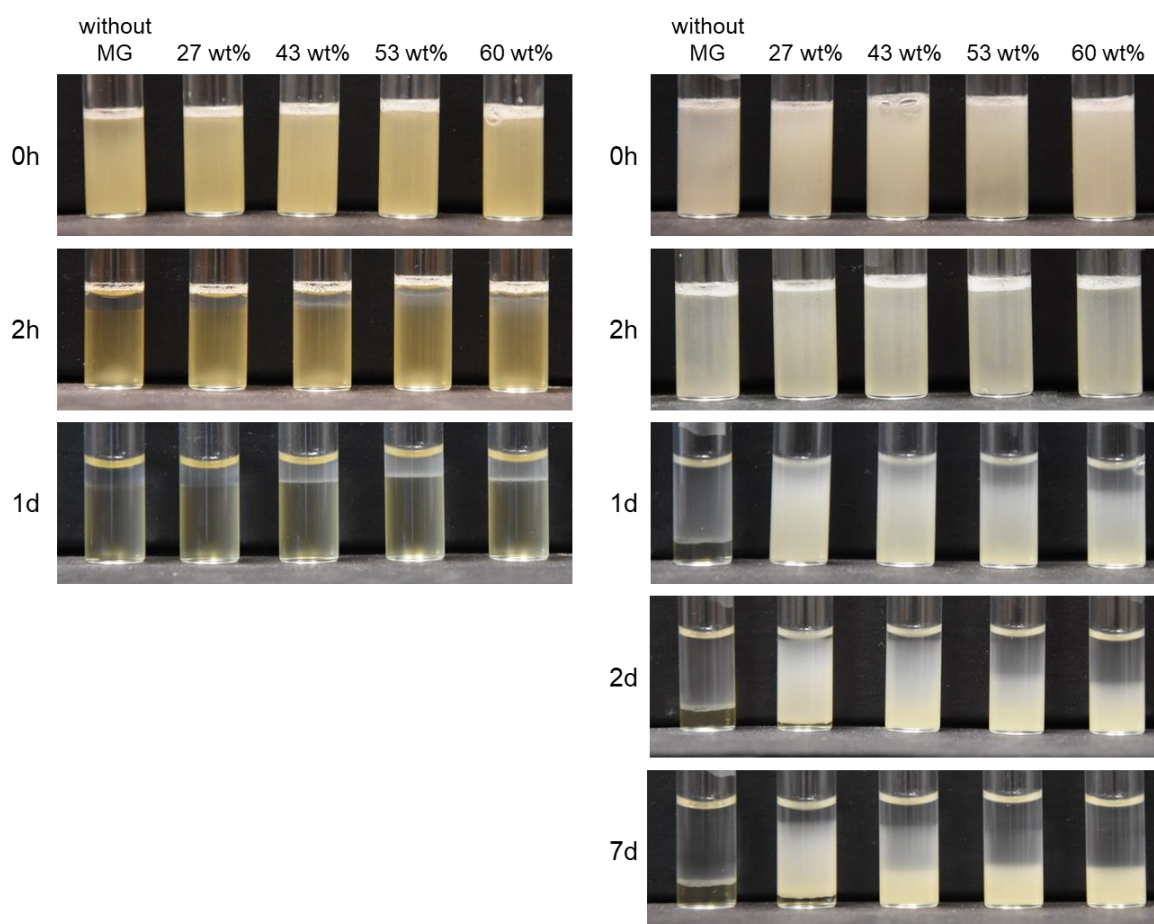


**Figure 5.4.** Photos of P/G and G/P emulsions at pH7 without or with 0.05 wt% neutral microgels with different weight fraction of DEX at different times after the preparation, as indicated in the figure

To quantify the stability of the emulsions, we measured the transmission profiles at different times during centrifugation at 470g and determined a characteristic stabilization time ( $t_c$ ), as was explained in section 2.2.3. The dependence of  $t_c$  on the weight fraction of DEX in the microgels is shown in **Figure 5.5** for G/P and P/G emulsions. For G/P emulsions,  $t_c$  increased sharply in the presence of microgels containing 43 wt% or more DEX. For P/G emulsions,  $t_c$  also increased with increasing % DEX, but remained much smaller than for G/P emulsions.

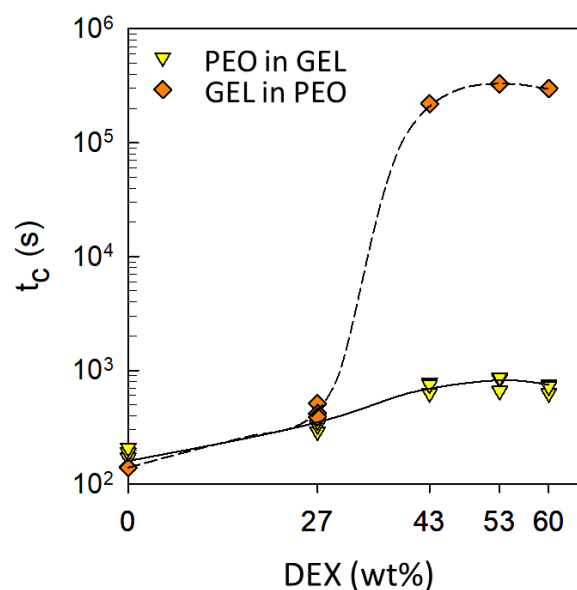


**Figure 5.5.** Characteristic stabilization times of P/G and G/P emulsions at pH7 with neutral microgels as a function of the weight fraction of DEX in the microgels.

### 5.1.2. Effect of the pH

GEL is not strongly charged between pH 6 and pH 9, but it has a sharply increasing positive or negative net charge density upon further decreasing or increasing the pH, respectively [46]. The effect of the pH on the microstructure of fresh G/P emulsions in the presence of neutral microgels with 53 wt% DEX is shown in **Figure 5.6**. The size of the GEL droplets was on average the same between pH 6 and pH 9 ( $13 \pm 2 \mu\text{m}$ ), but it was smaller at pH 5, 10.5 and 11, see **Figure 5.7**, because GEL partially mixed with the PEO phase [46]. GEL completely mixed with PEO below pH 4.5 and above 11.5. The mixing of GEL with the PEO phase at low and high pH is caused by the contribution of the counterion mixing entropy and its progressive character can be explained by the polydispersity of the GEL, with smaller chains becoming compatible at lower charge density. The microgels no longer adsorbed at the interface at pH 5, because the interfacial tension had become small. At high pH, the partition of microgels shifted to the PEO phase and the microgels had a tendency to form aggregates at the interface of GEL and PEO.

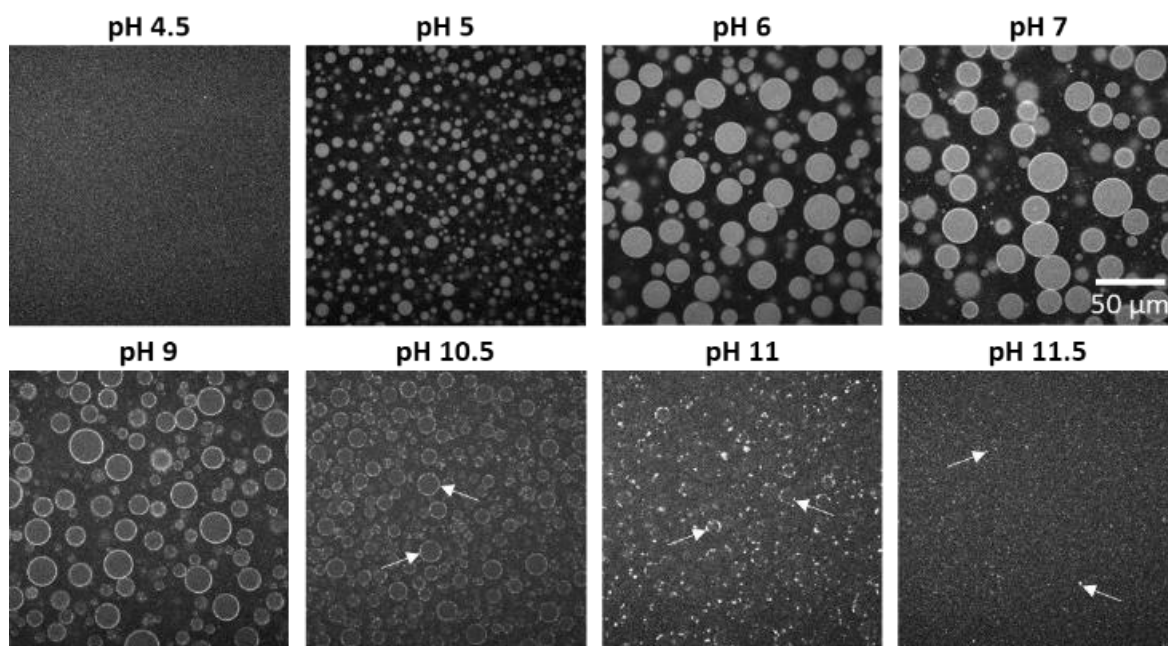


**Figure 5.6.** CLSM images of fresh G/P emulsions as a function of pH stabilized by neutral microgels with 53 wt% DEX. The arrows indicate microgel aggregates.

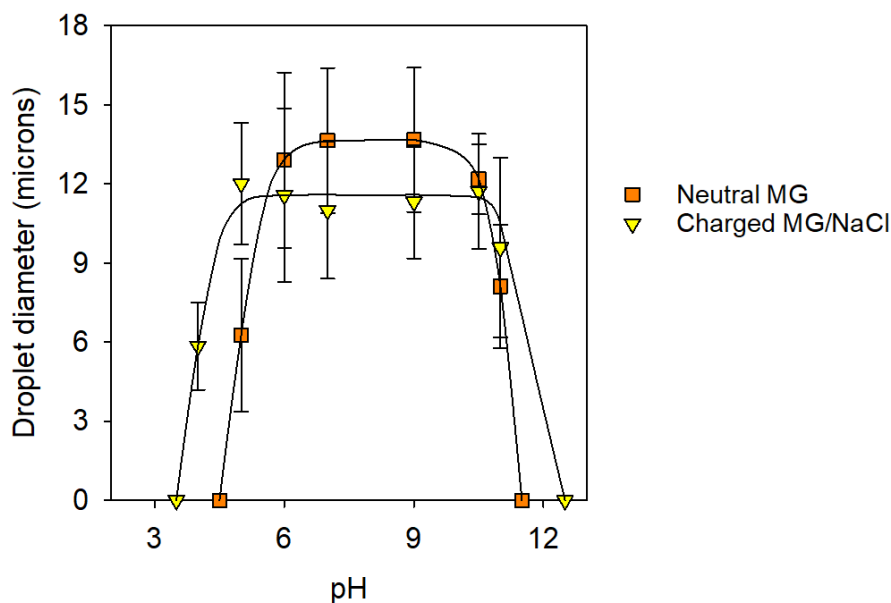


**Figure 5.7.** Droplet size of G/P emulsions stabilised by neutral microgels with 53 wt% DEX and charged microgels/NaCl as a function of pH.

The morphology of the emulsions at different pH was observed as a function of time during ageing, see **Figure 5.8**. The evolution of droplet size is shown in **Figure 5.9**. At all pH, the droplets grew with time, leading at pH 5 to the formation of a continuous GEL phase after

7 days. Between pH 6 and 9, the droplets coalesced and sedimented but remained stable for at least one week. At pH 11, the microgels tended to aggregate leading to deformed and aggregated droplets, that remained nevertheless stable for at least 1 week. Measurements of the characteristic stabilization time as a function of the pH showed that the system was most stable close to neutral pH, see **Figure 5.10**.

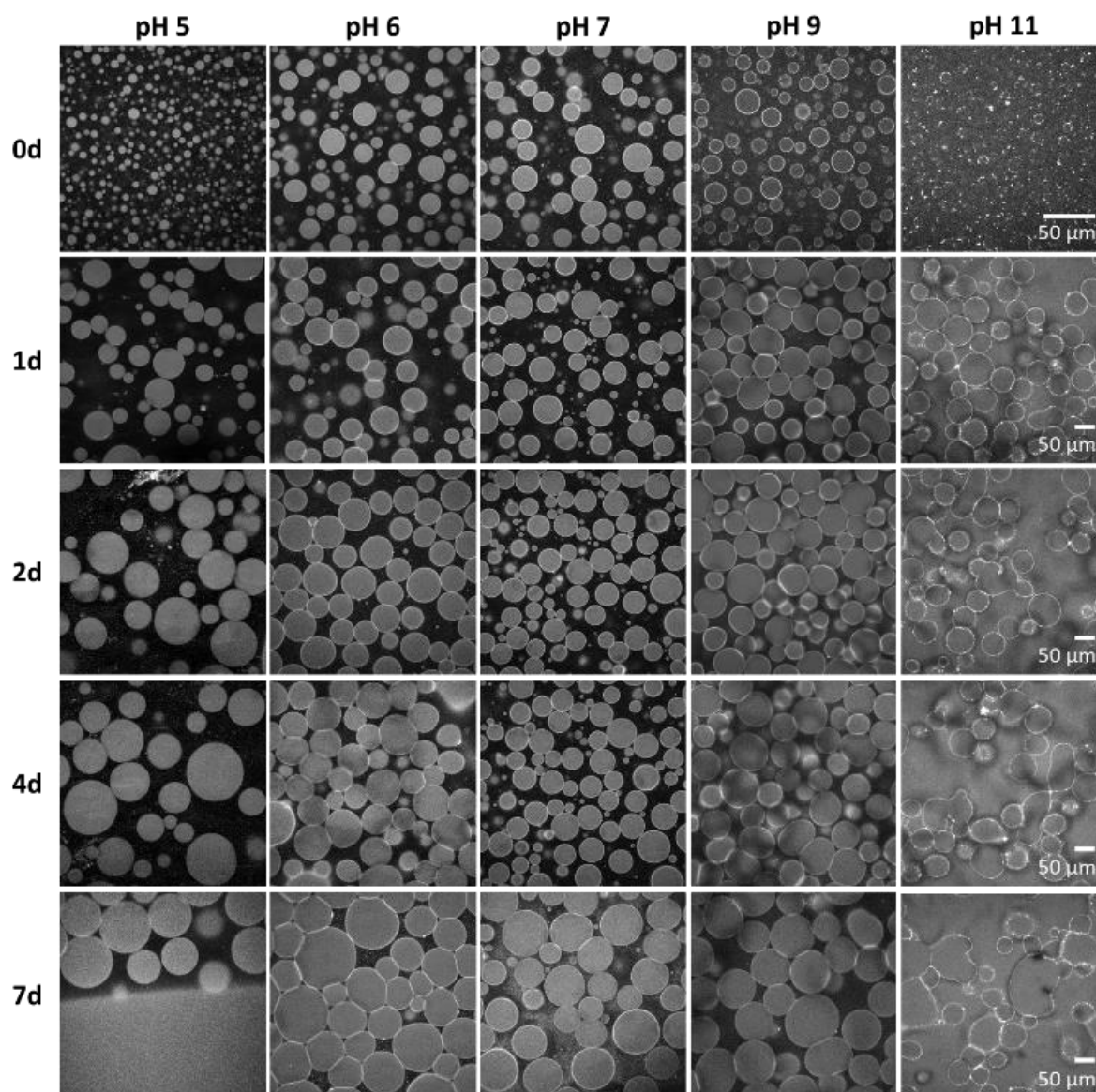


**Figure 5.8.** CLSM images of G/P emulsions at different pH stabilized by neutral microgels with 53 wt% DEX as a function of time. Notice that the scale of the images of the fresh emulsions is different from that of the aged emulsions.

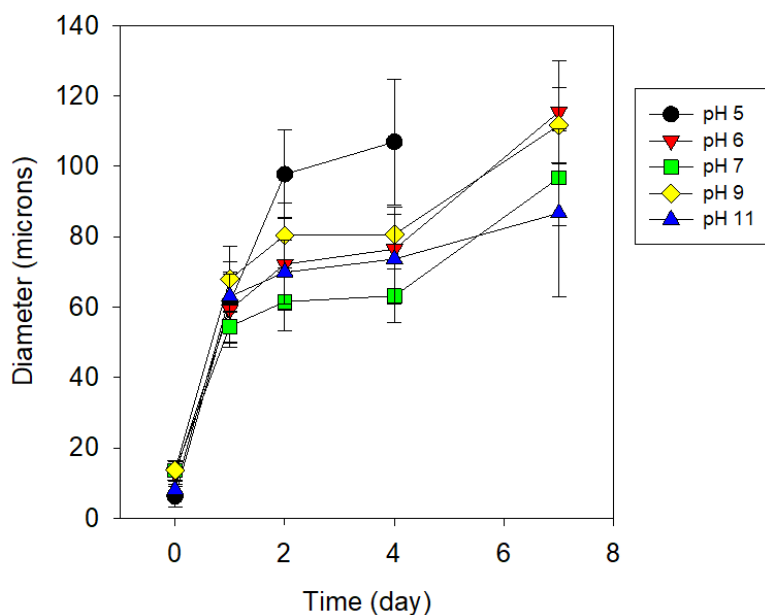


**Figure 5.9.** Evolution of droplet size in G/P emulsions stabilized by neutral microgels with 53 wt% DEX at different pH as a function of time.

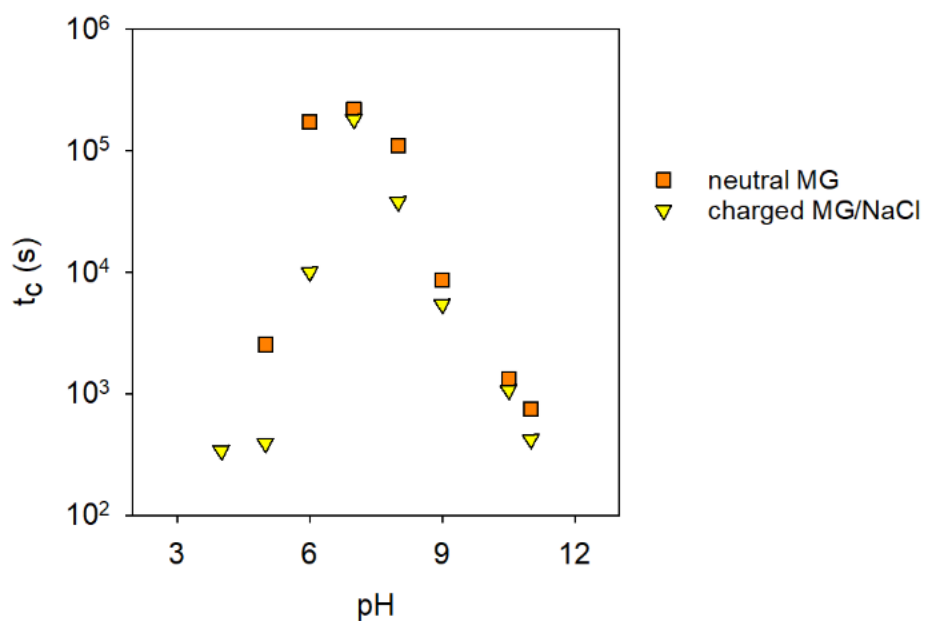


**Figure 5.10.** Characteristic stabilization times of G/P emulsions with neutral microgels (53 wt% DEX) in water or charged microgels in 100 mM NaCl as a function of the pH.



### 5.1.3. Effect of charge on the microgels

The presence of charged units inhibited the adsorption of the microgels at the W/W interface of G/P emulsions at pH 7, see **Figure 5.11**, so that they no longer stabilized the emulsion. However, after adding 100 mM NaCl, the charged microgels did adsorb at the interface and the emulsion was stable for at least one week showing weak growth of the droplet size, whereas P/G emulsions destabilized within 1 day, see **Figure 5.12**.

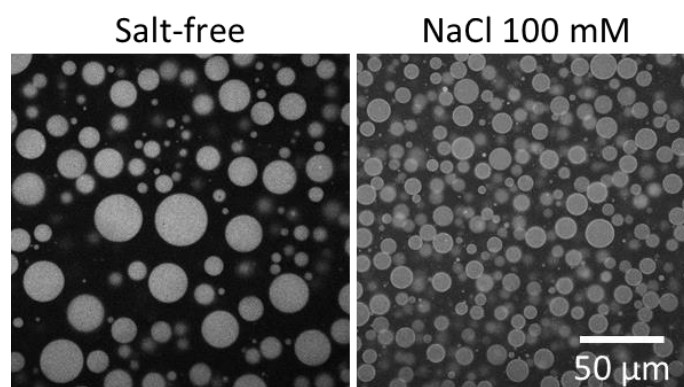


**Figure 5.11.** CLSM images of emulsions of G/P emulsions at pH7 stabilized by charged microgels in water and NaCl 100 mM.

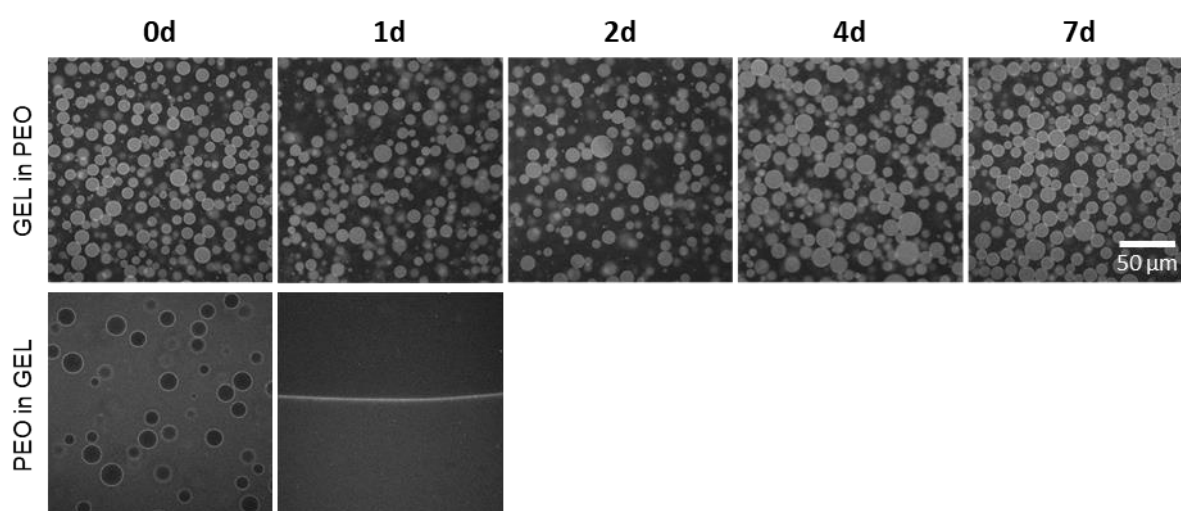


**Figure 5.12.** CLSM images of G/P and P/G emulsions at pH7 stabilized by charged microgels in NaCl 100 mM as a function of time.

The pH range over which the GEL phase is separated is slightly wider in the presence of 100 mM NaCl (from pH 3.5 to 12.5). There is not much difference in droplet size from pH 5 to pH 10.5 and it was close to that with neutral microgels ( $11 \pm 2 \mu\text{m}$ ). Here also the droplet size decreased at lower (pH 4) and higher (pH 11), see **Figure 5.7**. The effect of pH on the stability of the G/P emulsion with charged microgels in NaCl was similar to that with neutral microgels showing a maximum stability at neutral pH, see **Figure 5.10** and **Figure 5.13**. The coalescence of droplet is very limited between pH 7 and pH 9, while the droplet size increased more quickly at pH 6 and pH 10.5, see **Figure 5.14**.

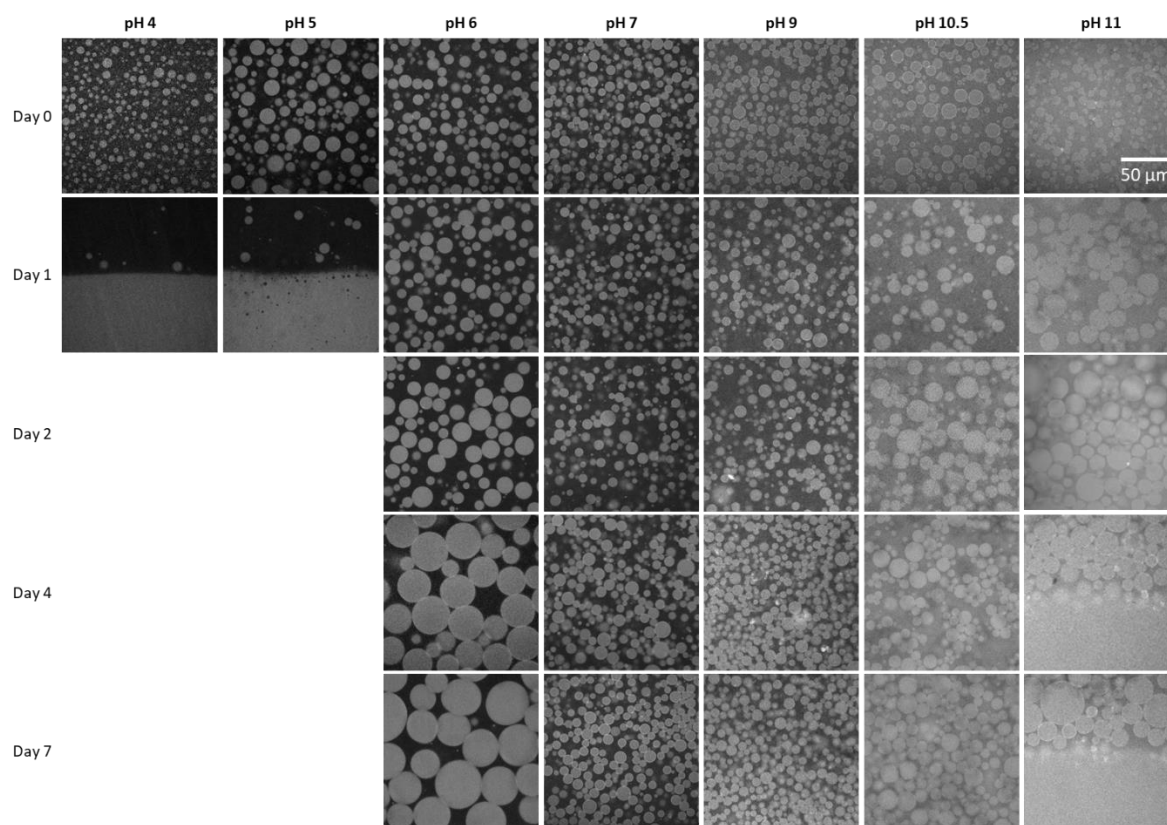


**Figure 5.13.** CLSM images of G/P emulsions at different pH stabilized by charged microgels in NaCl 100 mM as a function of time as indicated in the figure.

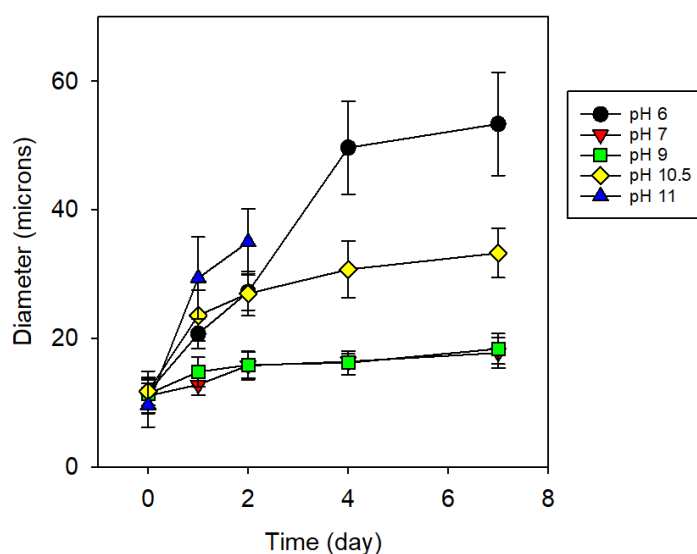


**Figure 5.14.** Evolution of droplet size in G/P emulsions stabilized by charged microgels in NaCl 100 mM at different pH as a function of time.

The system become unstable and started to form a continuous phase of GEL after 1 day at lower pH and after 4 days at higher pH. However, there was not a significant effect of adding salt on the morphology and stability of emulsions in the presence of neutral microgels. The effect of adding neutral or charged microgels on the morphology and stability of GEL-PEO emulsions around neutral pH, where GEL is weakly charged, was similar to that on DEX-PEO emulsions and was discussed in more detail in chapters 3 and 4. Quantitative differences were observed as might be expected, notably that more salt was needed for the G/P emulsions (100 mM) to induce adsorption of microgels at the interface than for the D/P emulsions (10 mM). However, the main difference between the two systems is that GEL becomes more strongly charged at high and low pH causing changes in the morphology and stability of the emulsion as a function of pH.

## 5.2. Interaction between gelatin and dextran droplets

Binary W/W emulsions D/P and G/P with the same PEO concentration in the continuous phase were mixed to form a DEX and GEL in PEO (DG/P) emulsion with the same volume fraction of dispersed DEX and GEL droplets. The emulsions were stabilized before mixing with neutral microgels in water or with charged microgels in 100 mM NaCl. The two binary emulsions were subsequently mixed either gently without perturbing the droplets or using a vortex, which mixes all of components homogeneously.

### 5.2.1. Morphology

In first instance, G/P and D/P emulsions at pH 7 were put into contact with each other on a microscopy slide and the interaction between the droplets was monitored by CLSM. The GEL and DEX droplets can be easily distinguished in the images, because the microgels partition preferentially to the GEL phase (grey) while it is relatively lower in DEX and PEO (black). Coalescence between droplets of the same phase was strongly inhibited by the adsorbed layer of microgels. However, surprisingly, when droplets of different phases met each other, they immediately coalesced forming Janus-like droplets with two compartments, see **Figure 5.15**. Droplet intensity profiles before and after the coalescence are also shown in **Figure 5.16**.

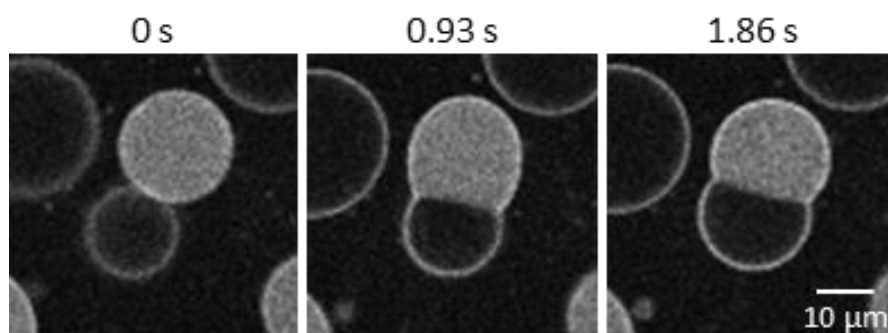


**Figure 5.15.** CLSM images during coalescence of a GEL (grey) and a DEX (black) droplet covered with neutral microgels with 53 wt% DEX.

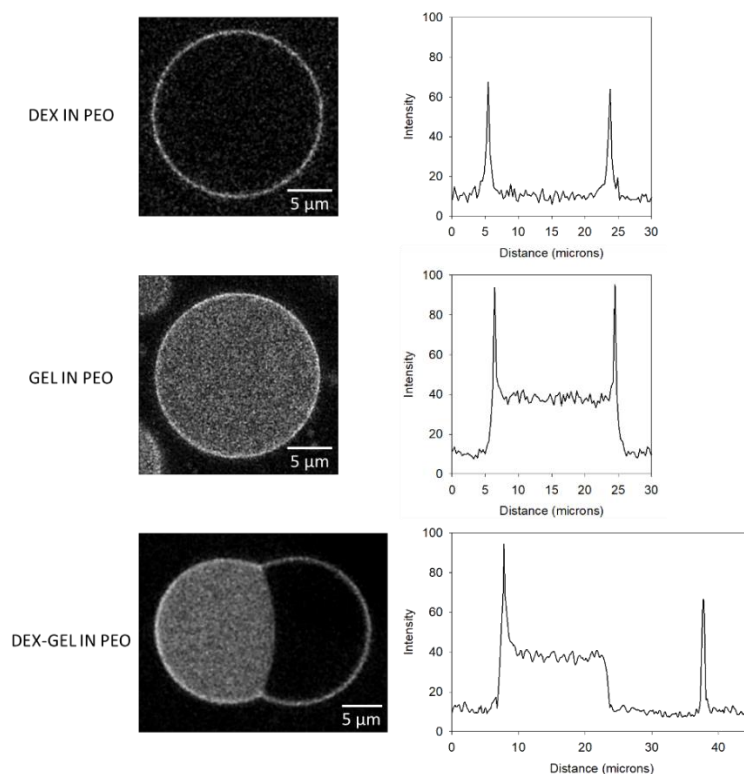


**Figure 5.16.** Fluorescence intensity profiles of neutral microgels with 53 wt% DEX throughout DEX and GEL droplets before and after coalescence.

The microgels strongly partitioned to the GEL phase, which can explain why the microgels did not adsorb at the DEX-GEL interface. Indeed, we found that also in binary emulsions of DEX and GEL the microgels did not form a layer at the interface and had no stabilizing effect. In DEX-PEO emulsions the excess microgels preferred the PEO phase implying that the interfacial tension of the microgels with each phase increased in the order:  $\gamma_{MGG} < \gamma_{MGP} < \gamma_{MGD}$ . The microgels did not adsorb at the DEX-GEL interface, because the interfacial tension between the DEX and GEL ( $\gamma_{DG}$ ) is less than the difference between the interfacial tension of the microgels with GEL ( $\gamma_{MGG}$ ) and with DEX ( $\gamma_{MGD}$ ):  $\gamma_{DG} < |\gamma_{MGG} - \gamma_{MGD}|$  [55].

**Figure 5.17** shows top and side views of a GEL and a DEX droplet covered by neutral microgels. The side views show that a monolayer of microgels with a diameter of about 0.2  $\mu\text{m}$  is formed at the interface, in agreement with the diameters measured by light scattering.

The top views show that the individual microgels appear to form a network at the interface leaving small pores of the bare DEX and GEL surface exposed. These microgels layers are sufficiently robust to inhibit coalescence when DEX or GEL droplets collide with each other. However, when a DEX droplet collides with a GEL droplet, the microgels move to the GEL phase so as to minimize contact with the DEX phase, because  $\gamma_{MGD}$  is much larger than  $\gamma_{MGG}$ , and leave a bare DEX-GEL interphase behind.

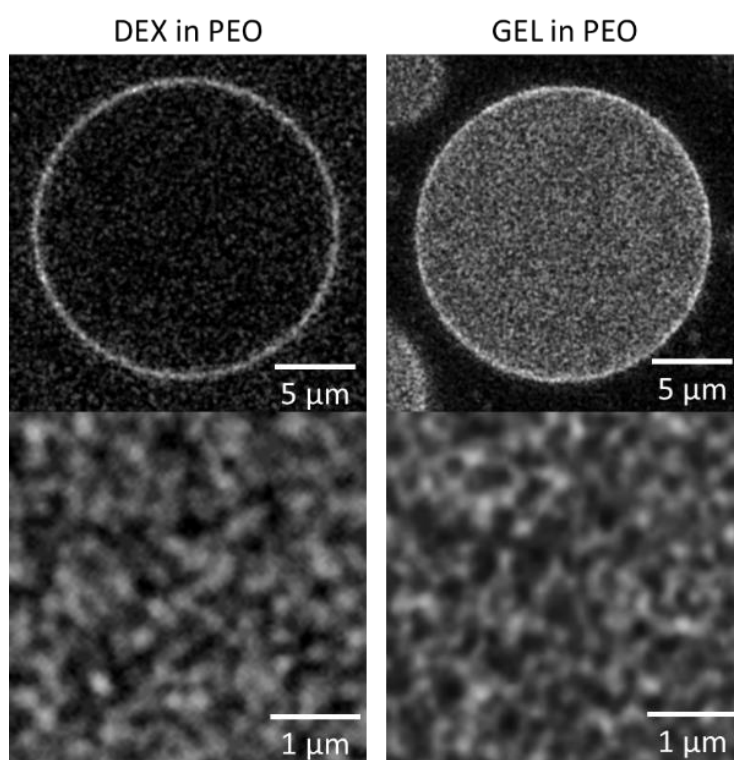


**Figure 5.17.** CLSM images of side and top views of DEX and GEL droplets covered with neutral microgels with 53 wt% DEX suspended in a continuous PEO phase.

As the interpenetration of the two emulsions continued, strings of alternating GEL and DEX droplets were formed that branched. The same network morphology was obtained after vortex mixing the two emulsions, see **Figure 5.18**. The contact angles of each phase ( $\theta_{DEX}$ ,  $\theta_{GEL}$ , and  $\theta_{PEO}$ , see figure 7c) were determined from the images as was explained elsewhere [46] ( $\theta_{PEO} = 130 \pm 1.5^\circ$ ,  $\theta_{DEX} = 98 \pm 1.2^\circ$ ,  $\theta_{GEL} = 132 \pm 1.7^\circ$ ) and were found to be very close to those in the absence of particles ( $\theta_{PEO} = 137 \pm 1.6^\circ$ ,  $\theta_{DEX} = 98 \pm 1.3^\circ$ ,  $\theta_{GEL} = 125 \pm 1.8^\circ$ ).

Emulsions stabilized with charged microgels in the presence of 100 mM NaCl showed similar behaviour, but the contact angles were different ( $\theta_{\text{PEO}} = 133 \pm 2.5^\circ$ ,  $\theta_{\text{DEX}} = 145 \pm 2.6^\circ$ ,  $\theta_{\text{GEL}} = 82 \pm 3.1^\circ$ ). Addition of salt can have an effect on the interfacial tension if one of the phases is a polyelectrolyte [79]. However, the contact angles for emulsions without microgels or with neutral microgels were the same with and without salt within the experimental error, showing that this effect was negligible here and does not explain the difference between the neutral and charged microgels.

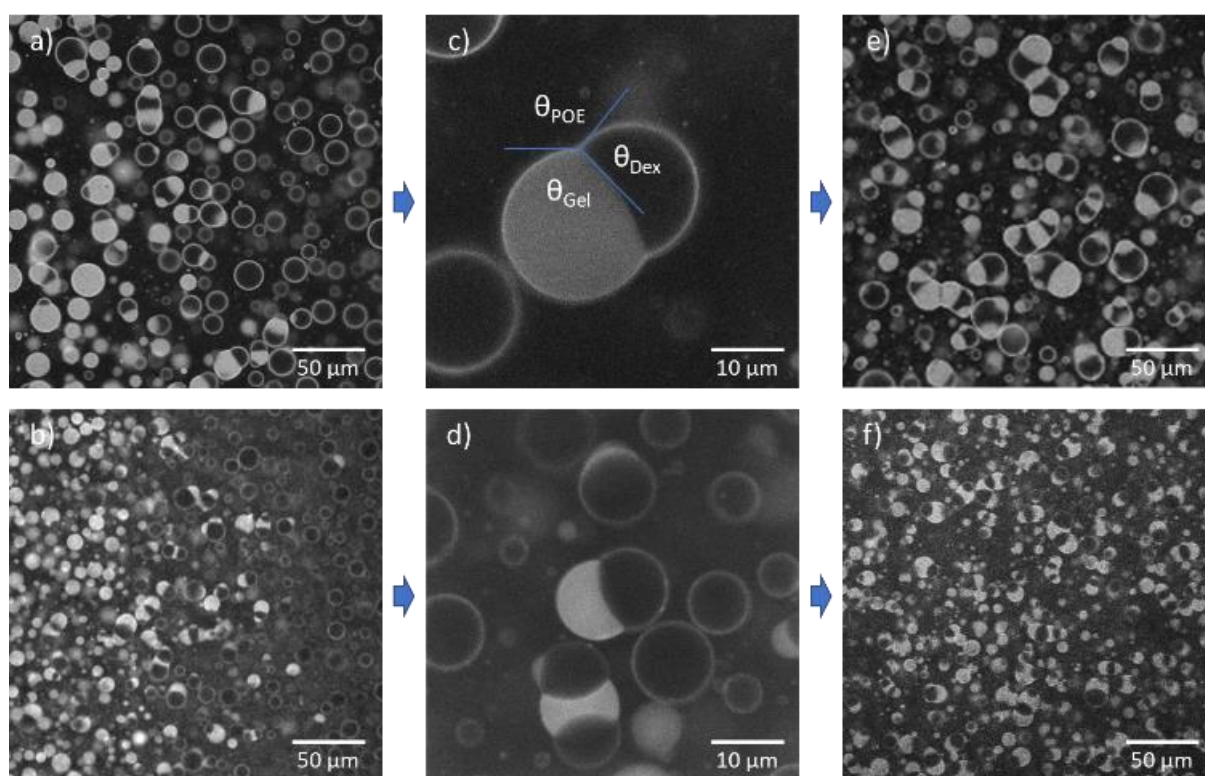


**Figure 5.18.** CLSM images of the contact area between D/P and G/P emulsions at pH7 stabilized by neutral microgels in water (a) and charged microgels in 100 mM NaCl (b) with close-ups of Janus droplets shown in figs. c and d, respectively. Images of the emulsions after vortex mixing are shown in figures e and f, respectively.

Elsewhere, it was shown for the same system in the absence of microgels that the contact angles depend on the pH close to the critical value [46]. **Figure 5.19** shows CLSM images of the mixed emulsions containing neutral microgels at different pH. Similar results were obtained in the presence of charged microgels in NaCl 100 mM, see **Figure 5.20**.



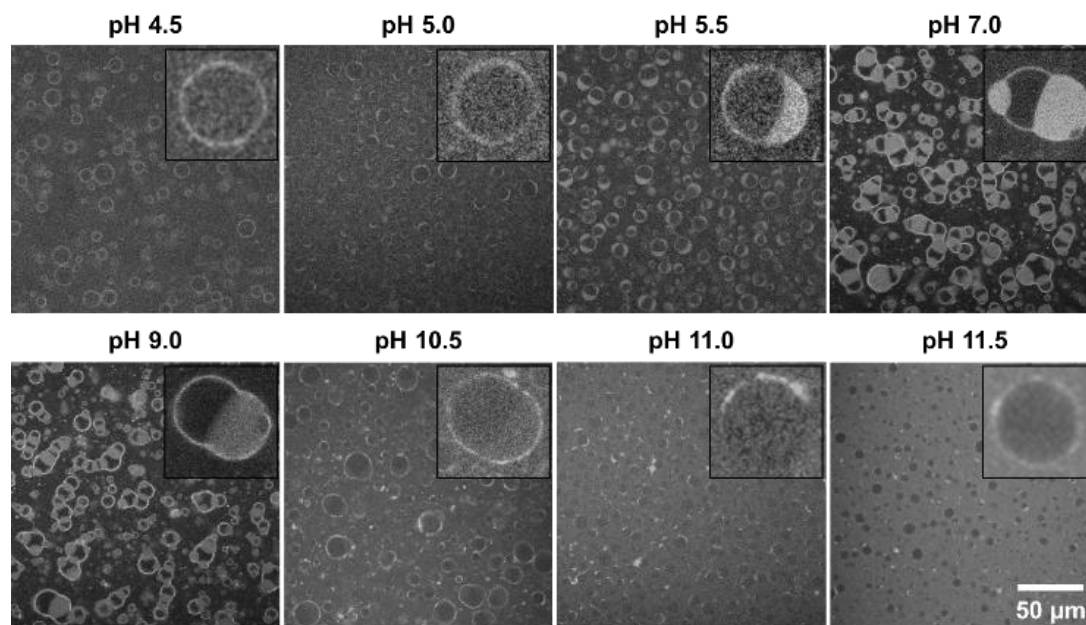


**Figure 5.19.** CLSM images of DG/P emulsions stabilized by neutral microgels (53 wt% DEX) at different pH indicated in the figure. The inserts show a close-up of a single droplet.

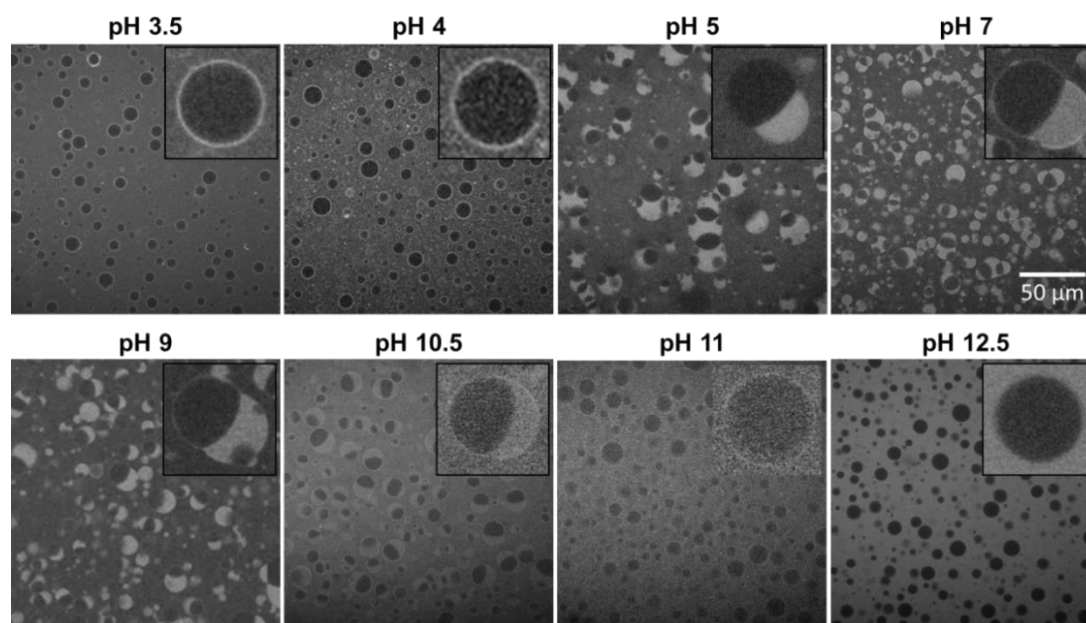


**Figure 5.20.** CLSM images of DG/P emulsions stabilized by charged microgels in NaCl 100 mM at different pH. The inserts show a close-up of a single droplet.

The contact angles are shown as a function of the pH in **Figure 5.21** for DG/P emulsions. In all cases,  $\theta_{\text{GEL}}$  reduced sharply when the pH approached the high or low critical value, whereas  $\theta_{\text{PEO}}$  and  $\theta_{\text{DEX}}$  increased. The decrease of  $\theta_{\text{GEL}}$  is caused by the increased compatibility



between the GEL and the PEO mentioned above. Below and above a critical low and high pH, respectively, all GEL mixed with the PEO, whereas close to the critical values the GEL phase completely wetted the DEX droplets. As was explained in more detail elsewhere [54], wetting of DEX droplets by the GEL phase is expected when the interfacial tension between the PEO and DEX phase is larger than the sum of the interfacial tensions between the GEL phase and the two other phases:  $\gamma_{PD} > \gamma_{PG} + \gamma_{DG}$ . In these emulsions, the microgels no longer formed a homogeneous layer around the droplets, see **Figure 5.19**, because the interfacial tension between the PEO and GEL had become very small. However, when the GEL phase was fully dissolved into the continuous PEO phase, microgels could again be observed at interface between the DEX phase and the mixed PEO/GEL phase.

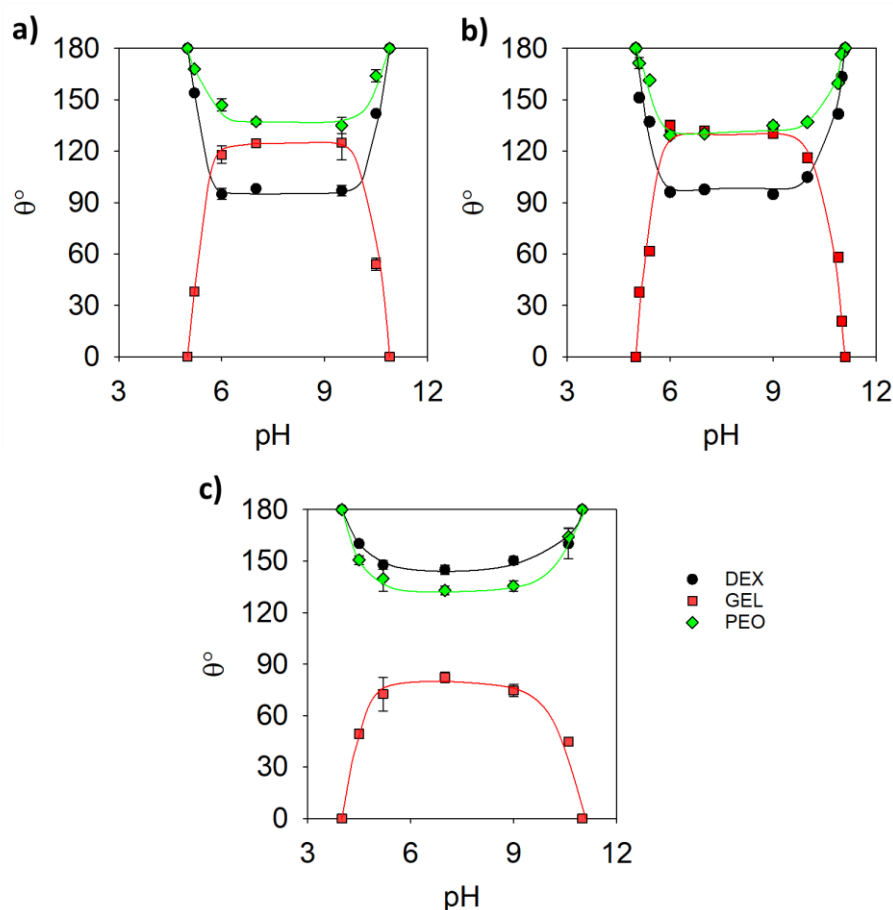


**Figure 5.21.** Contact angles of the DEX, GEL, and PEO phase as a function of the pH in three-phase systems: non-stabilized (a), stabilized by neutral microgels (53 wt% DEX) (b) and by charged microgels in NaCl 100 mM (c)

As was mentioned in the Introduction, measurements of the contact angles allows one to calculate the interfacial tensions between the different phases relative to each other [54]:

$$\gamma_{PD}/\gamma_{DG}=\sin(\theta_G)/\sin(\theta_P)$$

$$\gamma_{PD}/\gamma_{PG}=\sin(\theta_G)/\sin(\theta_D)$$

$$\gamma_{PG}/\gamma_{DG}=\sin(\theta_D)/\sin(\theta_P)$$

Since the GEL/DEX interface is not covered, we are able to calculate the effect of the microgels on the interfacial tension of the PEO/DEX and PEO/GEL interfaces relative to that of the bare DEX/GEL interface. Using the values of the contact angles at pH 7 given above, which were approximately the same between pH 6 and pH 9, we found  $\gamma_{PD} = 1.2 \times \gamma_{DG}$ ,  $\gamma_{PD} = 1.0 \times \gamma_{DG}$  and  $\gamma_{PD} = 1.3 \times \gamma_{DG}$ , for the bare P/D interface, covered with neutral microgels and covered with charged microgels respectively. For the P/G interface, the corresponding values are  $\gamma_{PG} = 1.4 \times \gamma_{DG}$ ,  $\gamma_{PG} = 1.3 \times \gamma_{DG}$  and  $\gamma_{PG} = 0.7 \times \gamma_{DG}$ . The largest effect was found for the P/G interface with the charged microgels, see **Figure 5.22**.

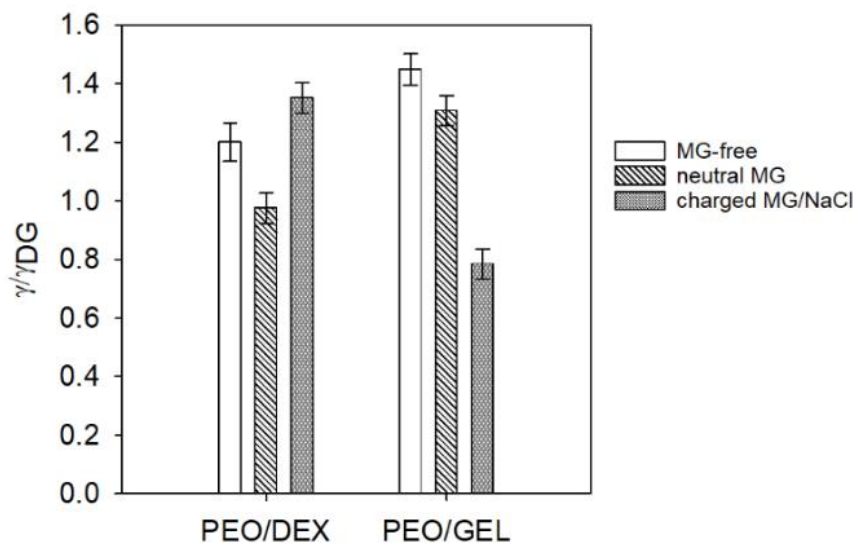


**Figure 5.22.** Interfacial tension of the bare PEO/DEX and PEO/GEL interfaces and the interfaces covered with neutral microgels (53 wt% DEX) or charged microgels in NaCl 100 mM

### 5.2.2. Stability

The droplet size of the DG/P emulsion at pH 7 containing neutral microgels, slowly increased over a period of days showing that a limited amount of coalescence between droplets of the same type still occurred in particular for DEX droplets, see **Figure 5.23**. After one week standing, large DEX droplets had sedimented, but a continuous layer of DEX was not observed, and a network of alternating droplets could still be observed in most of the sample.

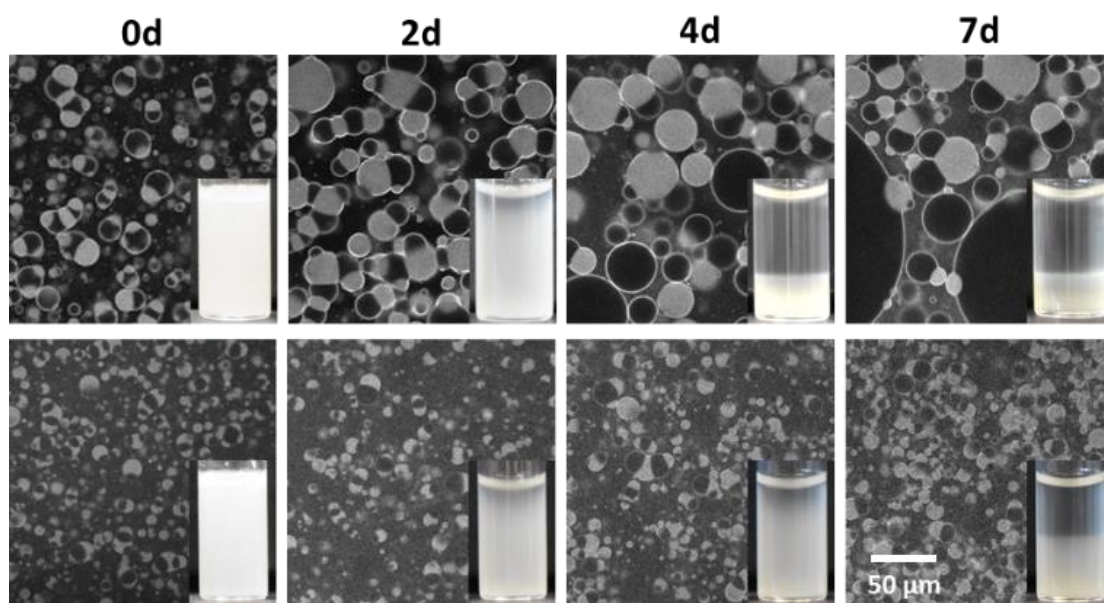


**Figure 5.23.** CLSM images of DG/P emulsions at pH7 stabilized by neutral microgels (53 wt% DEX) (top) and charged microgels in NaCl 100 mM (bottom) at different times.

The evolution of the transmission profiles during centrifugation showed that the stability of DG/P emulsions was higher than that of D/P emulsions and lower than that of G/P emulsions, see **Figure 5.24**, which confirms the CLSM observations during ageing under gravity. These different evolutions can be explained by the fact that the microgels more strongly inhibited coalescence of GEL droplets than of DEX droplets. The droplets in DG/P emulsions containing charged microgels and 100 mM NaCl did not grow significantly for a period of at least one week, see figure 10, which can be explained by the high stability of both the G/P and D/P emulsions at these conditions.

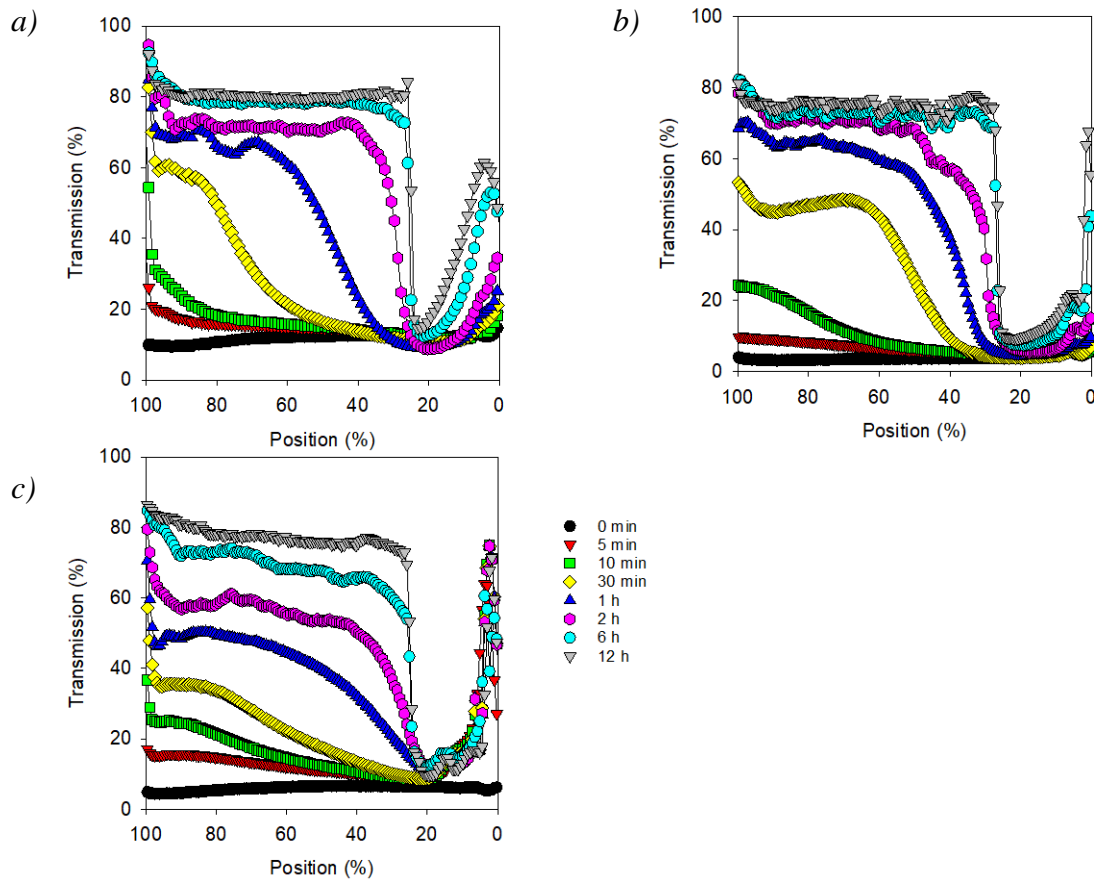


**Figure 5.24.** Transmission profiles of D/P (a), G/P (b), DG/P (c) at pH 7 during centrifugation in the presence of neutral microgels.

The evolution of the morphology of DG/P emulsions with neutral microgels at different pH is shown in the **Figure 5.25**. Both decreasing and increasing the pH made the emulsions less stable, which can be explained by the decrease of the stability of the G/P emulsion discussed in section 5.1.2. At pH 11, the microgels aggregated at the interface, which led to flocculation of the droplets similar to what was observed in binary G/P emulsions. Interestingly, at pH 4.5 and 11.5 when all GEL had mixed with the PEO, the binary emulsion containing only DEX droplets was again much more stable.

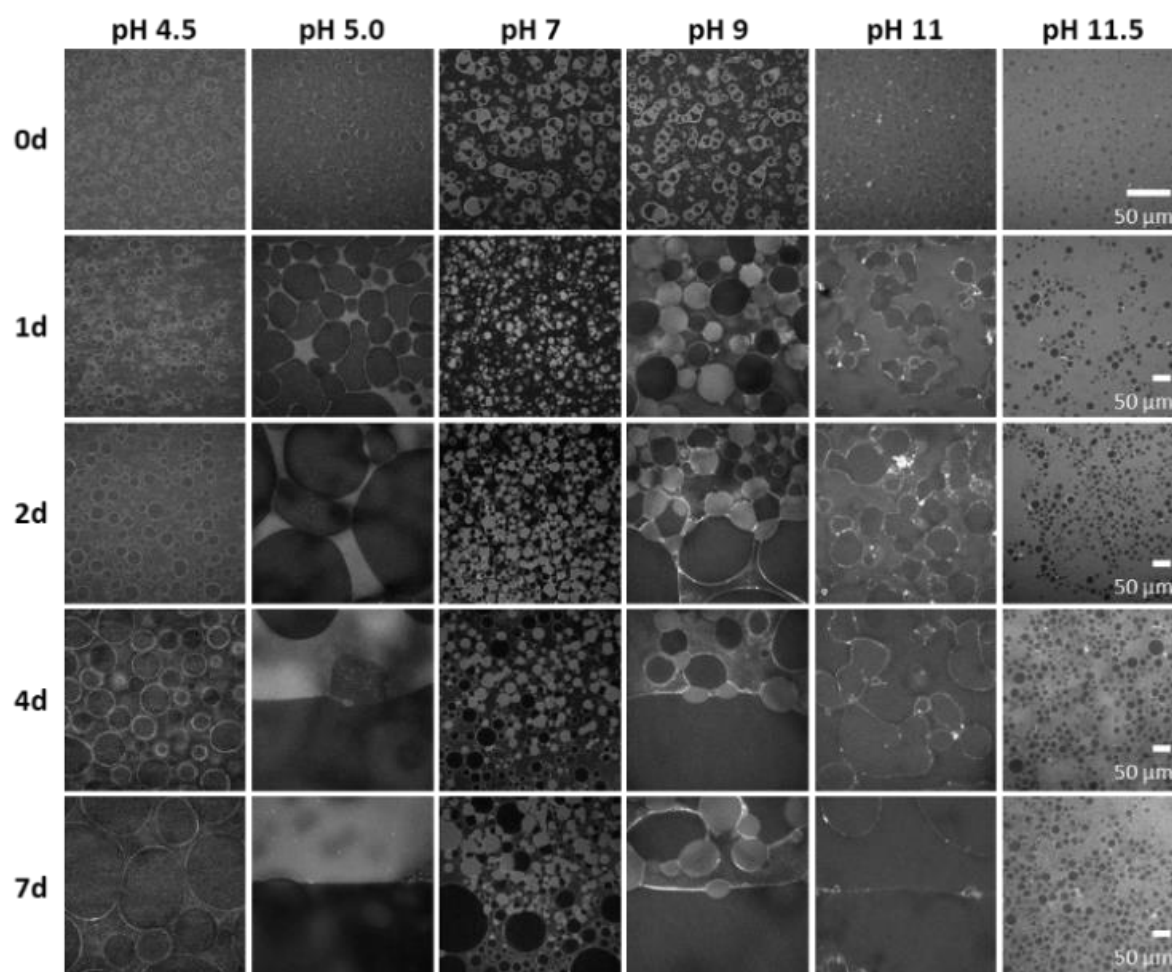


**Figure 5.25.** CLSM images of DG/P emulsions with neutral microgels at different pH and ageing times as indicate in the figure.

The effect of the pH on the stability was quantified by measuring the characteristic time of stabilization during centrifugation, see **Figure 5.26**, and confirmed the CLSM observations under gravity.  $t_c$  was maximum close to pH 7 decreasing both at lower or higher pH. However, when GEL was fully mixed with PEO below or above the lower or upper critical pH, the emulsion of DEX droplets dispersed in the mixed PEO/GEL phase was again much more stable.

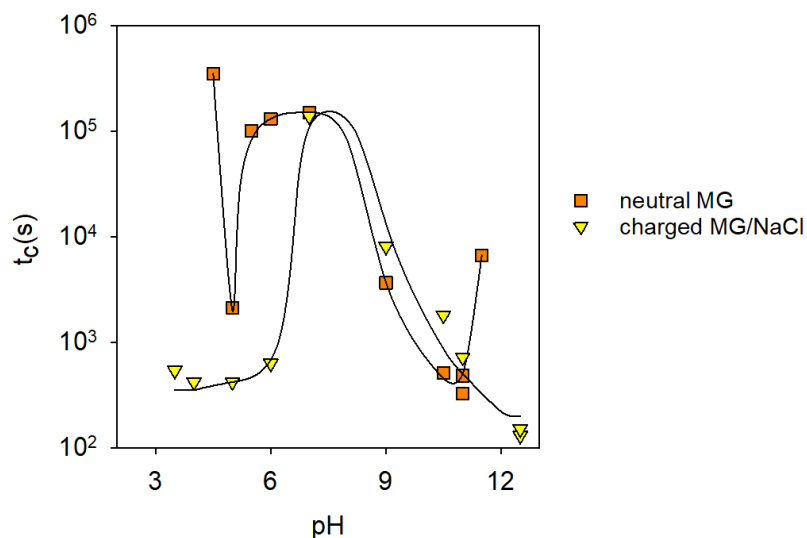


**Figure 5.26.** Characteristic stabilization times of DG/P emulsions stabilized by neutral microgels (53 wt% DEX) and charged microgels in NaCl 100 mM as a function of pH.

The evolution of the microstructure of DG/P emulsions with charged microgels in NaCl 100 mM was also monitored at different pH, see **Figure 5.27**. In this case the emulsion was not very stable at  $\text{pH} \leq 6$  where it fully destabilized after two days. This can be explained by the lower stability of the G/P emulsion with charged microgels at lower pH discussed in section 5.1.3. However, the emulsion remained stable for at least one week between pH 7 and pH 10.5. In this case, the stability of the emulsion did not improve again at low and high pH when all GEL mixed with the continuous PEO phase. For both types of microgels, the  $t_c$  was maximum close to neutral pH, but the stability with neutral microgels was better at lower pH, whereas that with charged microgels it was better at higher pH, see **Figure 5.26**.

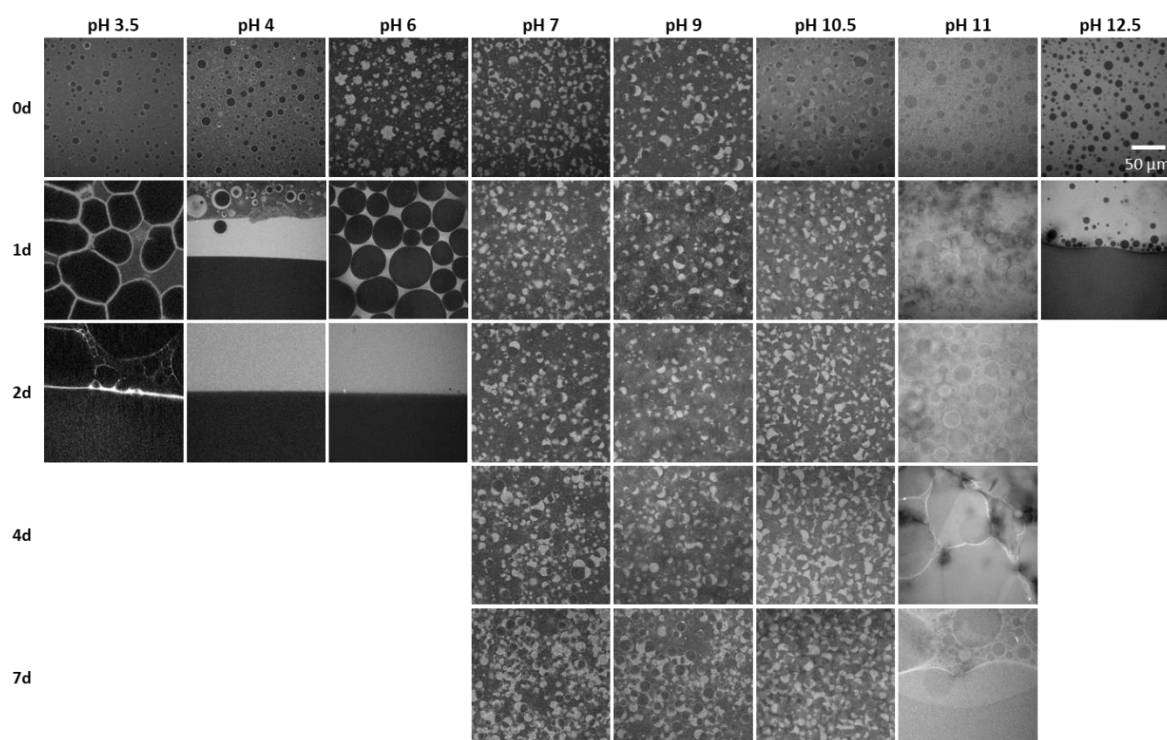


**Figure 5.27.** CLSM images of DG/P emulsions with charged microgels at different pH and ageing time as indicate in the figure.

## Conclusion

W/W emulsions of droplets of a fish GEL phase dispersed in a continuous PEO phase (G/P) can be stabilized by bishydrophilic microgels consisting of a mixed DEX and NIPAM network, if the DEX content is larger than about 40 wt%. When charged groups are introduced into the microgels, they can only stabilize the emulsion in the presence of salt. The inverse emulsion (P/G) cannot be effectively stabilized by these microgels at room temperature.

The interaction between dispersed droplets of different phases can be studied by mixing two emulsions with a common continuous phase. When stabilized DEX and GEL droplets dispersed in a common continuous phase of PEO are gently mixed, they immediately coalesce upon collision forming a Janus-like droplet with two distinct compartments and no microgels at the GEL/DEX interface. Coalescence is favoured by the fact that the microgels prefer to reside in the GEL phase rather than at the GEL/DEX interface. When the two emulsions are

fully mixed, a network is formed of alternatively associated droplets. No spontaneous coalescence is expected if the particles stabilize all three interfaces in the aqueous three phase system.

The contact angles that each phase makes with the other phases are controlled by the relative interfacial tensions, which depend on the pH. By comparing the contact angles with and without microgels adsorbed at the PEO/GEL and PEO/DEX interfaces, the effect of the microgels on the effective interfacial tension could be determined. Neutral microgels had little effect, but charged microgels reduced the interfacial tension between GEL and PEO significantly. If the dispersed droplets of the two stabilized W/W emulsions contain different ingredients, mixing the emulsions offers the opportunity to bring these ingredients in contact with each other in a controlled manner. Would these ingredients be reactive, this process opens interesting perspectives in controlling the initiation time of a reaction kinetic between them.





## **Chapter 6. Structure and stabilization of Water-in-Water emulsions in the presence of two types of microgels**

Synergetic effects on the stability of adding two types of particles has been noted earlier for O/W emulsions [29-31], but not yet for W/W emulsions. The objective of the investigation presented in this chapter was therefore to study the effect of adding two different types of particles on the microstructure and stability of a W/W emulsion. The effect of adding both protein microgels and bishydrophilic microgels was studied for a model W/W emulsion formed by mixing PEO and DEX. I first show the behavior of the particles in the PEO or DEX phase and then of mixtures of emulsions stabilized by each type of microgel. Furthermore, I will discuss the effect of adding one type of microgel to an emulsion stabilized with the other type of microgel. The mixtures were prepared either by gently mixing without breaking the dispersed droplets or by strongly shearing with a vortex mixer. The arrangement of particles at the interface was monitored using CLSM and the effect on the microstructure and stability of the emulsions was evaluated during aging.

|  |            |
|--|------------|
| <b>1. Microgels in water and pure PEO and DEX phases .....</b>   | <b>119</b> |
| <b>2. Mixtures of emulsions .....</b>                            | <b>120</b> |
| 2.1 Gently mixed emulsions .....                                 | 120        |
| 2.2. Vortex mixed emulsions.....                                 | 125        |
| <b>3. Stabilization with microgel co-aggregates.....</b>         | <b>131</b> |
| <b>4. Mixtures of an emulsion and a microgel suspension.....</b> | <b>134</b> |
| <b>Conclusion.....</b>   | <b>138</b> |

### 6.1. Microgels in water and pure PEO and DEX phases

The bishydrophilic (BIS) and protein (PRO) microgels were prepared as described in chapter 2.1. The BIS used in this chapter contained 60 wt% DEX at  $M_w = 6$  kDa,  $DS = 12$ . Before discussing the effect of the microgels in the emulsions we show their behaviour in water, DEX (15.8 wt%) and PEO (8.2 wt%), see **Figure 6.1**. Whereas the BIS and PRO remained well-dispersed in water and DEX, they immediately co-aggregated in PEO. PRO strongly prefers contact with DEX over PEO. Therefore, we speculate that in PEO the PRO stick to the DEX within the BIS. During ageing, co-aggregation continued slowly forming larger aggregates.

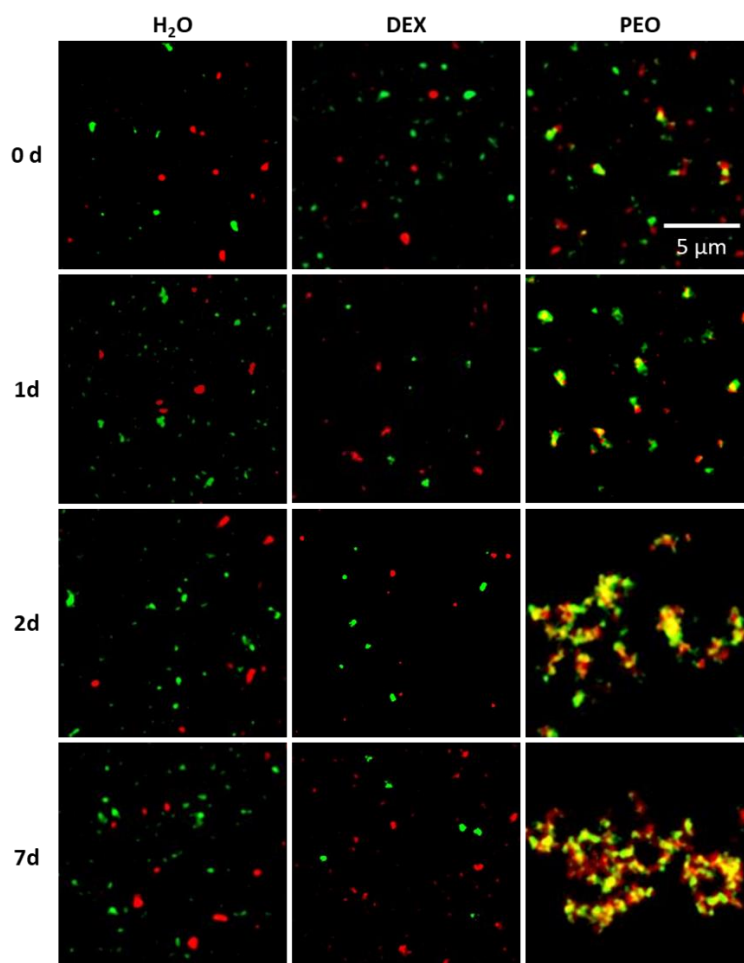


**Figure 6.1.** CLSM images of the mixture of BIS and PRO in water, the DEX phase and the PEO phase as a function of time.

## 6.2. Mixtures of emulsions

### 6.2.1. Gently mixed emulsions

D/P and P/D emulsions were prepared with BIS at 0.05 wt% or PRO at 0.2 wt%, as described in section 2.1.3. The microstructures of the emulsions were observed with CLSM, see **Figure 6.2**. Both types of microgels spontaneously adsorbed at the interface and formed a layer around the droplets. PRO could effectively stabilize the P/D emulsion for at least one week, while the D/P emulsion destabilized within one day. The excess of PRO partitioned preferentially to the DEX phase. BIS stabilized both systems for over a week, but more coalescence between droplets was observed during ageing for the D/P emulsion. When the concentration of microgels was divided by two, emulsions that were stable at the higher concentration destabilized after 2 days, see **Figure 6.3**.

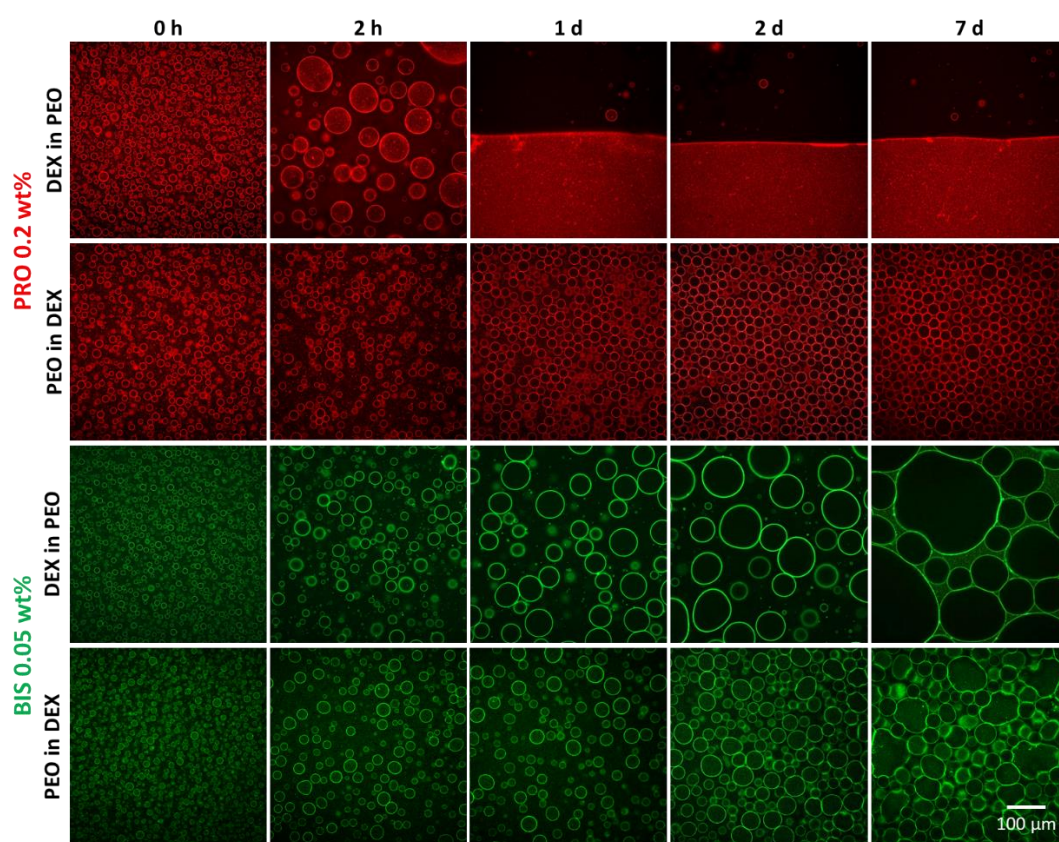


**Figure 6.2.** CLSM images of the evolution of D/P and P/D emulsions containing 0.2 wt% PRO (red) or 0.05 wt% BIS (green) as indicated in the figure.

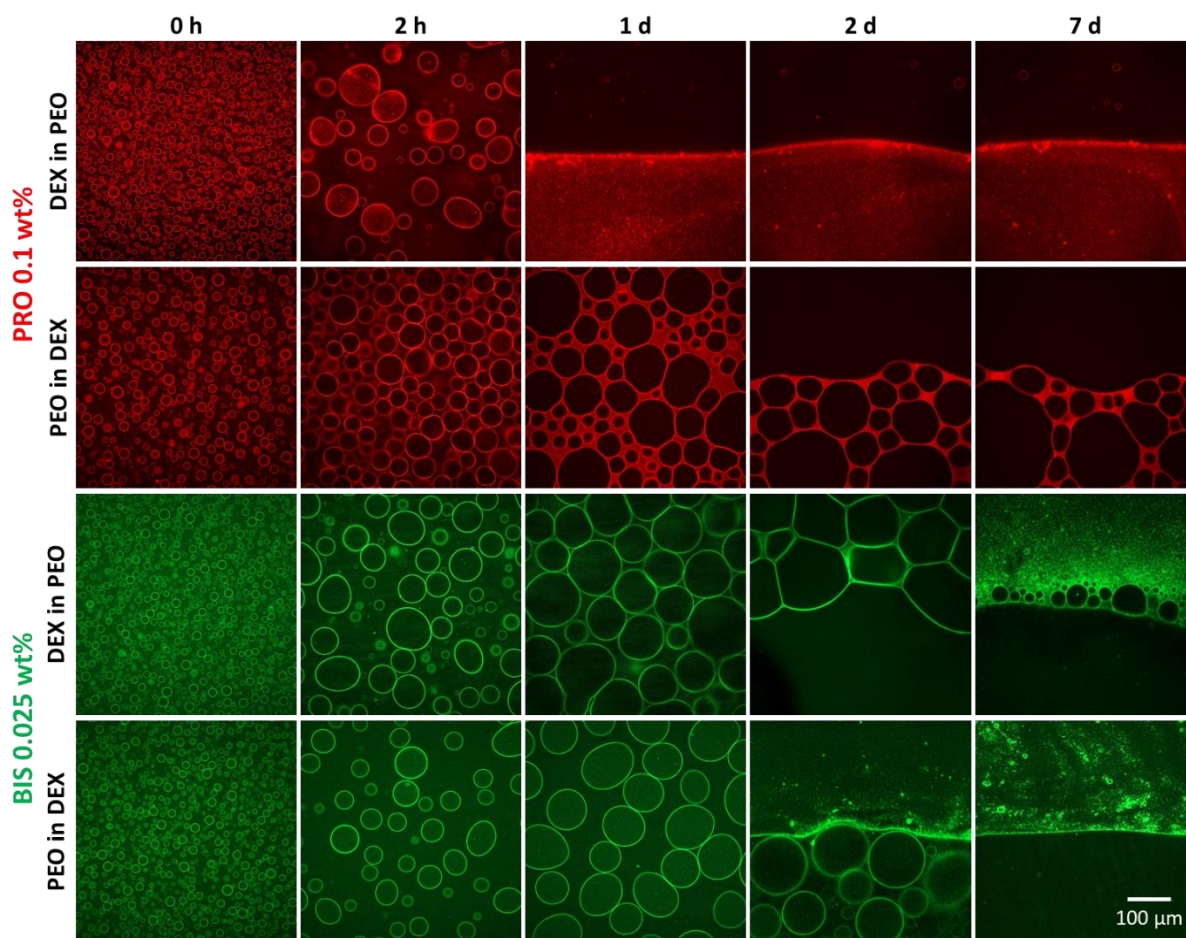


**Figure 6.3.** CLSM images of the evolution of D/P and P/D emulsions containing 0.1 wt% PRO (red) or 0.025 wt% BIS (green) as indicated in the figure.

Emulsions containing BIS were gently mixed with emulsions containing PRO without breaking the droplets. **Figure 6.4** shows that for D/P emulsions the PRO-covered and BIS-covered DEX droplets coalesced immediately upon collision, forming droplets with hybrid layers, whereas droplets stabilized with the same microgels did not coalesce or more slowly. However, in mixtures of P/D emulsions, no coalescence was observed. The different behaviors of D/P and P/D emulsion mixtures are clearly related to the strong difference in the stability of these emulsions in the presence of PRO.



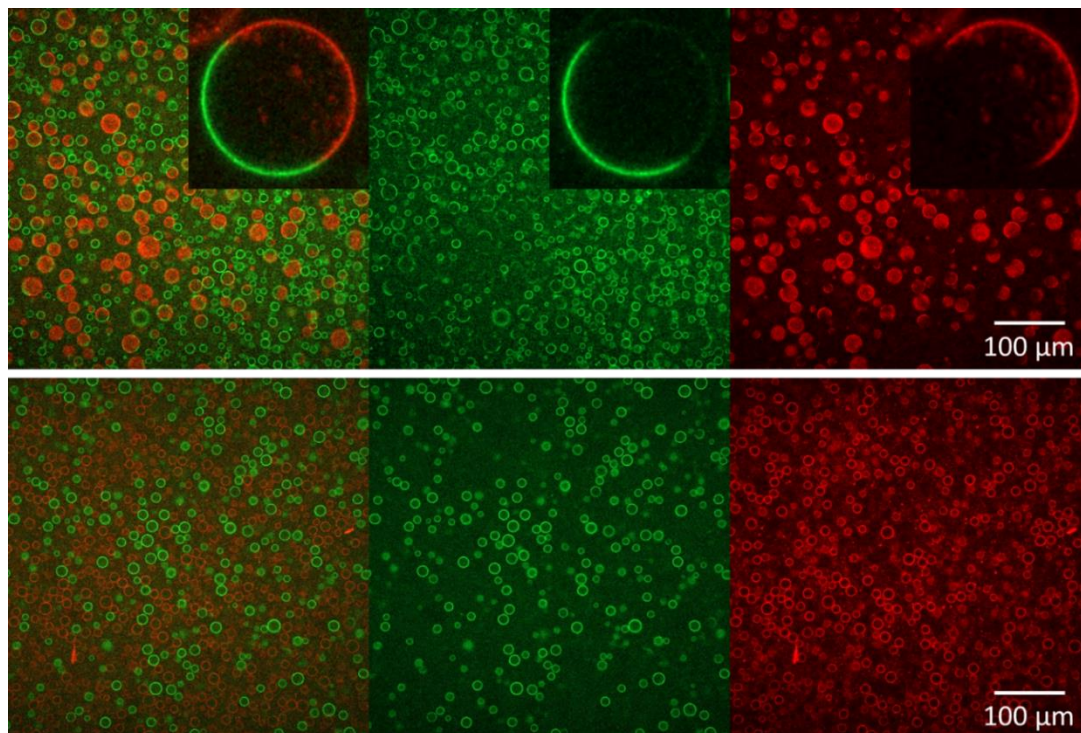


**Figure 6.4.** CLSM images of gently mixed PRO-covered (red) and BIS-covered (green) DEX droplets dispersed in PEO (top) as well as PEO droplets dispersed in DEX (bottom). The inserts show a close up of a droplet with a hybrid layer formed after coalescence. From left to right, the merged signal of the two microgels, the BIS signal and the PRO signal.

**Figure 6.5** shows the evolution of a gentle mixture of D/P emulsions as a function of time. After 1 day, BIS covered the whole droplet surface and PRO was expelled towards the DEX phase. It shows that once enough BIS is present to cover the interface, the system can increase its free energy by releasing PRO from the interface and thereby avoid contact of PRO with PEO in favor of contact with DEX. As might be expected, the DEX droplets covered with BIS behaved similarly to D/P containing only BIS at the same concentration, shown in **Figure 6.2**. In mixed P/D emulsions, the droplets covered by BIS or PRO evolved independently as in the individual emulsions showing significant coalescence of the BIS-covered droplets, but not for the PRO-covered droplets, see **Figure 6.6**. Similar observations were made for mixed emulsions with only half the amount of microgels, see **Figure 6.7** and **Figure 6.8**, but the emulsions were less stable as was found for the individual emulsions.

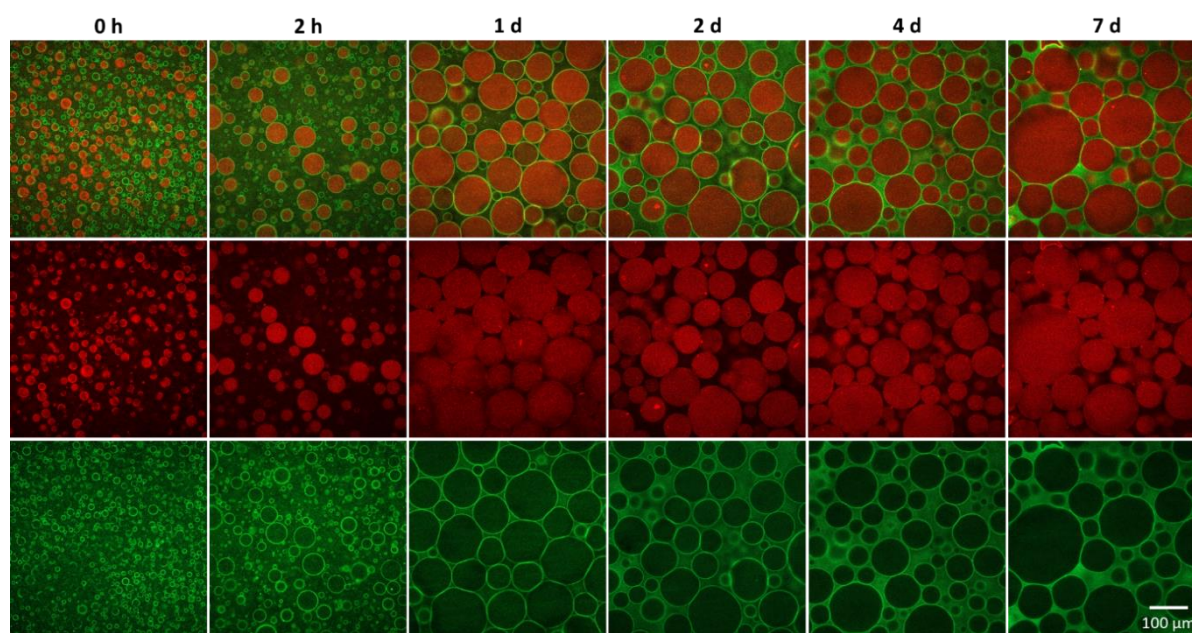


**Figure 6.5.** CLSM images of a mixture of PRO-covered and BIS-covered DEX droplets dispersed in PEO after gently mixing as a function of time, with the merged signal of two particles (top), the PRO signal (red, middle) and the BIS signal (green, bottom). The mixture contained 0.05 wt% BIS and 0.2 wt% PRO.

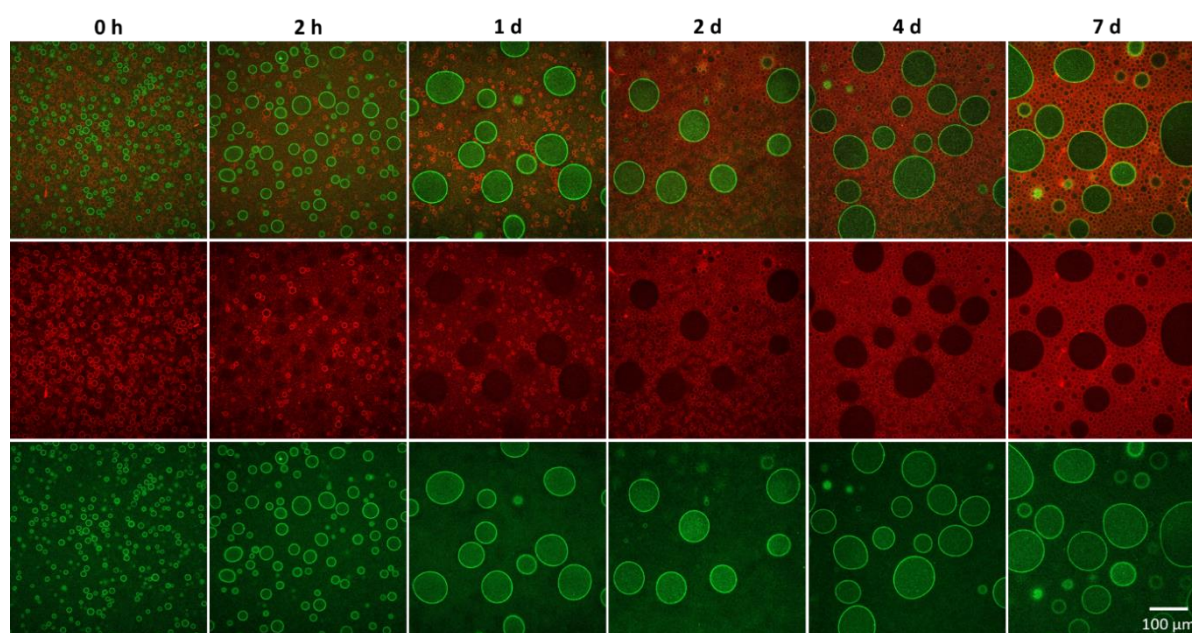


**Figure 6.6.** CLSM images of the mixture of PRO-stabilized and BIS-stabilized PEO droplets dispersed in DEX after gently mixing as a function of time, with the merged signal of two particles (top), the PRO signal (red, middle) and the BIS signal (green, bottom). The mixture contained 0.05 wt% BIS and 0.2 wt% PRO.



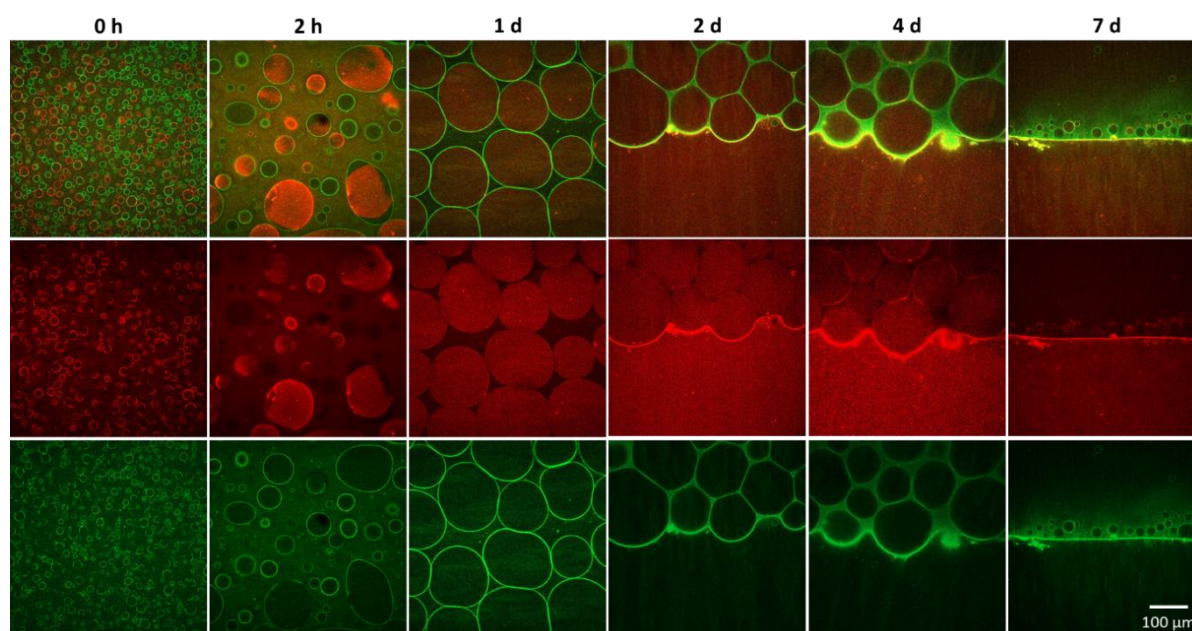


**Figure 6.7.** CLSM images of a mixture of PRO-covered and BIS-covered DEX droplets dispersed in PEO after gently mixing as a function of time, with the merged signal of two particles (top), the PRO signal (red, middle) and the BIS signal (green, bottom). The mixture contained 0.025 wt% BIS and 0.1 wt% PRO.

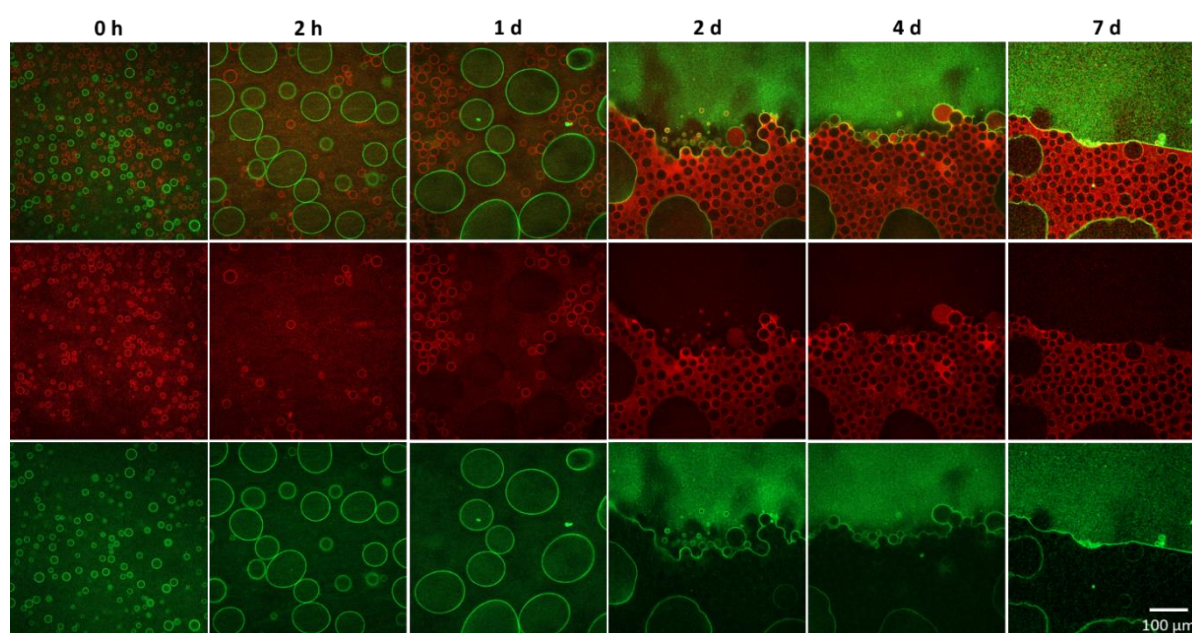


**Figure 6.8.** CLSM images of a mixture of PRO-covered and BIS-covered PEO droplets dispersed in DEX as a function of time, with the merged signal of two particles (top), the PRO signal (red, middle) and the BIS signal (green, bottom). The mixture contained 0.025 wt% BIS and 0.1 wt% PRO.

## 6.2.2. Vortex mixed emulsions

**Figure 6.9** shows images of droplets formed after mixing PRO and BIS stabilized D/P emulsions using a vortex mixer. In this case, droplets with a mixed layer of PRO and BIS microgels were formed. The layer thickness was determined from cross-cut images and was found to be about 230 nm and 380 nm for BIS or PRO, respectively, which corresponds well to the hydrodynamic diameter of the microgels measured by dynamic light scattering. Interestingly, the peak positions of the PRO and BIS layer were not the same and showed that the PRO preferred to be situated closer to the DEX phase due to its higher affinity with DEX.

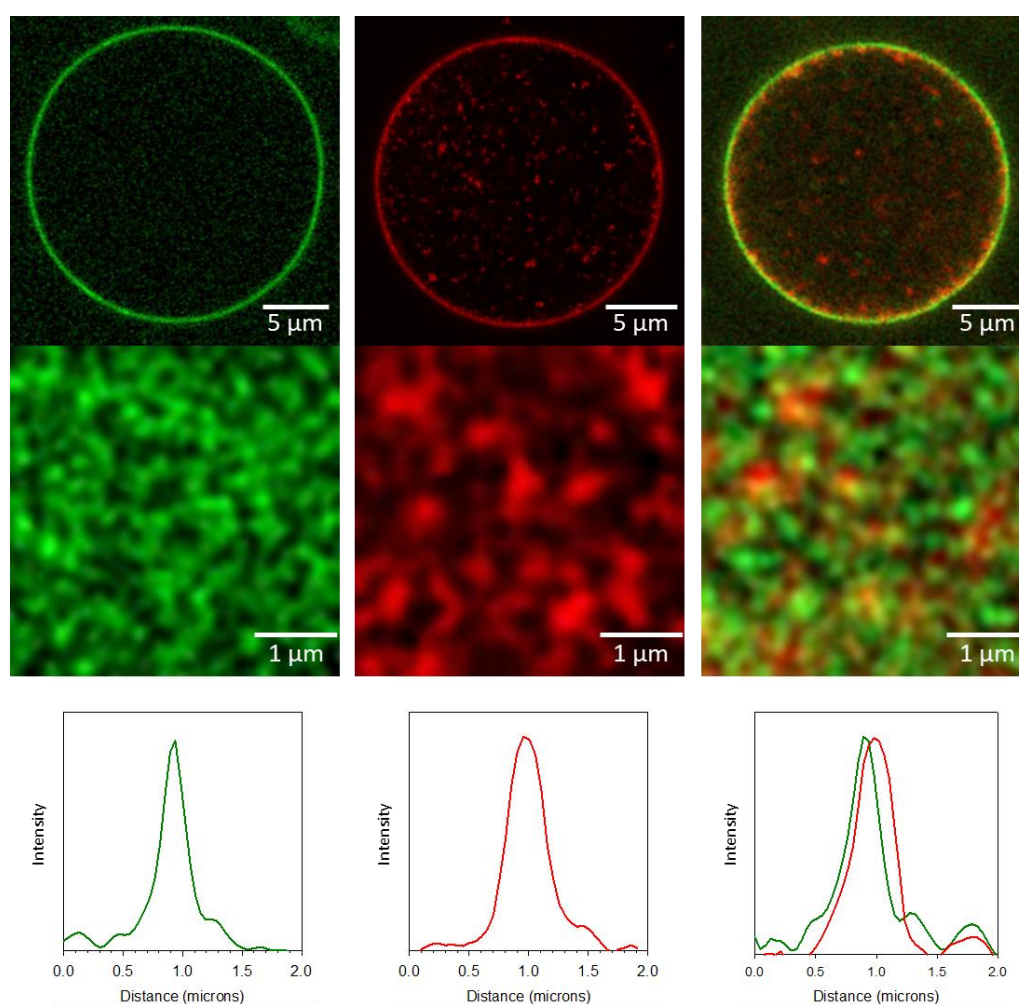


**Figure 6.9.** CLSM images of cross-cut and top views of DEX droplets covered by BIS (left), PRO (center) and a mixture of BIS and PRO (right) suspended in a continuous PEO phase. Fluorescence intensity profiles of a cut through the layers are also shown. The concentration of BIS was 0.05 wt% and that of PRO was 0.2 wt%.



A mixed layer was also formed in P/D emulsions, but in this case the PRO was more exposed to the continuous phase, see **Figure 6.10**. The distance between the peak positions was measured at different positions and in different droplets and was found to be  $74 \pm 30$  nm for D/P emulsions and  $65 \pm 44$  nm for P/D emulsions. The distance between the peak positions is much smaller than the layer thickness, which means that there is large overlap between the two types of microgels. Top views of the layer show that the two types of microgels are completely mixed with no sign of microphase separation.

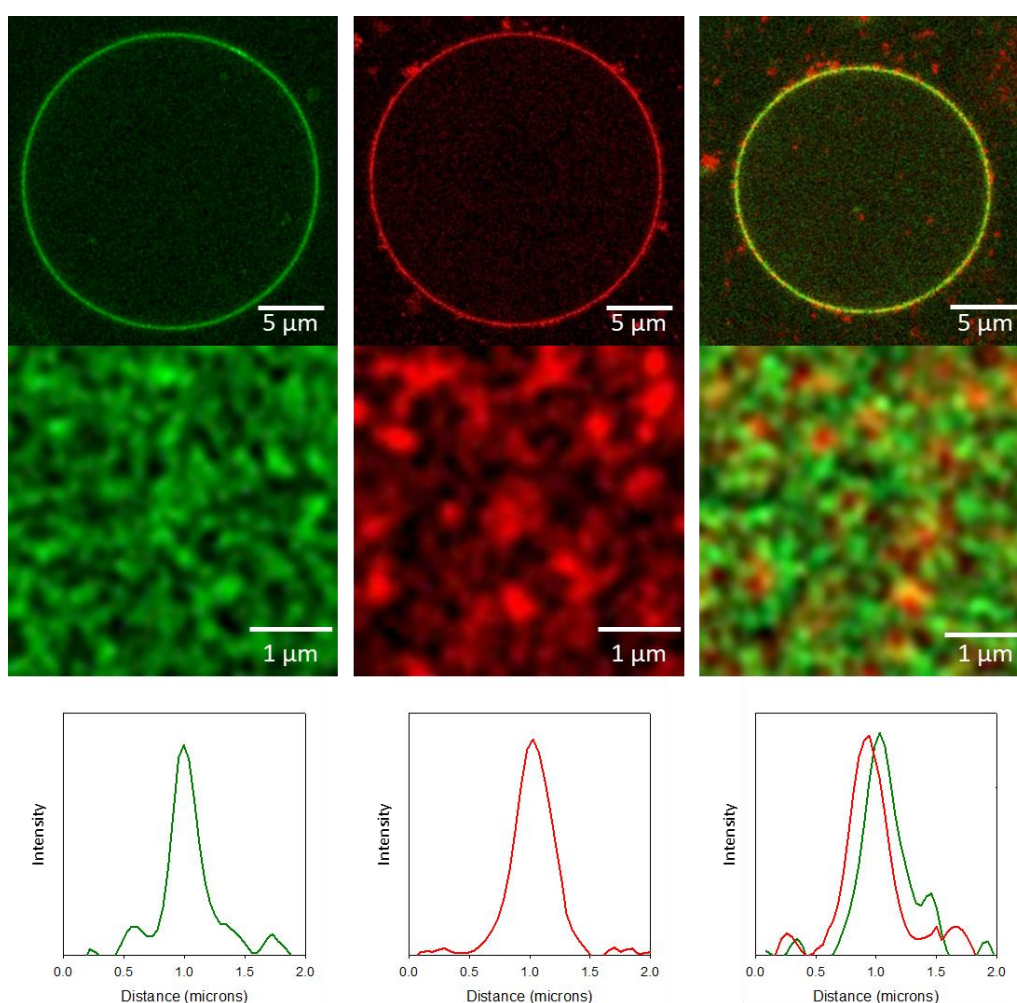


**Figure 6.10.** CLSM images of cross-cut and top views of PEO droplets covered by BIS (left), PRO (center) and a mixture of BIS and PRO (right) suspended in a continuous DEX phase. Fluorescence intensity profiles of a cut through the layers are also shown. The concentration of BIS was 0.05 wt% and that of PRO was 0.2 wt%.

An important observation is that by creating a mixed layer with both types of microgel, coalescence is significantly reduced compared with that in emulsions containing only one type, see **Figure 6.11** and **Figure 6.12**.

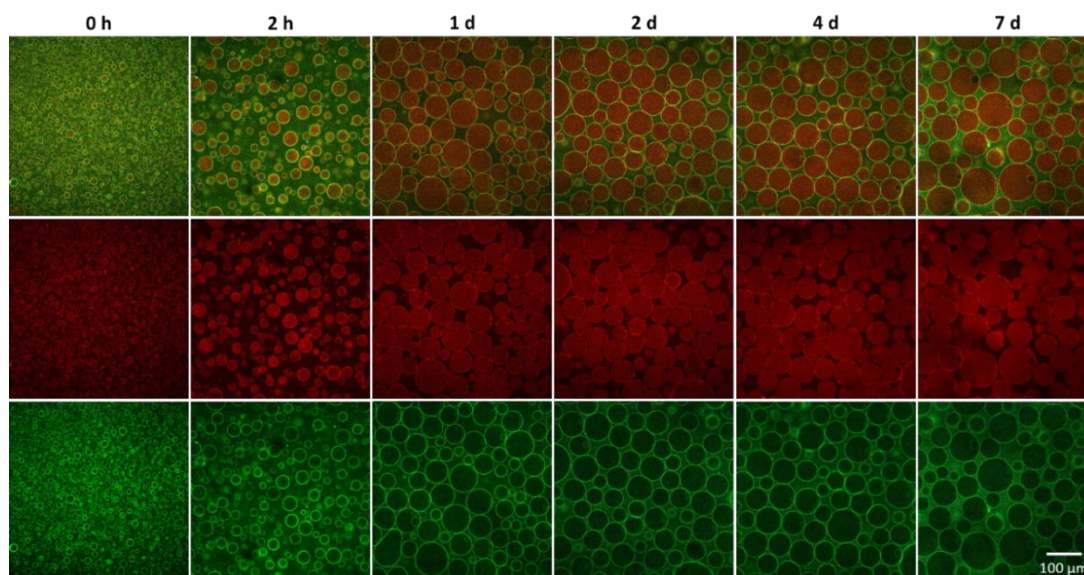


**Figure 6.11.** CLSM images of a mixture of PRO-covered and BIS-covered DEX droplets dispersed in PEO after vortexing. The merged signal of two particles (top), the PRO signal (red, middle) and the BIS signal (green, bottom) are shown. The concentration of BIS was 0.05 wt% and that of PRO was 0.2 wt%.

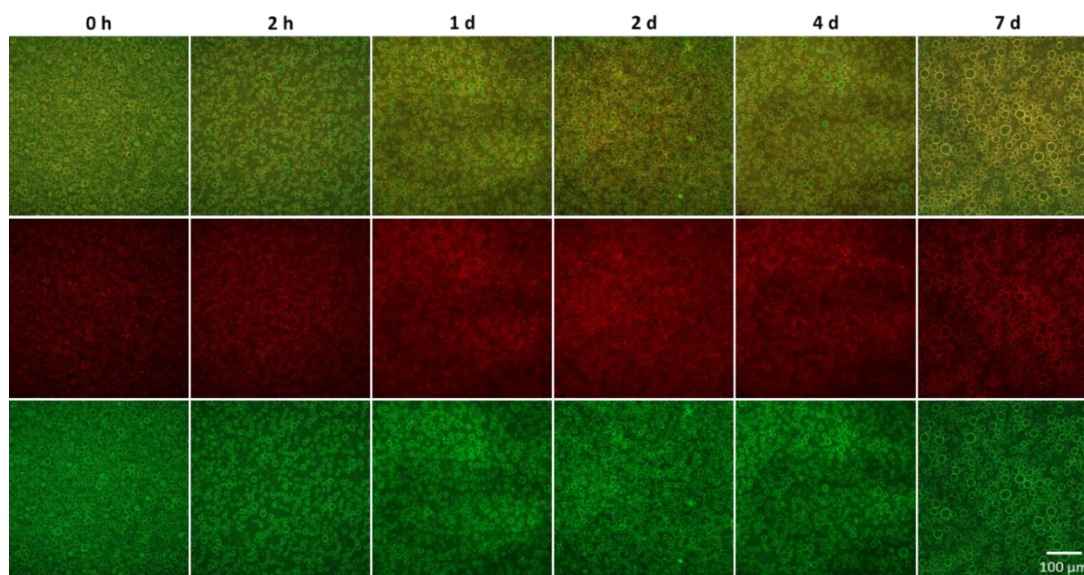


**Figure 6.12.** CLSM images of a mixture of PRO-covered and BIS-covered PEO droplets dispersed in DEX after vortexing. The merged signal of two particles (top), the PRO signal (red, middle) and the BIS signal (green, bottom) are shown. The concentration of BIS was 0.05 wt% and that of PRO was 0.2 wt%.



When the concentration of microgels was reduced by half, the distance between the two peaks became negligible, see **Figure 6.13** and **Figure 6.14**, but the stability was still slightly improved compared to emulsions with single type, see **Figure 6.15** and **Figure 6.16**.

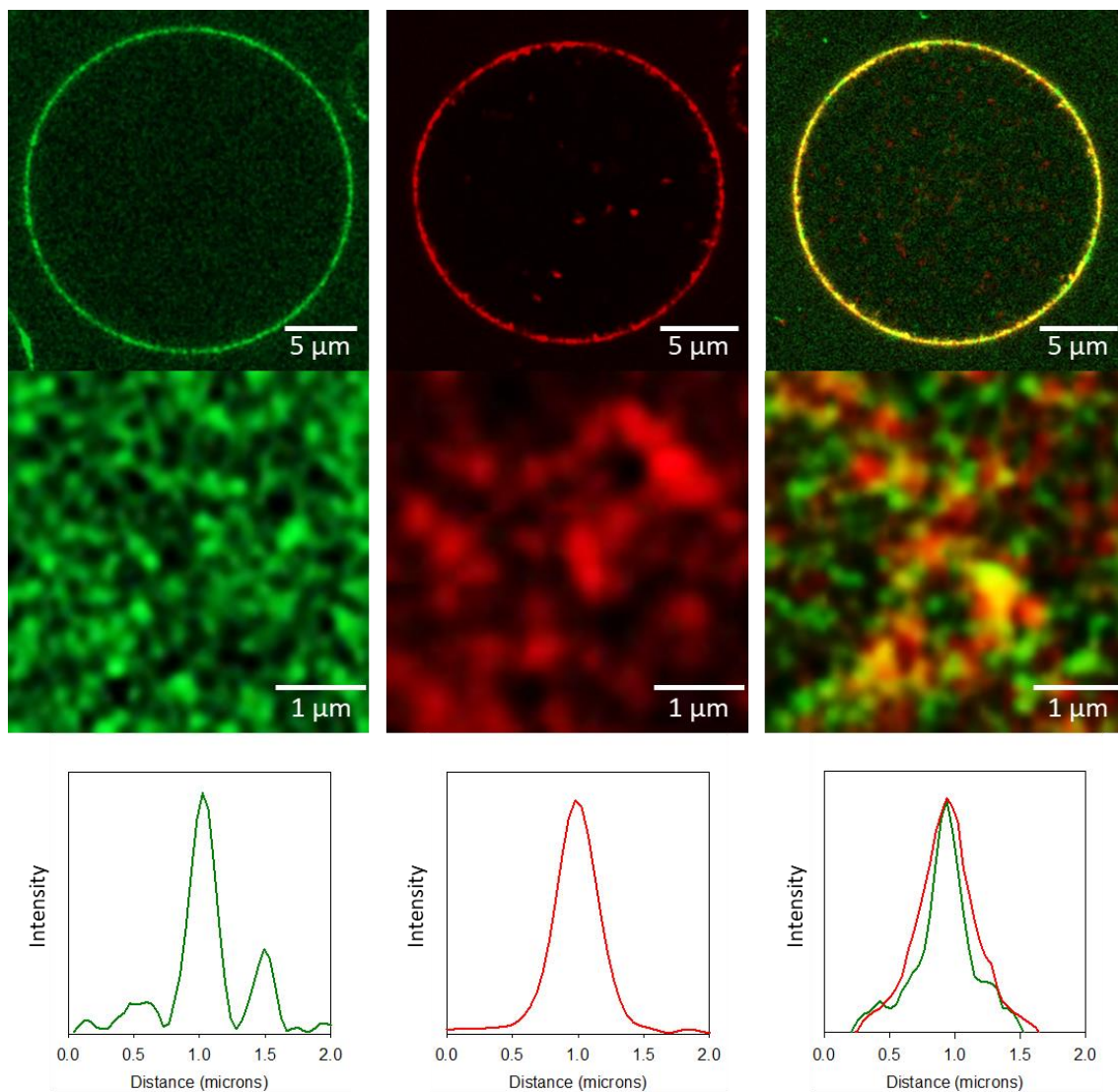


**Figure 6.13.** CLSM images of cross-cut and top views of DEX droplets covered by BIS (left), PRO (center) and a mixture of BIS and PRO (right) suspended in a continuous PEO phase. Fluorescence intensity profiles of a cut through the layers are also shown. The concentration of BIS was 0.025 wt% and that of PRO was 0.1 wt%.

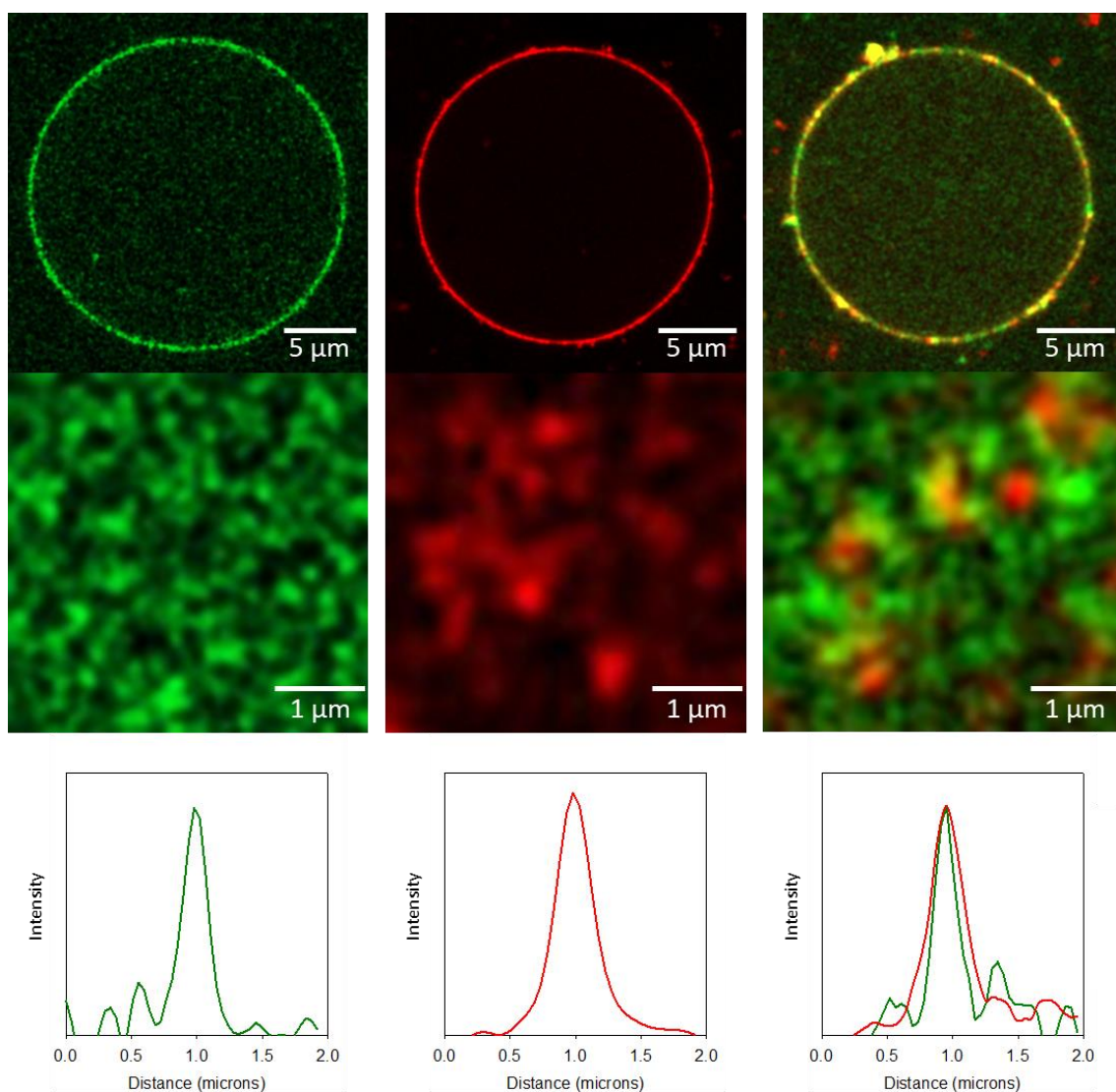


**Figure 6.14.** CLSM images of cross-cut and top views of PEO droplets covered by BIS (left), PRO (center) and a mixture of BIS and PRO (right) suspended in a continuous DEX phase. Fluorescence intensity profiles of a cut through the layers are also shown. The concentration of BIS was 0.025 wt% and that of PRO was 0.1 wt%.



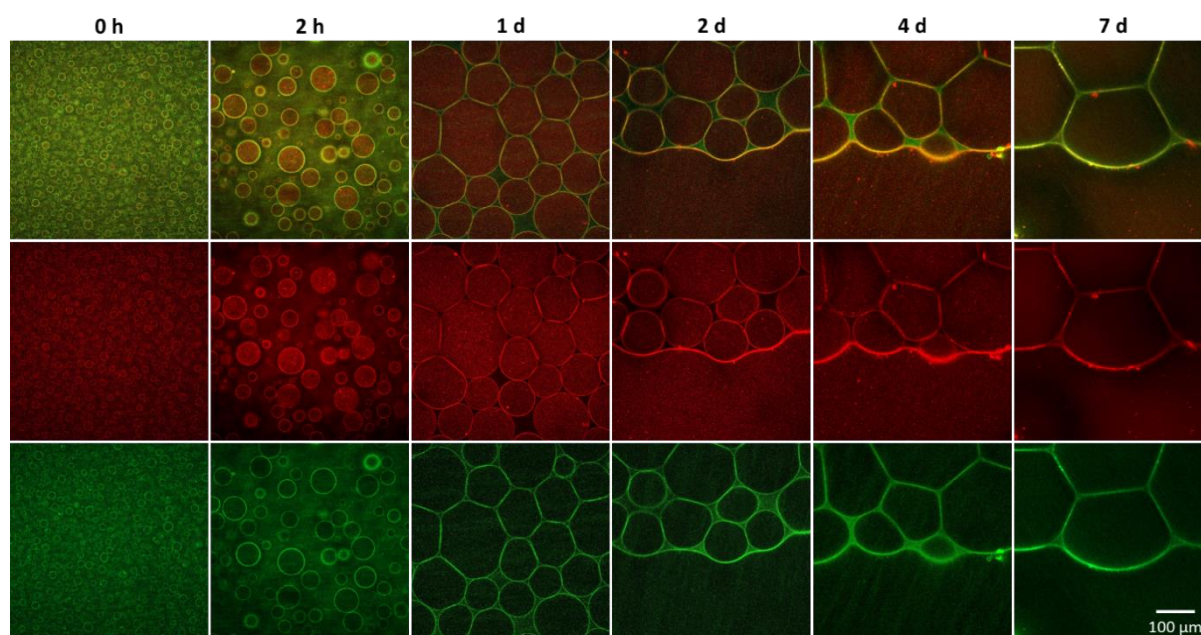


**Figure 6.15.** CLSM images of a mixture of PRO-covered and BIS-covered DEX droplets dispersed in PEO after vortexing. The merged signal of two particles (top), the PRO signal (red, middle) and the BIS signal (green, bottom) are shown. The concentration of BIS was 0.025 wt% and that of PRO was 0.1 wt%.

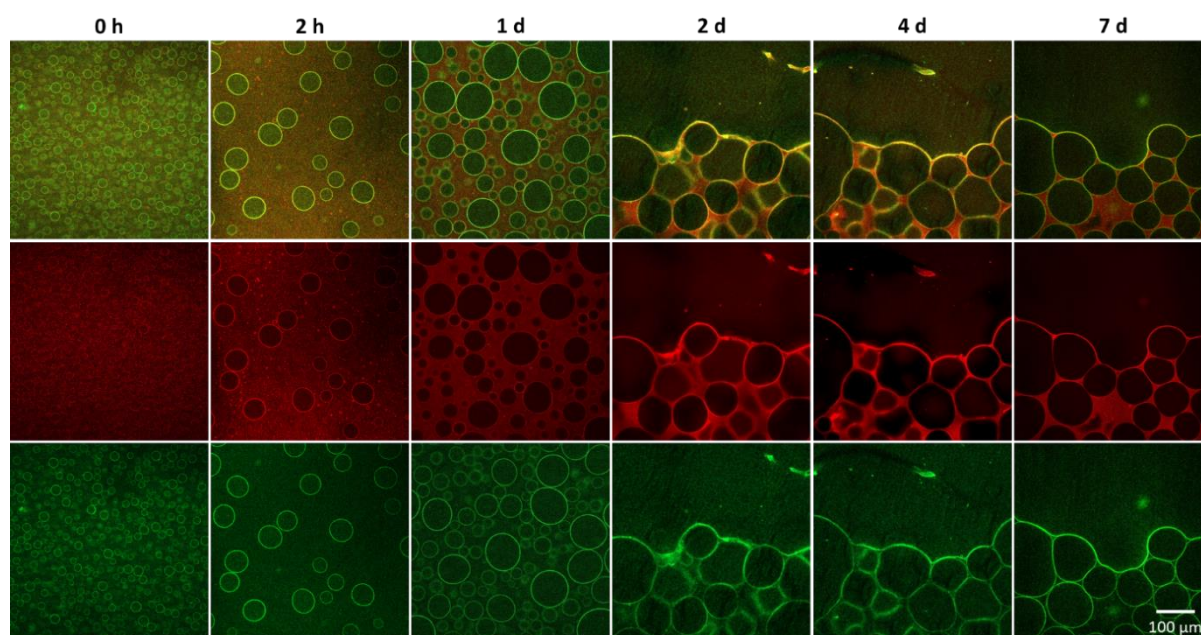


**Figure 6.16.** CLSM images of a mixture of PRO-covered and BIS-covered PEO droplets dispersed in DEX after vortexing. The merged signal of two particles (top), the PRO signal (red, middle) and the BIS signal (green, bottom) are shown. The concentration of BIS was 0.025 wt% and that of PRO was 0.1 wt%.

### 6.3. Stabilization with microgel co-aggregates

For the emulsion mixtures discussed so far, the microgels were already situated at the interface before mixing. However, as was shown in section 6.1, if the microgels are mixed in the PEO phase, co-aggregates are formed, which may alter their effect on the emulsions. Therefore, we added a DEX solution to a PEO solution containing co-aggregated PRO and BIS and vortexed the mixture to form an emulsion. CLSM images show that in this case also a mixed layer is formed with the same thickness, but without preferential contact of PRO with the DEX phase, see **Figure 6.17**. Clearly, co-aggregation inhibited the arrangement of the microgels at the interface allowing the PRO to increase contact with the DEX phase.

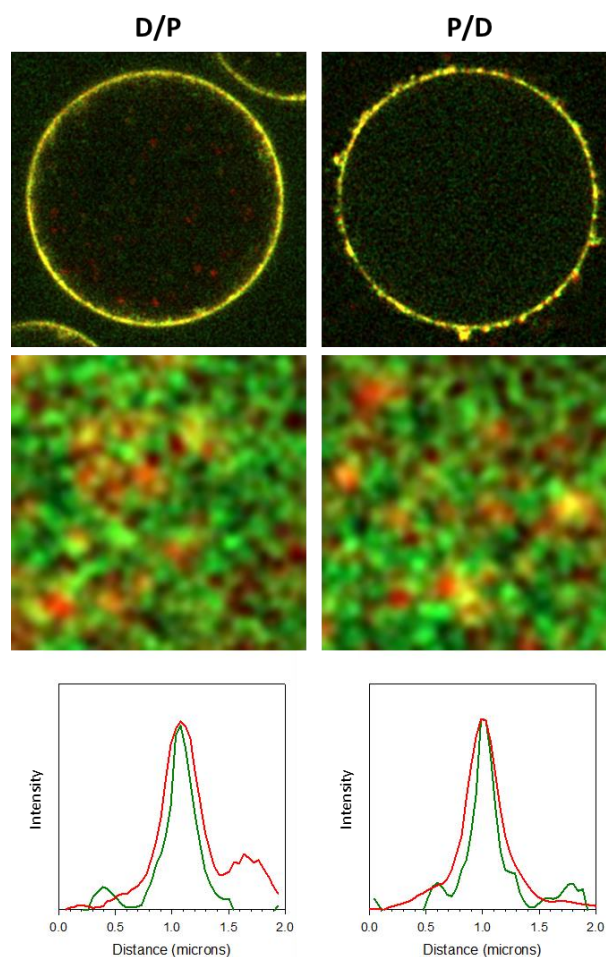


**Figure 6.17.** CLSM images of side and top views of D/P and P/D emulsions formed by PRO-BIS co-aggregates in PEO with DEX, with the fluorescence intensity profiles of microgels through the surface layer.



Slightly more coalescence was observed in these emulsion compared to when the microgels can arrange their position at the interface, see the **Figure 6.18** and **Figure 6.19**, but all emulsions were still stable during at least one week. Similar observations were observed when the concentration of microgels was reduced by two, but the emulsions were less stable, see **Figure 6.20** and **Figure 6.21**. Interestingly, the layers persist to some extent even when the emulsion destabilizes suggesting that the bonds between PRO and BIS microgels in the layer are quite strong. The effect of mixing the microgels in the DEX phase before forming the emulsions was also tested and gave the same results as the emulsion mixture, which was expected since PRO and BIS do not co-aggregate in the DEX phase.

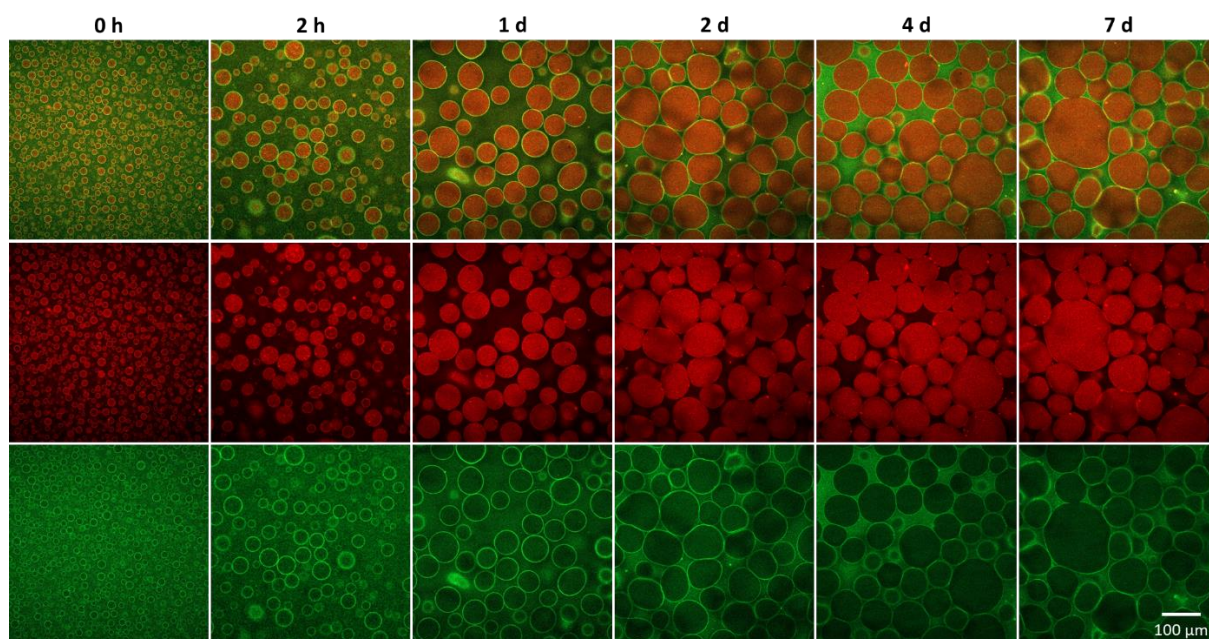


**Figure 6.18.** CLSM images of the D/P emulsions in the presence of PRO-BIS co-aggregates in as a function of time, with the merged signal of two particles (top), the PRO signal (red, middle) and the BIS signal (green, bottom). The concentration of BIS was 0.05 wt% and that of PRO was 0.2 wt%.

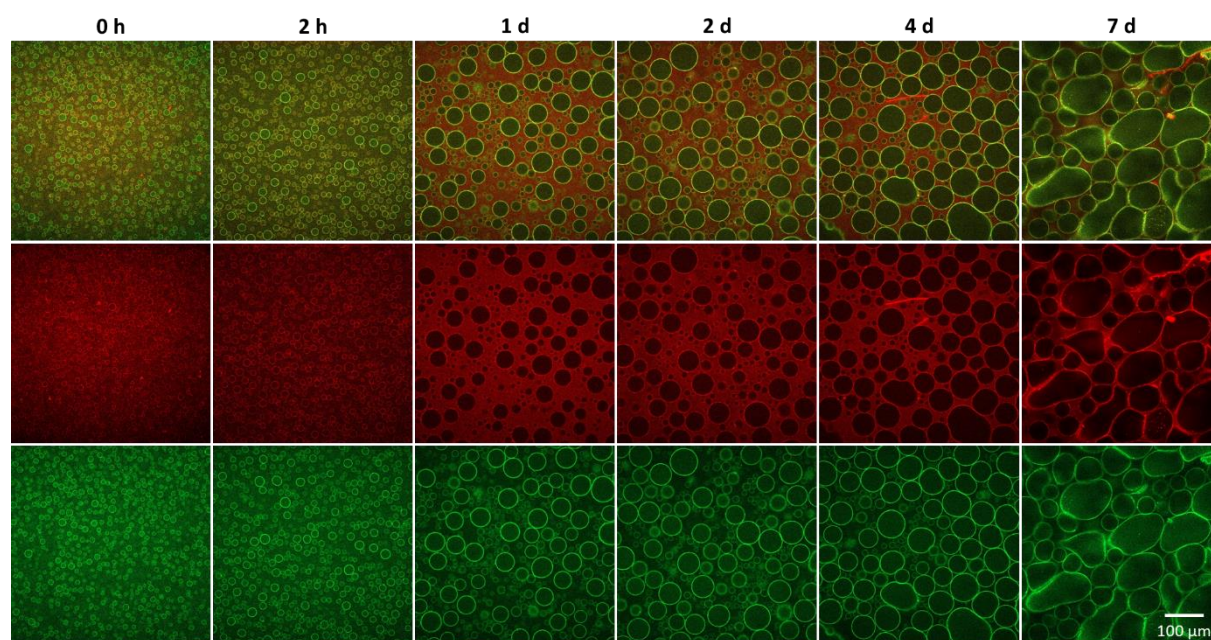


**Figure 6.19.** CLSM images of the P/D emulsions in the presence of PRO-BIS co-aggregates in as a function of time, with the merged signal of two particles (top), the PRO signal (red, middle) and the BIS signal (green, bottom). The concentration of BIS was 0.05 wt% and that of PRO was 0.2 wt%.

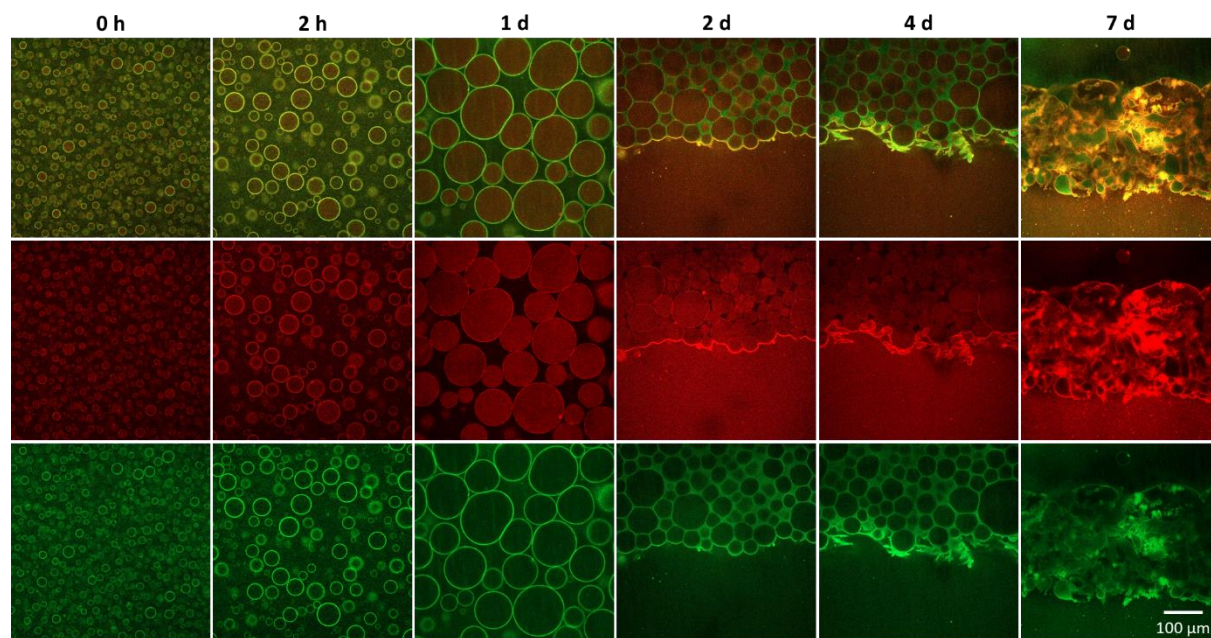


**Figure 6.20.** CLSM images of a D/P emulsion in the presence of PRO-BIS co-aggregates as a function of time, with the merged signal of two particles (top), the PRO signal (red, middle) and the BIS signal (green, bottom). The concentration of BIS was 0.025 wt% and that of PRO was 0.1 wt%.



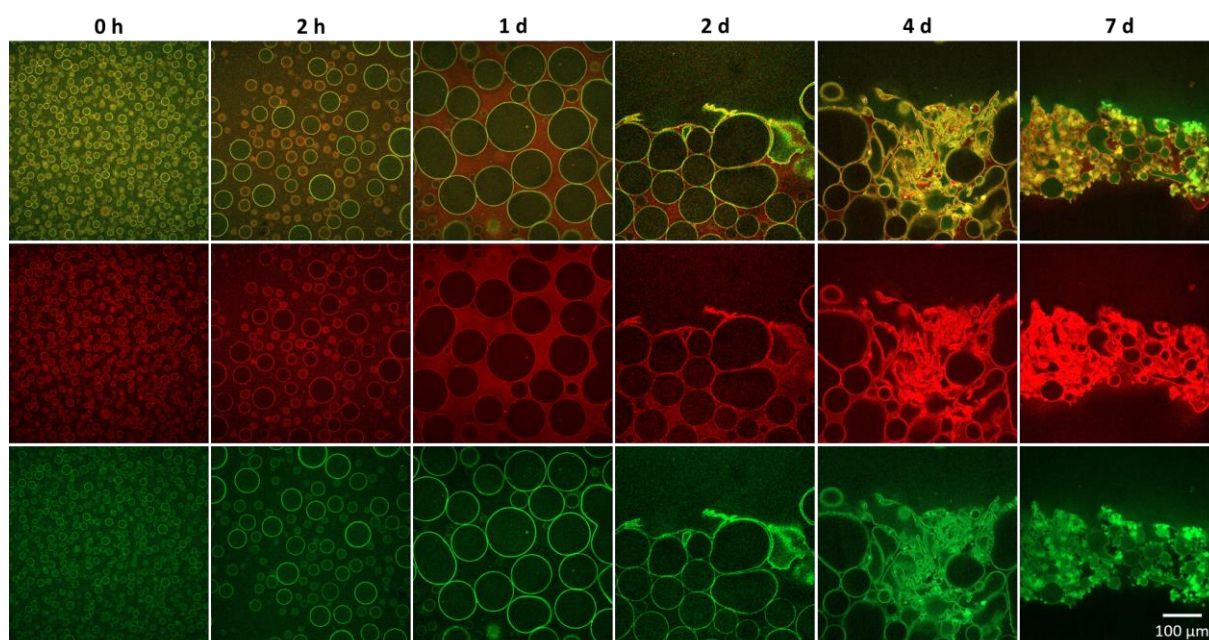


**Figure 6.21.** CLSM images of the P/D emulsions in the presence of PRO-BIS co-aggregates in as a function of time, with the merged signal of two particles (top), the PRO signal (red, middle) and the BIS signal (green, bottom). The concentration of BIS was 0.025 wt% and that of PRO was 0.1 wt%.

#### 6.4. Mixtures of an emulsion and a microgel suspension

We studied the interaction between one type of microgel suspended in the continuous phase and the droplet surface covered by the other type of microgel by gently mixing an emulsion with a suspension in the corresponding continuous phase in equal amounts. At concentrations of PRO and BIS in the mixture of 0.2 wt% and 0.05 wt%, respectively, it was found that PRO added to a D/P emulsion adsorbed spontaneously at the droplet surface covered by BIS, forming a second layer that was preferentially in contact with the DEX phase, see **Figure 6.22**. Interestingly, excess PRO penetrated through the BIS layer into the DEX droplets. When the DEX droplets were covered with PRO, the added free BIS also spontaneously adsorbed at the interface forming again a mixed layer with the PRO preferentially in contact with the DEX phase. The distance between the peak positions of the PRO and BIS layers was  $127 \pm 41$  nm for mixing with free PRO and  $124 \pm 33$  nm with free BIS.

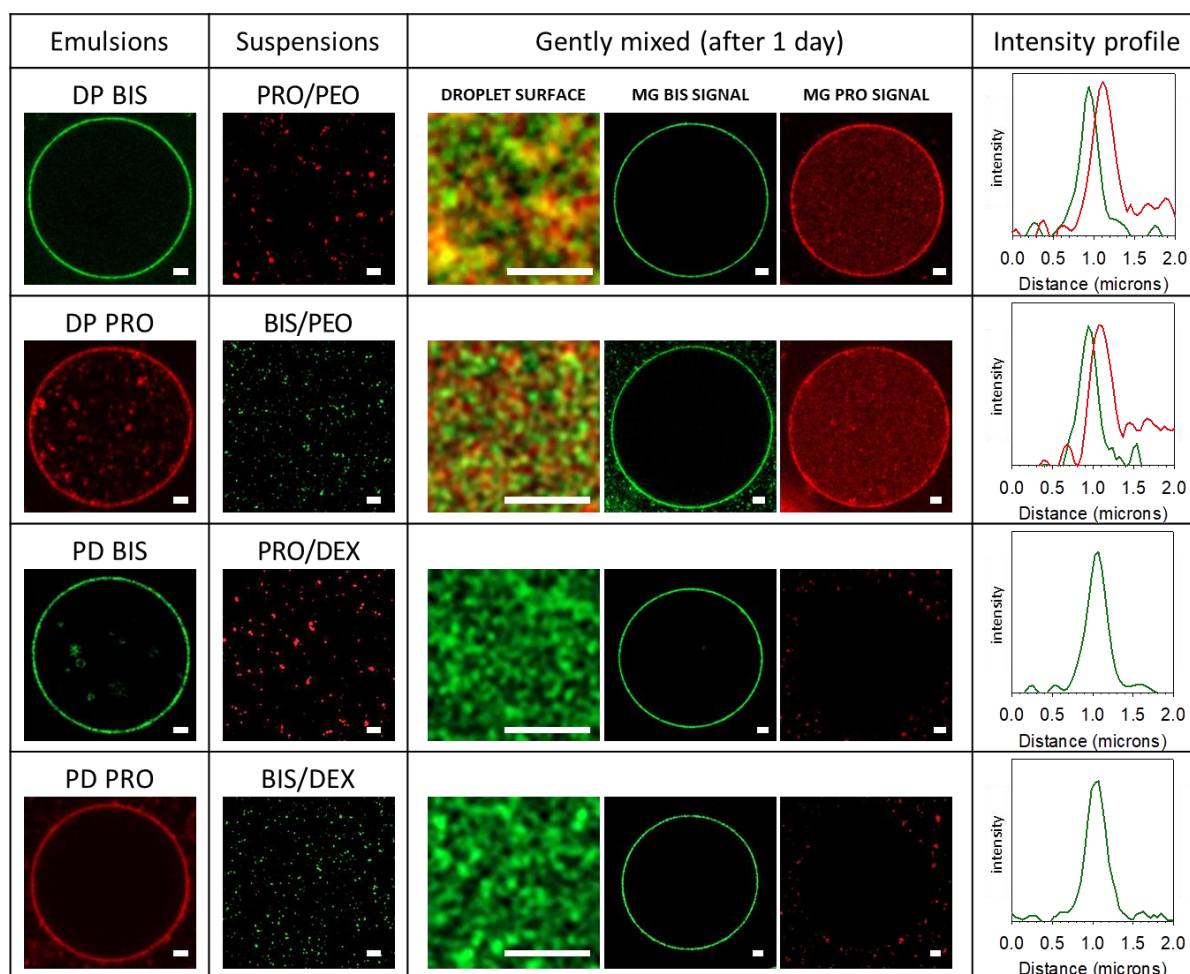


**Figure 6.22.** CLSM images of dispersed DEX and PEO droplets covered by BIS or PRO and suspensions of the microgels in the continuous phase. Also are shown images of the gently mixed systems and the corresponding fluorescence profiles of the layers. The scale bar represents 2  $\mu\text{m}$ . The concentration of BIS in the mixture was 0.05 wt% and that of PRO was 0.2 wt%.

PRO added to a P/D emulsion did not adsorb at the interface covered by BIS, but BIS added to a P/D emulsion adsorbed at the interface and replaced the PRO layer, which took several hours to complete. This intriguing phenomenon can be explained by the strong affinity of PRO with DEX. When PRO is dispersed in DEX and the DEX/PEO interface is already covered by BIS, there is no driving force for PRO to penetrate the BIS layer and be exposed to the PEO phase. For the same reason, the free energy can be reduced by releasing PRO at the interface to the DEX phase and covering the interphase with BIS. We note that spontaneous exchange of PRO microgels between the interface and the bulk does not occur, which means

that it is the presence of BIS that pushes the PRO from the interface. One might expect a similar replacement in the case of D/P emulsion. We speculate that this does not occur, because the two types of microgels meet on the outside of the droplet layer, i.e. in the PEO layer, which causes PRO to bind to BIS and remain stuck at the interface. Only excess PRO can penetrate into the DEX phase. There is an important difference with the gently mixed emulsions discussed in section 6.2.1, that also showed replacement of PRO by BIS at the interface in the case of D/P emulsions. In the latter case the replacement occurred after a BIS covered droplet had coalesced with a PRO covered droplet, whereas here free BIS microgels spontaneously penetrated the PRO layer.

The formation of a mixed layer significantly enhanced the stability of the D/P emulsion compared to that of the emulsion containing only one type of microgel at the same concentration, see **Figure 6.23** and **Figure 6.24**. As expected, the presence of free PRO in the P/D emulsion did not cause any change in stability compared with an emulsion containing only BIS, results not shown.

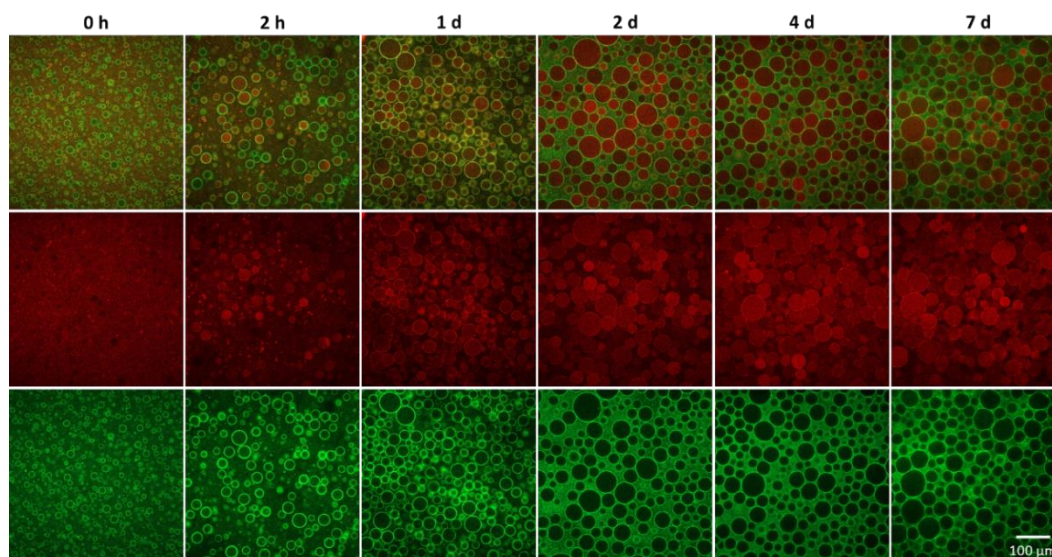


**Figure 6.23.** CLSM pictures of the mixture of BIS-stabilized D/P emulsions and suspension of PRO in PEO, with the merged signal of two particles (top), the PRO signal (red, middle) and the BIS signal (green, bottom). The concentration of BIS was 0.05 wt% and that of PRO was 0.2 wt%.



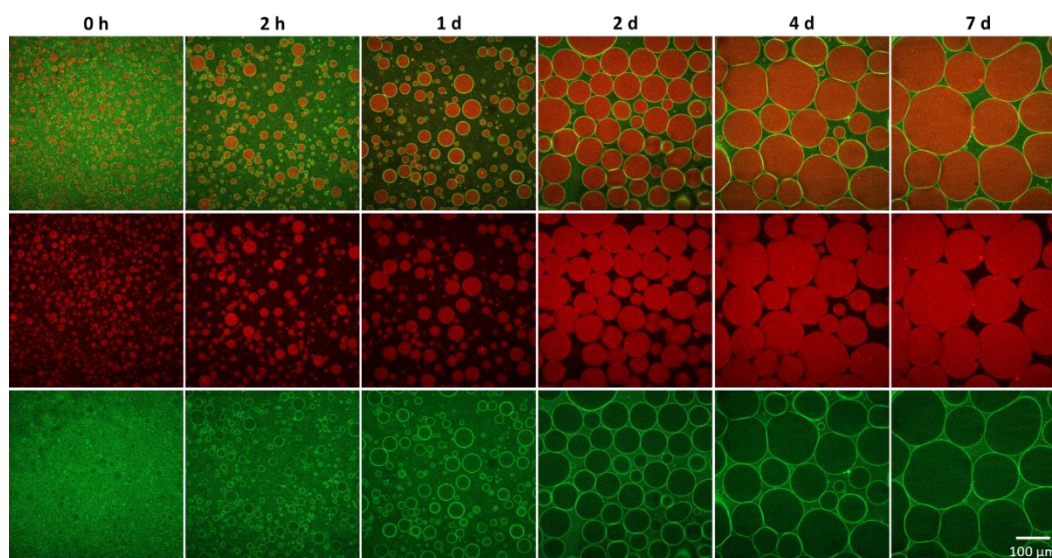


**Figure 6.24.** CLSM pictures of the mixture of PRO-stabilized D/P emulsions and suspension of BIS in PEO, with the merged signal of two particles (top), the PRO signal (red, middle) and the BIS signal (green, bottom). The concentration of BIS was 0.05 wt% and that of PRO was 0.2 wt%.

Similar observations were made when the microgel concentration was reduced by half, see **Figure 6.25**. However, for D/P emulsions the distance between the peak positions was smaller and BIS added to the P/D emulsion no longer replaced all PRO at the interface but formed a mixed layer. This is possibly due to the lower density of the PRO and BIS layers in the emulsions so that there is more space for the added microgel to adsorb and interact with the microgel at the interface. As always, the emulsions with less microgels were less stable, but they were more stable with a mixed layer than with only one type of microgel at the same concentration, results not shown. We note that when the mixtures were vortexed the microstructure and stability were the same and depended only on the composition independent of how the ingredient were mixed.

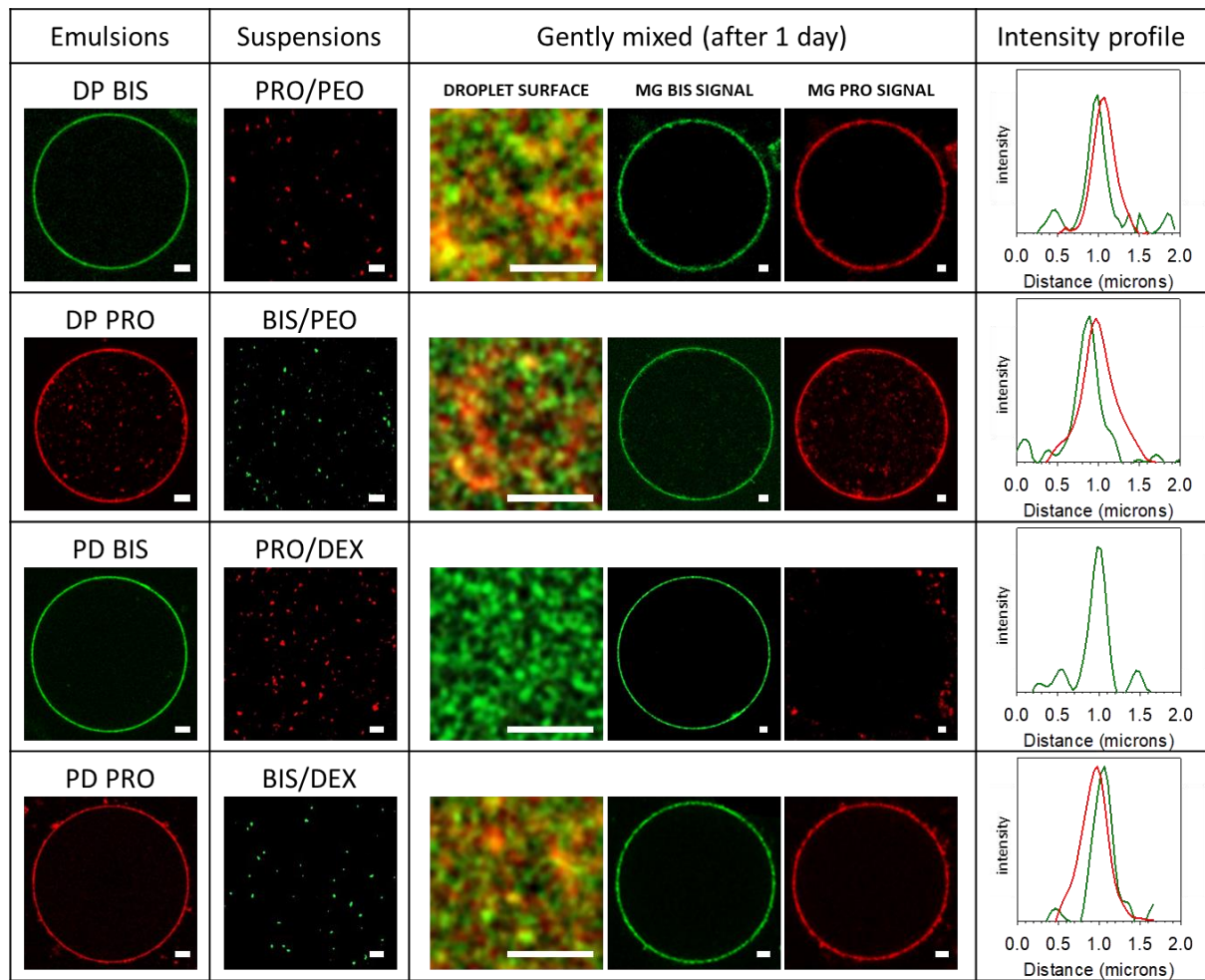


**Figure 6.25.** CLSM images of dispersed DEX and PEO droplets covered by BIS or PRO and suspensions of the microgels in the continuous phase. Also are shown images of the gently mixed systems and the corresponding fluorescence profiles of the layers. The scale bar represents 2  $\mu\text{m}$ . The concentration of BIS in the mixture was 0.025 wt% and that of PRO was 0.1 wt%.

## Conclusion

Synergetic effects on the stability of adding two types of particles has been noted earlier for O/W emulsions [29-31]. W/W behave quite differently, but here it is shown that it is equally possible to exploit the properties of different particles and their interaction at the interface. It was already shown that both PRO and BIS microgels can effectively stabilize W/W emulsions of PEO rich droplets dispersed in a DEX rich continuous phase, but PRO does not stabilize the inverse emulsion [11, 75]. In the presence of both microgels, the microstructure and stability

depend on how the mixture is prepared. For P/D emulsions, the PRO- and BIS-stabilized PEO droplets remain independently stable when they are gently mixed, but mixed layers are formed after vortex mixing. For D/P emulsions, the PRO- and BIS-stabilized DEX droplets coalesce with each other, and the PRO is expelled from the interface into the DEX phase, whereas mixed layers are again formed after vortex mixing. In the mixed layer, the PRO was situated slightly closer to the DEX phase, for which it has a high affinity, than the BIS layer.

BIS and PRO co-aggregate within the PEO phase, but not in water or in the DEX phase. When BIS and PRO are mixed in the PEO phase before adding DEX to prepare the emulsion, a mixed layer is again formed, but in this case the maximum fluorescence of the two microgel layers coincides. When free PRO is gently added to a BIS stabilized P/D emulsion, it remains in the continuous DEX phase, but when it is added to a D/P emulsion it spontaneously enters the interface forming a mixed layer and the excess migrates to the dispersed DEX droplets. When free BIS is gently added to a PRO stabilized D/P or P/D emulsion, it enters the interface and expels the PRO to the DEX phase. After vortexing these mixtures, the same mixed layers are obtained as after vortex mixing preformed PRO- and BIS-stabilized emulsion. In all cases mixed layers resulted in higher stability compared to emulsions with only one type of microgel at the same concentration.





## General conclusion

The research presented in this thesis significantly advances in the understanding of W/W emulsion stabilization by using polymer microgels whose composition is tunable and sensitive to external stimuli aiming to adjust interactions such as temperature, ionic strength, or pH.

I conducted a thorough and systematic study on how particle composition affects its interfacial properties and the stability of emulsions. The approach here demonstrated that adjusting the bis-hydrophilicity of microgels, composed of DEX grafted with pNIPAM, is an efficient method to control emulsion stability. I found that the interfacial adsorption and particle affinity to both phases are dependent on the particle composition, with the optimal stability observed around 50-60 wt% DEX content. This thesis work also explored the significant impact of temperature on emulsion stability. Specifically, at the high content of pNIPAM, P/D emulsion becomes more stable at higher temperatures while D/P emulsions becomes less stable, which was previously noted by Merland et al [10].

The results also highlight that the introduction of charged groups into bis-hydrophilic microgels can alter their sensitivity to pH and ionic strength variations, further enhancing the control over emulsion stability. This study confirms that incorporating acrylic acid units into the microgels inhibits deswelling during heating due to strong electrostatic repulsion. Conversely, reducing the charge density by lowering the pH recovers the deswelling effect. Charged microgels show reduced stabilization efficiency compared to the neutral ones but can be optimized by adjusting the ionic strength of the solution. These behaviors underline the critical role of electrostatic interactions in determining the stability of W/W emulsions. This result clearly highlights the importance of particle/particle and particle/liquid interactions on the stability of W/W emulsions. This dual control mechanism offers chemists new tools for designing efficient and functional particle stabilizers.

The conclusions of the stabilization on the DEX-PEO W/W emulsions can be generalized to other W/W emulsion systems, as was shown for the GEL-PEO system. The same trend of stability dependence on microgel composition was found with the optimal composition to stabilize the G/P emulsion is when the DEX content is about 50 wt%.

The interaction between dispersed droplets of different phases by mixing emulsions with a common continuous phase was investigated. The observed coalescence of droplets and the formation of Janus-like structures demonstrated the complex dynamics at the interface. The presence of microgels at the interface and their preference for residing in specific phases suggest that one can control droplet interactions and stability in mixed emulsions. Different active ingredients could be enclosed in dispersed droplets so that mixing the emulsions offers the opportunity to bring these ingredients in contact with each other in a controlled manner. This process opens interesting perspectives in controlling the initiation time of a reaction kinetic between them.

Additionally, the effect of using two different particles on W/W emulsions was investigated, by adding both bishydrophilic microgels and protein particles. The organization of the two types of particles at the interface is pathway dependent. When gently mixed, protein and bishydrophilic microgel-stabilized droplets can remain independently stable or coalesce with each other depending on the phase composition, but mixed layers are always formed after vortex mixing. The combination of the different particle types that were studied enhanced the stability, suggesting that mixed layers at the interface may be more effective than single particle types. This finding provides a pathway for optimizing emulsion properties for a specific combination of applications.

Despite these advancements, there remain many unresolved issues in the stabilization of Pickering W/W emulsions. Future research can focus on a detailed rheological study of emulsions under various conditions to deepen our understanding and improve the practical

applications of these findings. It would also be of interest to study more precisely the permeability of microgel membrane under various conditions (dilution, salt, pH, etc).

Overall, this study provided a comprehensive framework for understanding and controlling the stability of W/W emulsions through the manipulation of particle composition. It offers valuable insights for chemists and material scientists in designing and developing efficient particle stabilizers with potential new functionalities. This work also opened new possibilities in encapsulation and controlled reactions, expanding the use and application of W/W emulsions across various industries such as food science, pharmaceuticals, and cosmetics.



## References

- [1] W.J. Frith, Mixed biopolymer aqueous solutions—phase behaviour and rheology, *Advances in Colloid and Interface Science*, 161(1-2), 2010, 48-60.
- [2] Y. Chao, H.C. Shum, Emerging aqueous two-phase systems: from fundamentals of interfaces to biomedical applications, *Chemical Society Reviews*, 49(1), 2020, 114-142.
- [3] C.D. Keating, Aqueous Phase Separation as a Possible Route to Compartmentalization of Biological Molecules, *Accounts of Chemical Research*, 45(12), 2012, 2114-2124.
- [4] N. Martin, Dynamic Synthetic Cells Based on Liquid–Liquid Phase Separation, *ChemBioChem*, 20(20), 2019, 2553-2568.
- [5] D. Forciniti, C.K. Hall, M.R. Kula, Interfacial tension of polyethyleneglycol-dextran-water systems: influence of temperature and polymer molecular weight, *Journal of Biotechnology*, 16(3-4), 1990, 279-296.
- [6] E. Dickinson, Microgels—an alternative colloidal ingredient for stabilization of food emulsions, *Trends in Food Science Technology*, 43(2), 2015, 178-188.
- [7] J. Esquena, Water-in-water (W/W) emulsions, *Current Opinion in Colloid & Interface Science*, 25, 2016, 109-119.
- [8] T. Nicolai, B. Murray, Particle stabilized water in water emulsions, *Food Hydrocolloids*, 68, 2017, 157-163.
- [9] R.A. de Freitas, T. Nicolai, C. Chassenieux, L. Benyahia, Stabilization of water-in-water emulsions by polysaccharide-coated protein particles, *Langmuir*, 32(5), 2016, 1227-1232.
- [10] T. Merland, L. Waldmann, O. Guignard, M.C. Tatry, A.L. Wirotius, V. Lapeyre, P. Garrigue, T. Nicolai, L. Benyahia, V. Ravaine, Thermo-induced inversion of water-in-water emulsion stability by bis-hydrophilic microgels, *Journal of Colloid and Interface Science*, 608, 2022, 1191-1201.
- [11] B.T. Nguyen, T. Nicolai, L. Benyahia, Stabilization of Water-in-Water Emulsions by Addition of Protein Particles, *Langmuir*, 29(34), 2013, 10658-10664.
- [12] M. Pavlovic, A. Plucinski, L. Zeininger, B.V.K.J. Schmidt, Temperature sensitive water-in-water emulsions, *Chemical Communications*, 56(50), 2020, 6814-6817.
- [13] D.M.A. Buzza, P.D. Fletcher, T.K. Georgiou, N. Ghasdian, Water-in-water emulsions based on incompatible polymers and stabilized by triblock copolymers—templated polymersomes, *Langmuir*, 29(48), 2013, 14804-14814.
- [14] D.C. Dewey, C.A. Strulson, D.N. Cacace, P.C. Bevilacqua, C.D. Keating, Bioreactor droplets from liposome-stabilized all-aqueous emulsions, *Nature Communications*, 5(1), 2014, 4670.

- [15] N. Coudon, L. Navailles, F. Nallet, I. Ly, A. Bentaleb, J.-P. Chapel, L. Béven, J.-P. Douliez, N. Martin, Stabilization of all-aqueous droplets by interfacial self-assembly of fatty acids bilayers, *Journal of Colloid and Interface Science*, 617, 2022, 257-266.
- [16] T. Hanazawa, B.S. Murray, Effect of Oil Droplets and Their Solid/Liquid Composition on the Phase Separation of Protein–Polysaccharide Mixtures, *Langmuir*, 29(31), 2013, 9841-9848.
- [17] B.P. Binks, H. Shi, Phase inversion of silica particle-stabilized water-in-water emulsions, *Langmuir*, 35(11), 2019, 4046-4057.
- [18] E. Ben Ayed, R. Cochereau, C. Dechancé, I. Capron, T. Nicolai, L. Benyahia, Water-in-water emulsion gels stabilized by cellulose nanocrystals, *Langmuir*, 34(23), 2018, 6887-6893.
- [19] T. Hoare, R. Pelton, Functional group distributions in carboxylic acid containing poly(N-isopropylacrylamide) microgels, *Langmuir*, 20(6), 2004, 2123-2133.
- [20] K. Geisel, L. Isa, W. Richtering, The compressibility of pH-sensitive microgels at the oil-water interface: higher charge leads to less repulsion, *Angew Chem Int Ed Engl*, 53(19), 2014, 4905-9.
- [21] P. Masse, E. Sellier, V. Schmitt, V. Ravaine, Impact of electrostatics on the adsorption of microgels at the interface of Pickering emulsions, *Langmuir*, 30(49), 2014, 14745-56.
- [22] M.M. Schmidt, S. Bochenek, A.A. Gavrillov, Potemkin, II, W. Richtering, Influence of Charges on the Behavior of Polyelectrolyte Microgels Confined to Oil-Water Interfaces, *Langmuir*, 36(37), 2020, 11079-11093.
- [23] M.H. Kwok, J. Ambreen, T. Ngai, Correlating the effect of co-monomer content with responsiveness and interfacial activity of soft particles with stability of corresponding smart emulsions, *J Colloid Interface Sci*, 546, 2019, 293-302.
- [24] W.M. Aumiller Jr, B.W. Davis, N. Hashemian, C. Maranas, A. Armaou, C.D. Keating, Coupled enzyme reactions performed in heterogeneous reaction media: experiments and modeling for glucose oxidase and horseradish peroxidase in a PEG/citrate aqueous two-phase system, *The Journal of Physical Chemistry B*, 118(9), 2014, 2506-2517.
- [25] S. Mytnyk, A.G. Olive, F. Versluis, J.M. Poolman, E. Mendes, R. Eelkema, J.H.J.A.C. van Esch, Compartmentalizing supramolecular hydrogels using aqueous multi-phase systems, *Angewandte Chemie*, 129(47), 2017, 15119-15123.
- [26] T. Nicolai, J.P. Machado, Effect of the interfacial tension on droplet association in aqueous multiphase systems, *Langmuir*, 37(19), 2021, 5909-5915.
- [27] Y. Beldengrün, V. Dallarís, C. Jaén, R. Protat, J. Miras, M. Calvo, M.J. Garcia-Celma, J. Esquena, Formation and stabilization of multiple water-in-water-in-water (W/W/W) emulsions, *Food Hydrocolloids*, 102, 2020, 105588.
- [28] Y. Song, A. Sauret, H. Cheung Shum, All-aqueous multiphase microfluidics, *Biomicrofluidics*, 7(6), 2013.

- [29] T. Nallamilli, B.P. Binks, E. Mani, M.G. Basavaraj, Stabilization of Pickering emulsions with oppositely charged latex particles: influence of various parameters and particle arrangement around droplets, *Langmuir*, 31(41), 2015, 11200-11208.
- [30] M. Benyaya, M.A. Bolzinger, Y. Chevalier, S. Ensenat, C. Bordes, Pickering emulsions stabilized with differently charged particles, *Soft Matter*, 19(25), 2023, 4780-4793.
- [31] B.P. Binks, S. Lumsdon, Transitional phase inversion of solid-stabilized emulsions using particle mixtures, *Langmuir*, 16(8), 2000, 3748-3756.
- [32] F.M.F. Barros, B.L. Pelegrini, C. Chassenieux, M.M. de Souza Lima, L. Benyahia, Rheology and structure of Pickering emulsions undergoing transitional phase inversion using a mixture of hydrophilic and hydrophobic silica particles, *Colloids and Surfaces A: Physicochemical and Engineering Aspects*, 644, 2022, 128801.
- [33] M.W. Beijerinck, Über Gallbildung und Generationswechsel bei *Cynips calicis* und über die Circulansgalle, Müller 1896.
- [34] P.Å. Albertsson, Partition of proteins in liquid polymer-polymer two-phase systems, *Nature*, 182(4637), 1958, 709-711.
- [35] X. Zhang, Z. Cai, L. Wang, S. Xie, W. Zong, Unlocking Liquid-Liquid Separation: Exploring the marvels of aqueous Two-Phase systems, *Microchemical Journal*, 2024, 110445.
- [36] P.J. Flory, Principles of polymer chemistry, Cornell university press 1953.
- [37] K. Bergfeldt, L. Piculell, P. Linse, Segregation and association in mixed polymer solutions from Flory-Huggins model calculations, *The Journal of Physical Chemistry*, 100(9), 1996, 3680-3687.
- [38] B. de Jong, Coacervation, *Proc. Royal Acad. Amsterdam*, 1929, pp. 849-856.
- [39] L. Piculell, B. Lindman, Association and segregation in aqueous polymer/polymer, polymer/surfactant, and surfactant/surfactant mixtures: similarities and differences, *Advances in Colloid and Interface Science*, 41, 1992, 149-178.
- [40] V.Y. Grinberg, V. Tolstoguzov, Thermodynamic incompatibility of proteins and polysaccharides in solutions, *Food hydrocolloids*, 11(2), 1997, 145-158.
- [41] J.F. Pereira, J.A. Coutinho, Aqueous two-phase systems, *Liquid-phase extraction*, Elsevier, 2020, pp. 157-182.
- [42] J. Ryden, P. Albertsson, Interfacial tension of dextran-polyethylene glycol-water two-phase systems, *Journal of Colloid and Interface Science*, 37(1), 1971, 219-222.
- [43] Å. Gustafsson, H. Wennerström, F. Tjerneld, The nature of phase separation in aqueous two-polymer systems, *Polymer*, 27(11), 1986, 1768-1770.
- [44] P.G. Mazzola, A.M. Lopes, F.A. Hasmann, A.F. Jozala, T.C. Penna, P.O. Magalhaes, C.O. Rangel-Yagui, A. Pessoa Jr, Liquid-liquid extraction of biomolecules: an overview and update of the main techniques, *Journal of Chemical*



Technology & Biotechnology: International Research in Process, Environmental & Clean Technology, 83(2), 2008, 143-157.

[45] M.W. Edelman, E. Van Der Linden, R.H. Tromp, Phase separation of aqueous mixtures of poly (ethylene oxide) and dextran, *Macromolecules*, 36(20), 2003, 7783-7790.

[46] Y. Meng, E. Nicol, T. Nicolai, Exploiting multiple phase separation to stabilize water in water emulsions and form stable microcapsules, *Journal of Colloid and Interface Science*, 617, 2022, 65-72.

[47] M. Iqbal, Y. Tao, S. Xie, Y. Zhu, D. Chen, X. Wang, L. Huang, D. Peng, A. Sattar, M.A.B. Shabbir, Aqueous two-phase system (ATPS): an overview and advances in its applications, *Biological procedures online*, 18, 2016, 1-18.

[48] G. Balakrishnan, T. Nicolai, L. Benyahia, D. Durand, Particles trapped at the droplet interface in water-in-water emulsions, *Langmuir*, 28(14), 2012, 5921-5926.

[49] M. Vis, J. Opdam, I.S. Van't Oor, G. Soligno, R. Van Roij, R.H. Tromp, B.H. Ern , Water-in-water emulsions stabilized by nanoplates, *ACS Macro Letters*, 4(9), 2015, 965-968.

[50] R.H. Tromp, M. Vis, B. Ern , E. Blokhuis, Composition, concentration and charge profiles of water–water interfaces, *Journal of Physics: Condensed Matter*, 26(46), 2014, 464101.

[51] J. Rowlinson, Liversidge Lecture. The surface of a liquid, *Chemical Society Reviews*, 7(3), 1978, 329-343.

[52] J. Guzowski, P.M. Korczyk, S. Jakiela, P. Garstecki, The structure and stability of multiple micro-droplets, *Soft Matter*, 8(27), 2012, 7269-7278.

[53] H.C. Shum, Y.j. Zhao, S.H. Kim, D.A. Weitz, Multicompartment polymersomes from double emulsions, *Angewandte Chemie International Edition*, 50(7), 2011, 1648-1651.

[54] J.S. Rowlinson, B. Widom, *Molecular theory of capillarity*, Courier Corporation 2013.

[55] B.P. Binks, T.S. Horozov, *Colloidal Particles at Liquid Interfaces: An Introduction*, *Colloidal Particles at Liquid Interfaces*, Cambridge University Press, Cambridge, 2006, pp. 1-74.

[56] H. Firoozmand, B.S. Murray, E. Dickinson, Interfacial structuring in a phase-separating mixed biopolymer solution containing colloidal particles, *Langmuir*, 25(3), 2009, 1300-1305.

[57] A. Gonzalez-Jordan, T. Nicolai, L. Benyahia, Enhancement of the particle stabilization of water-in-water emulsions by modulating the phase preference of the particles, *Journal of colloid and interface science*, 530, 2018, 505-510.

[58] W.J. Ganley, P.T. Ryan, J.S. van Duijneveldt, Stabilisation of water-in-water emulsions by montmorillonite platelets, *Journal of colloid and interface science*, 505, 2017, 139-147.

- [59] A. Gonzalez-Jordan, T. Nicolai, L. Benyahia, Influence of the protein particle morphology and partitioning on the behavior of particle-stabilized water-in-water emulsions, *Langmuir*, 32(28), 2016, 7189-7197.
- [60] M. Inam, J.R. Jones, M.M. Perez-Madrigo, M.C. Arno, A.P. Dove, R.K. O'Reilly, Controlling the size of two-dimensional polymer platelets for water-in-water emulsifiers, *ACS central science*, 4(1), 2018, 63-70.
- [61] B.T. Nguyen, W. Wang, B.R. Saunders, L. Benyahia, T. Nicolai, pH-responsive water-in-water Pickering emulsions, *Langmuir*, 31(12), 2015, 3605-3611.
- [62] M. Moutkane, L. Benyahia, T. Nicolai, Stable protein microcapsules by crosslinking protein particles in water in water emulsions, *Colloids and Surfaces A: Physicochemical and Engineering Aspects*, 656, 2023, 130353.
- [63] J. Zhang, J. Hwang, M. Antonietti, B.V. Schmidt, Water-in-water pickering emulsion stabilized by polydopamine particles and cross-linking, *Biomacromolecules*, 20(1), 2018, 204-211.
- [64] M. Ossenbach-Sauter, G. Riess, G. Champetier, Propriétés émulsifiantes des copolymères séquencés. Emulsions du type eau dans eau, *CR Seances Acad. Sci., Ser. C*, 283, 1976, 269-272.
- [65] L. Nan, Y. Cao, S. Yuan, H.C. Shum, Oil-mediated high-throughput generation and sorting of water-in-water droplets, *Microsystems & nanoengineering*, 6(1), 2020, 70.
- [66] S.D. Hann, K.J. Stebe, D. Lee, Awe-somes: All water emulsion bodies with permeable shells and selective compartments, *ACS applied materials & interfaces*, 9(29), 2017, 25023-25028.
- [67] R.H. Tromp, R. Tuinier, M. Vis, Polyelectrolytes adsorbed at water–water interfaces, *Physical Chemistry Chemical Physics*, 18(45), 2016, 30931-30939.
- [68] J. Chen, J. Guo, X. Yang, T. Nicolai, Water-in-water-in-water emulsions formed by cooling mixtures of guar, amylopectin and gelatin, *Food Hydrocolloids*, 118, 2021, 106763.
- [69] X.T. Phan, D. Durand, T. Nicolai, L. Donato, C. Schmitt, L. Bovetto, On the crucial importance of the pH for the formation and self-stabilization of protein microgels and strands, *Langmuir*, 27(24), 2011, 15092-15101.
- [70] B.J. Berne, R. Pecora, *Dynamic light scattering: with applications to chemistry, biology, and physics*, Courier Corporation 2000.
- [71] J.B. Boitte, C. Vizcaino, L. Benyahia, J.M. Herry, C. Michon, M. Hayert, A novel rheo-optical device for studying food complex systems under controlled double plate shear, 2012.
- [72] G. Badolato, F. Aguilar, H. Schuchmann, T. Sobisch, D. Lerche, Evaluation of long term stability of model emulsions by multisample analytical centrifugation, *Surface and interfacial forces—from fundamentals to applications*, Springer 2008, pp. 66-73.

- [73] S. Kuchler, C. Schneider, D. Lerche, T. Sobisch, Process optimisation for making stable emulsions using accelerated dispersion analysis by multisample analytical centrifugation, *Labplus Int*, 20(14), 2006.
- [74] L. Tea, F. Renou, L. Benyahia, T. Nicolai, Assessment of the stability of water in water emulsions using analytical centrifugation, *J Colloids Surfaces A: Physicochemical Engineering Aspects*, 608, 2021, 125619.
- [75] L. Waldmann, D.N.T. Nguyen, S. Arbault, T. Nicolai, L. Benyahia, V. Ravaine, Tuning the bis-hydrophilic balance of microgels: A tool to control the stability of water-in-water emulsions, *Journal of Colloid and Interface Science*, 653(Pt A), 2024, 581-593.
- [76] R. Liu, M. Fraylich, B.R. Saunders, Thermoresponsive copolymers: From fundamental studies to applications, *Colloid and Polymer Science*, 287(6), 2009, 627-643.
- [77] J. Es Sayed, C. Lorthioir, P. Perrin, N. Sanson, PEGylated NiPAM microgels: synthesis, characterization and colloidal stability, *Soft Matter*, 15(5), 2019, 963-972.
- [78] K.R. Peddireddy, T. Nicolai, L. Benyahia, I. Capron, Stabilization of Water-in-Water Emulsions by Nanorods, *ACS Macro Letters*, 5, 2016, 283-286.
- [79] M. Vis, V.F. Peters, E.M. Blokhuis, H.N. Lekkerkerker, B.H. Ern e, R.H. Tromp, Decreased interfacial tension of demixed aqueous polymer solutions due to charge, *Physical review letters*, 115(7), 2015, 078303.

**Titre :** Stabilisation des émulsions eau-dans-eau par les microgels bishydrophiles

**Mots clés :** Emulsion, Microgel, Bishydrophile, Stability

**Résumé :** Les émulsions Eau-dans-Eau (E/E) sont obtenues en mélangeant deux types de polymères incompatibles en solution aqueuse, qui ont tendance à se séparer en deux phases distinctes. Ces systèmes ont suscité l'intérêt en tant que moyen simple de former des micro-compartiments tout aqueux capables d'encapsuler différents types de molécules. En comparaison aux émulsions Huile-dans-Eau, l'interface séparant les phases aqueuses est plus épaisse et présente une tension interfaciale deux à trois ordres de grandeur plus faible. Pour ces raisons, la stabilisation des émulsions E/E ne peut s'obtenir par des petits tensioactifs, mais nécessite des particules de taille suffisamment grande pouvant s'adsorber spontanément à l'interface et ainsi présenter une barrière contre la coalescence des gouttelettes. La stabilisation de ces émulsions par des particules, grâce à l'effet Pickering, a donc ouvert le champ d'applications dans les domaines de l'encapsulation de principes actifs, des biocapteurs ou encore du biomimétisme cellulaire. Si plusieurs études ont rapporté l'efficacité de divers types de particules dans la stabilisation des émulsions E/E, une compréhension plus approfondie et systématique des effets de la nature chimique des particules sur la stabilité des émulsions reste peu explorée.

Le travail de thèse vise à étudier les mécanismes de stabilisation des émulsions E/E par des microgels polymères dont la composition est modulable tout en étant sensibles à certains stimuli externes pour ajuster les interactions comme la température, la force ionique ou le pH. Les microgels sont composés de dextran (DEX) greffé de poly(N-isopropylacrylamide) (pNIPAM) leur conférant un caractère bishydrophile inédit.

Plusieurs techniques ont été mises en œuvre pour étudier les émulsions produites comme la diffusion de lumière, la microscopie confocale à balayage laser, la centrifugation analytique combinée à de la turbidimétrie...

Les résultats de ce travail ont montré qu'il est possible de moduler l'adsorption des particules aux interfaces liquide/liquide et leur affinité avec les deux phases en moduler le ratio du DEX, avec un optimum de compositions vers 50 wt%. La thermosensibilité du pNIPAM a permis d'inverser la stabilité des émulsions en traversant la température de transition de phase volumique (VPTT) du pNIPAM.

Par la suite, par l'incorporation d'unités d'acide acrylique dans les microgels, il a été possible de les rendre sensibles à la variation du pH ou la force ionique par ajout de sel, qui par ailleurs se révèlent non équivalentes vis-à-vis du comportement des émulsions pour un état de charge donné. Ce résultat met clairement en exergue l'importance des interactions particule/particule et particule/liquide sur la stabilité des émulsions E/E.

L'étude a été ensuite étendue, à des systèmes triphasiques en montrant la complexité du comportement de ces émulsions qui conduisent de manière étonnante à des structures en chapelet de gouttelettes Janus alors que les émulsions de départ sont parfaitement stables contre la coalescence.

La dernière partie de ce travail a porté sur l'étude d'un mélange des microgels bishydrophiles avec de particules de protéine. Cette stratégie a permis d'optimiser la stabilité des émulsions E/E mais également la structuration et l'organisation des deux types de particules à l'interface.

**Title:** Stabilization of water-in-water emulsions by bishydrophilic microgels

**Keywords:** Emulsion, Microgel, Bishydrophile, Stability

**Abstract:** Water-in-Water (W/W) emulsions are obtained by mixing two types of incompatible polymers in an aqueous solution, which tend to separate into two distinct phases. These systems have attracted interest as a simple way of forming all-aqueous micro-compartments capable of encapsulating different types of molecules. Compared to oil-in-water emulsions, the interface separating the aqueous phases is thicker and has an interfacial tension two to three orders of magnitude lower. For these reasons, the stabilization of W/W emulsions cannot be achieved by small surfactants but requires particles large enough to spontaneously adsorb at the interface and thus provide a barrier against droplet coalescence. The stabilization of these emulsions by particles, through the Pickering effect, has thus opened up applications in the fields of active ingredient encapsulation, biosensors, cellular biomimicry, etc. While several studies have reported the effectiveness of various types of particles in stabilizing W/W emulsions, a deeper and more systematic understanding of the effects of the chemical nature of the particles on the stability of the emulsions remains underexplored.

The thesis work aims to study the stabilization mechanisms of W/W emulsions by polymer microgels whose composition is tunable and sensitive to external stimuli aiming to adjust interactions such as temperature, ionic strength, or pH. The microgels are composed of dextran (DEX) grafted with poly(N-isopropylacrylamide) (pNIPAM), giving them a novel bishydrophilic character.

Several techniques were employed to study the produced emulsions, such as light scattering, laser scanning confocal microscopy, analytical centrifugation combined with turbidimetry,...

The results of this work have shown that it is possible to modulate the adsorption of particles at the liquid/liquid interfaces and their affinity with the two phases by adjusting the DEX ratio, with an optimal composition around 50 wt%. The thermosensitivity of pNIPAM allowed for the inversion of emulsion stability by crossing the volume phase transition temperature (VPTT) of pNIPAM. Subsequently, by incorporating acrylic acid units into the microgels, it was possible to make them sensitive to pH or ionic strength variations by adding salt, which, moreover, are not equivalent with respect to the behavior of the emulsions for a given charge state. This result clearly highlights the importance of particle/particle and particle/liquid interactions on the stability of W/W emulsions.

The study was then extended to triphasic systems, demonstrating the complexity of the behavior of these emulsions, which surprisingly lead to necklace-like structures of Janus droplets even though the initial emulsions are perfectly stable against coalescence.

The final part of this work focused on the study of a mixture of bishydrophilic microgels with protein particles. This strategy optimized the stability of W/W emulsions as well as the structuring and organization of the two types of particles at the interface.

## RÉSUMÉ LONG EN FRANÇAIS

Les émulsions Eau-dans-Eau (E/E) sont obtenues en mélangeant deux types de polymères incompatibles en solution aqueuse, qui ont tendance à se séparer en deux phases distinctes. Ces systèmes ont suscité l'intérêt en tant que moyen simple de former des micro-compartiments tout aqueux capables d'encapsuler différents types de molécules. En comparaison aux émulsions Huile-dans-Eau, l'interface séparant les phases aqueuses est plus épaisse et présente une tension interfaciale deux à trois ordres de grandeur plus faible. Pour ces raisons, la stabilisation des émulsions E/E ne peut s'obtenir par des petits tensioactifs, mais nécessite des particules de taille suffisamment grande pouvant s'adsorber spontanément à l'interface et ainsi présenter une barrière contre la coalescence des gouttelettes. La stabilisation de ces émulsions par des particules, grâce à l'effet Pickering, a donc ouvert le champ d'applications dans les domaines de l'encapsulation de principes actifs, des biocapteurs ou encore du biomimétisme cellulaire. Si plusieurs études ont rapporté l'efficacité de divers types de particules dans la stabilisation des émulsions E/E, une compréhension plus approfondie et systématique des effets de la nature chimique des particules sur la stabilité des émulsions reste peu explorée.

Le travail de thèse vise à étudier les mécanismes de stabilisation des émulsions E/E par des microgels polymères dont la composition est modulable tout en étant sensibles à certains stimuli externes pour ajuster les interactions comme la température, la force ionique ou le pH. Les microgels sont composés de dextran (DEX) greffé de poly(N-isopropylacrylamide) (pNIPAM) leur conférant un caractère bishydrophile inédit. Plusieurs techniques ont été mises en œuvre pour étudier les émulsions produites comme la diffusion de lumière, la microscopie confocale à balayage laser, la centrifugation analytique combinée à de la turbidimétrie...

Le premier but de cette étude est d'évaluer la capacité des microgels bis-hydrophiliques de stabiliser des émulsions E/E en fonction de leur composition. De ce faire, la fraction

massique de DEX a été variée de 27 à 60 %. Le taux de substitution est de 12 % à 20 %. Les DEX avec des masses molaires de 6000 et de 40000 Mw sont utilisés lors de la synthèse. Des émulsions modèles formées par des mélanges de DEX ( $M_w = 4.5-6.5 \times 10^5$  g/mol) et de polyéthylène glycol (PEO) ( $M_w = 2 \times 10^5$  g/mol) ont été utilisées avec des gouttelettes de la phase DEX dispersées dans la phase PEO (DEX/PEO ou D/P) ou inversement (PEO/DEX ou P/D). La microstructure de l'émulsion a été déterminée par le microscope confocal, voir la **Figure R1**. Les images montrent que les particules se mettent à l'interface entre les deux phases en formant une couche autour de gouttelettes. L'affinité des microgels pour les deux phases peut être modulée par la composition de microgels. En effet, ces particules préfèrent la phase de PEO à faible fraction de DEX (27 %) et la partition dans la phase de DEX augmente quand la fraction DEX dans les particules augmente. Par ailleurs, il a été constaté que la quantité de microgels à l'interface augmente aussi avec la fraction de DEX.

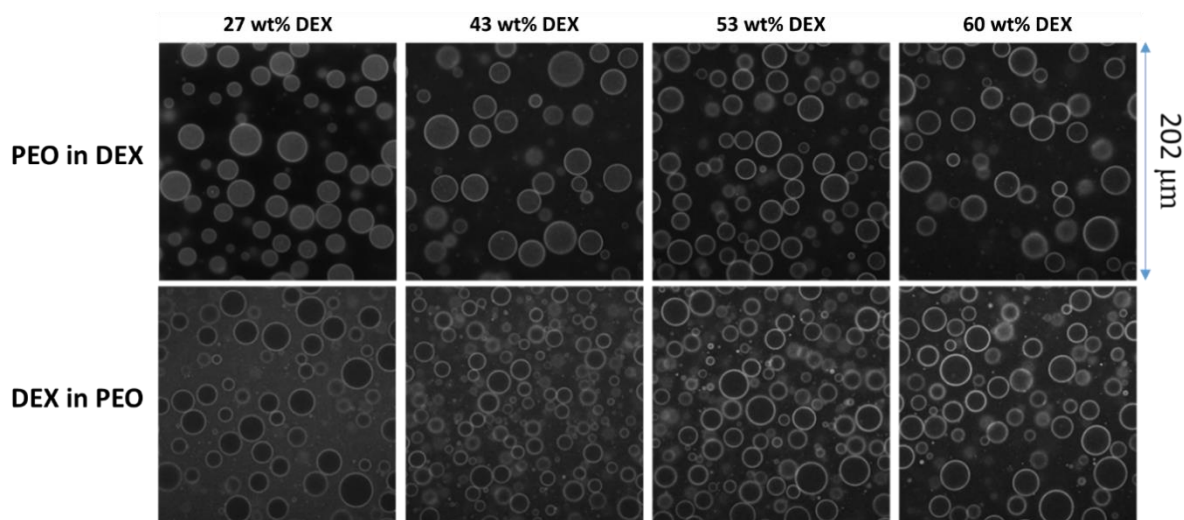


**Figure R1.** Microstructures des émulsions P/D et D/P stabilisées par les microgels avec différentes teneurs en DEX dont la composition est comme indiquée dans la figure.

L'étude examine l'effet de la force centrifuge et de la température sur la stabilité des émulsions contenant des microgels à différentes compositions, voir la **Figure R2**. À 20 °C, une



augmentation du pourcentage de DEX dans les microgels ralentit la vitesse de coalescence. Les microgels peuvent stabiliser les émulsions D/P plus que les émulsions P/D.

L'émulsion D/P était beaucoup moins stable à 50 °C qu'à 20 °C, quelle que soit la voie de préparation. Concernant l'émulsion P/D, le chauffage de l'échantillon avant l'émulsification a conduit à une meilleure stabilité en présence de microgels avec moins de 50 % DEX. L'émulsion avec microgels à 50 % DEX était plus stable lorsqu'elle était chauffée après l'émulsification. Enfin, avec des microgels à 60 % DEX, les deux émulsions chauffées étaient moins stables qu'à 20 °C.

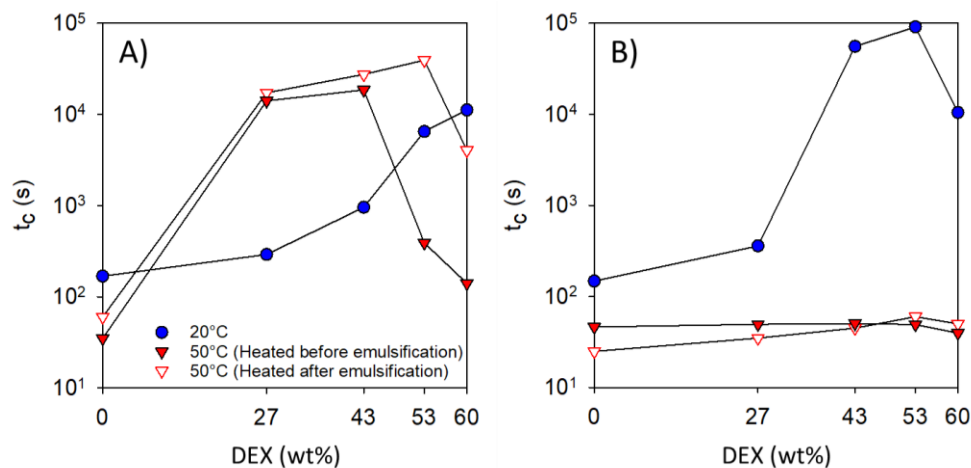


**Figure R2.** Temps caractéristiques des émulsions A) P/D, B) D/P en fonction de la fraction DEX dans les microgels à 20 °C et 50 °C, pour des émulsions préparées dans différentes conditions. 0 % DEX correspond à l'émulsion sans particules.

Les résultats de ce travail ont montré qu'il est possible de moduler l'adsorption des particules aux interfaces liquide/liquide et leur affinité avec les deux phases en modulant le ratio du DEX, avec un optimum de compositions vers 50 %. La thermosensibilité du pNIPAM a permis d'inverser la stabilité des émulsions en traversant la VPTT du pNIPAM lorsque la proportion de pNIPAM est dominante dans la particule.

Un deuxième objectif est d'étudier l'effet de charge sur la stabilité avec les microgels sensible au pH dont la structure est modifiée avec l'acide acrylique (AA). Les microgels chargés ont les mêmes compositions que pour les microgels neutres de 27 % DEX, mais 14 % en moles d'unités NIPAM sont remplacées par des unités AA ( $F_{AA} = 14\%$  en moles) lors de la synthèse.

Les microgels chargés gonflent dans l'eau en raison des interactions électrostatiques. La diminution de la densité de charge en diminuant le pH ou en écrantant l'interaction par l'ajout de NaCl provoque un dégonflement des microgels. Nous constatons que l'introduction de charges dans ces microgels inhibe le dégonflement lors du chauffage en raison de la forte répulsion électrostatique dans l'eau pure et en présence de sel. L'effet de dégonflement pendant le chauffage est restauré lorsque la densité de charge est réduite en diminuant le pH. À faible pH, le dégonflement commence à des températures plus basses lorsque davantage d'unités NIPAM sont remplacées par des unités AA neutres.

Les études de stabilisation avec des microgels chargés et pH-sensibles sont réalisées. Elles révèlent que la présence de charges diminue drastiquement l'adsorption des microgels à l'interface et les émulsions deviennent instables, voir la **Figure R3**.

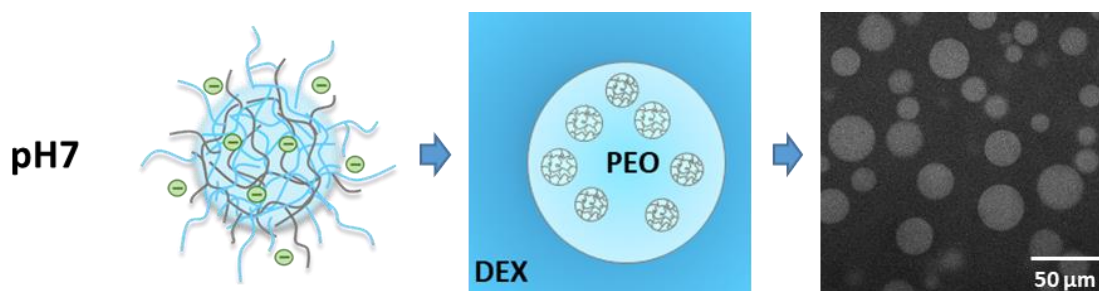


**Figure R3.** *Microstructure de PEO/DEX en présence de microgels chargés*

A pH 3, bien que réduire la densité de charge en abaissant le pH ait un effet sur la taille, les microgels chargés ne s'adsorbent pas à l'interface et n'ont pas eu d'effet significatif sur la stabilité, voir la **Figure R4**. Cependant, le fort effet de la température sur la stabilisation de l'émulsion P/D a été restauré avec les microgels chargés à faible pH, ce qui est absent à pH neutre.

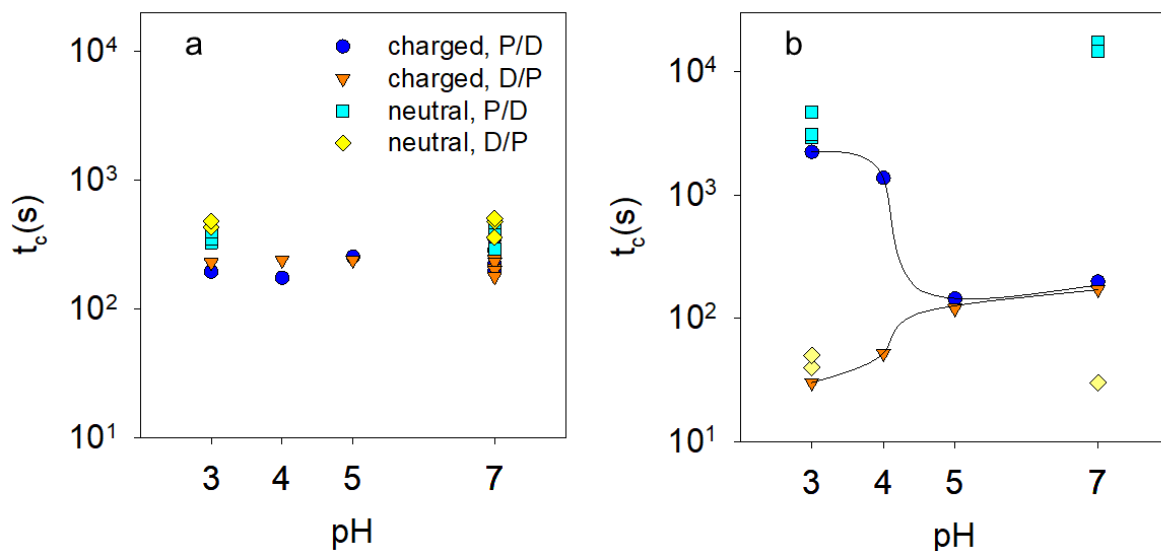


**Figure R4.** Temps caractéristiques des émulsions P/D et D/P à 20 °C (a) ou 50 °C (b) avec des microgels neutres ou des microgels chargés ( $F_{AA} = 14 \text{ mol}\%$ ) à différents pH.

L'écrantage des charges par augmentation de la force ionique tend à rétablir l'adsorption des microgels et à améliorer la stabilité, voir la **Figure R5**. En particulier, les microgels neutres équivalents ne peuvent pas stabiliser l'émulsion D/P à haute température, alors que les microgels chargés stabilisaient cette émulsion aussi bien à basse qu'à haute température si plus de 20 mM de NaCl étaient ajoutés.

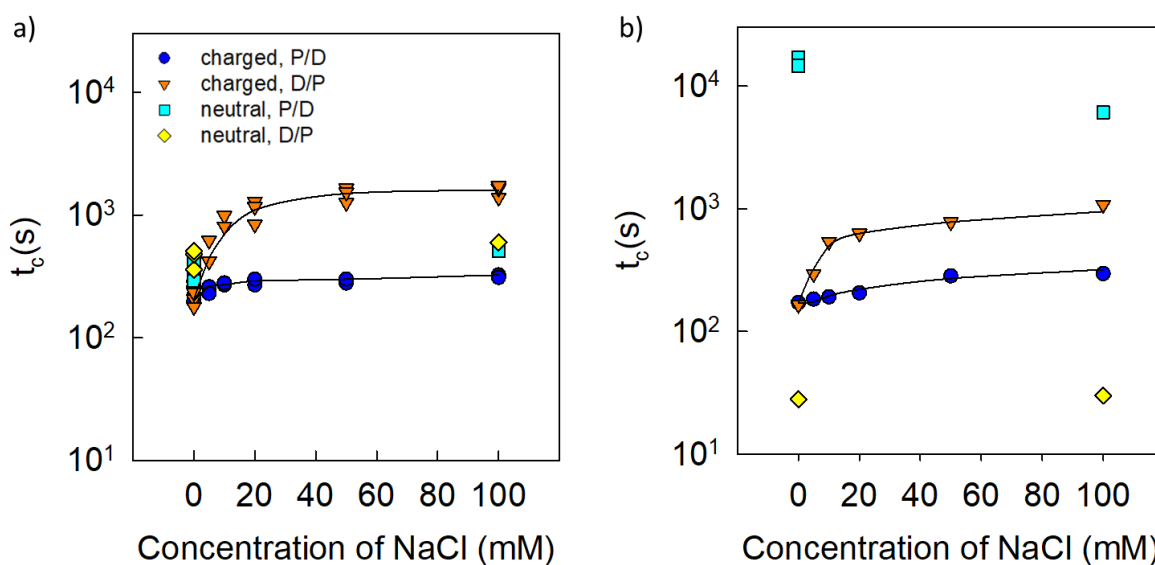


**Figure R5.** Temps caractéristiques des émulsions avec des microgels neutres et chargés ( $F_{AA} = 14 \text{ mol}\%$ ) dans différentes concentrations de NaCl à 20 °C (a) et 50 °C (b).

Par l'incorporation d'unités d'acide acrylique dans les microgels, il a été possible de les rendre sensibles à la variation du pH ou la force ionique par ajout de sel, qui par ailleurs se révèlent non équivalentes vis-à-vis du comportement des émulsions pour un état de charge donné. Ce résultat met clairement en exergue l'importance des interactions particules/particules et particule/liquides sur la stabilité des émulsions E/E.

Pour étendre le potentiel des microgels à d'autres émulsions E/E, nous avons étudié leur effet sur la stabilité des émulsions biphasiques formées de gélatine de poisson (GEL) et de PEO. On constate que les microgels se mettent à l'interface GEL et PEO, formant une couche continue à la surface de gouttelettes de GEL, voir la **Figure R6**. Bien que les microgels préfèrent la phase dispersée de GEL, ils peuvent bien stabiliser l'émulsion GEL/PEO. La dépendance de la stabilité sur la fraction de DEX dans les microgels est similaire à celle des émulsions D/P en ce sens que  $t_c$  augmente fortement en présence de microgels contenant 43 % ou plus de DEX.

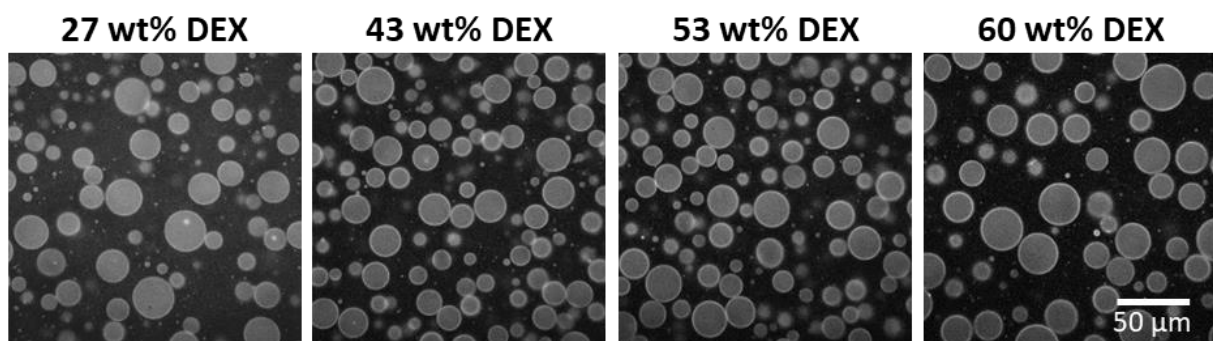


**Figure R6.** *Microstructures de GEL/PEO en présence de microgels avec différentes teneurs en DEX comme indiqué dans la figure*

Une première étude d'un système triphasique a été mise en œuvre en mélangeant deux émulsions avec une phase continue commune. Dans ce cas, deux émulsions bien stables DEX/PEO et GEL/PEO ont été mélangées pour obtenir des gouttelettes de DEX et de GEL dispersées dans une phase continue de PEO.

La coalescence entre les gouttelettes de la même phase a été fortement inhibée par la couche adsorbée de microgels. Cependant, lorsque des gouttelettes de phases différentes se sont rencontrées, elles se sont immédiatement associées pour former des gouttelettes de type Janus à deux compartiments, voir la **Figure R7**. Au fur et à mesure que l'interpénétration des deux émulsions se poursuit, des chaînes de gouttelettes alternées de GEL et de DEX se formaient et se ramifiaient.

Les angles de contact de chaque phase du système stabilisé par des microgels neutres sont proches de ceux observés en l'absence de particules. Les émulsions stabilisées avec des microgels chargés en présence de 100 mM de NaCl ont montré un comportement similaire, mais les angles de contact étaient différents, ce qui implique des changements dans les tensions interfaciales. L'effet le plus important a été trouvé pour l'interface P/G avec les microgels chargés.

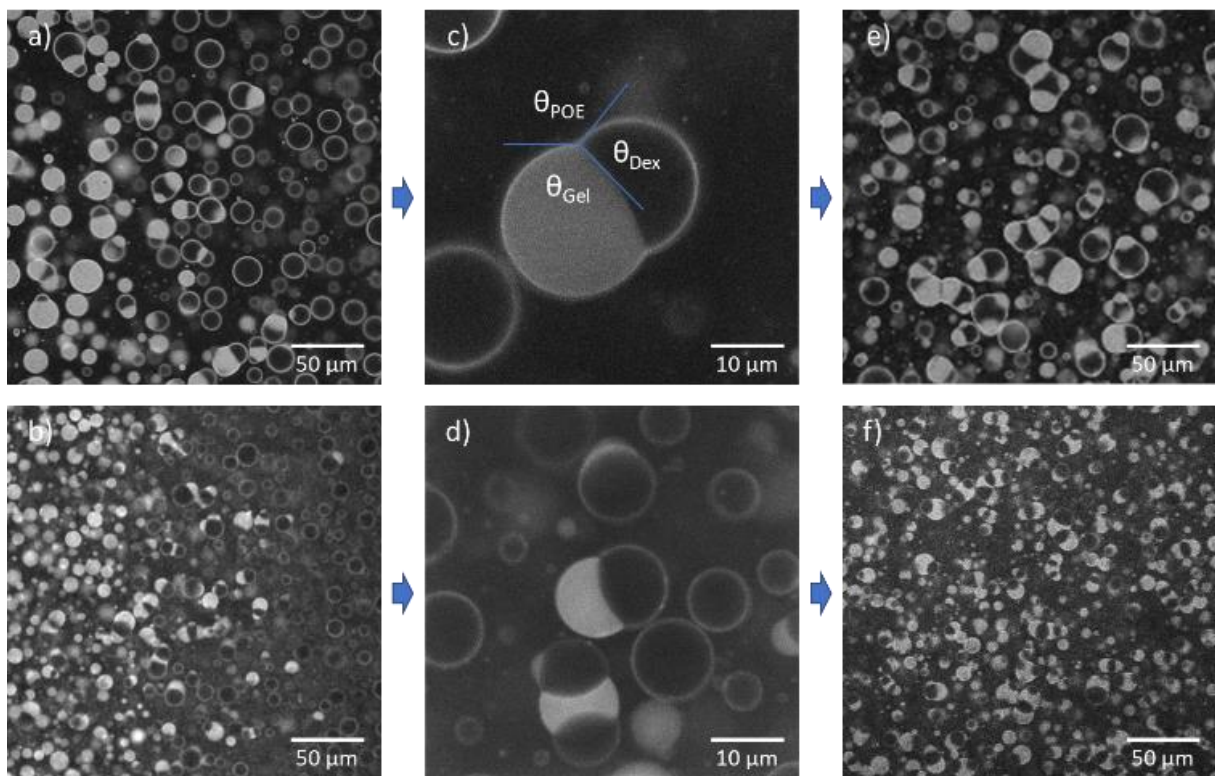


**Figure R7.** Images CLSM de la zone de contact entre les émulsions D/P et G/P à pH7 stabilisées par des microgels neutres dans l'eau (a) et des microgels chargés dans 100 mM NaCl (b) avec

*des gros plans des gouttelettes Janus montrées dans les figures c et d, respectivement. Les images des émulsions après un mélange au vortex sont montrées dans les figures e et f, respectivement.*

Si les gouttelettes dispersées des deux émulsions W/W stabilisées contiennent des ingrédients différents, le mélange des émulsions offre la possibilité de mettre ces ingrédients en contact les uns avec les autres de manière contrôlée et de déclencher une réaction entre eux.

La dernière partie de la thèse est consacrée principalement au mélange de deux différents types de microgels dans la stabilisation d'émulsions E/E. Une étude de l'effet de l'ajout de microgels de protéines (PRO) et de microgels bishydrophiles (BIS) à l'émulsion de PEO et de DEX a été mise en œuvre. Les microgels protéiques ont été produits en chauffant la solution aqueuse de protéine de lactosérum. Les deux types de microgels s'adsorbent spontanément à l'interface et forment une couche autour des gouttelettes. PRO peuvent stabiliser efficacement l'émulsion P/D mais pas D/P. Les PRO excédentaires sont partitionnés en priorité dans la phase DEX. Les BIS choisis peuvent stabiliser les deux systèmes, mais une plus rapide coalescence des gouttelettes a été observée pour l'émulsion D/P.

Les émulsions contenant BIS ont été doucement mélangées avec des émulsions contenant PRO sans casser les gouttelettes. La **Figure R8** montre que, dans les émulsions D/P, les gouttelettes DEX recouvertes de PRO et de BIS ont coalescé immédiatement après contact, formant des gouttelettes avec des couches hybrides. Cependant, dans les émulsions P/D, aucune coalescence n'a été observée.



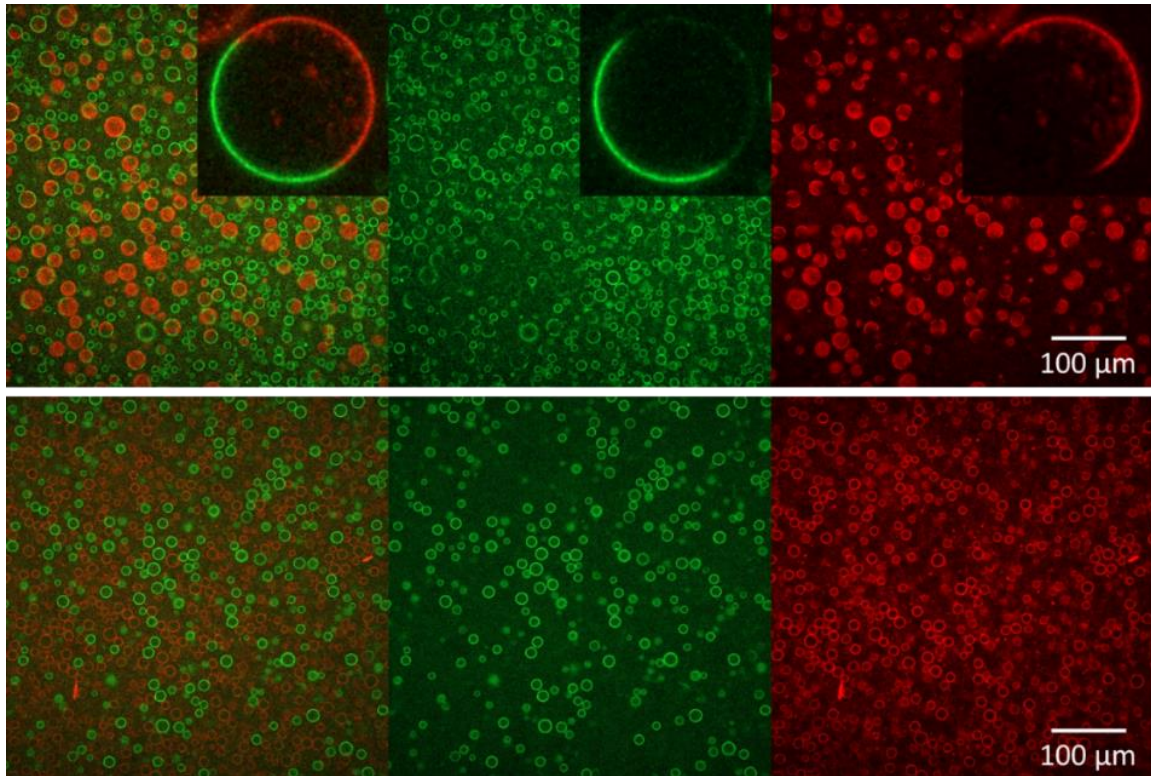


**Figure R8.** Microstructures de gouttelettes DEX recouvertes de PRO (rouges) et de BIS (vertes) dispersées dans du PEO (en haut) ainsi que de gouttelettes de PEO dispersées dans du DEX (en bas) après un mélange doux. Les inserts montrent un gros plan d'une gouttelette avec une couche hybride formée après coalescence. De gauche à droite, le signal fusionné des deux microgels, le signal de BIS et le signal de PRO.

La **Figure R9** présente des images de gouttes formées après mélange de deux émulsions D/P stabilisées par PRO et BIS à l'aide d'un vortex. Ces gouttes montrent une couche mixte de PRO et de BIS, avec une épaisseur de couche d'environ 230 nm pour le BIS et 380 nm pour le PRO, correspondant aux diamètres hydrodynamiques mesurés par diffusion dynamique de la lumière. PRO a une préférence pour se situer plus près de la phase DEX en raison de sa plus grande affinité. La distance entre les pics des couches PRO et BIS est de  $74 \pm 30$  nm pour les émulsions D/P et de  $65 \pm 44$  nm pour les émulsions P/D, indiquant un chevauchement significatif entre les microgels. Les microgels sont complètement mélangés sans séparation de phases, ce qui réduit considérablement la coalescence par rapport aux émulsions contenant un seul type de microgel.



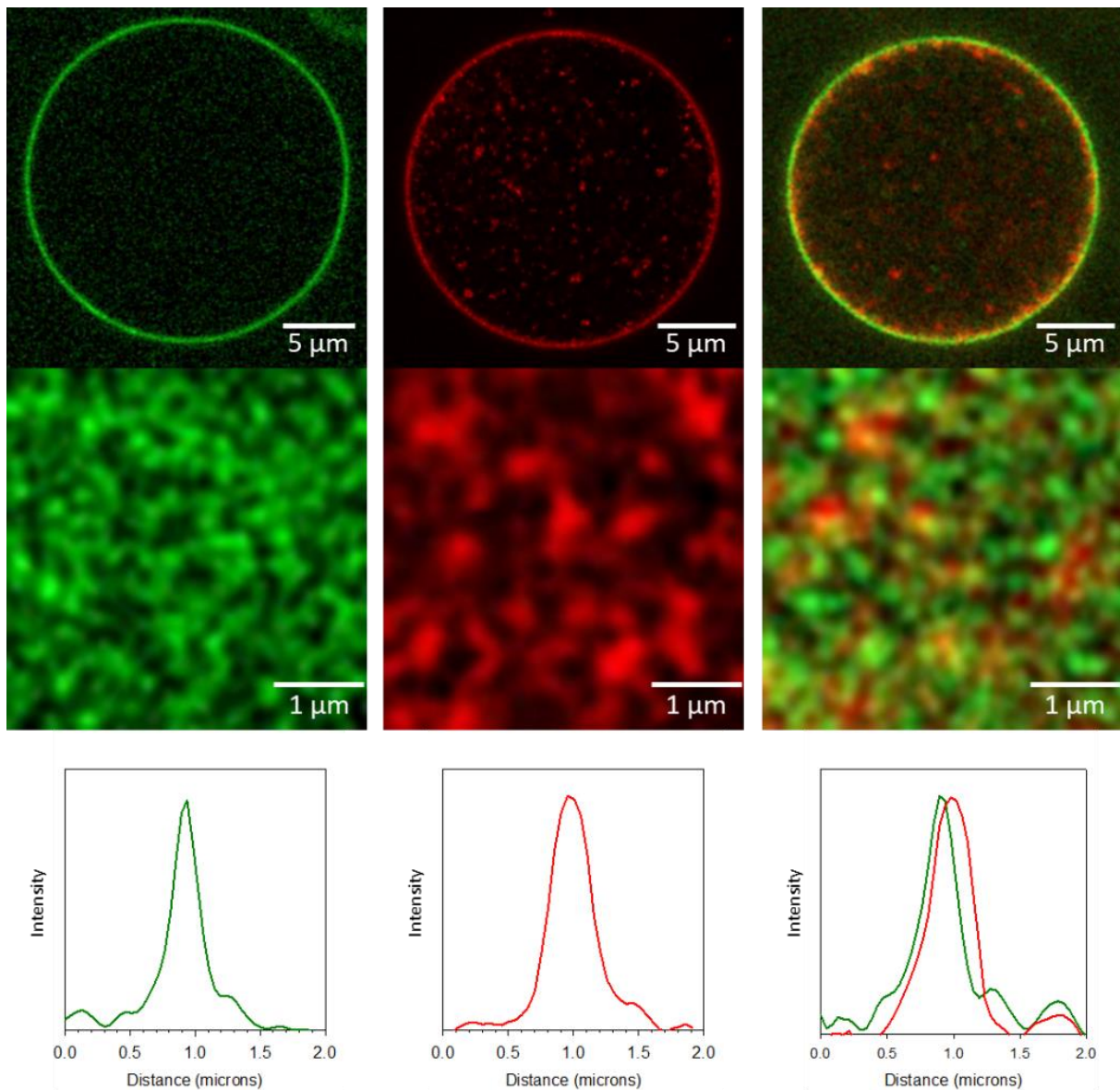


**Figure R9.** *Microstructure de vues transversales et de dessus de gouttelettes de DEX couvertes par BIS (gauche), PRO (centre) et par un mélange de BIS et PRO (droite) suspendues dans une phase PEO continue. Les profils d'intensité de fluorescence à travers les couches sont également présentés.*

Les microgels BIS et PRO restent bien dispersés dans l'eau et le DEX, mais co-agrègent rapidement dans le PEO car PRO s'attache au DEX des BIS dans le PEO. Lorsqu'une solution de DEX est ajoutée à du PEO contenant ces co-agrégats, une couche mixte se forme sans contact préférentiel du PRO pour le DEX. Cette co-agrégation empêche le réarrangement des microgels à l'interface.

Enfin, l'attention est portée sur l'interaction entre un type de microgel en suspension dans la phase continue et la surface des gouttelettes recouverte par l'autre type de microgel en mélangeant doucement, voir la **Figure R10**. Dans une émulsion D/P, PRO ajoutés s'adsorbent spontanément sur les gouttelettes recouvertes de BIS, formant une seconde couche en contact avec la phase DEX, et peut même pénétrer la couche de BIS. Inversement, lorsque les gouttelettes sont recouvertes de PRO, le BIS libre s'adsorbe également à l'interface, créant une couche mixte. Dans une émulsion P/D, le PRO ne s'adsorbe pas sur les gouttelettes recouvertes de BIS, mais le BIS ajouté remplace progressivement la couche de PRO, en raison de l'affinité élevée du PRO pour le DEX.

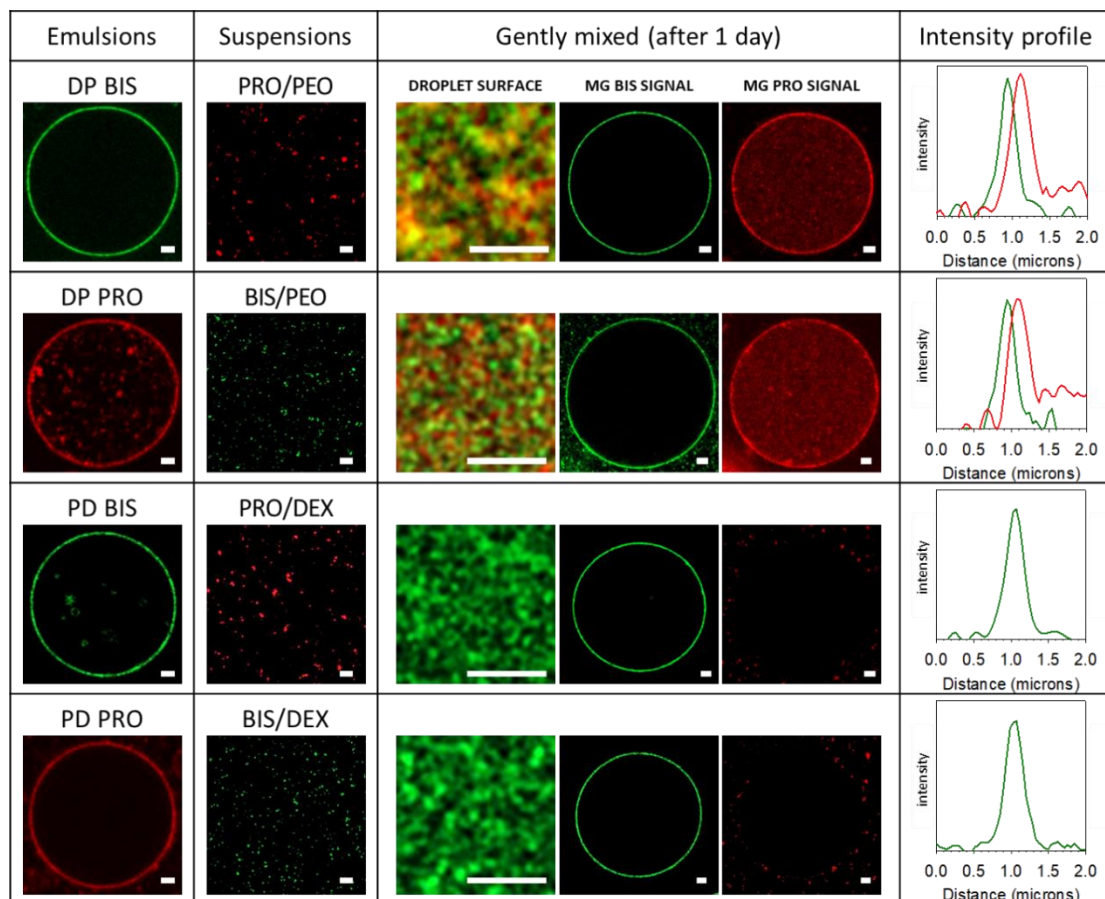


**Figure R10.** Microstructures de gouttelettes dispersées de DEX et PEO recouvertes de BIS ou PRO et de suspensions de MG en phase continue et les systèmes doucement mélangés et des profils de fluorescence correspondants des couches. La barre d'échelle représente 2  $\mu\text{m}$ .

La combinaison des différents types de particules étudiés a amélioré la stabilité, ce qui suggère que les couches mixtes à l'interface pourraient être plus efficaces que les types de particules uniques. Cette stratégie a permis d'améliorer la stabilité des émulsions E/E mais également la structuration et l'organisation des deux types de particules à l'interface. Cette découverte ouvre la voie à l'optimisation des propriétés de l'émulsion pour une combinaison des applications spécifiques.

En conclusion, cette thèse a fourni un cadre complet pour comprendre et contrôler la stabilité des émulsions E/E par la manipulation de différents paramètres et conditions. Elle offre des informations précieuses aux chimistes et aux scientifiques des matériaux pour la conception et le développement de stabilisateurs de type particulaire avec de nouvelles fonctionnalités. Ce travail a également ouvert de nouvelles possibilités d'encapsulation et de contrôle de réactions, élargissant l'utilisation et l'application des émulsions E/E dans diverses industries telles que l'alimentation, les produits pharmaceutiques et les cosmétiques.

